A field-based modelling framework of the ecohydrology of schistosomiasis

THÈSE N^{O} 8239 (2018)

PRÉSENTÉE LE 16 FÉVRIER 2018
À LA FACULTÉ DE L'ENVIRONNEMENT NATUREL, ARCHITECTURAL ET CONSTRUIT
LABORATOIRE D'ÉCOHYDROLOGIE
PROGRAMME DOCTORAL EN GÉNIE CIVIL ET ENVIRONNEMENT

ÉCOLE POLYTECHNIQUE FÉDÉRALE DE LAUSANNE

POUR L'OBTENTION DU GRADE DE DOCTEUR ÈS SCIENCES

PAR

Francisco Javier PEREZ SAEZ

acceptée sur proposition du jury:

Prof. T. I. Battin, président du jury
Prof. A. Rinaldo, directeur de thèse
Prof. J. Utzinger, rapporteur
Prof. J. Remais, rapporteur
Prof. M. Salathé, rapporteur

ÉCOLE POLYTECHNIQUE
FÉDÉRALE DE LAUSANNE
Suisse
2018

Il vaut mieux avoir de la poussière aux pieds,
que de l'avoir aux fesses.
— Proverbe africain

Acknowledgements

I would like to thank Andrea Rinaldo for the opportunity he has given me to embark on this thesis, for his culture of curiosity-driven research, and for guidance and advice throughout the years. This thesis would not have been possible without the financial support of the Swiss Agency for Development and Cooperation through the Projet 3E Afrique, Burkina Faso-2iE partie scientifique.

I was fortunate to share this research journey with Théophile Mande the whole way through, from whom I learned a great deal about Burkina Faso, science and life more in general. I am also grateful for the guidance of Natalie Ceperley during the first year of the thesis, and all the open-minding chats since then. I thank Lorenzo Mari and Enrico Bertuzzo for their support and for insightful discussions. These four years have been rich not only on the scientific plane, but also at the personal level, and for this I must thank the whole ECHO lab for its fantastic working environment and for the fact that I have learned something from each and every one of its members: from Pierre the taste for outdoors and exploration, may it be in the ruggedness of the Alps or of Ouagadougou's streets; from Flavio that deepness of thought is not (always) contradictory with lightness of spirit, and attain their greatest harmony in the act of skiing; from Jean-Marc navigation techniques in the meanders of international cooperation; from Anna the value of communication and listening; from Bernard what being a field hydrologist is all about, as opposed to the "salon" hydrologists that can be found these days; from Andrea (G.) that with great power, must come great bravery, which with great modesty, give great Jungle Speed players; from Silvia what a real piadina tastes like, how science and art find their way to mingle, and, more importantly, that romanesco broccoli are not as innocuous as one may think; from Damiano I failed to learn juggling and shooting hoops, but I was able to learn from the way he made people smile, laugh, and brighten, even when singing questionable italian culinary songs; from Ana-Clara the marvels of the mix of paõ de queijo, kindness, and cachaça, with due slowness, of course; from Luca I wish I had been able to retain more of his encyclopedic knowledge about world capitals, cycling, and much more, but I have certainly learned about dedication and commitment, may it be to science or teaching; from Paolo the embracing panache of classroom teaching, the sparkle of varying moustache styles, and the importance of empathy in both these aspects of life, and beyond; from Joseph the craftsmanship of poised nonchalant humour, the infinite possible uses of "ohala", and the discovery of the Garamont font; and finally, from Jonathan I learned to unleash one's creativity in unsuspected ways, across multiple media, and how valuable it is to have an outstanding office mate in shiny and less shiny days.

I thank my family for their unconditional love and support.

Finally I thank you Sophie for making it all have meaning.

Lausanne, 1 February 2018

Summary

Successful control of schistosomiasis, a water-borne parasitic disease, is challenged by the intricacy of the worm's lifecycle, which depends on aquatic snail intermediate hosts, and involves environmental, ecologic, and socio-economic factors. Current strategies rely on deworming through mass drug administration which however do not protect against reinfection and the persistence of hotspots. It is recognized that multifaceted approaches will be necessary to reach elimination, whose development will require a renewed focus on the disease's social-ecological drivers. Taking cue from the hydrological underpinning of these drivers, this Thesis aims at developing an ecohydrological approach to schistosomiasis with a view to identifying and exploiting the points in which its cycle can be broken.

Schistosomiasis is a poverty-reinforcing disease affecting more than 150 million people in sub-Saharan Africa, being the parasitic disease causing the largest health burden after malaria. However, the impairing morbidity it causes has been undervalued in the past, qualifying it as a neglected tropical disease. Moreover, water resources development often exacerbate transmission, posing scientific and ethical challenges in addressing the ensuing trade-off between economic development and public health. The relevance of this Thesis' work lies in furthering tools to offset this trade-off by unlocking the predictive appraisal of the social-ecological drivers of transmission.

An integration of fieldwork applied in Burkina Faso (West Africa) and theoretical methods are employed to address this aim. This Thesis establishes the use of spatially explicit mathematical models of schistosomiasis at the national-scale, allowing to study the effect of human mobility and spatial heterogeneity of transmission parameters. Weekly ecological samplings of snail abundance and continuous environmental monitoring were preformed at three sites along the country's climatic gradient, leveraged through ecological modelling. A novel methodology for the large-scale prediction of river network ephemerality allowed for refined snail species distribution models, and the analysis of the disease's geography in link with socio-economic covariates. Finally, surveys and participatory workshops shed light on local-scale water contact patterns.

The obtained results substantiate the stance that hydrology is a first-order control of disease transmission. Stability analysis of the spatially explicit model generated additional insight into the impact of the expansion of suitable snail habitat due to water resources development, highlighting the interplay between local and country-wide effects driven by human mobility. Models of snail ecology revealed key hydrological drivers, and disputed density feedbacks. Uncovered phase shifts between permanent and ephemeral habitats were adequately reproduced at the national scale through model regionalization. Characterization and predictions of hydrological ephemerality improved the estimation of the snails' ecological range, mirroring the disease's geography. Finally a national-scale association between ephemerality and disease risk was observed, possibly due to human-water contacts aggregation, as supported by preliminary results at village-level. The future incorporation of these ecohydrological findings into spatially explicit models of schistosomiasis is considered promising for optimizing control strategies and attaining disease elimination.

Key words: schistosomiasis; ecohydrology; spatially explicit mathematical modelling; Burkina Faso; water resources development; hydrological ephemerality;

Résumé

Le succès du contrôle de la schistosomiase, une maladie d'origine hydrique, dépend de la capacité a agir sur la complexité du cycle de vie du parasite qui dépend d'escargots aquatiques comme hôtes intermédiaires, et implique des facteurs environnementaux, écologiques et socio-économiques. Les stratégies actuelles reposent l'administration de masse de médicaments qui, cependant, ne protègent pas contre la réinfection. Il est reconnu qu'une approches multisectorielles sera nécessaire pour éliminer la maladie, mais nécessitera une attention renouvelée sur ses aspects socio-écologiques. Misant sur le lien entre l'hydrologie et la transmission de la maladie, cette thèse vise à développer une approche écohydrologique de la schistosomiase en vue d'identifier et d'exploiter les levier pour interrompre sa transmission.

La schistosomiase est une maladie affectant plus de 150 millions de personnes en Afrique subsaharienne. Cependant, la morbidité qui en découle a été sous-évaluée dans le passé. De plus, le développement des ressources en eau exacerbe souvent la transmission, ce qui pose des défis scientifiques et éthiques dans l'arbitrage qui s'ensuit entre le développement économique et la santé publique. Cette thèse vies donc aux développement d'outils pour dépasser ce compromis en comprenant mieux les facteurs socio-écologiques de la transmission.

Une combinaison de travail de terrain au Burkina Faso (Afrique de l'Ouest) et d'outils théoriques a été utilisée pour atteindre ce but. Cette thèse établit l'utilisation de modèles mathématiques spatialement explicites de la schistosomiase à l'échelle nationale, permettant d'étudier l'effet de la mobilité humaine et de l'hétérogénéité spatiale des paramètres de transmission. Des échantillonnages écologiques de l'abondance des escargots ont été faits sur trois sites le long du gradient climatique du pays, mis à profit par la modélisation écologique. Une méthodologie novatrice pour la prédiction à grande échelle de l'éphéméralité du réseau fluvial a permis d'améliorer des modèles spatiaux de répartition des espèces d'escargots, et l'analyse de la géographie de la maladie en lien avec des facteurs socio-économiques. Enfin, des enquêtes et des ateliers participatifs ont permis d'appréhender les schémas de contact avec l'eau à l'échelle locale.

Les résultats obtenus justifient l'hypothèse selon laquelle l'hydrologie est un facteur crucial dans la transmission de la maladie. L'analyse de la stabilité du modèle spatialement explicite a permis de mieux comprendre l'impact de l'expansion de l'habitat des escargots du au développement des ressources en eau, soulignant l'interaction entre les liés à la mobilité humaine. Les modèles de l'écologie des escargots ont mis en évidence des oscillations différées de la population des escargots entre les habitats permanents et éphémères, correctement reproduits par les modèles à l'échelle nationale. Les prédictions de d'éphéméralité ont permis de mieux prédire les zones de présence des escargots, reflétant la géographie de la maladie. Enfin, une association à l'échelle nationale avec le risque de la maladie a été observée, probablement en raison de l'agrégation des contacts avec l'eau, comme le prouvent les résultats obtenus au niveau des villages. L'incorporation future de ces résultats écohydrologiques dans des modèles spatialement explicites de la schistosomiase est considérée comme prometteuse pour optimiser les stratégies de lutte et parvenir à son élimination.

Mots clefs : schistosomiase ; écohydrologie ; modélisation mathématique ; Burkina Faso ; l'éphéméralisme hydrologique ; développement des ressources en eau

Table of contents

List of Figures

List of Tables

1 Introduction

1.1 Human schistosomiasis

1.1.1 Disease burden and parasite lifecycle

Schistosomiasis is a chronic debilitating neglected tropical disease (NTD) caused by flatworms of genus *Schistosoma.* Global estimates suggest that at least 200 to 250 million people were infected in the early 2000s [*Steinmann et al.*, 2006; *Global Burden of Disease 2013 Collaborators*, 2015; *Global Burden of Disease Collaborative Network*, 2017]. If untreated, the two main forms of the disease, intestinal and uro-genital schistosomiasis, have life-long effects, including kidney failure, heightened HIV risk, bladder cancer, and liver fibrosis [*King et al.*, 2005; *Gryseels et al.*, 2006; *Secor*, 2012]. Children typically bear the highest parasite burden, which has been associated to stunted growth, anaemia, cognitive deficits and school drop-outs [*King*, 2010]. The burden of schistosomiasis is second only to malaria among parasitic diseases, claiming an estimated 3 million disability-adjusted life years (DALYs) per year in the past decade [*Global Burden of Disease Collaborative Network*, 2017; *Heinrich et al.*, 2017]. However, it is to be noted these figures have been criticized by researchers working on the disease as they argue for a 4-50 fold higher disability weight [*King and Dangerfield-Cha*, 2008]. Despite significant gains made in combating this disease in the last 15 years, and that elimination is envisaged in certain countries (see section 1.1.2), 190 million people were estimated to still be infected in 2016 [*Global Burden of Disease Collaborative Network*, 2017]. The vast majority of these (85.5%) live in sub-Saharan Africa (SSA) where the reduction in the number of people infected has been the slowest (Fig.1.1a), showing a marked heterogeneous spatial distribution of infection prevalence among countries (Fig. 1.1b).

Intestinal and uro-genital schistosomiasis in SSA are mainly caused by *Schistosoma mansoni* and *S. haematobium* respectively. Both parasites present a complex life cycle (Fig. 1.2), consisting of two reproductive phases, asexual in aquatic snail intermediate hosts and sexual in the human host (the Asian schistosome *S. japonicum* can also reproduce in other mammals, mainly in water buffalos), linked by two water-mobile larval phases (for a thorough description of *Schistosoma*'s lifecycle see *Jamieson* [2017]). Mated adult schistosomes secrete eggs that either exit the human host through urine (*S. haematobium*) or faeces (*S. mansoni*), or remain trapped in the tissues surrounding the venules around the bladder or the gross intestine. When entering water, eggs hatch into a free-swimming larval stage named miracidium having a lifespan of about one day. Within this lifetime, miracidia can seek and infect snail intermediate hosts [*Jamiesson and Haas*, 2017]. A number of genera of these small aquatic gastropod molluscs are present in SSA [*Brown*, 1980], among which two are compatible with human schistosomes: *Bulinus* spp.

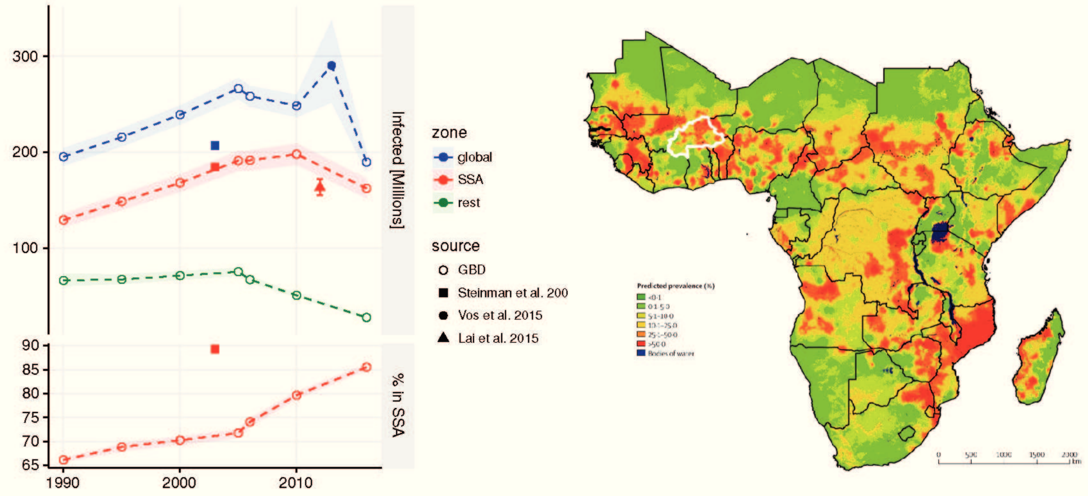

Figure 1.1 – The burden of schistosomiasis in sub-Sahara Africa (SSA) and the world. *Left*) Global estimates of the number of people living with schistosomiasis infection and the percentage of which live in SSA from the Global Burden of Disease Study (GBD) [*Global Burden of Disease Collaborative Network*, 2017; *Global Burden of Disease 2013 Collaborators*, 2015], prevalence-based estimates from a literature review (square) [*Steinmann et al.*, 2006], and predictions from a Bayesian geo-statistical model (triangle, only for SSA) [*Lai et al.*, 2015]. *Right*) Prevalence of *Schistosoma* spp. infection in school-aged children in SSA, from 2000 onward estimated by [*Lai et al.*, 2015][1]. Highlighted in white are the administrative boundaries of Burkina Faso where the relevant fieldwork of this Thesis has been carried out (see Chapter 2).

and *Biomphalaria* spp. for *S. haematobium* and *S. mansoni*, respectively. When schistosome and snail species are compatible, each miracidium will undergo asexual reproduction and produce hundreds to thousands of cercariae, the second larval stage, per day. The maturation time of miracidia within the snail hosts, here defined as the pre-patent period, is temperature- and species-dependent varying between 15 days and 4-5 weeks [*Anderson and May*, 1979]. Although snails can keep reproducing during this period, the infection can cause modifications of the snail's life history including gigantism [*Gérard and Théron*, 1997; *Kalinda et al.*, 2017b], as well as fecundity compensation depending on environmental conditions [*Gleichsner et al.*, 2016].

Once cercaria are released into water, they can infect a human host within 24-72h by penetrating the skin, losing their tail and morphing into a schistosomule. The schistosomule then migrates in the cardio-vascular system of the host, matures, and mates in the veins leading to the liver. The mated pairs migrate to the venules around the bladder (*S. haematobium*) or the intestinal lumen (*S. mansoni*). At this point sexual reproduction takes place and the female schistosomes start laying eggs at a rate of 150 or 300 per day for *S. haematobium* and *S. mansoni* respectively [*Loker*, 1983]. A fraction of the eggs (around 50% for *S. mansoni* [*de Vlas*, 1996], unestimated for *S. haematobium*) make it back into the environment through excreta by tunneling their way to the bladder or the intestinal lumen, thus completing the cycle. Egg excretion starts 5 or 6 weeks after infection for intestinal and 13 weeks for uro-genital schistosomiasis. Once mated, schistosomes live an average of 3-10 years in the human body, however infections lasting up to 40 years have been reported [*Fulford et al.*, 1995; *Colley et al.*, 2014].

The morbidity associated to schistosomiasis is due to the lesions caused by the eggs excreted throughout

---

[1] Reprinted and modified from The Lancet, 3099, Lai et al. (2015), Spatial distribution of schistosomiasis and treatment needs in sub-Saharan Africa: a systematic review and geostatistical analysis., 1–14, Copyright (2015), with permission from Elsevier (Liscence # 4191290638017).

the parasite's life in the tissues surrounding the veins in which they are logged [*Colley et al.*, 2014]. Organ-specific uro-genital schistosomiasis pathology concerns the uro-genital system causing cystitis, uretitis, and bladder cancer; the intestinal form affects the colon, liver and spleen and both forms can lead to pulmonary hypertension, sexual dysfunction, central nervous system lesions and spinal cord syndromes [*King and Dangerfield-Cha*, 2008]. Generalized morbidity of schistosomiasis is due to the continuous accumulation of eggs in the tissues resulting in chronic inflammation and sustained immune response [*Gryseels et al.*, 2006]. The effects of this chronic immunitary reaction includes anaemia, stunting, caloric undernutrition, impaired cognitive development, decreased work output, and infertility [*King and Dangerfield-Cha*, 2008]. Schistosomiasis has also been associated to a higher risk of contracting HIV both for adults and for children [*Mbabazi et al.*, 2011; *Bustinduy et al.*, 2014]. School-aged children and young adolescents are typically the age classes with the highest eggs excretion, with egg-prevalence often decreasing with age into adulthood, although these patterns vary between settings [*Colley et al.*, 2014]. Event though it is still debated among researchers and practitioners, this pattern is assumed to result from the accumulation of worms since the infection onset very early in the child's life (around 2 years of age [*Stothard and Gabrielli*, 2007]) during frequent water contacts which typically peak in the early adolescence [*Chandiwana*, 1987], with a decreasing egg-output with age due to the mounting of an immunological response and/or the reduction in exposure [*Colley et al.*, 2014]. Mathematical models combining epidemiological and immunological processes have suggested that the immunological reaction to *S. haematobium* is mainly driven by dying worms in the human host, leading to a mounting of a long-lasting protective antibody response [*Mitchell et al.*, 2012]. This response is thought to consist of the reduction of worm fecundity which, explains lower egg production in older individuals, already exposed to schistosomes, rather than providing protection against re-infection [*Mitchell et al.*, 2012]. Due to the very early onset of the possible infections and the life-long impacts in terms of cognitive impairment and labour capacity, schistosomiasis is a poverty-reinforcing disease jeopardizing the infected individual's capacity to overcome risk factors associated to the parasite's lifecycle [*King*, 2010], leading to a disease-induced poverty trap [*Ngonghala et al.*, 2017].

1.1.2 Strategies and measures for disease control and elimination

The intricate lifecycle of *Schistosoma* spp. provides multiple intervention pathways for disease control, which include reducing worm burden in the human host using anthelminthic drugs, managing the population of the snail intermediate host, reducing contamination of waterbodies due to open defecation and urination, and limiting exposure during human-water contacts [*Rollinson et al.*, 2003; *Utzinger et al.*, 2011]. This section provides a brief account of the historical evolution from morbidity control to disease elimination, as well as its limits and margins for the improvement of the suite of available control measures with regards to the parasite's ecology.

From control to elimination In the absence of safe and affordable anti-schistosomal drugs and vaccines, early control efforts in the 1940s mainly consisted of snail control through the use of molluscicides along with improved access to clean water, sanitation and hygiene (WASH) [*Sandbach*, 1976]. The discovery of praziquantel in the 1970s shifted control strategies towards mass drug administration (MDA) [*Engels et al.*, 2002], with a focus on morbidity control in highly endemic countries, i.e. the reduction of worm burden and its associated disability [*Rollinson et al.*, 2003]. Since the early 2000s, encouraged by the World Health Organization (WHO) through the adoption of the World Health Assembly (WHA) resolution WHA54.19 [*World Health Organization*, 2001], and embodied by the Schistosomiasis Control Initiative (SCI) [*Fenwick et al.*, 2006], morbidity control through MDA has been the backbone of most national

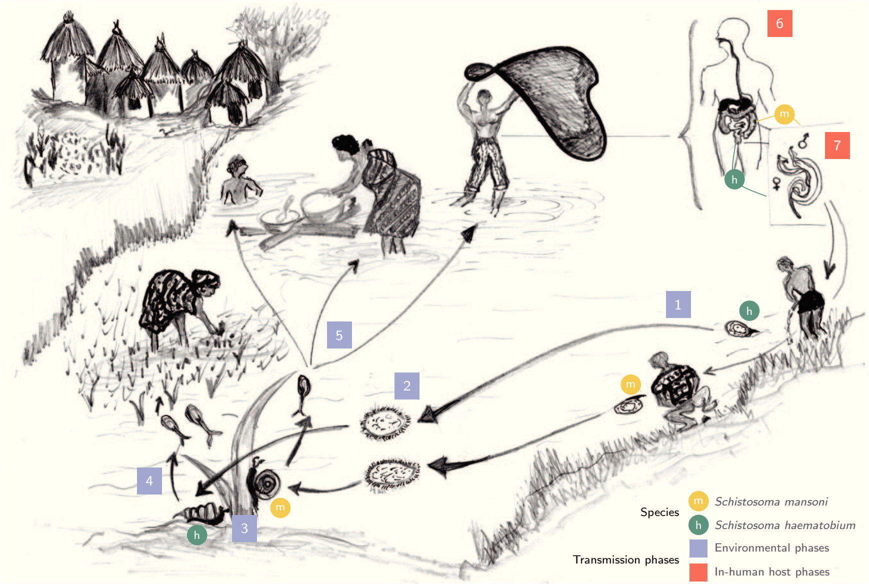

1 Egg excretion into the environment through urine and faeces. 2 Hatching into the first larval stage - 0.1 mm long miracidia. 3 Infection of the snail intermediate host, *Bulinus* or *Biomphalaria*, within 12 h of hatching. 4 Maturation and asexual reproduction of parasite in the snail intermediate host leading t emission of the second larval stage - 1mm long cercaria - after a pre-patent period of 1 month.
5 Human infection through skin penetration during prolonged water contacts within 24 h of cercarial emission.
6 Parasite migration and maturation in the human final host during 1-3 months 7 Mature schistosomes lodged in the capillary veins around the bladder or the intestinal lumen undergo sexual reproduction resulting in a daily release of around 150 to 300 eggs during the 3-5 yr lifespan of the schistosomes.

Figure 1.2 – Schistosome life cycle and infection phases

control strategies. These control strategies have had important gains in terms of reduction of disease prevalence and the intensity of infection [*Fenwick et al.*, 2006; *Wang et al.*, 2008]. In recent years schistosomiasis has moved up on the global health agenda with WHA resolutions WHA65.21 [*World Health Organization*, 2012a] and WHA66.12 [*World Health Organization*, 2013b] and the London Declaration on NTDs [*World Health Organization*, 2012c], with a paradigm shift from morbidity control to disease elimination as a public health problem (threshold on the prevalence of high intensity infections), and complete elimination (transmission interruption) in selected regions by 2020 [*World Health Organization*, 2013a].

Mass drug administration and its limits There currently exists no clinically-approved vaccine for human schistosomiasis [*Egesa et al.*, 2017; *Bergquist and McManus*, 2017], and most countries with national schistosomiasis control or elimination programmes rely solely on preventive chemotherapy [*Sokolow et al.*, 2016], despite WHO recommendations on combining MDA with alternative public health interventions [*World Health Organization*, 2013a]. Since its discovery in the 1970s praziquantel remains the drug of choice for most health authorities in countries with national schistosomiasis control programmes [*Fenwick et al.*, 2003]. Praziquantel has been shown to have a good efficacy against adult *S. haematobium* and *S. mansoni*, but less against the juvenile form of both species [*Gönnert and Andrews*, 1977; *Fenwick et al.*, 2003]. Concerns about its widespread use have been voiced due to the possible emergence of drug resistance [*Doenhoff et al.*, 2008], a thesis proposed as the an explanation, although not unambiguously validated, of lower, cure rates than expected in areas undergoing regular MDA [*Picquet et al.*, 1998; *Danso-Appiah and de Vlas*, 2002]. Chemotherapy, however does not protect against subsequent cercarial penetration and worm development, thus presenting the risk of morbidity control failure due to re-infection [*Mutapi et al.*, 1999; *N'Goran et al.*, 2001], possibly leading to persistent hotspots of transmission despite multiple rounds of MDA [*Pennance et al.*, 2016; *Kittur et al.*, 2017; *Wiegand et al.*, 2017]. Despite an increase in MDA coverage of school-aged children in the past 10 years, the 75% target of the WHO guidelines has not been met in many endemic countries due to institutional, operational, and budgetary impediments, with an average global coverage of 53.7% (36.5% when accounting for adults) of the population at risk in 2016 [*World Health Organization*, 2017b]. Furthermore, recent modelling studies suggest that community wide treatment is cost-effective across endemicity levels [*Lo et al.*, 2015], including preschool-aged children who are known to be parasitized very early on [*Stothard and Gabrielli*, 2007; *Stothard et al.*, 2013; *Bustinduy et al.*, 2017]. However the scaling of MDA alters the immunological interactions between human hosts and parasites, in particular for school-aged children, with potential benefits on the short-term (accelerated acquisition of protective immunity), but with the risk of a strong rebound overshooting pre-treatment infection intensity on the the longer due to depressed antibody levels in the population if MDA is interrupted and residual transmission remains [*Mitchell et al.*, 2014]. The future impacts of more frequent MDA campaigns with greater spatial coverage on schistosome biology and disease immunoepidemiology are therefore non-trivial, and will require close and constant monitoring in the coming years [*Mutapi et al.*, 2017]. Beyond the challenges associated with the estimation of current treatment needs at the sub-national level [*Schur et al.*, 2012], the district prevalence-based WHO thresholds for determining MDA frequency -developed for morbidity control- have been criticized due to the risk of under-treating areas with high transmission localities if elimination is to be achieved [*Tchuem Tchuenté et al.*, 2017; *Lo et al.*, 2017]. Another operational consideration is the importance of the timing of MDA with respect to the potentially seasonal dynamics of transmission highlighted in several settings [*Augusto et al.*, 2009; *Ahmed et al.*, 2012; *Tchuem Tchuenté et al.*, 2013; *Senghor et al.*, 2015], and mentioned in the WHO schistosomiasis control guidelines for endemic countries [*World Health Organization*, 2013a, p. 37]. Despite the large potential gains in transmission reduction, there still is a lack of a clear methodological approach for the quantification of transmission seasonality at the national scale, depending both on the fluctuations of snail abundance and human-water contacts, and the planning of MDA timing at the national level. In the face the shortcomings of MDA, a multifaceted approach is needed for reaching elimination targets, including measures for the management of snail populations, improved access to WASH, and the development of novel surveillance and rapid diagnostic tools for the monitoring of transmission in low-endemicity settings [*Utzinger et al.*, 2011; *Rollinson et al.*, 2013; *Lo et al.*, 2017; *Stothard et al.*, 2017; *Tchuem Tchuenté et al.*, 2017].

Snail control As mentioned above, snail control was the main control tool before the advent of praziquantel, and a number of chemical or plant-based molluscicides were tested and used in control programmes [*McCullough et al.*, 1980; *Suter et al.*, 1986; *Sturrock*, 1995; *Izah and Angaye*, 2016]. Indeed, retrospective analyses have suggested a notable disease-curbing role of local snail abundance management using chemical-based molluscicides [*King et al.*, 2015], and the importance of snail control in past successes of disease elimination [*Sokolow et al.*, 2016]. Biological control of snail populations have also been proposed using natural predators [*Maharaj et al.*, 1992; *Kloos et al.*, 2004; *Michelson*, 2009; *Sokolow et al.*, 2015; *Swartz et al.*, 2015] or snail competitors [*Pointier et al.*, 1991]. In China, an alternative method to snail control was implemented through environmental modification to reduce habitat suitability, although with mixed results [*Xu et al.*, 2015a]. Moreover, the high costs of this method would hinder its application in sub-Saharan countries [*Tchuem Tchuenté et al.*, 2017]. The challenge of the control of the intermediate host resides in its high cost with respect to praziquantal distribution, the technical and operational challenges it poses for it to be successful, and in the impossibility of the complete elimination of snail populations from all transmission sites at the national level [*Hostettmann*, 1984]. Snail control, in particular molluscicides application, is therefore considered as a potential complementary control measure to MDA [*World Health Organization*, 2013a], in particularly at sites characterized by highly seasonal transmission in a limited number of water access points [*Hostettmann*, 1984]. The regained attention in snail control has fostered the WHO to issue a new manual directed at program managers in endemic countries [*World Health Organization*, 2017a]. However, the manual underlines the context-dependence of snail control effectiveness, and the importance of optimal use of molluscicide application that have been a major obstacle in historical control programmes, especially in seasonal climates [*King et al.*, 2015]. As voiced by *Shiff* [2017], only very general indications are found on intervention timing with respect to the season of the year (rainy vs. dry), habitat type (permanent vs. ephemeral, natural vs. man-made), and snail species responsible for transmission [*World Health Organization*, 2017a, p. 14]. The development of successful snail control strategies therefore requires a thorough understanding of the snail intermediate hosts' ecology, and a suitable framework for quantifying the effectiveness of control measures as a function of intervention timing, spatial coverage and other operational as well as logistical constraints.

Reducing exposure and contamination through WASH and health education Schistosomiasis' transmission cycle depends on the parasite's eggs reaching waterbodies (contamination), successful infection and multiplication inside the snail intermediate hosts, and subsequent cercarial penetration of human skin during water contacts (exposure). Access to clean water sources, sanitation infrastructure and hygiene (WASH) are linked to both exposure and contamination through direct and indirect pathways which have the potential to curb transmission (see *Grimes et al.* [2015] for a review). Access to safe water sources and sanitation have been associated with lower odds of both uro-genital and intestinal schistosomiasis in meta-analysis, geo-statistical models, and more recently in the framework of mapping protocols of the national control program of Ethiopia [*Soares Magalhães et al.*, 2011; *Grimes et al.*, 2014, 2016]. However, uncertainty remains on the strength and general validity of this associations in part due to the lack of structured randomized trials providing clear supportive evidence [*Grimes et al.*, 2014; *Campbell et al.*, 2017]. Indeed, the link between access to WASH, its actual use, and its effect of transmission are strongly dependent on local attitude and practices with respect to water-contact patterns and access to water and sanitation infrastructure [*Aagaard-Hansen et al.*, 2009]. In light of these considerations, WASH is seen as a crucial component of the long-term control of NTDs, calling for additional research initiatives [*Campbell et al.*, 2017], and being incorporated in the WHO strategy for 2015-2020 [*World Health Organization*, 2016]. Despite of these developments, still there is a lack of tools and methodologies for guiding WASH interventions at the national level that address the local specificity of the underlying physical and ecological factors conditioning transmission dynamics. Local conditions are dependent, among others, of the temporal and spatial heterogeneity in water contact patterns and their effect on parasite re-invasion and disease persistence. Following another model of intervention, the national control program of China has adopted an approach which includes the mechanization of agriculture to reduce the use of water buffaloes (a mammalian host of *S. japonicum*). This intervention limits human-water contacts during agricultural activities with significant results in reducing transmission alongside MDA and snail control [*Xu et al.*, 2015a]. Although the impact in China is encouraging, this type of interventions cannot yet be contemplated in SSA due to the financial costs for implementation, and specificities of the environmental and socio-economic conditions favouring transmission in the sub-continent [*Tchuem Tchuenté et al.*, 2017]. Health education to reduce transmission is also deemed important in sustaining the gains of MDA and other control methods [*Kloos*, 1995; *Asaolu and Ofoezie*, 2003], even if results in terms of the reduction of exposure, contamination, and schistosomiasis incidence vary in the context of different case-studies [*Uchoa et al.*, 2000; *Hu et al.*, 2005]. Recent results from educational entertainment using animated cartoons for inducing behavioral change suggest that innovative strategies for health education could become an essential component of national control programmes in the future [*Bieri et al.*, 2013;

Essé et al., 2017].

Moving towards surveillance-response systems A strong consensus exists on the need for a country- or even site-specific multifaceted approach to eliminate schistosomiasis [*Utzinger et al.*, 2011; *Tchuem Tchuenté et al.*, 2017]. However, there are no general guidelines or methodologies for the choice control measures and guidance on how to tailor them to the climatic, ecological, and socio-economic specificities of endemic countries in SSA. It can be appreciated throughout the previously described interventions that these are dependent to many factors impinging on their effectiveness and associated costs. In fact, most control and elimination programmes are centrally managed by the ministry of health in endemic countries, with the responsibility of defining strategies and making resource allocation decisions at national level [*Sokolow et al.*, 2015]. The elimination of schistosomiasis will require the development and deployment of dedicated surveillance-response systems (SRSs) [*Zhou et al.*, 2013; *Bergquist et al.*, 2015] to: i) appropriately measure the evolution of transmission at the national scale and individuate persistent hotspots and parasite re-introductions in cleared areas, and ii) rapidly deploy response packages tailored to the specific environmental, ecological and socio-economic conditions supporting transmission. This is deemed crucial not only for schistosomiasis, but also for the other water-borne diseases and NTDs affecting low income countries [*Tambo et al.*, 2014]. In the case of schistosomiasis, this entails taking into account the intrinsic spatially varying climatic, environmental, and socio-economic conditions underpinning transmission [*Brooker*, 2002; *Liang et al.*, 2007], as well as extrinsic factors such as the effect of human mobility and migration patterns in parasite dispersion and introduction [*Gurarie and Seto*, 2009; *Cao et al.*, 2015]. Moreover the lack of accurate rapid diagnostic tests for schistosomiasis means that national control programmes rely on annual parasitological sampling in a small number of villages as indicators of disease progression and control effectiveness at regional or national scales, with all the associated uncertainty these comport [*Stothard*, 2009; *Stothard et al.*, 2014, 2017]. Given the limited resource conditions in which the national health ministries in SSA operate, to reach elimination it will be paramount to develop tools for the design and optimization of spatially embedded SRSs accounting for the specificities of schistosomiasis transmission, and which incorporate all the available sources of epidemiological data [*Yang et al.*, 2012b]. Challenges to the implementation of such tools include the design of socio-ecological and epidemiological data collection protocols, both in space and time, and procedures for information extraction from the produced data for supporting the intervention decision-making process [*Bergquist et al.*, 2015]. Mathematical and statistical modelling is considered an important (and cost-effective) tool in the design and operation of SRSs for the integration of the numerous factors that affect transmission, as exemplified by the Chinese experience aiming at the elimination of *S. japonicum* in the country [*Feng et al.*, 2016]. Although most needed, an approach which allows for the unique features of *S. haematobium* and *S. mansoni* transmission does not exists nowadays in endemic countries in SSA.

1.2 Hydrology and the social-ecological drivers of transmission

1.2.1 The *social-ecological* nexus of schistosomiasis

A *leitmotif* that emerges from the previous overview of strategies and measures for schistosomiasis elimination is that the complexity of the parasite's life cycle depicted in Fig. 1.2 is both an opportunity for, and an obstacle to successful disease control, depending on whether its salient features are adequately taken into account [*Utzinger et al.*, 2011; *Tchuem Tchuenté et al.*, 2017]. As previously stated, disease transmission dynamics depend on environmental, ecological and and socio-economic factors, which determine its persistence in endemic areas [*Yang et al.*, 2015], and its spread into disease-free regions often due to anthropogenic alterations of the natural environment [*Southgate*, 1997], or climate change [*Zhou et al.*, 2008]. *Utzinger et al.* [2011] defined the combination of these factors as the *social-ecological system* in which schistosomiasis is embedded, echoing *Stokols* [1996]'s definition of a social-ecological framework for community health promotion which has been more widely advocated for all helminthic diseases [*Gazzinelli et al.*, 2012]. In reference to schistosomiasis, two main aspects were highlighted by *Utzinger et al.* [2011]: 1) the social and behavioural aspects of the contamination of waterbodies by human excreta and the subsequent exposure to cercariae, and 2) the ecology of the snail intermediate hosts with a strong emphasis on the impact of water resources development on disease risk. Indeed, the construction of dams for irrigation and water management purposes, often in response to water scarcity [*Barbier et al.*, 2009], has been associated with higher schistosomiasis risk (both uro-genital and intestinal) throughout SSA, in particular in the Sahel [*Steinmann et al.*, 2006]. This exacerbated risk is due on one hand to the expansion of suitable habitats for the snail intermediate hosts [*Boelee et al.*, 2009], and on the other to the potential changes the construction or reservoir have on local population densities and human water-contact patterns [*Cecchi*, 2007]. Indeed, the water surfaces created by reservoir construction and the irrigation systems that often accompany them provide ideal aquatic conditions for the snail intermediate hosts, and foster new economic activities in addition to agriculture, such as fishing, or cattle herding, which can be at the origin of important migration patterns in rural areas [*Cecchi*, 2007; *Ayantunde et al.*, 2017]. The impact of water resources development on schistosomiasis has been widely stressed in the literature [*Steinmann et al.*, 2006; *Utzinger et al.*, 2011; *Rollinson et al.*, 2013; *Van Bocxlaer et al.*, 2014], and embodies the interaction among ecological and socio-economic factors in disease transmission and persistence through the alterations induced by dam construction. On the other hand, the hydrological underpinning of the schistosome's transmission cycle, in particular regarding snail ecology, and human-water contacts, has received marginal attention in SSA even though it can be seen as a first order control and the water-dependent survival and circulation of miracidia and cercariae between the aquatic intermediate snails and human definitive hosts [*Colley et al.*, 2014]. Risk profiling studies have considered multiple environmental and socio-economic covariates using generalized linear mixed models (GLMMs) with spatial random effects (i.e. geo-statistical models), while hydrological characteristics that condition transmission are limited to yearly precipitation amounts and distances to waterbodies [*Raso et al.*, 2006; *Soares Magalhães et al.*, 2011; *Lai et al.*, 2015; *Walz et al.*, 2015a; *Yang et al.*, 2015]. A similar trend can be observed in the field of mathematical models of disease transmission applied to guiding and evaluating MDA strategies in SSA (elaborated in section 1.2.4 and 3.2). The links between hydrology and schistosomiasis could provide useful insight into disease transmission, but have not been explored consequently by research studies in SSA. Before expanding this argument through a review of the literature on the hydrological studies of schistosomiasis in general, and more particularly in SSA, a brief account on past ecological studies of the snail intermediate hosts, and of human-water contacts, is given below, placing due attention to their hydrological controls.

1.2.2 Historical studies of the ecology of the snail intermediate host

Two genera of snails of the *Planorbidae* family (pulmonate, freshwater snails) are responsible for the transmission of human schistosomiasis in SSA, *Bulinus* spp. for *S. haematobium* and *Biomphalaria* spp. for *S. mansoni* [*Madsen*, 2017]. Both snail genera are hermaphrodites and can reproduce through self-fertilization (selfing) [*Jarne et al.*, 1993]. Their population dynamics is characterized by strong seasonal fluctuation [*Cridland*, 1958; *Webbe*, 1960; *Dazo et al.*, 1966; *Hira*, 1975; *Klumpp and Chu*, 1977; *Rollinson*, 2011], in particular in temporary habitats, with population bursts and crashes [*Cridland*, 1957; *Poda et al.*, 1994, 1996]. Moreover, the growth, fecundity, and death rates of both genera depend strongly on temperature [*Shiff*, 1964a; *McCreesh and Booth*, 2014a]. Though both genera are capable of surviving periods of desiccation through aestivation, *Biomphalaria* spp. snails are much less adapted than most species of *Bulinus* to prolonged dry spells, which severely increase snail mortality [*Rubaba et al.*, 2016]. Laboratory estimates of the mean lifespan of *Biomphalaria pfeifferi* under aestivation reach about 40 days [*Badger and Oyerinde*, 1996], whereas species of *Bulinus* (in particular *B. truncatus*, *B. senegalensis*, and *B. forskalii*) have evolved to survive burrowed beneath temporary ponds and streams which have water only for a couple of months per year [*Brown*, 1980; *Woolhouse and Taylor*, 1990].

From a historical perspective, the scientific endeavor of the medical malacology of schistosomiasis was fostered by WHO strategic focus on snail control in the 1950s which prompted a thorough investigation and description of the biology and occurrence of the intermediate in SSA [*Mandahl-Barth*, 1957a,b] (for a broader historical overview see *Madsen* [2017]). A number of studies since then (some of which are cited above) have focused on the ecology of these species, in particular looking into the seasonal fluctuations of snail abundance in relation to environmental variables in different types of habitats in SSA. A more comprehensive overview of the ecology of both genera across habitats, climatic, and environmental conditions, as described above, is currently missing in the literature. In the absence of such an overview, this section proposes a metadata analysis of a review of ecological studies of *Bulinus* spp. or *Biomphalaria* spp. in SSA that have addressed snail population dynamics[1]. For each article, the geo-localization, sampling technique, type of habitat, identified species, habitat ephemerality (whether it periodically dries out or not), monitored environmental covariates, test for schistosomal infection, and duration of the study were recorded, differentiating them by prospected habitat when reported. A total of 78 articles were retained which contained timeseries data on the ecology of either *Bulinus* spp. or *Biomphalaria* spp., covering 268 distinct habitats in 143 unique locations in SSA and Northern Africa (details in Fig. 1.3). In fact, it is recognized these are a small fraction of the numerous historical studies on the taxonomic identification and large and small scale ecological range determination of both species across the continent, but only these were found to cover snail ecology from a population dynamics point of view (the most comprehensive references on the general ecology of snails of medical importance in SSA is the book by *Brown* [1980], and it's re-edition *Brown* [1994]; see [*Rollinson*, 2011] for a more recent review for *Biomphalaria* spp.). From the review of it appears that population dynamics studies have mainly been done in Easter and Western Africa, with very few works covering the humid tropical agro-ecozone of central Africa (Fig. 1.3a). The bulk of these studies were made in the 1980s and 1990s, with a constant decline in their numbers since the 2000s up to date (Fig. 1.3b). Similarly, the number of studied habitats per article (for which disaggregated data was reported) reached a peak in the 1980s and 1990s (median of 4 habitats per study) and decline steadily afterwards (Fig. 1.3a)[2]. Moreover the majority of the studies had less than 15 consecutive months of ecological data, thus barely covering a succession of 2 yearly seasonal cycles (Fig. 1.3b)[3]. The majority of investigations have focused on *Bulinus* spp., particularly on *B. globosus* and *B. truncatus*, with *Biomphalaria pfeifferi* being the most studied (and widespread) intermediate host of *S. mansoni*, (Fig. 1.3d). Natural habitats, both ephemeral and permanent, were well represented in the data (rivers, ponds, lakes), on the other hand among man-made habitats reservoirs were much less covered than irrigation canals and ditches (Fig. 1.3e). Moreover environmental covariates were reported

---

[1] The Library of the École Polytechnique Fédérale de Lausanne is gratefully acknowledged for support in retrieving the articles for this review. Although the review has been updated to cover works published in 2017, the results presented here do not include the contributions of the present Thesis which constitute the content of Chapter 4.

[2] The "exception confirming the rule" comes from the very recently published work by *Gouvras et al.* [2017], which surveyed 15 distinct sites during 4 years along the shores of Lake Victoria, although the data were reported as aggregates for all sampling sites in the paper thus counting only as one in Fig. 1.3c [*Gouvras et al.*, 2017]. In total, 33/78 articles reported aggregated snail counts from multiple habitats (sums or averages).

[3] Again, there are notable exceptions to the rule which are the study by *Noda et al.* [1995] which report 7 years of fortnightly counts in 7 distinct habitats, and *Kariuki et al.* [2013] reporting 12 years of data although aggregated annually.

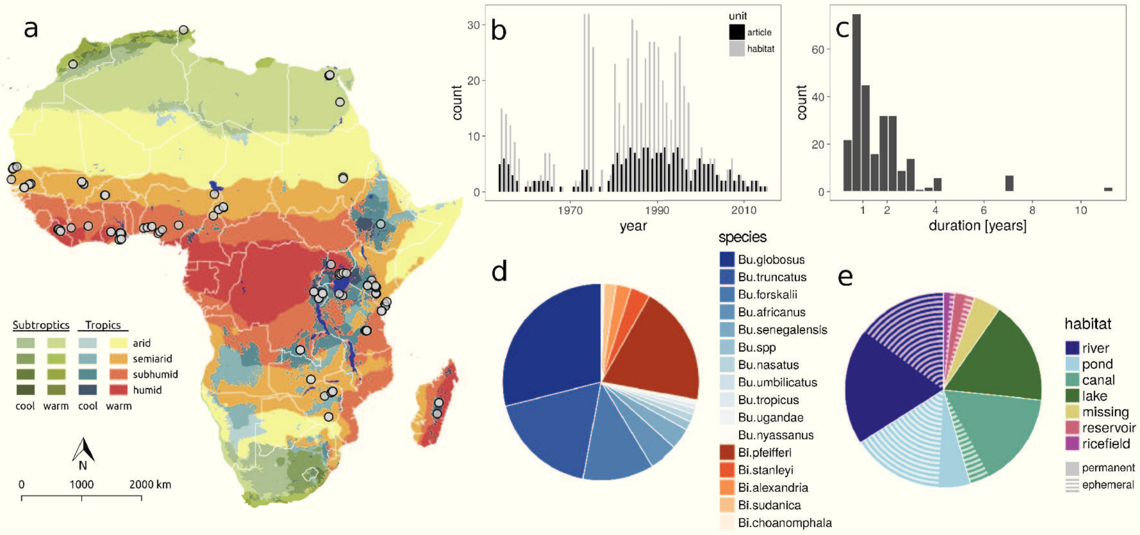

Figure 1.3 – Review of past ecological studies of the snail intermediate hosts of *S. haematobium* and *S. mansoni* in Africa. Data from 78 articles with timeseries data regarding snail population dynamics, covering 268 habitats in 143 distinct locations. a) Map of the historical study locations (gray points) shown against the 16 agro-ecological zones of Africa (data from *Sebastian* [2009], waterbodies in dark blue). b) Number of published studies (black) and unique habitats (grey) for which timeseries data is available in each year. c) Histogram of the duration of the studies (length of the timeseries) per habitat in each study (median: 1.25 yr, mean: 1.66 yr). d) Partitioning of the data by species of *Bulinus* spp. (blue) and *Biomphalaria* spp. (orange). e) Partitioning of the data by type of habitat and whether it dries out periodically (ephemeral habitat, white hatching) or not (full color).

for only 148/266 habitats. Although highlighting the interest that snail population dynamics has drawn in the past, the results of the review thus stress the miss-match between the scientific community's call for taking snail ecology into account in control and elimination strategies [*Utzinger et al.*, 2011; *Rollinson et al.*, 2013; *Tchuem Tchuenté et al.*, 2017], and the actual effort put into field ecological studies of their population dynamics which have steadily decreased in quantity (number of studies) and comprehensiveness (number of distinct habitats/study) in the past 30 years.

If observational studies constitute a foundation on which our understanding of the ecology of the snail intermediate hosts (and arguably of any other taxa) is built, the quantification of natural population dynamic rates is essential in disentangling the main drivers of seasonal and inter-annual abundance fluctuations [*Schneider*, 2009]. Moreover, a quantitative ecological appraisal allows for the coupling of mathematical models of snail and parasite transmission dynamics for the evaluation of transmission seasonality and the optimization of interventions, which is a crucial aspect of environmentally transmitted diseases [*Garchitorena et al.*, 2017] (cf. section 3.2). The work by Shiff in the early 1960s is a remarkable example of the investigation of key ecological rates both in a natural temporary pond in former Rhodesia (now Zimbabwe) and in laboratory experiments, showing the strong seasonal temperature-dependent variations of natural rates of increase in *Bulinus globosus* [*Shiff*, 1964a,b,c] [1]. Of particular ecological relevance is the relative importance of environmental forcings known to operate across natural and man-made habitats in SSA, with respect to density feedbacks which have been reported in laboratory or controlled field experiments [*Jobin and Michelson*, 1967; *Thomas and Benjamin*, 1974; *Mangal et al.*, 2010; *McCreesh et al.*, 2014]. It is worth noting, various assumptions have been made regarding density

---

[1] Examples of other noteworthy studies include *O'Keeffe*'s work in Kenya in the 1980s [*O'Keeffe*, 1985a,b], and *Odermatt*'s work in Tanzania in the 1990s [*Odermatt*, 1994].

feedbacks in mathematical models of disease transmission which account for the dynamics of snail populations, often without an ecological justification with respect to the studied species and habitat (see section 3.2 for a detailed account). Negative density feedbacks (*sensu Herrando-Pérez et al.* [2012]) have been at the heart of a debate on whether they must be seen as a key ecological process for the demography of the intermediate hosts of schistosomes in natural habitats, sparked by the seminal attempt to model the population dynamics of *Schistosoma* intermediate hosts by *Jobin and Michelson* based on *Shiff*'s field and laboratory data [*Shiff*, 1964c; *Jobin and Michelson*, 1967]. A limited number of ecological modelling studies have followed in these early investigations' footsteps in SSA, most of which relating to *Woolhouse*'s work on *Bulinus globosus* and *Biomphalaria pfeifferi* in permanent streams in the Zimbabwe's highveld in the late 1980s [*Woolhouse*, 1988a; *Woolhouse and Chandiwana*, 1989, 1990a,c; *Woolhouse*, 1992b]. These studies first described the large seasonal fluctuations in snail abundance, and the effect of variations in discharge on the hydrological dispersal and spatial structuring of snail populations [*Woolhouse and Chandiwana*, 1989, 1990c; *Woolhouse*, 1992b]. *Woolhouse and Chandiwana* [1990a] then moved on to use mathematical models to highlight the role of water temperature in driving the population dynamics of *Bulinus globosus*, and further considered the effect of rainfall in the form of an instantaneous reduction of snail abundance and recruitment due to snail dispersal by advection. Density feedbacks were not included in the model as the population dynamics of *B. globosus* were labelled as "density vague" (*sensu Strong* [1986]) suggesting that, under natural conditions, snail abundance is controlled by adverse environmental conditions preventing crowding levels at which negative density feedbacks are appreciable, although no statistical or model-comparison tests were made to verify this assumption [*Woolhouse and Chandiwana*, 1990a]. More recently, a comprehensive modelling analysis expanding *Woolhouse and Chandiwana*'s framework was performed by *Remais et al.* [2007] to investigated the role of environmental covariates on the recruitment and mortality of *Oncomelania hupensis* (the amphibious intermediate host of *S. japonicum*) in irrigation canals in China. Temperature and water level fluctuations were found to be the main drivers of snail population dynamics (as opposed to density feedbacks), and the best-fitting model adequately reproduced seasonal abundance patterns [*Remais et al.*, 2007]. Another path has been followed by *McCreesh and Booth* [2014a,b] focusing on the effect of temperature on the ecology of *Biomphalaria* spp. and cercariogenesis using an individual-based approach parameterised with laboratory data on snail fecundity, development, and mortality as a function of temperature, which also included negative density feedbacks. Having been designed to answer pressing questions on the effect of changing temperature on schistosomiasis from the biological perspective [*McCreesh and Booth*, 2013; *Kalinda et al.*, 2017b,a], this approach is less suitable for disentangling ecological drivers of snail ecology in natural habitats from time series data of population counts, in particular for ephemeral habitats. The latest modelling work of snail ecology in SSA (published after the study reported in Chapter 4 of this Thesis) addressed the seasonal variations of *Bulinus* spp. abundance in temporary ponds in Kenya by incorporating a model for the variation of available habitat/resources which modulates growth and death rates, discarding temperature effects and density feedbacks [*Gurarie et al.*, 2017]. The explicit modelling of available resources as a function of precipitation is a noteworthy development with respect to previous studies, however it remains unclear to which extent this approach is extensible across climatic conditions at the national scale, and whether it is adaptable to other habitat types and hydrological conditions in which resource availability may not be the main driver of snail ecology [*Woolhouse and Chandiwana*, 1990a].

The paucity of quantitative analysis on the population dynamics of these keystone species of the *Schistosoma* lifecycle [*Esch et al.*, 2001; *Stothard et al.*, 2017] magnifies the sparsity and growing scarcity of field studies in SSA highlighted by the literature review (Fig. 1.3). This trend is in sharp contrast with the numerous, and necessary, species distribution studies on the ecological range of *Bulinus* spp. and

Biomphalaria spp. in the continent (cf. section 1.2.4), probably owing to the wider availability of historical species occurrence data with respect to ecological timeseries [*Stensgaard et al.*, 2013]. Moreover, the hydrological drivers of snail ecology have not been systematically been accounted for in past studies, and by no means in a manner allowing for formal model identification and comparison across different types of habitats and climates, save for the study of *Oncomelania hupensis* in China although only one habitat was considered in that case [*Remais et al.*, 2007]. As a matter of fact, hydrological insight has also been lacking from species distribution models despite the well known importance of discharge fluctuations on snail presence and abundance in streams and rivers (this argument is further expanded section 1.2.4) [*Brown et al.*, 1994]. The conclusions that may be drawn from this section echo *Shiff* [2017]'s very recent call to gain insight from research performed between the 1950s and 1990s which focused on fieldwork and emphasized transmission control, thus bringing to the fore the need for renewed interest in the ecology of the snail intermediate hosts of schistosomiasis, and more particularly on its manifest but often disregarded hydrological drivers.

1.2.3 Socio-economic determinants, human-water contacts, and mobility

Socio-economic and behavioural factors are intrinsically linked to the poverty-related and reinforcing nature of schistosomiasis due to their association to the risks of exposure through human-water contacts, and contamination by egg-baring human excreta reaching waterbodies (section 1.1.2) [*King*, 2010]. The accurate quantification of contamination rates by excreta poses obvious methodological challenges since they depend not only on the degree of open defecation and subsequent transport due to rainfall or treading by humans or animals [*Chandiwana*, 1986; *Vercruysse et al.*, 2001], but also on unavoidable micro-urination [*Grimes et al.*, 2015], and hygienic bathing practices [*Sow et al.*, 2008]. On the other hand, regarding exposure there has been considerable effort put into characterizing human-water contact patterns as a function of demographic and socio-economic covariates in numerous settings [eg. *Klumpp and Webbe*, 1987; *Chandiwana*, 1987; *Bundy et al.*, 1990], and their modulation by access to water infrastructure [eg. *Krauth et al.*, 2015; *Kosinski et al.*, 2016]. The joint analysis of water contact patterns and individual infection status has lead to the identification of occupational and recreational activities associated to higher odds of schistosomiasis in some settings, such as recreational bathing and regular crossing of streams [*Dalton*, 1976; *Lima e Costa et al.*, 1991; *Kloos et al.*, 1998], even though a clear link between water contact patterns and infection intensity cannot be systematically drawn at the individual level in all transmission settings [*Scott et al.*, 2003; *Sow et al.*, 2011]. Moreover, the spatial patterns of water contacts have been associated to the micro-epidemiology of schistosomiasis, in particular with the reduction of infection risk with distance to the closest waterbody or irrigation canal, although the strength of the association depends markedly on the setting and the spatial configuration of households and waterbodies, and is further blurred by the mixing of heterogeneous human-water contacts among a finite number of water contact points [*Chandiwana and Woolhouse*, 1991; *Kloos et al.*, 1997; *Clennon et al.*, 2006; *Seto et al.*, 2013; *Meurs et al.*, 2013]. Of possibly greater importance for schistosomiasis control and elimination is the role of heterogeneities in individual water-contact characteristics and spatial occurrence in the strength of transmission at the community level. Noteworthy is the fact that mathematical models which allow for spatial and individual heterogeneity suggest that differences in exposure/contamination within a population tend to favour parasite invasion and disease persistence with respect to an equivalent but homogeneous one [*Barbour*, 1978; *Ofoezie et al.*, 1998; *Woolhouse et al.*, 1998]. In a similar fashion, the concentration of contacts in a limited set of water sources exacerbates community-wide transmission, thus suggesting the potential efficacy of targeted vs. blanket interventions for chemotherapy, snail control, and WASH in the disease elimination phase [*Mari et al.*, 2017a], although with its associated caveats [*Woolhouse et al.*, 1997]. Based upon this, hydrology comes to view as a crucial factor underlying schistosomiasis transmission as it constitutes the first order control on the spatial and temporal availability of surface water, prior to its eventual anthropogenic modification, thus constraining the degree of human-water contact clustering with possible implications for elimination efforts, especially in strongly seasonal climates.

Human mobility is also an important factor due to its role in the persistence and expansion of schistosomiasis in and from endemic areas [*Bella et al.*, 1980; *Appleton et al.*, 1996; *Cetron et al.*, 1996; *Kloos et al.*, 2010]. Indeed, population genetic studies have revealed a strong genetic diversity of schistosomes within and among individuals, and lack of geographical population sub-structuring across spatial scales (village to regional), thus suggesting a strong mixing of parasites due to human mobility and migration patterns [*Davies et al.*, 1999; *Sire et al.*, 2001; *Standley et al.*, 2010]. The spread of intestinal schistosomiasis in Northern Senegal following the construction of the Diama dam in the 1980s serves a striking example of the role of human mobility in the onset of parasite invasion of a river network, here due to multiple parasite introduction by migrants coming to work in the newly established agricultural areas and, the successful invasion of previously snail-free areas by *B. pfeifferi* [*van den Broeck et al.*, 2015]. Interestingly, the issues of human mobility and migration raised by the construction of these dams links back to climate and hydrology since they were built as a preemptive measure to avoid the repetition of the losses caused by the strong long-lasting West-African drought in the 1970s [*Handschumacher et al.*, 1992; *Le Barbé et al.*, 2002]. Tools to account for the effect of human mobility, and possibly its interdependence with water resources development, on disease transmission risk therefore comes to light as an additional crucial component of future schistosomiasis elimination strategies in endemic countries.

1.2.4 A review of hydrology in schistosomiasis transmission studies

As stressed throughout the previous sections, hydrology intervenes at multiple levels in the transmission cycle of schistosomiasis. However, a limited number of studies have investigated it comprehensively, as opposed to other water-borne diseases [eg. *Rinaldo et al.*, 2017]. Indeed, river networks provide ecological corridors that are continuously subject to modification by climatic, geomorphologic and ecohydrologic drivers which support both freshwater and terrestrial biodiversity [*Fagan*, 2002; *Bertuzzo et al.*, 2007; *Muneepeerakul et al.*, 2008; *Rodriguez-Iturbe et al.*, 2009; *D'Odorico et al.*, 2010; *Konar et al.*, 2013], including the pathogens affecting the human communities living along them [*Lara et al.*, 2011; *Rinaldo et al.*, 2017]. Hydrology underlies water-borne disease outbreaks through its direct impact on the pathogenic agent's survival and ecology (or of primary and intermediate hosts) and through their (mostly) downstream transport, prompting infections to spread within and across human communities, as in the case of cholera [*Gatto et al.*, 2012; *Mari et al.*, 2012a; *Rinaldo et al.*, 2017]. Apart from schistosomiasis, hydrology also plays a key role in the endemicity of other parasitic diseases by determining habitat presence and suitability for the parasite's vectors, such as for malaria [*Bomblies et al.*, 2008; *Bomblies and Eltahir*, 2009] and onchocerciasis (river blindness) [*Servat et al.*, 1990]. As previously presented, in the case of schistosomiasis hydrology is a key driver of the occurrence and ecology of the snail intermediate hosts, but can also be seen as a first order control on the spatial and temporal configuration of the waterbodies in which human-water contacts can occur, and indirectly linked to water resources development.

Widening the scope from SSA to a global perspective suggests that hydrology has been considered in studies covering different aspects of the transmission cycle. A selection of works focusing on the link between hydrology and schistosomiasis is given in Table 1.1. Four main topics emerge: i) the effect of hydrology on snail population dynamics, ii) snail spatial distribution as a function of some form of hydrological process or index, iii) hydrological transport of cercariae and dispersal of snails at various spatial and temporal scales, and iv) a direct quantification of the effect of hydrology on disease transmission. As a preliminary remark it is interesting to note that the majority of the identified studies (19/32) have focused on the *Oncomelania hupensis-S. japonicum* system in mainland China, and only 12 studies have investigated the link between hydrology and schistosomiasis in SSA. Works on the population dynamics of the intermediate snail host have been largely covered in section 1.2.2. Additional approaches other than mathematical modelling include regression analysis [*Seto et al.*, 2008] and time series modelling [*Wu et al.*, 2015].

Snail occurrence Works on the spatial occurrence of the snail intermediate hosts in direct link with hydrological processes and characteristics have been surprisingly rare. A noteworthy example of the potential of hydrological insight in understanding and potentially predicting the snail's ecological range is the work by *Appleton* [1975] linking the occurrence of *Bi. pfeifferi* to distinct geological formation associated to different hydrological regimes over a 100km stretch of the river network crossing South Africa and Swaziland. The results of this work show how snail occurrence is linked to permanent lentic (still) habitats allowed by weathered bedrock, as opposed to seasonal flows in river stretches with sandy substrates. At a large spatial scale, *Zhou et al.* [2002] explored the link between exceptional flooding in the Yangtze River following the 1998 El Niño event [*Shankman et al.*, 2006], and the expansion of suitable habitats for *O. hupensis* through the classification of flooded areas from satellite imagery. It is important to note that only studies in which hydrological processes are explicitly taken into account are reported in Table 1.1, thus not setting aside the numerous works on the characterization of snail ecological ranges using gridded environmental covariates that have been done in SSA [*Stensgaard et al.*, 2006, 2013; *Moser et al.*, 2014; *Pedersen et al.*, 2014; *Manyangadze et al.*, 2016, eg.]. Indeed, most of these analysis used aggregated values of annual rainfall or soil moisture and distances to waterbodies as covariates in species distribution models, always together with temperature and vegetation indices, but without leveraging hydrological concepts nor insights despite the fact both *Biomphalaria* spp. and *Bulinus* spp. are aquatic snails, as opposed to *Oncomelania hupensis* which is amphibious (see *Walz et al.* [2015a] for a review of the use of remote sensing products in schistosomiasis risk mapping, highlighting the under-use of products providing insight into the prediction of suitable snail habitats and other aspects of the transmission cycle). Following a multifaceted approach, *Krauth et al.* [2016] performed a multivariable correspondence analysis linking environmental to the abundance of *B. pfeifferi* and *Bulinus* spp. in rivers and ponds in Northern Côte d'Ivoire, concomitantly monitoring water contacts at the collection points and parasitological data in neighboring villages. Their study highlighted differences in habitat preferences between snail species, with a descriptive rather than predictive aim, but the approach is a compelling example of study design aiming at providing a comprehensive picture of the disease transmission process including snail ecology, water contact patterns, and parasitology.

Transport and dispersal Transport studies have focused either on advection of cercariae using caged mouse experiments [*Radke et al.*, 1961; *Lowe et al.*, 2005], or of the snail intermediate hosts with mark-recapture approaches over short distances (≤ 1km)[*Marti and Tanner*, 1988; *Woolhouse*, 1988b; *Akullian et al.*, 2012]. At larger spacial scales snail dispersal has been investigated using landscape connectivity measures as formalized in *Remais et al.* [2010] which take into account the drainage network and landuse, most of the time in conjunction with population genetic studies correlating estimated migration among sub-populations and various distance measures [*Chlyeh et al.*, 2002; *Clennon et al.*, 2007; *Hauswald et al.*, 2011; *Head et al.*, 2016]. Among the latter, *Clennon et al.* [2007] bears the strongest hydrological mark by using gridded estimates of soil moisture to determine *B. nasatus* field-validated migration pathways and connectivity between waterbodies across their study area in Kenya (≈5km).

Transmission to humans Of great interest are the appraisals of hydrology directly with respect to disease transmission in terms of infection intensity and prevalence in humans. Two types of studies have addressed this issue, first the ones hereafter termed "correlation" studies in which hydrologic factors were compared to a measure of disease transmission severity to humans (prevalence in the most cases). Among these, *Appleton* [1975] reported lagged increased transmission of intestinal schistosomiasis in Botswana after intense flooding events. *Li et al.* [2016] associated lower water levels in the Yangtze river following the construction of the three Gorges dam to higher *S. japonicum* prevalence despite the reduction in snail densities [*Wu et al.*, 2015], possibly due to increases in human-water contacts, though it is thought that on the long run the dams will accelerate rather than delay progress towards elimination [*Zhou et al.*, 2016]. Using clustering analysis of schistosomiasis cases around known transmission sites, *Clennon et al.* [2006] and subsequently *Mutuku et al.* [2011] have highlighted the importance of floods and droughts in shaping the abundance and spatial configuration of waterbodies in seasonal climates and the ensuing impacts on disease micro-epidemiology. A distinct suite of studies addressed the role of hydrology on the transmission cycle of schistosomiasis through mechanistic mathematical models, in terms of what *Liang et al.* denote as the environmentally-modulated "internal potential" of disease transmission [*Liang et al.*, 2007]. With a strong emphasis on process realism, these models expanded the classical mean-worm burden modelling framework (cf. section 3.2) focusing on within-village transmission by accounting for the effect of water flow on cercarial infectivity and miracidial hatching success in irrigation canals [*Liang et al.*, 2002, 2007; *Remais et al.*, 2008, 2009; *Remais*, 2010], seasonally varying human-water contacts among in multiple sites (through questionnaires) [*Liang et al.*, 2002, 2007; *Remais et al.*, 2008, 2009; *Remais*, 2010; *Xiang et al.*, 2013], and rainfall-driven snail population dynamics [*Remais et al.*, 2009; *Remais*, 2010]. Notably, one such study coupled a hydrologic module within the disease dynamics model to better account for variations in discharge on larval infectivity (no infectivity if discharge bellow certain threshold), even if its effect was not incorporated into the population dynamics model of the intermediate hosts [*Remais et al.*, 2009]. Using a similar but simplified framework, the role of hydrologic transport of larvae [*Xu et al.*, 2006; *Gurarie and Seto*, 2009], and snails [*Ciddio et al.*, 2016], has also been broached as a potentially important factor for disease persistence and re-invasion. These studies however did not take into account climate-dependent hydrological fluctuations on the effect on transmission. An different approach to account for spatial variation in hydrological factors on disease risk has been propose by *Walz et al.* which developed habitat suitability indices based on topological traits derived from high resolution imagery. These include water velocity and sink depth using terrain slope, and stream order using automated drainage network extraction algorithms [*Walz et al.*, 2015b]. While this approach bridges a gap with respect to previous geo-statistical modelling approaches which had considered a limited scope of remote sensing products with minimal hydrological insight, mirroring the state of affairs in snail species distribution modelling (again, see *Walz et al.* [2015a] for a review), it falls short in accounting for the dynamical nature of disease transmission, and only partially captured observed spatial variations in disease prevalence [*Walz et al.*, 2015b]. As previously noted, for all study types involving hydrology, there has been a larger effort put into accounting for environmental (and hydrological) drivers on transmission using mathematical models for *S. japonicum* in China with respect to *S. mansoni* and *S. haematobium* in SSA.

Table 1.1 – Review of selected studies on the role of hydrology on the transmission of schistosomiasis. The spatial scale refers to the length of the longest axis of the study area.

	Country	Scale	Methods	Habitat	Organism	Factor
i. Snail population dynamics						

^{a,b} articles published after Chapters 4 and 3 of this Thesis in which the chapters are cited

Continued on next page

Table 1.1 – Hydrology review - continued

	Country	Scale	Methods	Habitat	Organism	Factor
Woolhouse and Chandiwana [1990a,c]; *Woolhouse* [1992b]	Zimbabwe	500 m	Mathematical modelling	River	*Bu. globosus;* *Bi. pfeifferi*	Rainfall
Liang et al. [2002]	China	3 villages	Mathematical modelling	Irrigation canals	*O. hupensis*	Rainfall
Remais et al. [2007]	China	1 village; 50 m	Mathematical modelling	Irrigation canals	*O. hupensis*	Rainfall
Seto et al. [2008]	China	100km	Regression analysis	Rivers; flooded areas	*O. hupensis*	Water level; Rainfall
Wu et al. [2015]	China	50km	Time series modelling	Rice fields; flooded areas	*O. hupensis*	Water level
Gurarie et al. [2017][a]	Kenya	5km	Mathematical modelling	Ponds	*Bulinus* spp.	Rainfall
ii. Snail spatial occurrence						
Appleton [1975]	South Africa	100km	Ecological sampling	Rivers	*Bi. pfeifferi*	Geology; discharge
Zhou et al. [2002]	China	100km	Image classification	Flooded areas	*O. hupensis*	Flooding
Levitz et al. [2013]	Uganda	2km	Ecological sampling	Lake	*Bi. pfeifferi*	Wave action
Krauth et al. [2016]	Côte d'Ivoire	150km	Correspondence analysis	Rivers; ponds; reservoirs	*Bi. pfeifferi*; *Bulinus* spp.	Water velocity
iii. Transport and dispersal						
Radke et al. [1961]	Puerto-Rico	1km	Mouse caging	River	Cercariae	Advection
Marti and Tanner [1988]	Tanzania	100 m	Mark-recapture study	River	*Bu. globosus*	Advection
Woolhouse [1988b]	Zimbabwe	100 m	Mark-recapture study	river	*Bu. globosus*	Advection
Maszle et al. [1998]	China	4km	Hydrological transport modelling	Irrigation canal	-	Advection
Chlyeh et al. [2002]	Morocco	1km	Population genetics	Irrigation canal	*Bu. truncatus*	Advection
Lowe et al. [2005]	China	500 m	Mouse caging	Irrigation canal	Cercariae	Advection
Clennon et al. [2007]	Kenya	5km	Dispersal modelling	Ponds	*Bu. nasatus*	Drainage network
Hauswald et al. [2011]	China	50km	Population genetics; Distance correlations	Rivers	*O. hupensis*	Drainage network
Remais et al. [2010]	China	50km	Dispersal modelling	Rivers; flooded areas	*O. hupensis*	Drainage network
Akullian et al. [2012]	China	100 m	Mark-recapture study; dispersal modelling	Rivers	*O. hupensis*;cercariae	Advection
Head et al. [2016]	China	50km	Population genetics; dispersal modelling	Rivers; flooded areas	*O. hupensis*	Drainage network
iv. Transmission to humans						
Liang et al. [2002, 2007]	China	3 villages	Mathematical modelling	Irrigation canals	*O. hupensis*;cercariae; miracidia; humans	Rainfall
Clennon et al. [2006]; *Mutuku et al.* [2011]	Kenya	5km	Spatial statistics	Ponds	Humans	Drainage network; drought; flooding
Xu et al. [2006]	China	227 villages; 50km	Mathematical modelling	Rice fields	Cercariae; miracidia	Drainage network
Appleton et al. [2008]	Botswana	200km	Regression analysis	Rivers	Humans	Discharge
Remais et al. [2008]	China	2 villages	Mathematical and hydrological modelling	Irrigation canals	*O. hupensis*; cercariae; miracidia; humans	Rainfall; Discharge

[a,b] articles published after Chapters 4 and 3 of this Thesis in which the chapters are cited

Continued on next page

Table 1.1 – Hydrology review - continued

	Country	Scale	Methods	Habitat	Organism	Factor
Gurarie and Seto [2009]	Kenya	15 villages	Mathematical modelling	Rivers	Cercariae; miracidia	Drainage network
Remais et al. [2009]; *Remais* [2010]	China	1 village	Mathematical modelling	Irrigation canals	*O. hupensis*; cercariae; miracidia; humans	Rainfall; Discharge
Xiang et al. [2013]	China	50km	Mathematical modelling	Rice fields; flooded areas	Humans	Water level
Walz et al. [2015b]	Côte d'Ivoire; Burkina Faso	200km	Habitat suitability index	Rivers; ponds; lakes; reservoirs; rice fields	*Bi. pfeifferi; Bu. truncatus*	Water velocity; stream order; sinks
Ciddio et al. [2016][b]	Senegal	90 villages; 50km	Mathematical modelling	rivers; lakes	Snails; miracidia, cercariae	Drainage network
Li et al. [2016]	China	200km	Regression analysis	Rice fields; flooded areas	Humans	Water level

[a,b] articles published after Chapters 4 and 3 of this Thesis in which the chapters are cited

The picture that emerges from this selected review underlines the gap that exists in the accounting of hydrology in schistosomiasis transmission in SSA in terms of snail ecology and human infection dynamics. Indeed, since *Woolhouse and Chandiwana*'s seminal work in the late 1980s, the hydrological drivers of snail demography had not been investigated again up until very recently [*Gurarie et al.*, 2017, published after the content in Chapter 4 in this Thesis], and it is still lacking a comparison across habitat types and climatic conditions. Moreover, although there has been a notable rise in snail species distribution modelling studies, hydrological insight has not been leveraged beyond the use of aggregated environmental covariates [*Walz et al.*, 2015a]. Finally, most mathematical models that account for hydrology have been developed for and applied to the transmission of *S. japonicum* in China and its specificities in terms of intermediate host ecology (amphibious vs. aquatic snails), and mostly man-made landscape underpinning exposure and contamination (irrigation canals and rice fields). Attention is drawn to the fact that the outlook by the works by *Liang et al.* [2002], subsequently expanded by *Remais et al.* [2008], tends more to stress hydraulics (open channel flow in irrigation canals) rather than catchment hydrology. Along parallel lines equally important contributions have been made in substantiating the potential importance of hydrological transport of larvae and snails in disease persistence using mathematical models, as exemplified by *Gurarie and Seto* [2009]'s pioneering work on a network of 15 interconnected villages. However, the same mathematical framework can be used to investigate the effect of human mobility and parasite re-importation, as already proposed in *Gurarie and Seto* [2009] (cf. section 3.2), which will become increasingly important in the elimination phase of the disease [*Tchuem Tchuenté et al.*, 2017].

Within the perspective of transmission control for the elimination of schistosomiasis in SSA, a synthesis of the hydrological drivers of transmission together with its spatial embedding could provide important insight for the design and development of adequate surveillance-response systems and strategies. To this end it is argued as necessary to account for the hydrologic controls of i) snail spatial occurrence, ii) snail population dynamics, and iii) human exposure/contamination processes, within a framework allowing for the exploration of spatial connectivity. Building on the past 50 years of research developments [*Basáñez et al.*, 2012], mathematical modelling could very well keep providing insights into this parasite's complex lifecycle, this time from an ecohydrological perspective.

1.3 Thesis aim and outline

Moving from morbidity control to the elimination of schistosomiasis will require a renewed focus on transmission dynamics, with a particular emphasis on its social-ecological underpinning [*Utzinger et al.*, 2011; *Shiff*, 2017]. Schistosomiasis is a water-borne disease in that hydrology operates as a first order control on the disease cycle, chiefly on the spatial and temporal ecology of the snail intermediate hosts, and secondly as a physical determinant of the occurrence of waterbodies supporting exposure/contamination patterns. Yet, only few studies have taken hydrology into account in SSA, in particular with respect to the large-scale determination and prediction of transmission dynamics in strongly seasonal climates.

This Thesis therefore aims at developing an ecohydrological approach to schistosomiasis through the use of a modelling framework permitting a predictive appraisal of the spatial hydrological, ecological, and socio-economic determinants of disease transmission.

The content of this Thesis is organized as follows:

- Chapter 2 introduces the setting, Burkina Faso, and the three sites along its longitudinal climatic gradient in which the fieldwork for this Thesis was undertaken.
- Chapter 3 proposes a national-scale spatially explicit mathematical modelling framework building on previous modelling works, allowing for spatially varying snail habitat suitability, population-dependent contamination/exposure rates, and parasite spread through human mobility. An analytic expression of the dynamical stability of spatial disease transmission was derived for the disease-free equilibrium. This result was applied to the theoretical investigation the effect of human mobility on one hand, and water resources development modifications on snail occurrence on the other, on schistosomiasis in Burkina Faso. This work serves as a starting point in the spatially explicitly modelling of schistosomiasis at large spatial scales, and stressed the shortcomings in existing approaches, first and foremost the absence of a representation of the ecology of the snail intermediate hosts.
- Chapter 4 constitutes a first step in addressing this gap, and reports on field and modelling studies of the ecology of *Bulinus* spp. and *Biomphalaria pfeifferi* across natural and man-made habitats in the experimental sites. Weekly snail counts and high-resolution micro-meteorological data were combined into models of snail demography, which enabled the identification of density-feedbacks and hydrological drivers of snail ecology. The approach provides a promising tool for the spatial prediction of snail abundance fluctuations, and highlights the importance of habitat hydrological conditions (permanent vs. ephemeral) in driving the snail's population dynamics.
- Chapter 5 expands the investigation of the link between hydrology and schistosomiasis by developing a methodology for the national scale classification and prediction of hydrological ephemerality. The methodology is applied to determine the ephemerality of the country's whole river network, which is then incorporated into refined snail species distribution modelling and national-scale epidemiological analysis. Intestinal and uro-genital schistosomiasis are shown to have opposite associations with ephemerality, owing to snail occurrence for the former, and possibly to human-water contact patterns for the latter.
- Chapter 6 introduces a methodology for the extension of the ecological models developed in Chapter 4, together with the ephemerality predictions and ensuing species distribution models of Chapter 5 for the modelling of snail population dynamics at the national scale. Remote sensing data are shown to be suitable surrogates for ground measurements of temperature and precipitation in

reproducing the spatio-temporal patterns of snail abundance across habitat types. Although these results require further analysis and open questions for model refinement, they pave the way for incorporating snail ecology in the modelling framework introduced in Chapter 3.

- Finally Chapter, 7 elaborates on the integration of Chapters 6 and 3 into a unified modelling framework, and its future developments in light of preliminary results on water contact surveys and participatory mapping activities carried out in the three experimental sites. The second part of Chapter 7 draws a general discussion on the methods and results covered by this Thesis, advancing the relevance of a comprehensive ecohydrological approach to schistosomiasis, and the frame of action it provides for transmission control.

This Thesis is closed with a conclusion section summarizing results and recommendations for future research.

2 The field setting: Burkina Faso

2.1 Introduction

The development of mathematical models of disease transmission applied to policy-relevant questions relies on their connection with epidemiological data for the iterative process of model refinement and validation [*Finger*, 2017], ideally within a model-guided hypothesis formulation-verification framework based on field-collected ecological data [*Restif et al.*, 2012]. The fieldwork undertaken for this thesis was done in Burkina Faso, in the framework of a large scientific collaboration project (projet 3E: Eau, Energie et Environnment) between Switzerland and the *Institut International d'Ingénierie de l'Eau et de l'Environnement (2iE)* in Ougadaougou, Burkina Faso, and financed by the *Swiss Agency for Development and Cooperation*. As detailed below, schistosomiasis is a public health issue in the country, and the strong latitudinal gradient of climatic conditions make it a relevant and interesting case-study for the investigation of the ecohydrological drivers of schistosomiasis.

2.2 Geography and climate

Burkina Faso is a land-locked country in West Africa inhabited by 18 million people that is situated at the interface between the Sudanian and Sahelian climates [*Sivakumar and Faustin*, 1987; *PANA Burkina Faso*, 2007]. The country is characterized by a strong South-to-North gradient of increasing temperature and decreasing precipitation, and a marked seasonality with most of the precipitation occurring in the months of June-September [*PANA Burkina Faso*, 2007]. Annual precipitation ranges from 1,100 mm in the Sudanian South-West to less than 500 mm in the Sahel to the North (Fig. 2.1). The climate is characterized by a single rainy season, which spans from South to North with varying durations and arrival dates. Although rainfall may possibly decrease in the future, the change in timing and the decrease in predictability of the precipitation distribution across the season will be more noticeable [*Ibrahim*, 2012]. Years of late onset and early cessation of the rainfall season, resulting in a reduction in the growing period, are particularly problematic for agricultural production. An increase of temperature is also likely in the Sahel [*Sarr*, 2012]. Climate change could mean increased variability and a decrease of runoff up to 40% in the Volta River basin [*Sood et al.*, 2013]. The country spans a 600 m elevation range, making it relatively flat. Its territory is subdivided between the Volta, Niger and Comoé river basins (Fig. 2.1). The precipitation gradient creates a strong variation in vegetation characterized as three distinct types: Sahelian transition zone, Sudanian endemic center, and Guineo-Congolia/Sudanian transition zone. This floral gradient ranges from dense, humid forest to sparse scrub vegetation on crusted soils. Corresponding to the

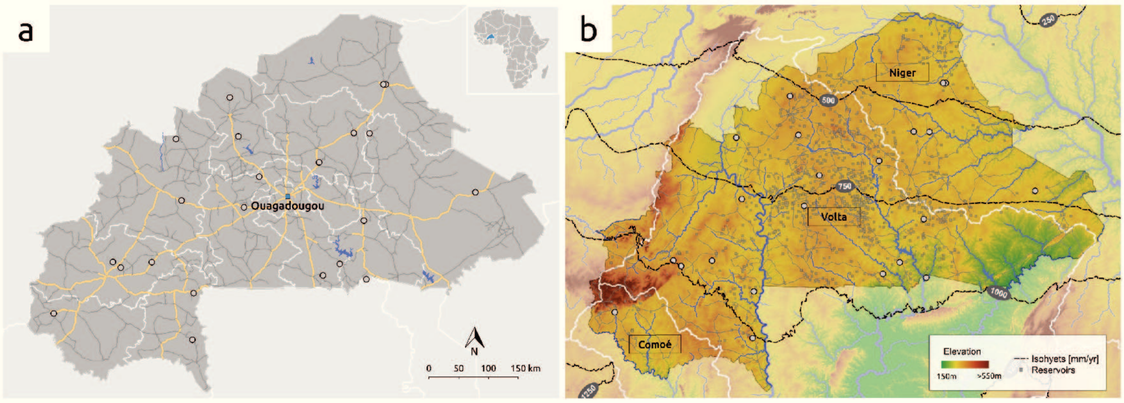

Figure 2.1 – Geography, climate and hydrography of Burkina Faso. a) Situation map and road network (national roads: yellow, regional roads: dark gray) of Burkina Faso, the capital Ouagadougou, and the sentinel sites of the Ministry of Health's schistosomiasis national control programme where regular (quasi-annual) parasitological surveys are done (white lines indicate first level administrative divisions). b) Climate, hydrology, and water resources development shown in terms of annual precipitation isohyets (isolines of equal precipitation amount, data from the 1960-1990 Worldclim dataset [*Hijmans et al.*, 2005]) by the three major watersheds of the country (white outlines), the river network (HydroSHEDS product at ≈ 500m resolution [*Lehner et al.*, 2008]), and man-made reservoirs (≈ 1500 dams, data from [*Cecchi*, 2007]).

gradients of natural flora and precipitation is a gradient of human livelihood activities and production ranging from rainfed cereal production and livestock herding in the North to irrigated market gardening, rice production, and fishing in humid parts. The high dependence on rainfed agriculture, particularly of cereal crops (millet, corn, and sorghum), places the population in a vulnerable position. Improved water management, conservation-agriculture, crop diversification and small irrigation schemes are seen as the most promising tools to adapt to the changing water resource [*Barbier et al.*, 2009; *Zorom et al.*, 2013]. To that end, dams ranging from small reservoirs for irrigation to large-scale dams for drinking water, hydropower, and industrial agriculture are being built since the droughts of the 1970s (Fig. 2.1b) [*Cecchi*, 2007].

2.3 Schistosomiasis in Burkina Faso

2.3.1 Prevalence and progress towards elimination

Schistosomiasis has been known in the country since the first demographic surveys in the 1950s [*Poda et al.*, 2004a] and has yet to be eliminated despite nation-wide control measures intitiated from 2004 to 2008 by the Schistosomiasis Control Initiative (SCI) [*Garba et al.*, 2006; *Touré et al.*, 2008; *Gray et al.*, 2010]. Both uro-genital and intestinal forms of the disease are present with very different historical geographical coverages (Fig. 2.2). Schistosomiasis has actively been monitored by the *Programme National de Lutte Contre la Schistosomiase (PNLS)*, the Burkinabe Health ministry's unit dedicated to schistosomiasis in 11 regions of Burkina Faso (Fig. 2.1a) [*Koukounari et al.*, 2011]. Ten years of MDA campaigns following the WHO guidelines have successfully controlled morbidity, lowering prevalence to about 5% at the national level from about 40% in the early 2000s [*Ouedraogo et al.*, 2016]. In the face of these achievements and in line with the London declaration and the WHA65.21 resolution, Burkina Faso has set the goal of eliminating the disease from the country, using MDA as its primary control measure.

Despite achievements in morbidity control, the road remains long to elimination, with more than 1

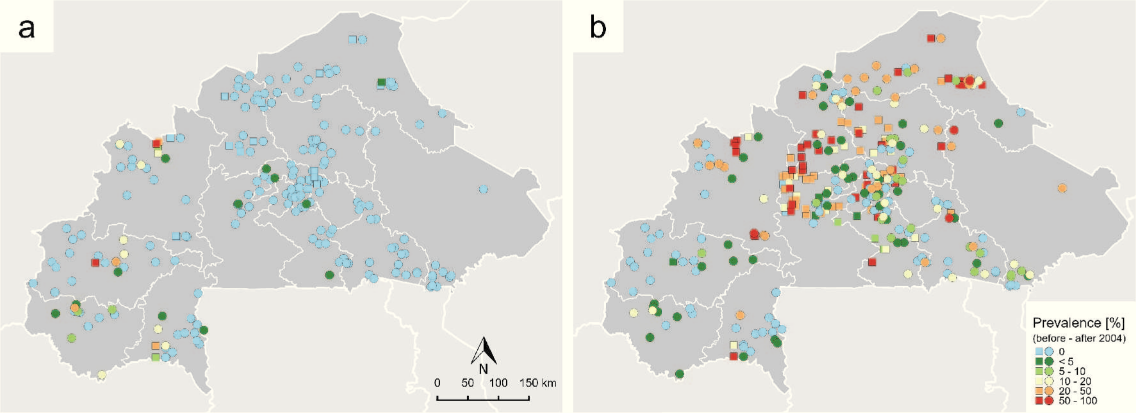

Figure 2.2 – Historical data on schistosomiasis prevalence in Burkina Faso. Data from the Global Neglected Tropical Diseases Database (http://www.gntd.org), and the Institut National de Recherche en Sciences de la Santé (IRSS, Ouagadougou BF). a) Intestinal schistosomiasis has been geographically constrained to the South-Western and Southern parts of the country, with recent expansion to the Sourou valley after the construction of the Léry dam at the North-Western border with Mali [*Poda et al.*, 2003]. b) Uro-genital schistosomiasis has been present throughout the country, with highest historical values found in the Northern Sahelian parts of the country.

million children estimated to still be infected with either of the two parasite species in the early 2010s [*Lai et al.*, 2015]. In fact, the recent evolution of prevalence has been jigsawed in some regions, sign of potentially ongoing re-infection, and persistent hotspots remain in specific areas such as in the Sahel for uro-genital schistosomiasis, and the Haut-Bassins for the intestinal form (Fig. 2.3). Moreover the state of infection in adults, which are not covered by MDA in the majority of regions, is mostly unknown (*Zida et al.* [2016] reported an overall prevalence of 8.5% in women older than 15 from two study areas in the Sahel and Centre, although strong heterogeneities were observed) and could fuel re-infection should MDA be interrupted. Accounting for the specificities in the socio-ecological drivers of disease transmission and considering alternative control strategies are therefore deemed necessary for attaining transmission interruption at the national scale [*Ouedraogo et al.*, 2016].

2.3.2 Social-ecological factors of disease transmission

The snail intermediate host present in Burkina Faso include five species of *Bulinus* for *S. haematobium*, and only *Biomphalaria pfeifferi* for *S. mansoni* [*Poda*, 1996; *Poda et al.*, 2004a; *Zongo et al.*, 2009]. Their spatial distribution is constrained by the strong South-to-North climatic gradient of the transition from Sudanian to Sahelian regimes [*Poda*, 1996]. Furthermore, the country-wide sampling undergone by *Poda* [1996] revealed the importance habitat type (natural or man-made), in addition to of climatic zones, on snail presence/absence [*Poda*, 1996]. Indeed, *B. pfeifferi* was seldom found beyond the 12th parallel and absent beyond the 14th [*Poda et al.*, 1994], correlating well with the observed historical range of intestinal schistosomiasis in the country [*Poda*, 1996; *Poda et al.*, 2004a]. Snail abundance in Burkina Faso, in particular, exhibits pronounced fluctuations determined by the precipitation patterns typical of the Sudano-Sahelian climate. These oscillations are clearly illustrated by the study conducted by *Poda et al.* for two *Bulinus* species transmitting uro-genital schistosomiasis, namely *B. truncatus* and *B. senegalensis* in a village East of Ouagadougou [*Poda et al.*, 1994, 1996]. The former is adapted to live in permanent relatively deep waters like reservoirs, the latter in temporary ponds, very common during the rainy season in Burkina Faso. Population abundance of both species proved to be strongly correlated to prolonged precipitation events conditioning the ephemeral habitat and to temperature oscillations in the

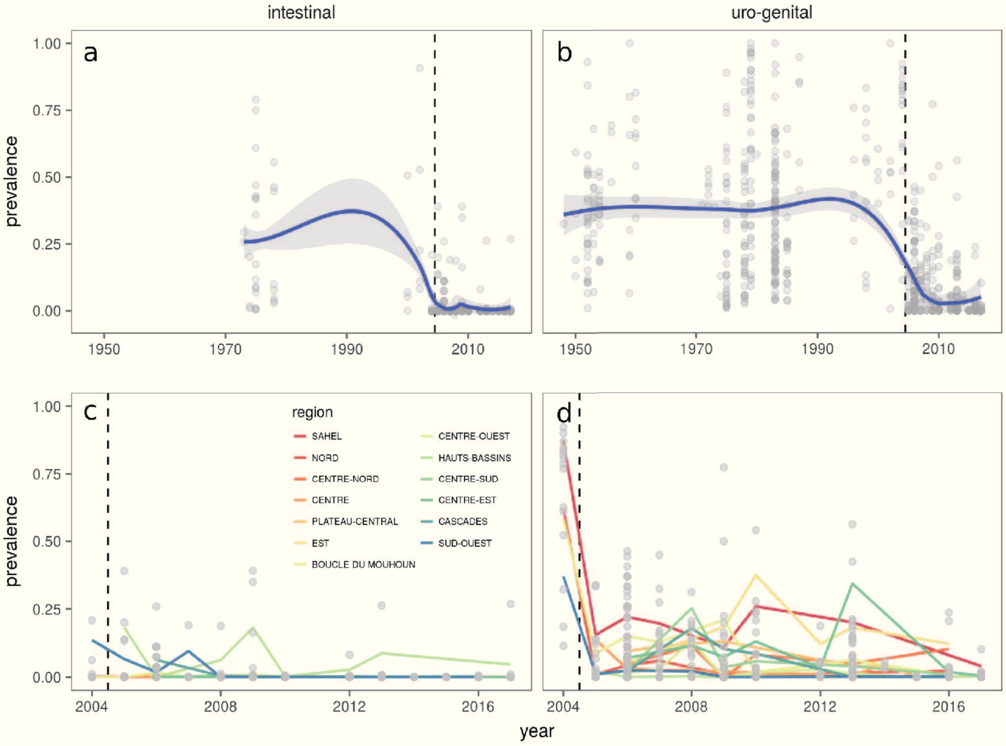

Figure 2.3 – Historical evolution of schistosomiasis prevalence in Burkina Faso. a,b) Historical prevalence data by village (points) and nation-wide trend (line and 95% CI obtained by local weighted least-squares smoothing of village prevalence against time) for intestinal and uro-genital schistosomiasis respectively. The dotted vertical line indicates the start of MDA campaigns in the country in 2004. c,d) Recent evolution of schistosomiasis as monitored in the 22 sentinel sites of the national schistosomiasis elimination programme (points), averaged by region (lines).

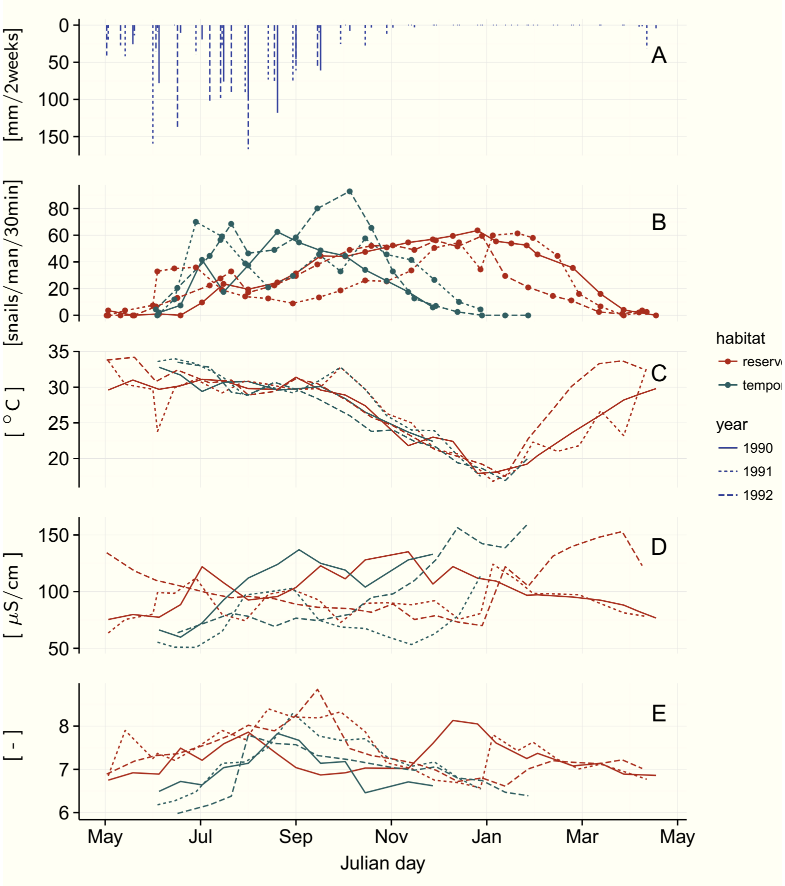

Figure 2.4 – Historical *Bulinus* spp. abundance and covariate data in Burkina Faso. Data were collected by Poda and collaborators during three years (1990, 1991 and 1992, indicated by full, dotted and dashed lines) [*Poda et al.*, 1996]. A) biweekly precipitation, B) *Bulinus* spp. abundance, C) water temperature, D) conductivity, and E) pH. Colours indicate data collected in a small reservoir (brown) and a temporary pond (turquoise), both located in the same area (inset). Note that the precipitation data are the same for both habitats. The interruption of the temporary pond time-series indicate the drying of the pond. Data from *Poda* [1996].

water reservoir (Fig. 2.4). A comprehensive litterature review suggests that these are the only multi-year ecological studies which have addressed the population dynamics of snail hosts in Burkina Faso, and both highlighted notable seasonal abundance fluctuations of *Bulinus* spp., and no such studies have been made for *Biomphalaria pfeifferi* in the country. From the exposure/contamination angle, exacerbating factors associated to schistosomiasis in the country relate to limited, although improving access to WASH, include incomplete access to safe drinking water (only 43% of the rural population has access to at least basic water as defined in *World Health Organization and UNICEF* [2017]), and very limited access to sanitation (48% of the rural population resorts to open defecation), and hygiene facilities (12% of the population have access to basic hygiene) [*World Health Organization and UNICEF*, 2017; *WASHwatch*, 2017].

Finally, as observed in many other schistosomiasis-affected countries, agricultural development and the implementation of large-scale irrigation schemes have induced anthropogenic perturbations of the underlying natural matrix affecting schistosomiasis distribution [*Poda et al.*, 2003; *Boelee and Madsen*, 2006; *Steinmann et al.*, 2006]. This fact is well illustrated by the construction of the Sourou valley dam (the

Léry dam) at the North-Western border with Mali in the late 1980s, which resulted in the range expansion of *Biomphalaria pfeifferi* along the Mouhoun river from the Bobo-Dioulasso region to the North [*Poda et al.*, 2003, 2004b]. Intestinal schistosomiasis followed shortly, possibly brought in by migrants coming from the endemic South of the country to work in the rice paddies, yielding an increase in prevalence from virtually zero to more than 60% among school-aged children in villages located around the Léry dam in about 10 years [*Poda et al.*, 2004b]. With a 5-fold increase in the number of small reservoirs in Burkina Faso in the past 60 years, and the perspective of future construction of large dams, these observations highlight the need to explicitly address the impact of water resources development on schistosomiasis transmission [*Boelee and Madsen*, 2006; *Cecchi*, 2007]. Echoing *Utzinger et al.* [2011], *Rollinson et al.* [2013], and *Tchuem Tchuenté et al.* [2017], an integrated approach to schistosomiasis control and elimination is therefore need to address the inherent contradiction between water resources development and livelihood preservation [*Südmeier-Rieux et al.*, 2006; *Abdelhak et al.*, 2012], the reshaping of local environmental, social and economic conditions and the persistence of schistosomiasis in Burkina Faso and the other endemic countries in SSA [*Steinmann et al.*, 2006].

2.4 Field work and data collection[1]

2.4.1 Site selection

Three villages were retained along the transition from the Sudanian to Sahelian climatic zones (Fig. 2.6) (see also [*Sivakumar and Faustin*, 1987]). The choice of these experimental sites accounted for the spatially varying climatic conditions in Burkina Faso, the habitat preferences of the snail intermediate hosts (Table 4.1), previously studied habitats (Table 2.1), and logistic constraints (site accessibility, travel time, total available budget). The sampling sites were selected to cover the range of habitats harboring snail hosts (see Table 4.1), including an irrigation canal, a temporary pond, one ephemeral stream and one permanent stream. Panamasso (11°23′23.4"N, 4°12′02.5"W) is a village adjacent to a small perennial stream in the South-Western part of the country. The Lioulgou site (12°00′38.8"N, 0°21′48.2"W) lies in the central part of the country in a lowland subject to flooding (with the creation of temporary ponds) during the wet season and mostly dry to very dry during the rest of the year (Fig. 2.6). Finally, Tougou (13°41′06.0"N, 2°14′22.2"W) is located in the Northern Sahelian climate next to a reservoir that feeds a network of permanent irrigation canals active year round. In total, four sampling locations were retained in the three experimental sites, one on the perennial stream in Panamasso, two in Lioulgou in the ephemeral stream draining the low-land and in a temporary pond, and one in Tougou within an irrigation canal.

The three villages are emblematic of the socio-economic, ecological, and hydrological factors which support schistosomiasis transmission, presenting adequate natural and man-made aquatic habitats for the snail intermediate hosts in which various livelihood-related activities take place (Fig. 2.7). Both Lioulgou and Panamasso are sentinel sites of the national schistosomiasis elimination programme and parasitological surveys are done on a quasi-annual basis [*Ouedraogo et al.*, 2016], highlighting ongoing transmission of *S. haematobium* and *S. mansoni* respectively (Fig. 2.8). On the other hand Tougou is not part of the ministry's monitoring programme, however the site was retained as to represent the Sahelian climatic zone because it has been an experimental site for hydrology research by the *Institut International d'Ingénieurie de l'Eau et de l'Environnement* (2iE, cf. section 2.1) for the past 10 years, and provided an opportunity for resource and data mutualisaition. Schistosomiasis is present in all three sites, the

---

[1] The content of this section is a detailed expansion of the fieldsite presentation in *Perez-Saez et al.* [2016]

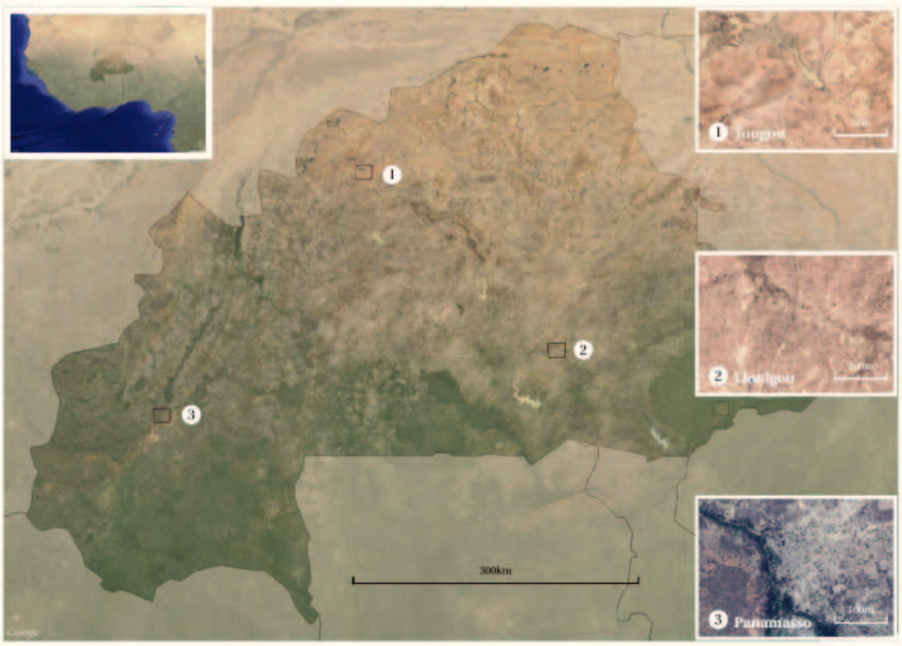

Figure 2.5 – Site selected for fieldwork. The satellite images (Google maps, May 2013, note the different scales) of the sites reveal their physical differences: *Tougou* Sahelian climate with almost no vegetation in the dry season period, organized around a small reservoir. *Lioulgou* Village depends on an ephemeral hydrological network the feeds the rice paddies to the North of the village. *Panamasso* Perennial backwater flows from South to Norht to the West of the village with abundant vegetation. Map data: Google, DigitalGlobe

intestinal form in Panamasso and the uro-genital form in Lioulgou and Tougou (Fig. 2.8). Despite 13 years of MDA, schistosomiasis is still well present in Panamasso in 2017 (27% of school-aged children infected), and presents a jigsawed pattern in Lioulgou which has seen its prevalence decline in 2016 (3%, from 56% in 2013). Parasitological sampling was done in Tougou in 2016 by the national health research institute (*Institut National de Recherche en Sciences de la Santé*, IRSS), showing low prevalence ($\approx 5\%$) in line with national trends (Fig. 2.3, [*Ouedraogo et al.*, 2016]).

2.4.2 Environmental monitoring

A total of 15 micro-meteorological Sensorscope[1] stations with three sensors each was deployed in the three sites, starting May 2014 in Tougou, June 2014 in Panamasso and July 2014 in Lioulgou (Fig. 2.6). The stations were equipped with sensors of key hydro-meteorological parameters including air temperature, water level, conductivity and temperature, and precipitation [*Mande et al.*, 2015] (Tables 2.1). Measurements were taken every 30 seconds and data were sent to a central server using the mobile phone network. Data were accessible online through a dedicated web portal (http://climaps.com). Additional temperature data loggers were placed in the temporary pond in Lioulgou because it was not covered by the wireless stations (Table 2.1).

---

[1] http://www.sensorscope.ch/

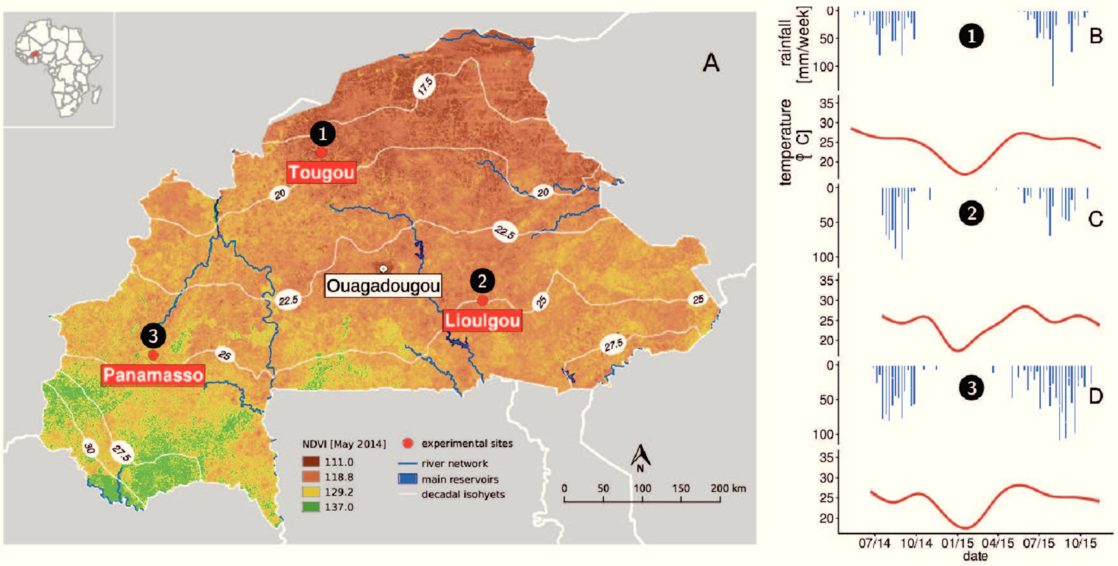

Figure 2.6 – A: Map of the South-North climatic gradient in Burkina Faso, highlihted by values of normalized difference vegetation index (NDVI) and average decadal precipitation isolines. The field sites chosen for the present study are marked with red dots. The state capital, Ouagadougou, is also shown. B-D: The right panels show measured cumulative weekly precipitation (blue bars) and average daily air temperatures (red lines) in the experimental sites of Tougou (B), Lioulgou (C) and Panamasso (D). Note the different starting measurement dates in each experimental site.

Figure 2.7 – Behaviours and socio-economic activities presenting a risk for local populations of exposure to schistosome cercariae in natural and man-made aquatic environments. *Left* Water contacts in an irrigation canal in Tougou. *Middle* Children bathing in a temporary pond in Lioulgou. *Right* Women washing dished in the stream crossing Panamasso.

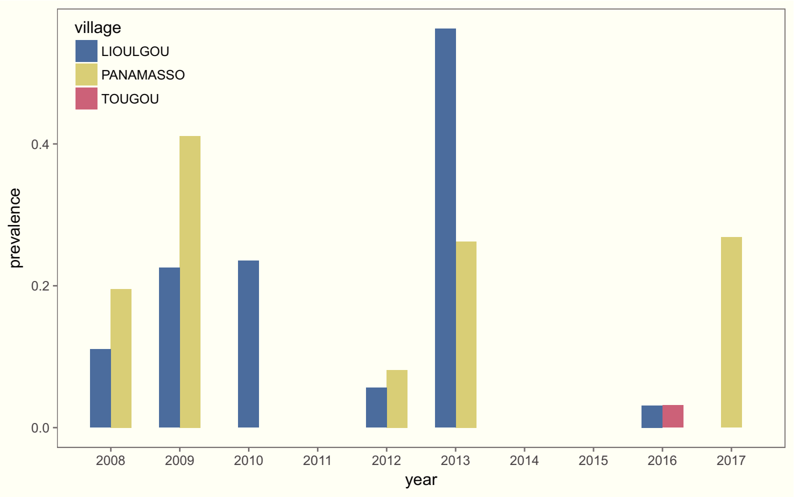

Figure 2.8 – Recent evolution of schistosomiasis prevalence in school-aged children in the experimental sites. Note that prevalence refers to the uro-genital form for Lioulgou and Tougou, and for the intestinal form for Panamasso. Data prior to 2016 are from *Ouedraogo et al.* [2016], and from the Institut National de Recherche en Sciences de la Santé (unpublished data provided by Dr. Zongo, IRSS) after 2016.

(a) Tougou reservoir (b) Tougou - open (c) Panamasso - weir in stream

(d) Tougou - irrigation canal (e) Lioulgou - field (f) Lioulgou - rice paddy

Figure 2.9 – Pictures of SensorScope stations installed in the three sites. *Tougou* 8 stations with 24 sensors including standard microclimatic (air,wind,temperature,precipitation), two soil moisture profiles of three sensors, water temperature, depth and conductivity in reservoir and irrigation canal. *Lioulgou* 3 stations with 8 sensors including standard microclimatic, soil sensor in field and in rice paddy and water temperature, depth and conductivity in rice paddy. *Panamasso* 3 stations with 9 sensors including standard microclimatic, soil moisture and water temperature, depth and conductivity in stream where a weir was built to estimate discharge.

Table 2.1 – Environmental covariates at sampling locations

		Water [a,b]			Air [c]	Precipitation [d]	
Village	Site	Temperature	Conductivity	Depth	Temperature	Sum [e]	Events [f]
Tougou	Canal	Yes	Yes	Yes	Yes	Yes	Yes
	Reservoir	Yes	Yes	Yes	Yes	Yes	Yes
Lioulgou	Stream	Yes[g]	-	-	Yes	Yes	Yes
	Pond	Yes	-	-	Yes	Yes	Yes
Panamasso	Stream	Yes	Yes	Yes	Yes	Yes	Yes

---

[a] Measurements made in Tougou and Panamasso using Decagon Devices CDT sensor, Decagon Devices, http://www.decagon.com/en/hydrology/water-level-temperature-electrical-conductivity/ctd-10-sensor-electrical-conductivity-temperature-depth/

[b] Measurements made in Lioulgou using TidBiT v2 Temp, Onset HOBO Data Loggers, Onset Computer Corporation, http://www.onsetcomp.com/products/data-loggers/utbi-001

[c] Measurements made using Decagon Devices VP-3 sensor, Decagon Devices, http://www.decagon.com/en/canopy/canopy-environment/vp-4-humidity-barometricpressure-temperature-and-vapor-pressure-sensor/

[d] Measurements made using Davis Rain Collector, Davis Instuments, http://www.davisnet.com/weather/products/weather_product.asp?pnum=07852

[e] Cumulative sum over 2 weeks and 1 month time windows preceding snail sampling dates

[f] A rainfall event is considered to be a day with total precipitation larger than 20 mm

[g] Only in 2015

2.5 Conclusion

Schistosomiasis elimination is envisaged in Burkina Faso, however pockets of transmission remain after more than 10 years of MDA. The strong climatic gradient in the country provides a representative setting for investigating disease transmission from an ecohydrological perspective. Three sites were retained along this climatic gradient, covering a range of suitable habitat types for the snail intermediate hosts. The automated environmental monitoring stations installed in each site open the door for the investigation of the hydrological drivers of the ecology of the snail intermediate hosts.

3 Development of a national-scale spatially explicit modelling framework

Spatial connectivity, either through human mobility or hydrological transport, can play a significant role in the persistence and (re-)invasion of water-borne diseases, and is an important aspect of disease ecohydrology. Its effect had been studied in previous theoretical works of schistosomiasis transmission applied to networks of villages at small scales (study areas <50 km), highlighting its potential importance in disease transmission. This Chapter lays the basis for national-scale spatially explicit modelling of disease transmission by extending previous approaches, in particular with respect to the derivation of stability conditions of parasite spread, to the modelling of human mobility, and to the incorporation of snail habitat suitability maps from commonly used species distribution models. An interesting feature of the framework is that it sheds new light on the interplay between spatial connectivity and water resources development on schistosomiasis transmission, here accounted for through modifications of the snail suitability maps, showing how the more populated (thus strongly connected within this framework) the location in which a dam is built, the stronger its effect will be on nation-wide transmission. Importantly, the end of the Chapter underlines the shortcomings of the model, drawing a roadmap for their development into useful decision support tools for surveillance-response systems[2].

3.1 Introduction

Patterns of water-borne disease are unique in their spatial complexity which arise from pathogen reproduction, transport and transmission through waterways and human mobility networks, and for the corresponding challenges to morbidity and transmission control. Indeed both micro- and macro-parasitic water-borne diseases are conditioned by spatially varying natural (environmental or climatic [*Pascual et al.*, 2000, 2002; *Finger et al.*, 2014]) and anthropogenic factors (water resources, [*Altizer et al.*, 2006; *McMichael et al.*, 2006; *Eisenberg et al.*, 2007] habitat availability and suitability [*Dejong et al.*, 2001], pathogen dispersal by river networks [*Bertuzzo et al.*, 2008, 2010; *Mari et al.*, 2012b; *Rinaldo et al.*, 2012], and human mobility [*Gurarie and Seto*, 2009; *Bertuzzo et al.*, 2011; *Chao et al.*, 2011; *Tuite et al.*, 2011; *Mari et al.*, 2012a]. This Chapter focuses on the transmission cycle of schistosomiasis in Burkina Faso. Dynamical models of schistosomiasis [*Macdonald*, 1965; *May and Anderson*, 1979], and their spatial extension to connected environments [*Gurarie and Seto*, 2009], provide the opportunity to show the

---

[2] The content of this Chapter has been adapted from *Perez-Saez et al.* [2015]: Perez-Saez, J., Mari, L., Bertuzzo, E., Casagrandi, R., Sokolow, S.H., De Leo, G.A., Mande, T., Ceperley, N., Froehlich, J.M., Sou, M., Karambiri, H., Yacouba, H., Maiga, A., Gatto, M., and Rinaldo A., 2015. A theoretical analysis of the geography of schistosomiasis in Burkina Faso highlights the roles of human mobility and water resources development in disease transmission. *PLoS Neglected Tropical Diseases*, 9(10), p.e0004127. https://doi.org/10.1371/journal.pntd.0004127

applicability of a general mathematical framework for analysing the disease invasion conditions and the resulting spatial patterns of human schistosomiasis which could inform control and elimination programs. With this goal, the spread of schistosomiasis and persistence in the context of Burkina Faso is addressed with an emphasis on the roles of human mobility and water resources development.

Human mobility is known to play a major role in the persistence and the expansion of the disease within and from endemic areas in Africa [*Bella et al.*, 1980; *Appleton et al.*, 1996; *Cetron et al.*, 1996; *Bruun and Aagaard-Hansen*, 2008] and Brazil [*Kloos et al.*, 2010]. Indeed people may become infected while performing their livelihood tasks away from home and importing the disease back in their home village. Furthermore infected migrants coming form endemic regions can introduce schistosomiasis in disease-free villages. This type of medium-to-long range contamination is indeed compatible with the successive focal transmission of the disease at the local level suggested by recent landscape genetics studies [*Criscione et al.*, 2010]. The socio-ecological and epidemiological specificities of the transmission of intestinal schistosomiasis in sub-Saharan Africa and Brazil may explain the different roles played by human mobility, a topic to be elucidated by future research. Given its importance for transmission in the African context, data regarding mobility patterns, possibly directly via cellular phone displacements, will be necessary to produce reliable predictive tools for disease elimination both in terms of re-appearance and of prioritization of directed interventions in Burkina Faso.

In line with such priorities, a novel mathematical exploration of an established model [*Gurarie and Seto*, 2009] is proposed and an application of the geography of the disease to the context of Burkina Faso. Special emphasis is placed on linking disease spread and human mobility and water resource development as a proof of concept for the usefulness of the implementation of these kind of tools for macroparasitic water-borne diseases like schistosomiasis.

3.2 A perspective on mathematical models of schistosomiasis

Mathematical modelling is deemed to be an important tool in reaching the resolutions fixed by the London Declaration and the World Health Assembly for the elimination of schistosomiasis (cf. section 1.1) by providing key insights into the dynamics of disease transmission, mechanisms underpinning its stability, and ways to brake it through control measures [*Basáñez et al.*, 2012; *Hollingsworth et al.*, 2015]. Mathematical modelling -expressing disease transmission in the form of dynamical systems using mechanistic approaches- is here distinguished from statistical models -linking indicators of diseases transmission (prevalence, mean infection intensity) to covariates through regression or one of its more sophisticated extensions, often including space using Bayesian geo-statistical approaches (see *Lai et al.* [2015] for a notable example). A perspective on mathematical models of schistosomiasis is given here, with a brief overview of the classical mean-worm-burden approach to model schistosomiasis transmission, and the state-of-the art in terms of spatially-explicit modelling of disease spread. The extention of the latter constitute the main focus of this Chapter.

3.2.1 Macdonald's model and its limitations

Mathematical modelling of schistosomiasis dates back to *Macdonald* [1965]'s seminal paper on disease transmission, marking a first step in discriminating between the transmission of micro-parasites, well captured by the Susceptible-Infected-Recovered (SIR) model [*Kermack and McKendrick*, 1932], and macro-parasites like schistosomes for which the worm burden, rather than binary infection status, is the variable of interest. The derivation of the mean-worm-burden approach developed by Macdonald, its subsequent developments, and its application to the investigation of alternative control strategies have been comprehensively reviewed elsewhere [*Anderson and May*, 1985; *Anderson*, 1987; *Woolhouse*, 1991, 1992a; *Barbour*, 1996; *Basáñez et al.*, 2012; *Anderson et al.*, 2016].

In *Macdonald* [1965], work the dynamics of the macro-parasitic disease is expressed in terms of the mean worm burden in a homogeneous human population, w, the prevalence of infection in the snail intermediate hosts, y, and the densities of cercariae and miracidia, c and m. Briefly, the model with the eplicit incorporation of larval stages reads:

$$\frac{dw}{dt} = a\theta c - \gamma w \tag{3.1a}$$

$$\frac{dy}{dt} = bm(1-y) - \nu y \tag{3.1b}$$

$$\frac{dc}{dt} = \pi_C N y - \mu_C c \tag{3.1c}$$

$$\frac{dm}{dt} = \pi_M \theta' H \frac{w}{2} - \mu_M m. \tag{3.1d}$$

The rate of change in the mean worm burden is given by the intensity of cercarial infection expressed as a probability of infection upon contact a times the exposure to contaminated water θ and cercarial density. Worms are assumed to die at rate γ. Density of cercariae is dynamically determined by the *per-capita* cercarial output from infect snails π_C and the number of infected snails Ny at time t, and limited by cercarial mortality μ_C. The rate of change in the prevalence of infected snail is given by the probability of infection of a susceptible snail $b(1-y)$ times miracidial density m and limited by snail mortality ν. Finally miracidial density is conditioned by the rate of miracidial output from humans π_M, the contamination rate θ' and the number of pairs of adult schistosomes, given by half of the mean worm burden times the number of human hosts H.

The main simplifying assumptions underlying this model are constant and well-mixed human and snail populations, and homogeneous human-snail contacts. In the face of the transmission cycle of schistosomiasis these assumptions appear as excessively unrealistic and greatly limit the usability of the proposed model for effective breaking of the transmission cycle. Significant improvements have been made in control-designed models taking into account the dynamics of the snail host populations [*Feng et al.*, 2002]. However the specificities of snail ecology have often been overlook. Density feedbacks have been either accounted for [for example in *Feng et al.*, 2004; *Ciddio et al.*, 2015; *Sokolow et al.*, 2015] or ignored [for example in *Liang et al.*, 2007; *Chiyaka and Garira*, 2009; *Gurarie et al.*, 2016] in transmission models of all three main species of schistosomes that considered snail population dynamics. Moreover, seasonal variation in vital rates which are the norm in SSA (see section 1.2.2) have typically been ignored, except occsaionally from a theoretical perspective by [*Ciddio et al.*, 2015; *Mari et al.*, 2017a]. Interestingly, a recent study has considered seasonally varying human-to-snail and snail-to-human force of infections rates for *S. japonicum* transmission, while considering a constant snail population, concluding that seasonality reduces transmission stability (in terms of the basic reproductive number) [*Gao et al.*, 2017]. Rare examples of proper weather-driven snail model formulation and identification within an applied mean-worm-burden framework are in *Remais et al.* [2009] and *Remais* [2010]. Expanding the one-population mean-worm-burden framework, age-stratified models of schistosomiasis have taken into account age-dependent water contacts and susceptibility and been used to predict requirements in terms of MDA coverage in school children and adults to reach the elimination of *S. mansoni*, arguing that current WHO guidelines should be enough for disease elimination if treatment is prolonged for 15 years

[*Anderson et al.*, 2015]. However, snail dynamics where ignored in this study under the premise that due their short lifespan with respect to schistosomes, they would not have an impact on the overall behavior of the transmission model [*Chan et al.*, 1995; *Anderson et al.*, 2015]. On the other hand, a modification of *Macdonald*'s approach allowing for different degrees of infection intensity categories (denoted "stratified worm burden" model in *Gurarie et al.* [2010]) which did allow for (non-seasonal) snail dynamics came to a different conclusion regarding *S. haematobium* suggesting the need for alternative control measures (snail control, WASH) in addition to MDA to reach elimination. These differences have been further highlighted by comparing the two modelling approaches on the same datasets, thus highlighted the importance of model assumptions on predictions regarding policy-relevant questions [*Truscott et al.*, 2017].

A common limitation of these models, also encountered in other human-parasites systems [*Vazquez-Prokopec et al.*, 2016], is that the intrinsic individual (e.g. water contact patterns, susceptibility), spatial (e.g. connectivity), and temporal (e.g. snail ecology, water contact patterns) heterogeneities characterizing schistosomiasis transmission are ironed out, and diluted into aggregated parasitological data [*Barbour*, 1996]. This has also been argued to explain the miss-match between the transmission potential in terms of the basic reproduction number R_0 predicted by the mean-worm-burden approach, and its observed stability and resilience [*Barbour*, 1996][1]. The acknowledge importance of heterogeneities - human-water contacts, spatial occurrence and temporal variations of snail abundance among others - in schistosomiasis transmission is reflected by its common labeling as a "focal" disease due to the large differences in transmission patterns that can be observed between neighboring villages [*Stothard et al.*, 2017]. The "focality" of schistosomiasis has often been voiced in terms of the measured rapid decrease in the correlation of prevalence among survey points with geographical distance [*Sturrock et al.*, 2010; *Knowles et al.*, 2017]. Thinking this observation through the end would strongly question the validity of using *Macdonald*-type models on parasitological data aggregated from distinct transmission settings (as done in *French et al.* [2015] by grouping villages based on baseline infection prevalence, but not by socio-ecological characteristics). However, this (arguably vague) concept of "focality" coexists with the recognition of distinct, and possibly well-defined, areas with common social-ecological characteristics explaining patterns of varying transmission strength within countries, as argued by *Brooker et al.* in terms of ecological zones (cf. Fig.1.3) [*Brooker et al.*, 2002][2], and fostered in the WHO's guide for national program managers in the design of stratified random sampling of villages and the choice of sentinel sites, respectively for the mapping and monitoring of disease prevalence at the national scale [*World Health Organization*, 2011, p. 27][3]. However, no methodology is given on how to define these ecozones in practice, particularly with the aim of schistosomiasis transmission control. Under the light of section 1.2, it can be argued that site-specific heterogeneities contemplated at the national level ensue in large part from the ecology of the snail intermediate hosts (species-dependent presence/absence, seasonal population dynamics), and to contamination/exposure patterns linked to the availability and spatial configuration of waterbodies (both natural and man-made), modulated by behavioral factors,

---

[1] Based on this observation, *Barbour* motivated the use of a prevalence-based approach in which individuals are considered either parasite-free or parasitized, and infection is represented as discrete, sporadic and intense events of worm uptake rather than as the "trickling" hypothesis of gradual worm accumulation embodied in *Macdonald*'s model. The prevalence-based model attained much higher values of R_0 (see Appendix A for the derivation of R_0 for *Macdonald*'s model), although at the cost of the loss of the capacity to track distinct levels of worm burden in the population. This approach has been subsequently adopted in various modelling works, in particular on *S. japonicum* [*Williams et al.*, 2002; *Rudge et al.*, 2013; *Gao et al.*, 2013, 2017], and possibly unawares in *Yakob et al.* [2014].

[2] This ecology-inspired approach to the spatial classification of schistosomiasis transmission areas has faded out since the advent of the widespread use of geo-statistical modelling for mapping disease risk, in which gridded environmental covariates enter in "raw" format into the model rather than in ecologically-meaningful pre-processed products (such as *Brooker et al.*'s ecozones).

[3] The WHO encourages using "homogeneous ecological zones" for the stratification of random village sampling and the choice of sentinel sites, defined as a "geographical area that is homogeneous in terms of humidity, rainfall, vegetation, population density and sanitation level." [*World Health Organization*, 2011, glossary at p. 10].

access to WASH, and spatial connectivity. Their incorporation into mathematical models of disease transmission is therefore a potentially important step towards improving the concordance between model predictions and varying observed transmission patterns within and among countries, but also for providing an objective and scalable methodology for the definition of geographical units meaningful for the implementation of necessarily spatial surveillance-response systems. Examples of the incorporation of climate and hydrology-driven models of the population dynamics of the snail intermediate hosts have been given section 1.2.4 for *S. japonicum*, but remain to be developed for SSA, and in a way that allows their spatial generalization. On the other hand, past works have already introduced spatially explicit models of disease transmission on which to build a national-scale approach to schistosomiasis modelling.

3.2.2 Spatially explicit dynamical models of disease spread

Mathematical models have proved useful in analyzing the spread of both micro- and macro- parasitic water-borne diseases in spatially explicit settings e.g. [*Gurarie and Seto*, 2009; *Bertuzzo et al.*, 2011; *Chao et al.*, 2011; *Tuite et al.*, 2011; *Rinaldo et al.*, 2012; *De Oliveira Duarte et al.*, 2014]. Indeed understanding the processes favouring schistosomiasis transmission appears highly important in the face of the risk of ineffective mass chemotherapy treatments.

Furthermore, social and hydrological connectivity for schistosomiasis have been discussed in the context of distributed human-snail contact sites [*Barbour*, 1978; *Woolhouse*, 1991], and formally developed in agent-based [*Hu et al.*, 2010] and connected metapopulation models [*Xu et al.*, 2006], building on the seminal model described in equation 3.1 for schistosomiasis. By relaxing the well-mixed and contact homogeneity assumptions [*Gurarie and Seto*, 2009] implemented a metapopulation-like approach on a set of n hydrologically connected villages and considers miracidial and cercarial transport in the water network, as well as human mobility. The model naturally expands from Macdonald's work by considering site-specific state variables yielding a $4n$-dimensional system that reads:

$$\frac{dw_i}{dt} = a\theta_i \sum_j c_j \omega_{ji} - \gamma w_i \tag{3.2a}$$

$$\frac{dy_i}{dt} = bm_i(1-y_i) - \nu y_i \tag{3.2b}$$

$$\frac{dc_i}{dt} = \pi_C N_i y_i + \sum_{j<i} s_{ij}^C r_{ij} \frac{V_j}{V_i} c_j - (\epsilon r_i + \mu_C) c_i \tag{3.2c}$$

$$\frac{dm_i}{dt} = \pi_M \sum_j \omega_{ij} \theta_i' H_j w_j + \sum_{j<i} s_{ij}^M r_{ij} \frac{V_j}{V_i} m_j - (\epsilon r_i + \mu_M) m_i. \tag{3.2d}$$

Hydrological connectivity is implemented through a distance-dependent transport survival rate $s_{ij} = e^{-\beta d_{ij}}$, whre β governs the exponential larvale decay with distance, for each larval stage from upstream to downstream villages with different volumes of contaminated water V. Net washout of larvae is given by a site-specific net hydrological output $r_i = \sum_{j<i} r_{ij}$. Human mobility is included by specific contact distribution fractions $\omega_{ij} \propto e^{-\alpha d_{ij}}$ with α being a measure of zonal social connectivity. Finally exposure and contamination contact rates $\{\theta, \theta'\}$ are made site-specific.

A theoretical network of connected villages was used by *Gurarie and Seto* [2009] to study the effect of varying connectivity parameters on the endemicity of the disease. These authors extended quantitatively the concept of the basic reproductive number R_0 for schistosomiasis transmission (for a derivation see

Appendix A) to a basic reproduction matrix (BRM) that includes connectivity among villages [*Gurarie and King*, 2005], in the same fashion as *Gatto et al.* [2012, 2013] characterized spatial epidemic risk for microparasitic water-borne disease. The analysis of the dominant eigenvalue of the BRM (if > 1 the disease is endemic in the network) was therefore used to investigate the impact of varying hydrological and social connectivity patterns on the endemic equilibrium point, highlighting a trade-off between the range of social connectivity and the strength of hydrological links in terms of endemicity risk in the network. Furthermore the BRM was used to test disease control interventions at the equilibrium by modifying the local R_0's (for instance by snail control) and comparing strategies by quantifying the effect on the overall risk reduction. Interestingly, the results suggested that applying control effort on highly connected nodes despite low disease burden would be a more efficient strategy than targeting the most affected nodes. Similar results were obtained using a slightly different model accounting for disease intensity in the population instead of the mean worm burden, which has the advantage of taking into account age-intensity distribution [*Gurarie et al.*, 2010].

Although the model proposed by *Gurarie and Seto* [2009] provides valuable insights in the role of connectivity among villages on a local scale, it has a number of shortcomings limiting its potential, most notably, and as argued in the previous section, the assumption of a constant snail populations. In fact, a peculiarity of the intermediate hosts of the pathogen is the pronounced seasonality of their population abundances. Both *Biomphalaria* and *Bulinus* spp. are characterized by yearly population crashes and bursts depending on local climatic and environmental drivers (cf. section 1.2.2). Seasonal fluctuations in snail population dynamics yield in turn seasonally varying disease transmission intensity, difficult to measure directly because of the slow dynamics of worm burden and the resulting symptom build-up [*van der Werf et al.*, 2003], and the practical limitations of existing cercariometric techniques based on water filtering [*Ouma et al.*, 2009], although promising advances in the use of environmental DNA could overcome some of these in the near future [*Stothard et al.*, 2017]. Yet this could be key in timing control interventions for disease elimination. Indeed the lack of appropriate diagnostic technologies impedes capturing a clear picture of the temporal evolution of the intensity of disease [*Stothard*, 2009] and may discourage forecasting time-varying transmission intensity based on snail population dynamics. However, understanding more thoroughly the ecohydrological drivers of seasonality in schistosomiasis transmission would allow to link hydro-meteorological projections, ecological dynamics and alternative disease control intervention strategies through suitable predictive models.

3.3 Materials and methods

3.3.1 The model

The mechanistic process model proposed by *Gurarie and Seto* [2009] expanded the seminal spatially implicit model of schistosomiasis by *Macdonald* [1965]. The extension proposes a connected metapopulation network of *n* villages. The system of differential equations is expressed in terms of the mean worm burden in human populations, W_i, the prevalence of infection in the snail intermediate hosts, Y_i, and the densities of cercariae and miracidia, C_i and M_i, the two intermediate larval stages of the parasite. Connectivity is accounted for by human mobility and hydrologic transport of larvae (while neglecting snail mobility). The parameters of this model and the values used for analysis are detailed in Table 3.1.

With the notation of this Chapter, the model of [*Gurarie and Seto*, 2009] can be written as:

$$\frac{dW_i}{dt} = a\left[(1-m_i)\theta_i C_i + m_i \sum_{j=1}^{n} Q_{ij}\theta_j C_j\right] - \gamma W_i \tag{3.3a}$$

$$\frac{dY_i}{dt} = bM_i(1-Y_i) - \nu Y_i \tag{3.3b}$$

$$\frac{dC_i}{dt} = \frac{\Pi_C}{V_i} N_i Y_i - \mu_C C_i - l_i^C C_i + \sum_{j=1}^{n} l_j^C P_{ji} S_{ji}^C \frac{V_j}{V_i} C_j \tag{3.3c}$$

$$\frac{dM_i}{dt} = \frac{\Pi_M}{V_i}\theta_i'\left[(1-m_i)H_i\frac{W_i}{2} + \sum_{j=1}^{n} m_j H_j \frac{W_j}{2} Q_{ji}\right] - \mu_M M_i - l_i^M M_i + \sum_{j=1}^{n} l_j^M P_{ji} S_{ji}^M \frac{V_j}{V_i} M_j. \tag{3.3d}$$

Here at each node i, the rate of change in the mean worm burden is given by the difference between the intensity of cercarial infection expressed as a probability of infection upon contact a times the exposure to contaminated water θ_i and cercarial density, and worm mortality at given rate γ. Density of cercariae is dynamically determined by the *per-capita* cercarial output from infected snails Π_C and the number of infected snails $N_i Y_i$ at time t, and limited by cercarial mortality μ_C. The rate of change in the prevalence of infected snails is given by the probability of infection of a susceptible snail $b(1-Y_i)$ times miracidial density and limited by snail mortality ν. Finally, miracidial density is determined by the rate of miracidial output from humans Π_M, the contamination rate θ_i' and the number of pairs of adult schistosomes, given by half of the mean worm burden times the number of human hosts H_i, divided by the volume of water V_i in which they are released (to obtain larval concentration in water). Human mobility is included by specific contact distribution fractions Q_{ij}. In the original version [*Gurarie and Seto*, 2009], the connectivity matrix is set to be proportional to distance between nodes, i.e. $Q_{ij} \propto e^{-\alpha d_{ij}}$ with α being a measure of zonal social connectivity. Hydrologic connectivity is implemented through a distance-dependent transport survival rate $S_{ij} = e^{-\beta d_{ij}}$ for each larval stage from upstream to downstream settlements with different volumes of contaminated water V_i. Model 3.3a differs slightly from the one proposed by *Gurarie and Seto* [2009] in the way it treats larval densities and human connectivity. Indeed, the volume of water V_i in which larvae are released is explicitly introduce in order have the state variable expressed as a concentration per unit volume (rather than general unit habitat as expressed by *Gurarie and Seto* [2009]). However, in the analysis presented in this Chapter all V_i to 1 so as restrain the analysis on the connectivity parameters. Regarding human connectivity, traveller contacts and local contacts are diffirenciated by the mobility parameter m instead of distributing the whole local contact parameters θ_i as a function of population and distance as proposed by [*Gurarie and Seto*, 2009] in the corresponding social contact matrix ω_{ij}. Indeed, in their approach m_i is implicitly considered to be constant and proportional to $H_i / \sum_j H_j e^{-\alpha d_{ij}}$ for local contamination and exposure rates.

By distinguishing between travellers and non-travellers its is assumed that contamination and exposure rates depend only on the physical characteristics of the site, and not on the traveller origin (captured by θ_i). This is reasonable when analyzing patterns on a national scale where the physical characteristics of the human settlements are heterogeneous (cites vs. towns vs. villages), and thus the contact rate at a visited location θ_j depends mainly on j. The main features of model 1 are (1) well-mixed and stationary human and snail populations at each village i (2) miracidial dispersal and cercarial uptake through human movement matrix Q_{ij} modulated by the fraction of moving people m_i, and (3) miracidial and cercarial dispersal through hydrologic connectivity matrices $P_{ji}S_{ji}^C$ and $P_{ji}S_{ji}^M$ modulated by the hydrologic transport rates $l_j^{C,M}$. By setting $\{m_i, l_j^{C,M}\} = 0 \ \forall i,j$ model 1 collapses to the local model of *Macdonald* [1965] expressed for each individual settlement, for which the local basic reproduction numbers are derived as $R_{0,i} = (ab\theta\theta'\Pi_C\Pi_M H_i N_i)/(2\gamma\nu\mu_C\mu_M V_i^2)$ (a complete derivation is given in

Table 3.1 – Model parameter description and values used in analysis of intestinal schistosomiasis in Burkina Faso

		Description	Value	Reference
State variables	W_i	Mean worm burden in village i	-	-
	Y_i	Infection prevalence in snail population in node i	-	-
	C_i	Cercarial density (per unit volume) in node i	-	-
	M_i	Miracidial density (per unit volume) in node i	-	-
Demographic and ecological parameters	H_i	Human population in node i	Inferred	*Bhaduri et al.* [2007]
	N_i	Snail population in node i	Inferred	*Phillips et al.* [2006]
	V_i	Water volume in node i	1	-
	a	Probability of successful cercarial infection in humans	10^{-5}	*Feng et al.* [2004]
	b	Probability of successful miracidial infection in snails	5×10^{-5}	*Feng et al.* [2004]
	θ_i, θ'_i	Local exposure and contamination rates	Range fixed	*Gurarie and Seto* [2009]
	Π_C	Cercarial emission rate/infected snail	100 [day^{-1}]	*Feng et al.* [2004]
	Π_M	Miracidial emission rate per worm pair	300 [day^{-1}]	*Feng et al.* [2004]
	μ_C	Per capita mortality rate of cercariae	3.04 [day^{-1}]	*May and Anderson* [1979]
	μ_M	Per capita mortality rate of miracidia	0.91 [day^{-1}]	*May and Anderson* [1979]
	γ	Per capita mortality rate of schistosome in host	1/5 [yr^{-1}]	*May and Anderson* [1979]
	ν	Per capita mortality rate of snails	1/0.1 [yr^{-1}]	*May and Anderson* [1979]
Connectivity parameters	m_i	Fraction of moving residents of node i	Fixed	-
	$Q_{i,j}$	Human mobility probability matrix of a traveler moving from i to j and back	Inferred	*Simini et al.* [2012]
	l_i^C, l_i^M	Hydrologic throughput rates of cercaria and miracidia	Not used	-
	P_{ji}	Hydrologic connectivity matrix (0/1 entries)	Not used	-
	S_{ji}^C, S_{ji}^M	$= e^{-\beta_{C,M} d_{ij}}$; transport survival rates of cercariae and miracidia between nodes separated by distance d_{ij}.	Not used	-
	$\beta_{C,M}$	Larval hydrologic survival exponents during transport	Not used	-

Appendix A). In this simple case, parasite invasion of the disease-free system depends locally on the condition $R_{0,i} > 1$. The above-mentioned model does not include detailed biological controls (worm mating probability, negative density feedback on within-host worm population) nor immunological ones (acquired immunity of human hosts). Although this could prove inadequate for the study of a particular village close to endemic equilibrium, these factors are deemed of secondary importance in the analysis of pathogen invasion conditions at the national level. The stability analysis of the model is carried out here for the reformulated version and extended to explore the spatial patterns of disease spread. Sensitivity analysis of model assumptions can be found in the original paper [*Gurarie and Seto*, 2009].

3.3.2 Parasite invasion conditions

Despite the complexity given by the spatially explicit formulation of model 3.3a, a rigorous stability analysis can be used to determine spatially explicit conditions for pathogen invasion. As the system is positive and the disease-free equilibrium is characterized by null values of the state variables, the bifurcation can only occur via an exchange of stability. Specifically, the disease-free equilibrium switches from stable node to saddle through a transcritical bifurcation, at which the Jacobian has one zero eigenvalue [*Kuznetsov*, 1995; *Rohani et al.*, 1999; *Gurarie and Seto*, 2009; *Gatto et al.*, 2012]. Parasite invasion is determined by the unstability of the disease-free equilibrium (DFE) $\mathbf{X_0} = [\mathbf{0}_n, \mathbf{0}_n, \mathbf{0}_n, \mathbf{0}_n]^T$, with $\mathbf{0}_n$ a $1 \times n$ null vector, n being the number of settlements. The stability properties of the DFE can be studied by analyzing the Jacobian linearised at the DFE, $\mathbf{J_0^*}$, which reads:

$$\mathbf{J_0^*} = \begin{bmatrix} \mathscr{A} & \mathscr{B} \\ \mathscr{C} & \mathscr{D} \end{bmatrix}, \tag{3.4}$$

where

$$\mathscr{A} = \begin{bmatrix} -\gamma\mathbf{I} & 0 \\ 0 & -\nu\mathbf{I} \end{bmatrix} \qquad \mathscr{B} = \begin{bmatrix} a(\mathbf{I}-\mathbf{m}+\mathbf{mQ})\boldsymbol{\theta} & 0 \\ 0 & b\mathbf{I} \end{bmatrix}$$

$$\mathscr{C} = \begin{bmatrix} 0 & \Pi_C\mathbf{V}^{-1}\mathbf{N} \\ \frac{\Pi_M}{2}\mathbf{V}^{-1}\boldsymbol{\theta}'(\mathbf{I}-\mathbf{m}+\mathbf{Q}^T\mathbf{m})\mathbf{H} & 0 \end{bmatrix}$$

$$\mathscr{D} = \begin{bmatrix} -\mu_C\mathbf{I}+\mathbf{T_C} & 0 \\ 0 & -\mu_M\mathbf{I}+\mathbf{T_M} \end{bmatrix}.$$

where: $\mathbf{I}$ is the identity matrix; $\mathbf{m}$, $\boldsymbol{\theta}$, $\mathbf{V}$, $\mathbf{N}$, $\boldsymbol{\theta}'$ and $\mathbf{H}$ are diagonal matrices whose non-zero elements are made up by the parameters m_i, θ_i, V_i, N_i, θ_i' and H_i, respectively; $\mathbf{Q} = [Q_{ij}]$ is the connectivity matrix for human mobility; $\mathbf{T_C} = \left(\mathbf{V}^{-1}\mathbf{P_C}^T\mathbf{V}-\mathbf{I}\right)\mathbf{l_C}$ and $\mathbf{T_M} = \left(\mathbf{V}^{-1}\mathbf{P_M}^T\mathbf{V}-\mathbf{I}\right)\mathbf{l_M}$, while $\mathbf{P_C} = [P_{ij}S_{ij}^C] = \mathbf{P}\circ\mathbf{S_C}$ (where $\circ$ is the Hadamard product) and $\mathbf{P_M} = [P_{ij}S_{ij}^M] = \mathbf{P}\circ\mathbf{S_M}$ are the transport matrices accounting for hydrologic connectivity and larval survival during transport, and $\mathbf{l_C}$ and $\mathbf{l_M}$ are diagonal matrices whose non-zero elements are the local values of l_i^C and l_i^M, respectively. After some manipulations (see Appendix A), the bifurcation condition $\det(\mathbf{J_0^*}) = 0$ can be reformulated as:

$$\det\left(\mathbf{I} - (\mathbf{I}-\mathbf{m})^2\mathbf{R_0} + \mathbf{R_0^M}(\mathbf{m},\mathbf{Q}) + \mathbf{T}(\mu_C,\mathbf{T_C},\mu_M,\mathbf{T_M})\right) = 0 \tag{3.5}$$

A generalized reproduction matrix (GRM) can be defined for the model of schistosomiasis transmission introduced in this Chapter as the sum of three matrices. One depends on local dynamics only; the other two (non-linearly) on spatial coupling mechanisms, reading,

$$\mathbf{G_0} = (\mathbf{I}-\mathbf{m})^2\mathbf{R_0} + \mathbf{R_0^M}(\mathbf{m},\mathbf{Q}) + \mathbf{T}(\mu_C,\mathbf{T_C},\mu_M,\mathbf{T_M})\,. \tag{3.6}$$

Parasite invasion conditions can therefore be decomposed into spatially explicit local conditions, $\mathbf{R_0}$, and connectivity-induced conditions $\mathbf{R_0^M}$ and $\mathbf{T}$ for mobility and hydrologic transport respectively. $\mathbf{R_0}$ is a diagonal matrix, whose non-zero elements are the local values R_{0i} of the basic reproduction number. $\mathbf{R_0^M}$ is a matrix depending on human mobility structure and magnitude, i.e.

$$\mathbf{R_0^M}(\mathbf{m},\mathbf{Q}) = \frac{ab\Pi_C\Pi_M}{2\gamma\nu\mu_C\mu_M}\mathbf{N}\mathbf{V}^{-1}\boldsymbol{\theta}'\left[(\mathbf{I}-\mathbf{m})\mathbf{mHQ} + \mathbf{Q}^T\mathbf{Hm}(\mathbf{I}-\mathbf{m}) + \mathbf{Q}^T\mathbf{m}^2\mathbf{HQ}\right]\boldsymbol{\theta}\mathbf{V}^{-1}.$$

$\mathbf{T}$ is another matrix depending on larval death rates and transport through the hydrologic network

$$\mathbf{T}(\mu_C,\mathbf{T_C},\mu_M,\mathbf{T_M}) = \frac{1}{\mu_C}\mathbf{V}\mathbf{T_C}\mathbf{V}^{-1} + \frac{1}{\mu_M}\mathbf{N}\mathbf{T_M}\mathbf{N}^{-1} - \frac{1}{\mu_C\mu_M}\mathbf{N}\mathbf{T_M}\mathbf{V}\mathbf{N}^{-1}\mathbf{T_C}\mathbf{V}^{-1}.$$

Ensuing from equations 3.5 and 3.6 the condition for parasite invasion can be stated in terms of the dominant eigenvalue g_0 of matrix $\mathbf{G_0}$, i.e. $g_0 = \max_k(\lambda_k(\mathbf{G_0}))$, with disease spread occurring if $g_0 > 1$. Bearing the operational use of this condition in mind, it is important to note that control measures that successfully lead to a stable DFE (thus driving g_0 below 1), for instance by providing improved sanitation

or the use of molluscicides, do not imply immediate transmission interruption, and the country may instead present non-zero parasite loads in the population and in the environment for some time. In ecological terms, the time to reach pathogen extinction corresponds to the relaxation time of the system [*Diamond*, 1972; *Tilman et al.*, 1994], $t_{\mathscr{R}}$, which is determined by the characteristic timescale of pathogen spread dynamics. The relaxation time of schistosomiasis transmission is therefore set by the dominant eigenvalue g_0 as $t_{\mathscr{R}} = 1/|\log(g_0)|$, and can be shown that the average time to transmission interruption amounts to $-5/\log(g_0)$ time units [*Mari et al.*, 2014a]. Based on this relation it is possible to associate a given socio-ecological setting in the country (i.e. a given value of g_0) to an estimate of the time for transmission to effectively die out once conditions for pathogen extinction are met ($g_0 < 1$).
Furthermore bifurcation analysis for water-borne disease models proved to be able to capture spatial patterns of the spread of the pathogen [*Gatto et al.*, 2013]. It is possible to show that the dominant eigenvector $\mathbf{g_0}$ of the GRM can be used to study the geography of disease spread in the case of macroprasitic infections, at least close to the transcritical bifurcation. In fact, $\mathbf{g_0}$ corresponds to the cercarial component $\mathbf{C}$ of the vector of state variables for trajectories diverging from the (unstable) DFE (see Appendix A). This corollary is of particular interest in the study of spatial patterns of disease spread. Indeed, close to an unstable DFE the dominant eigenvector of matrix $\mathbf{J_0}^*$, $\boldsymbol{\lambda}_{\max}(\mathbf{J_0^*})$, pinpoints the directions in the state space along which the system trajectories will diverge from the equilibrium. In other words, computing $\boldsymbol{\lambda}_{\max}(\mathbf{J_0^*})$ enables not only the quantitative analysis of conditions for the parasite to invade a connected set of spatial locations, but also to predict the direction of disease spread geographically in the time close to the onset. Of particular interest in the dominant eigenvector analysis is the mean worm burden compartment, $\mathbf{W}$, which in the case of schistosomiasis is an important measure of infection severity and the natural target of control interventions through antischistosomal treatments [*Fenwick et al.*, 2006; *Utzinger and de Savigny*, 2006]. At the bifurcation through which the DFE loses stability, spatial distribution of the mean worm burden can be computed in terms of $\mathbf{g_0}$ as $\mathbf{W} = (a/\gamma)(\mathbf{I} - \mathbf{m} + \mathbf{mQ})\boldsymbol{\theta}\mathbf{g_0}$ (see Appendix A).

3.3.3 Model implementation

Schistosomiasis control and elimination programs are implemented on at the national scales by centralized national institutions [*Rollinson et al.*, 2013], a nation-wide spatial scale is thus retained for investigating the modelling framework presented above. The dominant eigenvalue and eigenvector analysis was applied to the context of Burkina Faso, presented in Chapter 2. Briefly, both urinary and intestinal forms of the disease are present with very different historical geographical coverages, governed by the ecological ranges of their respective species of intermediate host [*Poda et al.*, 2004a]. The intestinal form of the disease will be used for the subsequent analysis given the proven importance of human movement in its geographical expansion in the country [*Poda et al.*, 2001]. The context of this study is the geographical extent of the country (Fig. 3.1) and the distribution of human settlements that consist the nodes of the connected network on which the disease is considered to spread.

Settlements and population - H_i A settlement is considered to be a geographic location having any number of permanent residents. The population of the settlements in Burkina Faso ranges from villages of less than 100 inhabitants to cities of more than 100,000 people, the urban area of the capital Ouagadougou housing more than 700,000. A settlement was considered to be a city if its population H_i is bigger than a definition threshold of 10,000 inhabitants, and a village if H_i is smaller than 2,000 inhabitants. The model was applied to $10,592$ settlements provided by a freely available database (courtesy of Humanitarian Response www.humanitarianresponse.inf). Population was obtained by assigning the sum of gridded

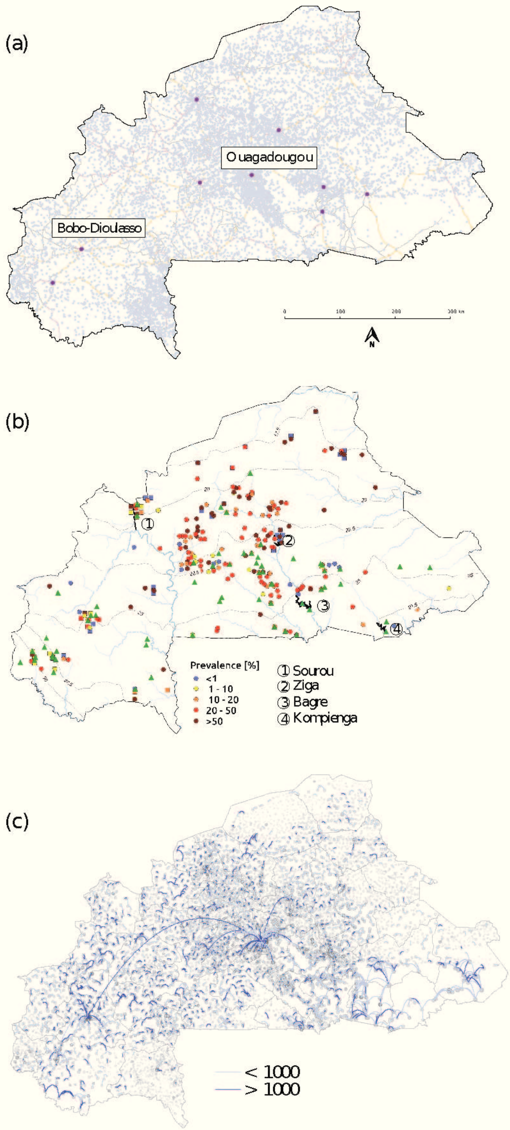

Figure 3.1 – Model implementation for Burkina Faso (a) *Road network and settlement distribution.* The principal transportation axes, the main cities (black points), including the capital, Ouagadougou and, the regional hub, Bobo-Dioulasso, and smaller settlements (grey) are represented. Villages from OCHA https://www.humanitarianresponse.info/en/operations/burkina-faso/dataset/burkina-faso-settlements-villages-towns-cities Road network from Open Street Map, data available under Open Database License (© *OpenStreetMap contributors*). (b) *Water resources and schistosomiasis.* Only the four largest dams of the country are shown (numbered 1-4) along with the major rivers and mean monthly precipitation isolines (isohyets). Historical prevalence of intestinal(urinary) schistosomiasis is represented in color-coded rectangles(circles). Data was extracted from the Global Neglected Tropical Diseases Database (www.gntd.org) and consists of published parisotological studies in Burkina Faso from 1955 to 2007 (the average prevalence over survey years was taken in villages where multiple surveys were available). Green triangles represent *B. pfeifferi* presence data compiled by [*Poda*, 1996]. (c) *Human mobility patterns.* Fluxes were predicted using the radiation model and the population density of each node. Point size is proportional to the $\log_{10}$ of settlement population. Fluxes are divided into higher and lower than 1,000 travellers (evaluated taking all of people in the node travelling) and displayed in the main figure for settlements larger than 5,000 people. The tow insets correspond to zooms on areas in the South-West and the East of the country with all fluxes larger than 1,000 travellers depicted, base maps from Open Street Map.

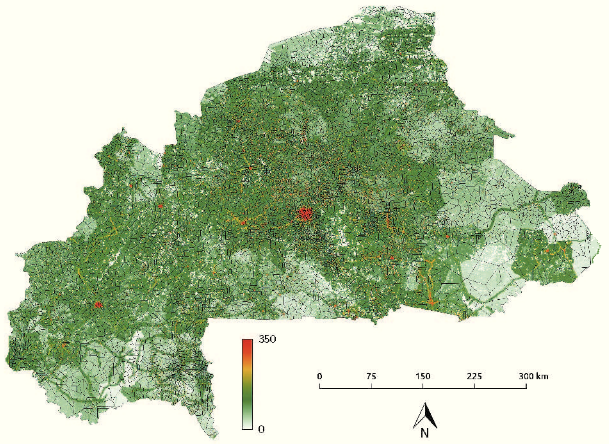

Figure 3.2 – Population distribution in Burkina Faso and Voronoi tessalation used for building the network. Population density is given at a resolution of ≈ 1 km^2 (from LandScan)

Landscan estimates of population density (Fig. 3.2) to the Voronoi polygons resulting from the spatial configuration of settlements.

Intermediate host distribution - N_i As mentioned in section 2.1, the intermediate host of intestinal schistosomiasis in Burkina Faso is *B. pfeifferi*. The ecological range of the species is determined by both climatic and hydrologic conditions, namely the presence of agricultural infrastructure such as small and large reservoirs [*Poda et al.*, 2003; *Boelee and Madsen*, 2006; *Steinmann et al.*, 2006]. Presence and abundance of the host determine the viability of the transmission cycle of the disease. In the mathematical framework proposed [*Gurarie and Seto*, 2009], the number of snails in a given node, N_i, is given. For surveillance-response programs at the national level, a probability of presence is retained as a proxy of snail abundance. Probability of presence can be modelled for entire landscapes based on underlying environmental covariates, preserving information about heterogeneity across sites. The Maximum Entropy (MaxEnt) approach by *Phillips et al.* [2006] is one of such methods that has proven its worth in comparison to other predictive methods, and has already been used in the specific case of modelling the distribution of the intermediate hosts of the two genus of schistosomes across Africa [*Stensgaard et al.*, 2013]. The MaxEnt framework is based on the distribution of presence records versus continuous environmental covariates, specifically species distribution is modelled by maximizing its distribution entropy, subject to the constraint of having the same expected value of each environmental variable than its empirical average [*Elith et al.*, 2011]. Available data for *B. pfeifferi* to implement MaxEnt modelling consisted of presence data obtained from the comprehensive literature review and field work of *Poda* [1996] in Burkina Faso, including a total of 64 unique sighting locations. For a detailed description of the sampling methodology the reader is referred to *Poda* [1996]; briefly, punctual samplings were performed throughout the country between 1984 and 1993, and standard identification keys were used for species discrimination. Modelling was performed in the freely available software provided by [*Phillips et al.*, 2006]. Section of features and natural environmental covariates for prediction was done according to the method proposed by [*Stensgaard et al.*, 2013]. The only anthropogenic covariate used is the distance to waterbodies, $\mathscr{D}_{water}$, which was produced by calculating the euclidean distance from each settlement to the closest water surface. Water surfaces were obtained at a 30m pixel resolution for all of Burkina Faso

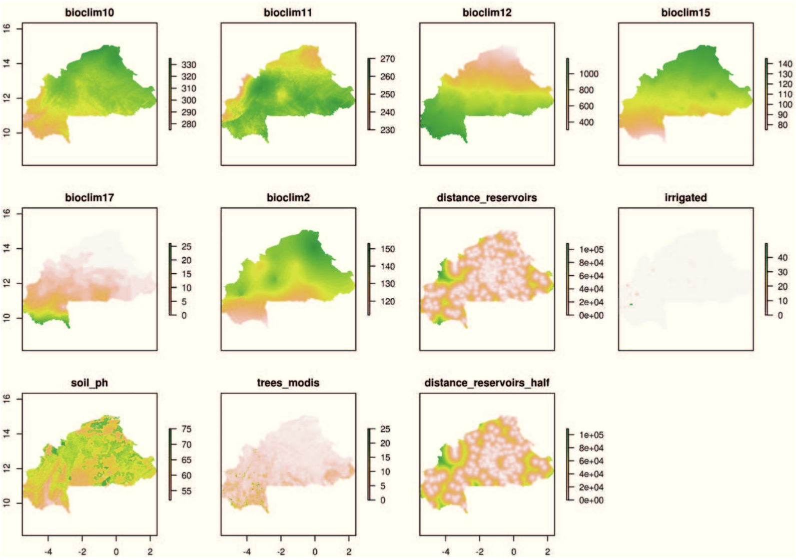

Figure 3.3 – Covariates used in the species distribution modelling of the snail intermediate host using MaxEnt. All data sources are analogous to those used in [*Stensgaard et al.*, 2013]

by Quadratic Discriminant Analysis of a mosaic of Landsat satellite images of 2014 (courtesy of the U.S. Geological Service). The resulting water surfaces were filtered and validated against the national spatial database of dams and small reservoirs [*Cecchi*, 2007]. Maps of the covariates used as inputs for MaxEnt are illustrated in Fig 3.3, and their relative importance for modelling the ecological range are presented in Fig 3.4. Interestingly the variable with both the most unique information and the most explanatory power was found to be the distance to reservoirs, thus supporting the need for investigating the role of water resources development in schistosomiasis transmission. The output of MaxEnt (probability of presence) was taken as proportional to the site-specific parameter N_i during model implementation.

Human mobility model - Q_{ij} No actual human mobility data, such as census or mobile phone records, are available for accurately estimating human mobility fluxes in Burkina Faso. Models of human mobility have grown popular and accurate with increasing access to big data on human behaviour, and are valuable tools to overcome data scarcity despite the strong assumptions that need to be made regarding, for instance, travel means and accessibility [*Lu et al.*, 2013; *Wesolowski et al.*, 2013]. Here the recently proposed radiation model is retained which has proven to correctly reproduce mobility patterns at the national and regional scales originally implemented in the context of the USA [*Simini et al.*, 2012], and proved to hold well for inter-city movement in West Africa [*Palchykov et al.*, 2014]. Specifically, the radiation model expresses the probability Q_{ij} that a person travelling out of node i reaches node j as:

$$Q_{ij} = \frac{H_i H_j}{(H_i + s_{ij})(H_i + H_j + s_{ij})} \tag{3.7}$$

where $H_i\,[H_j]$ is the population size of the origin [destination] node, and s_{ij} is the total population living within a radius d_{ij} around the origin, excluding the origin and destination populations, and d_{ij} being the distance between nodes i and j. The model has therefore the benefit of depending explicitly only on population density distribution in space to capture the structure of human mobility fluxes. The fraction of moving people, i.e. people visiting another node during a short period of time, m_i, is therefore the only free parameter modulating the strength of mobility-related connectivity in the spatial spread

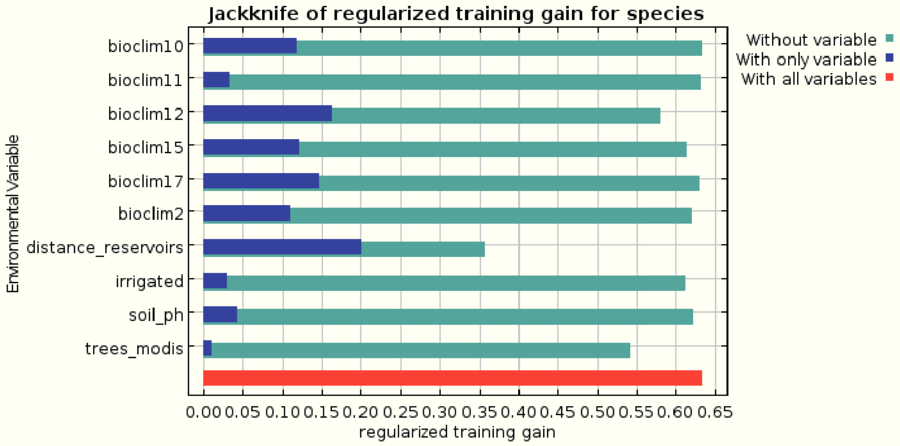

Figure 3.4 – Jackknife analysis of covariate importance. Results are shown for one fold of the fitting procedure. Importance is measured in terms of the regularized training gain of the MaxEnt model when removing a given variable (light blue) and using only that variable (dark blue). The former expresses the information contained in the given covariate that is different from other variables. The latter the specific explanatory power contained in the variable. The results show that distance to reservoirs is both the covariate with the largest explanatory power, and with the highest information content not contained in the other covariates.

of the disease. No empirical estimate of m are readily accessible for Burkina Faso, although values of $m \to 1$ are unlikely. The vector of human population $\mathbf{H}$ and Euclidean distances were used to produce a $10'592 \times 10'592$ matrix Q_{ij} of human mobility connections. Three forms of human mobility can be observed in Fig. 3.1: (1) strong local-level fluxes between low density populated areas, (2) large population centres interconnected by long-distance trips, and (3) medium-range fluxes in the basin of attraction of the two major cities (Ouagadougou and Bobo-Dioulasso).

A detailed study of the relative merits of radiation versus gravity-like models would be interesting, however it is limited at this point by the accessibility to data. Other mobility models such as the gravity model imply different underlying assumptions, but with no validation data for Burkina Faso available these would suffer from the same weakness of verifiability than the radiation model. Needless to say that the availability of real mobility data would overcome the need for modelling as observed mobility fluxes could be used directly (with caveats) [*Lu et al.*, 2013; *Finger*, 2017].

Exposure and contamination rates Successful human infection by cercariae strongly depends on water contact frequency and duration, which in turn are determined by the socio-economic activities of the populations [*Bruun and Aagaard-Hansen*, 2008; *Kpoda et al.*, 2013]. For this reason, urban areas are potentially less favourable schistosomiasis transmission sites given the lower human-to-water contact opportunities relative to the number of inhabitants, which needs to be encompassed into the single $\theta_i[\theta'_i]$ parameters of exposure[contamination] rate for the whole population of a node i. Although there have been examples of recent increases in agriculture around small reservoirs and other water bodies in urban areas [*Compaoré and Kaboré*, 1997; *Kêdowidé et al.*, 2010], the proportion of such contact patterns is not deemed representative of the majority of any urban settlement [*Ernould et al.*, 2000; *Bruun and Aagaard-Hansen*, 2008]. In the absence of detailed and nation-wide socio-economic surveys assessing exposure and contamination rates in Burkina Faso, the reduced probability of having population-wide high contamination and exposure rates in urbanized settlements has been translated into an inverse-logistic formulation for the exposure/contamination rates (here assumed to coincide, i.e. $\theta = \theta'$, as

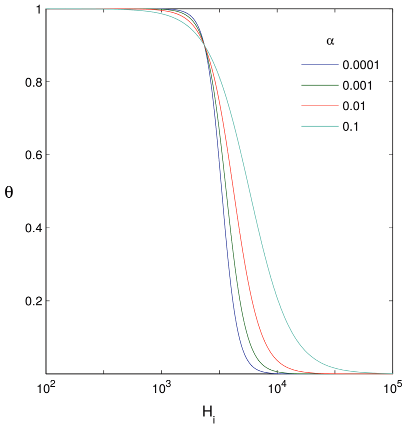

Figure 3.5 – Sigmoid functional forms for exposure/contamination. The curves are given here for $\theta_{MAX} = 1$ as a function of population in node i, H_i, and for values of α used in model exploration

in *Gurarie and Seto* [2009]) based on the size of each node. The hypothesis underlying this approach is therefore that, in Burkina Faso, densely populated and tertiarized urban centres should have low contamination/exposure rates with respect to small rural settlements were a number of socio-economic activities entail human-water contacts [*Zongo et al.*, 2012; *Kpoda et al.*, 2013]. The resulting contact rate θ_i in node i is thus:

$$\theta_i = \theta_{MAX} \left\{ 1 - \frac{1}{1 + a(\alpha) e^{-b(\alpha) S_{\log 10}(H_i)}} \right\}, \tag{3.8}$$

that is a sigmoid decreasing function of population size, where θ_{MAX} is a parameter indicating the maximum contact rate, while α controls the shape of the function. Specifically $a(\alpha)$ and $b(\alpha)$ are two positive coefficients that are selected so that cities have exposure equal to $\alpha\theta_{MAX}$, and imposing $\theta_i = 0.9 \cdot \theta_{MAX}$ for villages of exactly 2,000 inhabitants. In other words α can be seen as the percentage reduction in exposure/contamination rates due to urbanization for a settlement at the population threshold defining a city, here taken to be defined as a settlement of 10,000 inhabitants, with respect to the maximal rates observed in rural areas. $S_{\log 10}(H_i) = (\log_{10}(H_i) - \mu_{\log_{10}(\mathbf{H})})/(\sigma_{\log_{10}(\mathbf{H})})$ is the $\log_{10}$-transformed and standardized population density based on the mean, $\mu_{\log_{10}(\mathbf{H})}$, and the standard deviation, $\sigma_{\log_{10}(\mathbf{H})}$, of the log10 transform of the population vector $\mathbf{H}$. Illustrations of the resulting functional forms for different values of α are given in Fig 3.5. The choice of eq. 3.8 was made with the objective of discriminating between the very different settings of urban areas and rural settlements, and that other functional forms could have been chosen that respect the low vs. high contamination/exposure rates. Indeed the inclusion of small-scale heterogeneity between settlements of similar sizes (for which 3.8 would predict similar contact/exposure rates) depends on the presence and density of improved sources of water, of sanitation infrastructure, the ephemerality of the hydrological network and waterbodies, and other factors for which detailed geo-referenced data is not readily accessible. Furthermore this approach clearly lacks the accuracy of water contact surveys or direct observations of human-water contacts such as the ones provided for particular sites across Sub-Saharan Africa [*Kloos*, 1985; *Rudge et al.*, 2008], but at least enables a relative ranking of nodes at the national scale following the hypothesis that urbanization leads to a reduction in human-water contacts. A more accurate generalizable modelling of human-water contacts based on water and sanitation infrastructure data and resulting contamination and exposure rates for schistosomiasis would be of great use in reducing the uncertainty related to this particular point.

Hydrologic connectivity In equation 3.3a, hydrologic connectivity only concerns larval stages of the parasite. Survival times of both miracidia and cercariae are known to be on the order of hours [*Anderson et al.*, 1982], thus resulting in localized effects of this form of transport, as illustrated in *Gurarie and Seto* [2009] for a network of 15 connected villages. Because the context of the present analysis is all of Burkina Faso, it is deemed realistic to remove hydrologic transport of the larval stages of the parasite, since the only viable hydrologic transport routes at the national scale could be large rivers (Fig. 3.1), which are known to be unsuitable environments for larvae that have limited life spans. Nevertheless, all of the following analysis could be repeated including hydrologic transport by applying eq. 3.6 in its full version. On the other hand a form of hydrologic connectivity that was not considered in *Gurarie and Seto* [2009] is the passive dispersion of the snail intermediate host in streams and rivers. Indeed it has been observed that water velocities greater than 33cm/s may dislodge *Bulinus spp.* individuals that may be transported downstream [*Poda*, 1996]. Quite possibly, the threshold on velocity should have been translated into one on shear stress of the waterway bottom. However, the only available data on this kind of phenomenon in the fairly flat topography of Burkina Faso is an inconclusive study by *Poda* [1996] which measured snail dispersion during the rainy season of the order of 1 snail/30min on the Nazinon river (Volta Rouge). Given that this result is based on only 4 samplings, and no information was collected on snail provenance, transport distance and variability, and species, it was considered that there was not enough evidence to justify modifying eq. 3.3a to include snail transport at this stage. Field data on the transport of the intermediate hosts of schistosomiasis in Burkina Faso would help elucidate its importance and relevance in full transmission models.

3.4 Results and discussion

3.4.1 Pathogen invasion conditions and relaxation times

Because the real magnitude of human mobility in Burkina Faso is currently unknown, a wide range of possible scenarios are explored. It is assumed that the structure of the human mobility network is accurately captured by the radiation model, thus only the intensity of mobility fluxes are considered. In order to encompass all possible behaviours, although extremes are unlikely, in real large scale mobility patterns for example it is unlikely that as much as one half of the population would leave their home, values of the fraction of mobile population in the range $m \in [0,1]$ are considered. The relation between contamination and exposure rates and population density dependence also lacks ground-truthed data, and therefore it is explored through sigmoid contact functions (eq. 3.8) with $\alpha \in \{0.0001, 0.001, 0.01, 0.1\}$. Urban contamination and exposure rates can be seen as an increasing function of α. Not surprisingly, human mobility is found to strongly condition successful parasitic invasion of the system. Two opposite effects are illustrated in Fig. 3.6 with a dilution effect for fractions of mobile people increasing from $m = 0$ to $m \approx 0.3$; and an increase in the risk of disease spread for $m > 0.3$. Indeed for all investigated levels of urban contamination and exposure rates the dominant eigenvalue g_0 of the GRM falls below 1 for intermediate ranges of the fraction of mobile people and low values of θ_{MAX}. Beyond the specificities of model 1, these results are consistent with the conclusions of *Gurarie and Seto* [2009], at least close to the bifurcation and for the parameter region where $m < 0.5$. The parameter region in which the DFE is stable (gray shaded area in Fig. 3.6), thus preventing parasite invasion, is of similar sizes for all values of α, except for high levels of urban contact rates ($\alpha = 0.1$) for which pathogen invasion is observed for a wider range in the parameter space. This can be seen as the effect of coupling locations with high mobility (densely populated areas) with locations with high transmission potential (high contamination and exposure rates). All subsequent analysis therefore focused on the case that seemed the most realistic, namely intermediate urban contamination and exposure rates ($\alpha = 0.01$).

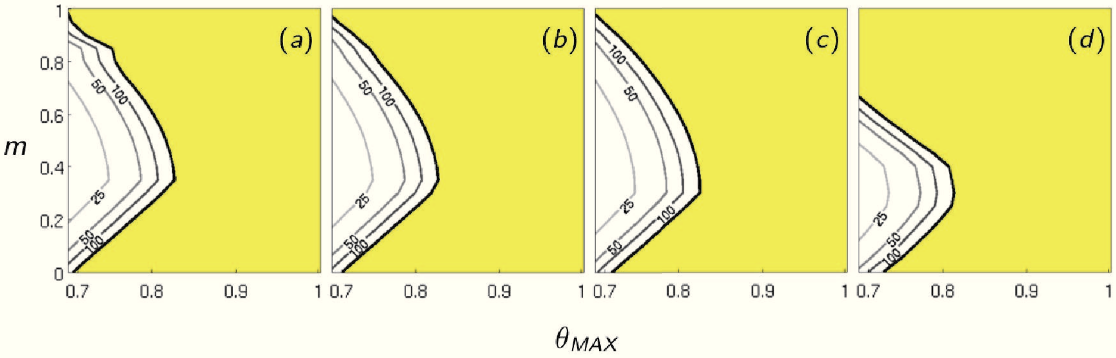

Figure 3.6 – Pathogen invasion conditions and average time to extinction for the Burkina Faso settlement network. The values of the dominant eigenvalue g_0 of the GRM are plotted for increasing values of $\alpha \in \{0.0001, 0.001, 0.01, 0.1\}$ (respectively in panels (a) to (d)), against values of maximal contamination and exposure rates θ_{MAX} and the fraction of mobile people m. Yellow indicates parameter combinations permitting parasitic invasion. Contours to the left of the stability boundary give parameter combinations yielding average times to pathogen extinction isolines $(5t_{\mathscr{R}})$ of 25, 50 and 100 years.

In addition to the stability of the DFE, the dominant eigenvalue of the GRM contains information on the average time for transmission to fade out in the case of unfavourable conditions for pathogen spread. The average times to extinction based on relaxation time isolines (constant $t_{\mathscr{R}}$) follow the shape of the stability boundary, with a logarithmic decrease of extinction time as a function of distance to the boundary $g_0 = 1$. The time to extinction is of the order of a century close to the stability line, and decreases sharply for small modifications of human mobility and contamination/exposure rates. Similarly to the stability conditions, the relaxation time is minimal at intermediate mobility levels for a given θ_{MAX}. Furthermore the shape of the time to extinction isolines suggests that a above the mobility threshold $m \approx 0.3$, reducing contamination/exposure rates would have a larger marginal reduction on the time to extinction than acting on mobility. Contextualizing these results in the framework of elimination programs, it may be argued that an extinction time of 100 years may be considered an effectively stable transmission scenario from a public health management point of view. In this perspective $g_0 = 1$ could be inappropriate as an operational indicator of transmission characteristics, and the threshold value should be chosen based on an acceptable relaxation time from a public health standpoint. Moreover the remark on the effect of the two parameters on relaxation time should be reformulated in terms of costs for it to be projected into disease control strategy design, and although the latter is of great practical interest it is beyond the scope of this work.

3.4.2 Predicted spatial patterns

Proof of concept for macro-parasitic dynamical systems The first element of the analysis explores the spatial patterns of disease spread by mapping the components of the dominant eigenvector of the linearised system around the DFE. When compared to the equilibrium state of the system, *Gatto et al.* [2013] showed that in the case of micro-parasitic water-borne diseases characterized by fast dynamics, $\mathbf{g}_0$ is an accurate predictor of the spatial distribution of cases both in the early phase of the outbreak and at the epidemic peak. In the perspective of mathematical modelling, schistosomiasis differs from cholera-like diseases in that it could be considered as a slow-fast dynamical system [*Auger et al.*, 2000], meaning having rate parameters spanning 3 orders of magnitude (see 3.1). Indeed, by definition, the dominant eigenvector of the Jacobian of the linearised system approximates well the trajectory close to the DFE,

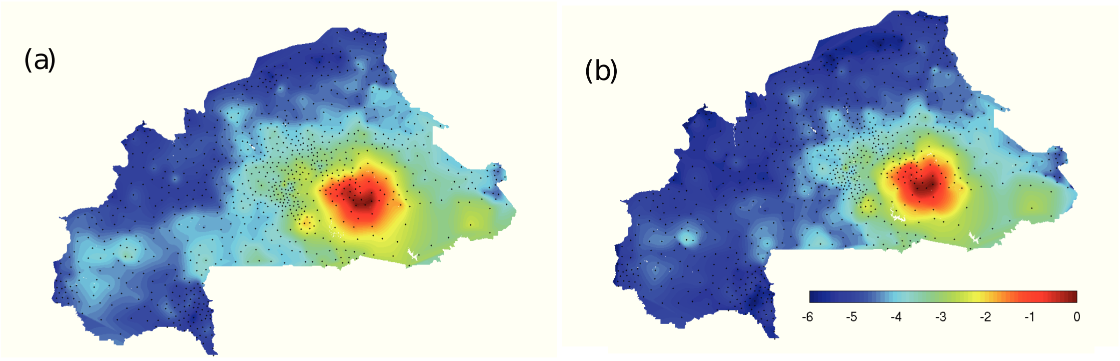

Figure 3.7 – Eigenvector analysis as predictive tool. Comparison of the equilibrium state of the system for a 1,000 node aggregated network for the parameter set $\{\alpha = 0.01, \theta_{MAX} = 0.31, m = 0.4\}$. (a) Spatial distribution of disease intensity at the equilibrium expressed as a linear interpolation of mean worm burden W_i at the aggregated network nodes (black dots) in $\log_{10}$-scale. (b) Spatial patterns of disease spread predicted by the rescaled dominant eigenvector $\mathbf{g_0}$ of the system at the transcritical bifurcation of the DFE in $\log_{10}$-scale.

but its predictive power of the endemic equilibrium remains to be verified. This is done by comparing the predicted spatial patterns of disease with the state of the system at the endemic equilibrium. The system at the national level has a prohibitively large number of state variables ($4 \times n \approx 40,000$) that prevents running the connected ordinary differential equations (ODE) system to endemic equilibrium using traditional numerical solvers on standard computing software. Specialized high-performance computing techniques could permit running the full system, but their discussion is beyond the scope of this work. To test the applicability of the eigenvector analysis to the full Burkina Faso settlement network, the analysis on an aggregated network of 1,000 nodes is first performed to prove the relevance of the approach for slow-fast systems. The aggregated network is obtained by geographical clustering (using the *k-means* algorithm) of the full 10'592 node network. Spatial patterns of disease spread are obtained by rescaling the dominant eigenvector $\mathbf{g_0}$ of the GRM to represent $\mathbf{W}$, the mean worm burden along model trajectories diverging from the DFE. The results illustrated in Fig. 3.7 show that at the transcritical bifurcation the rescaled dominant eigenvector reproduces well the spatial patterns observed at the endemic equilibrium of the system. Indeed the disease hotspot is accurately predicted by the dominant eigenvector approach. It is important to note that what a disease hotspot is defined as a geographical area for which the numerical simulation of the aggregated system yields high mean worm burden levels, and does not necessarily correspond to observed historical prevalence levels in the epidemiological data presented in Fig. 3.1. Indeed it is recalled that the aim of Fig. 3.7 is to test the correspondence between the system endemic equilibrium and spatial patterns predicted by the dominant eigenvector. In this regard the main discrepancy is in the predicted disease intensity levels in western parts of the country which are slightly under-predicted by the rescaled $\mathbf{g_0}$. These results prove that the method holds for the macro-parasitic dynamical system representation of schistosomiasis transmission, at least close to the transcritical bifurcation. This result illustrate the usefulness of the approach proposed in this Chapter in assessing the conditions for determining elimination thresholds, and their susceptibility to variations in transmission conditions.

Spatial patterns at the national level The eigenvector approach allows the analysis of schistosomiasis spread on the full network of Burkina Faso. The focus is put into studying spatial patterns for three mobility regimes along the $g_0 = 1$ contour line in Fig. 3.6 by tuning the free parameters (m and θ_{MAX}) to place the system precisely at the transcritical bifurcation that determines the instability of the DFE. It is

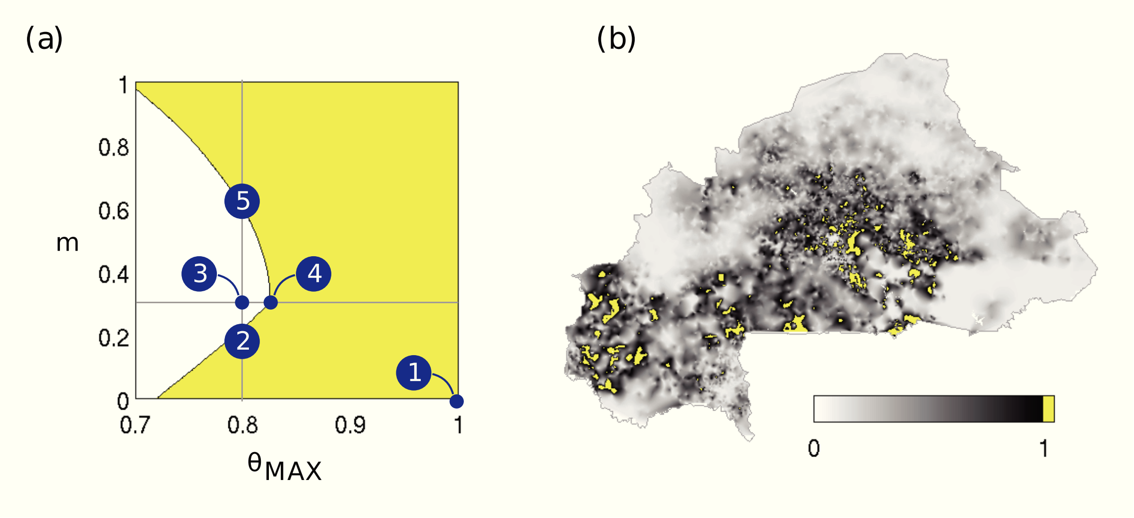

Figure 3.8 – Pathogen invasion conditions and local transmission risk. (a) Stability diagram of the DFE in terms of contamination and exposure rates and the fraction of mobile people for intermediate urban contamination/exposure rates($\alpha = 0.01$). Points in the white[yellow] area represent parameter combinations yielding a stable[unstable] DFE. Parasite invasion occurs when crossing the bifurcation curve (black line, $g_0 = 1$). (b) Local conditions of pathogen invasion risk in terms of R_0 for no human mobility and maximal contact rates (point (1) in panel a). Areas presenting $R_{0,i} > 1$ (in yellow) experience sustained pathogen invasion and schistosomiasis is introduced in the node. Even for maximal contact rates locally schistosomiasis-prone areas are restrained to the south-western and central parts of the country.

noteworthy that the dominant eigenvector analysis holds only close to the bifurcation which represents conditions tending towards elimination, thus relevant to surveillance-response strategies, as opposed to areas of high endemicity characterized by $g_0 >> 1$. Fig. 3.9 illustrates the effect of connectivity on disease spread in comparison to local pathogen invasion condition, expressed by the local basic reproduction number $R_{0,i}$ (panel (b) in Fig. 3.8, corresponding to point (1) in panel (a)). Local potential for pathogen invasion results from the interaction between local population density and snail presence. At low human mobility intensity the disease concentrates around the populated areas in the center of the country (panel (a), point (2) in Fig. 3.8(a)). By increasing mobility, the dilution effect causes the DFE to become stable and the pathogen cannot invade the country (point (3) in Fig. 3.8(a)). For parameter combinations yielding pathogen invasion at intermediate human mobility ($m = 0.3$), the spatial patterns of disease spread shift towards the South-East with the appearance of a second hotspot in an area with favourable local conditions (panel (b), point (4) in Fig. 3.8(a)). The effect of mobility is most visible when the majority of people are mobile ($m = 0.65$). Indeed, the South-Eastern hotspot takes over the central one and the disease spreading to the whole South-Eastern part of the country in areas where the local reproduction number is below 1, indicating unfavourable local conditions for transmission (panel (c), point (5) in Fig. 3.8(a)). It is interesting to note that the spatial patterns of disease spread on the aggregated network reproduce reasonably well the ones observed on the full network, thus supporting the assumptions made above. The capacity to predict the spatial patterns of the disease close to the disease free equilibrium could provide a tool for prioritizing surveillance sampling in those areas where schistosomiasis is predicted to pickup the most, thus were the re-invasion signal in the mean worm burden would be the strongest.

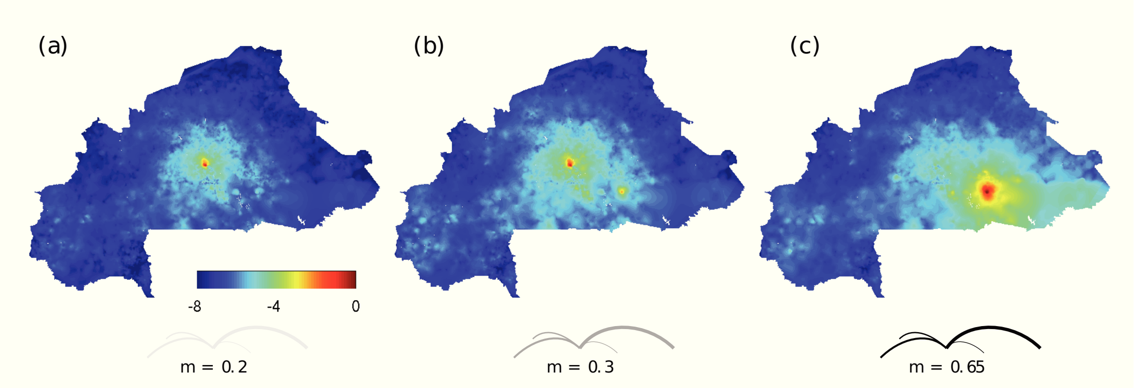

Figure 3.9 – Human mobility and spatial patterns of the disease in the case of intermediate urban schistosomiasis. (a-c) Predicted $\log_{10}$-rescaled values of the mean worm burden compartment **W** for increasing levels of human mobility ($m = 0.2, 0.3, 0.65$) along the bifurcation line (points d-e-f in panel a) and the $\theta_{MAX} = 0.8$ transect (points 2-4-5 in panel a).

3.4.3 Water resources development and human mobility

Water resources development directly impacts large-scale schistosomiasis transmission by altering the probability of presence of the intermediate snail host in the environment. This is explicitly accounted for in the approach presented here through the distance to water, $\mathscr{D}_{water}$, of a human settlement. To investigate the side-effects of water resources development on schistosomiasis in the country, *B. pfeifferi* probability of presence was re-evaluated using MaxEnt for alternative scenarios of water resources development by randomly removing existing reservoirs to consider different numbers of built dams expressed as a fraction ϵ of the existing ones, and the stability of the DFE recomputed for parameter combinations used in Fig. 3.6. The evolution of water resources development in Burkina Faso (a 5-fold increase in the number of reservoirs in the past 60 years [*Cecchi*, 2007]) was explored by varying ϵ in the set $\{0.25, 0.5, 0.75\}$ of existing reservoirs, which represents increasing numbers of built reservoirs. An illustration of the predicted changes in the ecological range of the intermediate host due to water resources development, in comparison with the current scenario, is given in Fig. 3.12. Uncertainty in the stability predictions induced by random removal of reservoirs was assessed by repeating the procedure 10 times for each value of ϵ and taking the 95% simulation enveloppe of the realizations of the resulting stability lines. The effect of water resources development on pathogen invasion is illustrated in Fig. 3.10 for the case of $\epsilon = 0.5$, results for the other two scenarios are similar and reported in Fig. 3.11. For all the reduced water resources development scenarios, the DFE tends to be stable for a wider set of mobility and contact parameters, for all levels of urban contamination and exposure rates. Examining the stability diagrams in Fig. 3.10, it becomes evident that human mobility plays an important role in the stability of the DFE, thus of pathogen invasion conditions, in these alternative scenarios. Indeed the interplay between human mobility and water resources development is greatly conditioned by the level of urban contamination/exposure rates. For $\alpha < 0.1$ the effect of building dams is most detrimental for low levels of human mobility ($m < 0.25$), while the bifurcation lines tend to be close to the invasion condition of the current scenario for $m > 0.8$. On the other hand, for high levels of urban transmission of schistosomiasis ($\alpha = 0.1$) human mobility accentuates the negative impact of the increasing number of dams by augmenting the gap between the bifurcations curves of the alternative and current scenarios $m > 0.6$. Furthermore, uncertainty in the stability of the DFE increases with the fraction of mobile people for all α's. These observations can be seen as the contribution of less connected settlements, where contamination and exposure are high, to the overall (in)stability condition of the DFE. By increasing

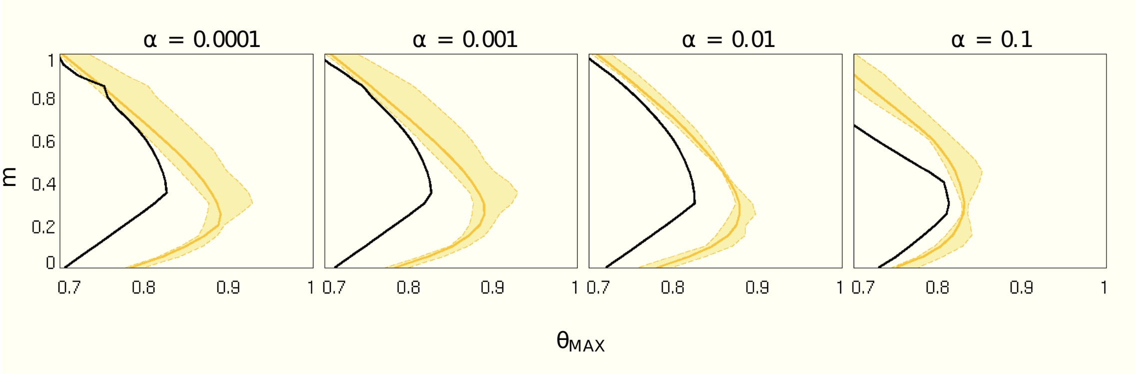

Figure 3.10 – Investigation of the side-effects of water resources development in terms of pathogen invasion conditions of schistosomiasis. The bifurcation curves ($g_0 = 1$) of the DFE are plotted for a level of water resources development corresponding to 50% of the existing reservoirs. Stability plots are given as a function of the maximal contamination and exposure rate parameter θ_{MAX} and the fraction of mobile people m. Yellow curves represent parasite invasion conditions for the alternative scenarios of water resources development, while black lines refer to the current situation (same as Figure 2), and are reported here for reference. Colour shadings represent 95% confidence intervals based on 10 scenario realizations by random removal of existing reservoirs. Regions to the right of the black and coloured lines correspond to conditions of pathogen invasion of the country, i.e. an unstable DFE, for the current and alternative scenarios respectively.

urban contamination and exposure rates, nodes with high connectivity also present high transmission, thus having a large impact on the stability of the system. When removing reservoirs that determine the number of snails in these key nodes, the stability region of the DFE expands. In other words, the system is more dependent on a small set of highly connected nodes, thus the construction of dams close to these points has a much larger effect on stability. The uncertainty associated to the location of the stability line is thus directly related to the random removal of the reservoirs influencing snail abundance in these key nodes. Human mobility therefore exacerbates the effect of water resources development on risk of pathogen invasion in the case of high urban contamination and exposure rates.

Although preliminary, these results illustrate the use of the proposed eigenvector analysis of the GRM to quantify the potential impacts of water resources development in a spatially explicit framework that includes connectivity mechanisms such as human mobility. In particular, the results of this Chapter concur with previous studies suggesting that strategies to mitigate negative effects on human health should become integral parts in the planning, implementation, and operation of future water resources development projects [*Steinmann et al.*, 2006]. In particular the interplay between the water resources development and connectivity induced by human mobility are deemed to be important in the risk of re-emergence of the disease if elimination is attained.

3.4.4 A roadmap for the implementation in Burkina Faso

Although the main focus of this work is on the system conditions requiring deployment of intervention measures in the perspective of elimination, thus far from the endemic equilibrium, an appropriate model would need to be developed and validated against historical data for the specific context of Burkina Faso. The first step in this direction would require the availability of comprehensive national scale data on disease prevalence and infection intensity that are not available on online sources. This data would allow the rigorous calibration of parameter values and the quantification of the associated uncertainty. The second step could consist in the improvement of simplifying assumptions of the model by [*Gurarie and*

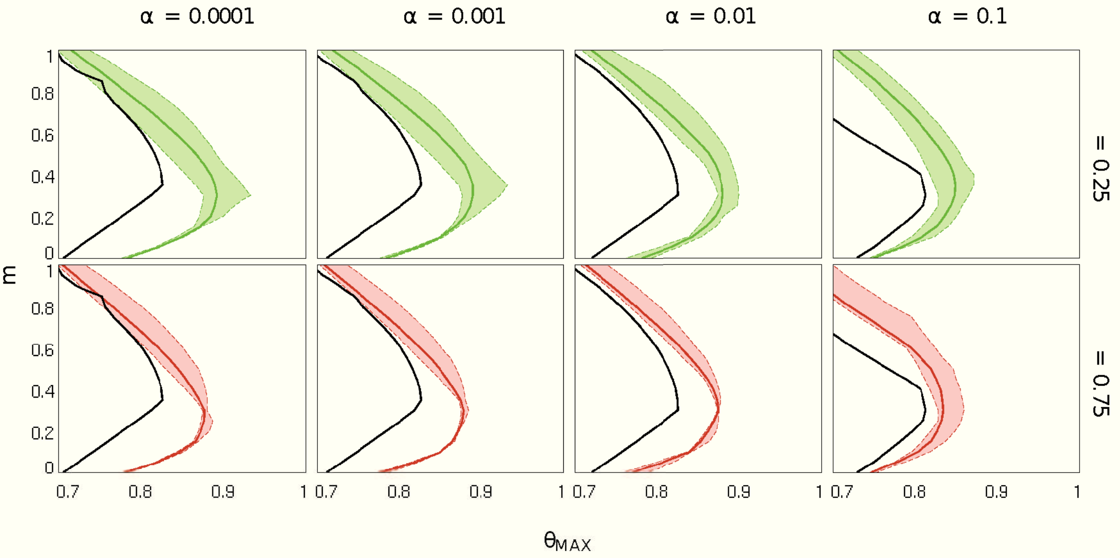

Figure 3.11 – Effects of water resources development in terms of pathogen invasion conditions of schistosomiasis. Legend as in Fig. 3.10. Coloured (green, red) curves represent parasite invasion conditions for the alternative scenarios of water resources development.

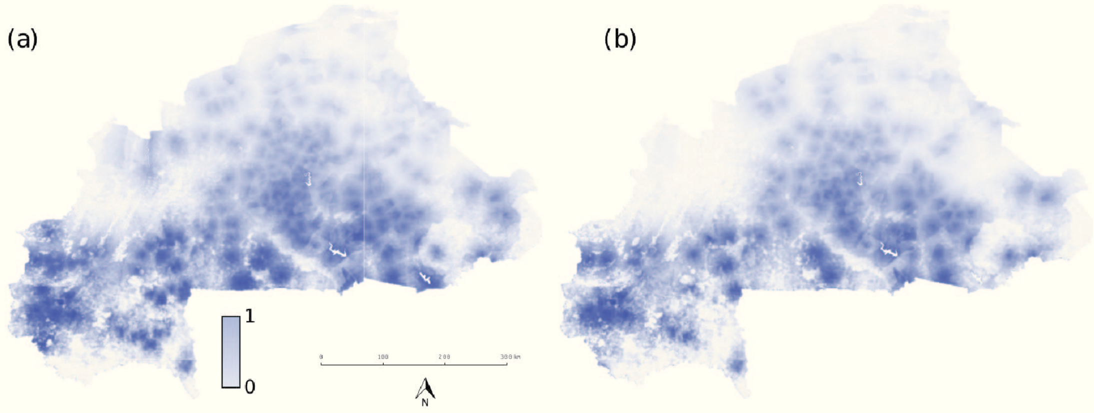

Figure 3.12 – Impact of water resources on the ecological range of the intermediate host. (a) B. pfeifferi *probability of presence for the current scenario of water resources development.* (b) *Probability of presence for an example of the alternative scenario with half the number of reservoirs ($\epsilon = 0.5$).* The predicted species distribution of *B. pfeifferi* by the MaxEnt approach reveals the importance of distance to water surfaces along with the influence of the North-South precipitation/temperature gradient which prevents the snail to colonize the Northern parts of the territory. The example of one realization of the scenario with half the reservoirs illustrates the reduction of the ecological range of the intermediate host, necessary but not sufficient condition for explaining the observed results.

Seto, 2009] and its implementation for Burkina Faso. Namely the assumptions are: (1) constant, although spatially heterogeneous, human and (2) snail populations, (3) population-dependent contamination and exposure rates, (4) no hydrologic transport of parasite larvae (5) nor of the snail intermediate host, and finally (6) mobility patterns imposed by population density. Here, parameter values were taken from previously investigated configurations, but field data collection would be needed to strengthen the use of the results presented here. If assumptions (1) and (4) are deemed to be reasonable for studying schistosomiasis at the country-level, the remaining points still need to be addressed. Snail population dynamics (2) needs to be explicitly modelled with respect to local environmental conditions governing its habitat and its population dynamics, mainly driven by hydrology [*Woolhouse and Chandiwana*, 1990a; *Poda et al.*, 1994; *Clennon et al.*, 2007]. Contact and contamination rates (3) strongly depend on human-water contacts driven by local socio-economic realities [*Utzinger et al.*, 2011; *Kpoda et al.*, 2013; *Grimes et al.*, 2014], and are of particular importance to quantify the success of control measures through education and access to clean water, sanitation and hygiene (WASH). Furthermore, the seasonal variation of the ecohydrologic parameters would need to be properly addressed and incorporated in the modelling framework [*Mari et al.*, 2014a]. For both of these aspects of particular use would be local hydro-climatic data at suitable temporal and spatial resolutions in Burkina Faso, to be assimilated along with remotely sensed data with of bridging the existing gaps in their use for schistosomiasis risk profiling [*Walz et al.*, 2015a]. Regarding human-water contacts a generalizable framework would need to be developed for the specific context of Burkina Faso based on detailed geo-referenced data on improved water sources, sanitation infrastructure and natural or man-made waterbodies, complemented by surveys and participatory-observant methods in distinct climatic, water resource availability and socio-economic contexts [*Zongo et al.*, 2012; *Kpoda et al.*, 2013]. This would reduce the uncertainty introduced with the population-density based approach presented here for estimating water-contact rates, with a particular focus on the seasonal dynamics of water contacts across the territory. Hydrological transport of the intermediate host regarding transport rates, variability, snail species specificities and seasonality are needed to evaluate the relevance of its inclusion the large-scale modelling framework propose in this Chapter. Finally, increasing access to human mobility data such as cell phone records would not only remove the necessity for modelling mobility patterns in the location where data are available (6) [*Buckee et al.*, 2013; *Wesolowski et al.*, 2013], but would also permit the validation of existing mobility models that are based on data from highly motorized countries [*Lu et al.*, 2013; *Palchykov et al.*, 2014] against the specific mobility characteristics of Sub-Saharan Africa for their use in the context of schistosomiasis study. Indeed a thorough comparison of available mobility models for the specific purpose of spatially explicit modelling of schistosomiasis.

3.5 Conclusion

By implementing dynamical system analysis techniques recently developed for water-borne diseases, the roles of human mobility and water resources development in the spread of intestinal schistosomiasis have been highlighted in Burkina Faso close with the goal of elimination. Human mobility was shown to play a role not only in the degree of success of invasion of the network of human settlements by the pathogen, but also in the spatial patterns of disease spread. For small fractions of mobile people, mobility induced a dilution effect of the parasite concentration in accessible waters leading to an effective prevention of parasite invasions, in agreement with previous results derived at much smaller spatial scales. Even in settings unfavourable to pathogen invasion, human mobility had a large effect on average times to metapopulation extinction of the pathogen. Above a threshold value, mobility prompted a systematic exacerbation of the disease by shifting its hotspots from the most populated areas (even where local conditions warrant local reproduction numbers larger than one) to more transmission-prone areas with higher contamination and exposure rates and snail abundance.

Predicting the spread of the disease based on water resources development was also investigated, specifically by quantifying the modification of the stability conditions of the disease-free equilibrium resulting from anthropogenic expansions of suitable habitats for *B. pfeifferi*, the snail acting as intermediate host in the life cycle of the parasite *S. mansoni*. By considering theoretical scenarios representative of pre-existing levels of water resources development in the country, the results in this Chapter have shown that the marked increase in the number of dams prompted by water development projects favoured pathogen invasion. For low urban schistosomiasis transmission, the greatest effects of water resources development were found to occur for low levels of human mobility, thus favouring localized transmission which maximizes the effect of each additional dam built. Interestingly, intense human mobility was also shown to exacerbate the impact of the building of the dams in the case of high levels of urban contamination and exposure rates.

This Chapter concludes that insight from the tools such as the ones develop here could directly inform national and regional control measures in the perspective of elimination in terms of pathogen invasion conditions and initial spatial spread, thus contributing to two of the points brought to the fore as research priorities for helminth modelling [*Basáñez et al.*, 2012]. Both prevention and intervention at regional scales, in fact, need to address the central role of human mobility in the perspective of the deployment of surveillance-response mechanisms and the localization of treatment measures. Controls of urban contamination and exposure rates, say by reducing contamination rates by control programs like WASH, could be measured against predicted disease burden reductions. Even at the current state of development, results of management alternatives obtained from mathematical models are potentially informative for epidemiological decisions in conditions of close-to-threshold transmission that will hopefully be in the near future the stage of elimination programs in sub-Saharan Africa and Burkina Faso. Indeed the proposed theoretical framework is an opportunity for the design of control indicators based both on timescales of pathogen extinction in addition to dynamical stability criteria. Overall, this Chapter supports the key role that mathematical toolboxes built on spatially explicit models of disease dynamics play for the prediction of the spatial patterns of schistosomiasis at regional scales.

4 Field and modelling studies on the ecology of the snail intermediate hosts

The population dynamics of the different species of snail intermediate hosts are key components in the appraisal of the socio-ecological drivers of the transmission cycle of schistosomes, in particular in seasonal climates, which impose strong fluctuations in environmental and hydrological conditions. Walking in the footsteps of the single previous study of the population dynamics of Bulinus spp. in Burkina Faso by Poda in the 1990's, this Chapter reports on field ecological sampling and environmental monitoring campaigns aiming at better understanding the ecohydrology of the distinct species of intermediate hosts across different natural and man-made habitats in the country. Although the ecological sampling methodology used here have not evolved since Poda's, what is novel in the work presented in this Chapter is the use of on-site micro-meteorological stations for continuous monitoring of environmental parameters, combined with the quantitative analysis of snail abundance timeseries data within a formal model comparison framework. This combination allowed to disentangle the ecological processes at hand, namely exogenous environmental forcing and density feedbacks. Beyond ecological insight per se, this work constitutes a first step in developing a methodology for the prediction of seasonal snail populations at the national scale[2].

4.1 Introduction

Insight into population dynamics of the intermediate hosts of human schistosomes is necessary to the understanding of the disease's ecology [*Plowright et al.*, 2008], and important to the optimization of control strategies, may it be the timing of MDA with respect to transmission seasonality, or snail population control [*Sturrock*, 1995; *Rollinson et al.*, 2013]. Snail population dynamics are typically seasonal in SSA, and have been shown to be strongly influenced by environmental conditions [*Shiff*, 1964c; *O'Keeffe*, 1985a; *Woolhouse and Chandiwana*, 1990a], although the effect of crowding on reproduction and death rates has been shown to play a role in laboratory experiments [*Jobin and Michelson*, 1967; *McCreesh et al.*, 2014]. Negative density feedbacks (*sensu Herrando-Pérez et al.* [2012]), i.e. the increase of mortality or decrease in fecundity with high population density, have been at the heart of a debate [*Shiff*, 1964c; *Jobin and Michelson*, 1967] on whether or not they must be seen as a key ecological process for the demography of the intermediate hosts of schistosomes. Density feedbacks have been alternatively accounted for [*Sokolow et al.*, 2015; *Feng et al.*, 2004; *Ciddio et al.*, 2015] or ignored [*Liang et al.*, 2007; *Chiyaka and Garira*, 2009] in spatially implicit mathematical models of schistosomiasis transmission

---

[2] The content of this chapter has been adapted from *Perez-Saez et al.* [2016]: Perez-Saez, J., Mande, T., Ceperley, N., Bertuzzo, E., Mari, L., Gatto, M. and Rinaldo, A., 2016. Hydrology and density feedbacks control the ecology of intermediate hosts of schistosomiasis across habitats in seasonal climates. *Proceedings of the National Academy of Sciences of the United States of America*, 113(23), pp.6427-6432. https://doi.org/10.1073/pnas.1602251113

that include snail demography. On the other hand, ecological studies have highlighted the role of environmental forcings in limiting snail abundance, including water temperature for *Bulinus globosus* in permanent streams in Zimbabwe [*Woolhouse and Chandiwana*, 1990a] and water level fluctuations for *Oncomelania hupensis* (the intermediate host of *S. japonicum*) in irrigation canals in China [*Remais et al.*, 2007]. *B. globosus*' population dynamics has been labeled as 'density vague' [*Woolhouse and Chandiwana*, 1990a] suggesting that, under natural conditions, snail abundance is controlled by adverse environmental conditions preventing crowding levels at which negative density feedbacks are appreciable. Occasionally, however, crowding was observed to occur in particularly favorable environments [*Sokolow et al.*, 2015]. Notably, a large body of literature exists on statistical methods for density feedback detection [*Dennis and Taper*, 1994; *Andreasen and Pugliese*, 1995; *Turchin*, 2003; *Brook and Bradshaw*, 2006].

Focusing on Burkina Faso, the intermediate hosts of the parasite species (*Bulinus* spp. for the former and *Biomphalaria pfeifferi* for the latter) have been observed in various types of natural and man-made habitats, either permanent or ephemeral (Table 4.1). From literature searches in standard online databases, only two field studies [*Poda et al.*, 1994, 1996] have addressed the ecology of snail hosts in Burkina Faso, and both highlighted notable seasonal abundance fluctuations of *Bulinus* spp. [*Poda et al.*, 1994, 1996]. This is in contrast with current assumptions of spatially explicit models of schistosomiasis transmission that neglect the dynamics of local snail abundance, which is typically assumed to be constant and treated as a parameter [*Gurarie and Seto*, 2009; *Perez-Saez et al.*, 2015]. Notably, the existing field studies had focused on two sites in similar climatic zones and did not address quantitatively the underlying ecological processes driving population dynamics, in particular density effects and drivers borne out of external environmental forcings.

Here, formal model selection, specifically structural risk minimization [*Corani and Gatto*, 2007] and other information criteria, are used to investigate the role, the relative importance, and the links among density feedbacks and environmental forcings and the fluctuating abundances of the intermediate hosts of schistosomiasis. Several population models are contrasted against field data gathered across different habitats chosen as representative of a broad range of conditions for endemic schistosomiasis throughout sub-Saharan Africa. Structural risk minimization allows to rank theoretical models of population dynamics thus clarifying the relevant covariates that explain empirical observations of snail abundance in the various sites under actual climatic forcings. As a result, statistical methods are developed based on model averaging capable of providing reliable local snail abundance projections, whose implications, like sensible generalizations of current spatially explicit epidemiological models, are discussed also in view of schistosomiasis control.

4.2 Materials and methods

4.2.1 Ecological sampling

Representative host species of both uro-genital and intestinal parasites were sampled over 15 months in the four sampling sites, in the three retained villages presented in Chapter 2. A time-based snail sampling technique was employed analogously to the one previously used in malacological studies in the country [*Poda et al.*, 1994; *Sokolow et al.*, 2015]. The sampling protocol consisted of systematically scooping the investigated habitats for 30 minutes using a 2 mm metal mesh mounted on a wooden pole of 1.5 m [*Hairston et al.*, 1958; *Sokolow et al.*, 2014]. The number of collected snails and sampling metadata were recorded in dedicated sampling sheets. *Bulinus* spp. or *Biomphalaria* spp. specimens were stored in dated collection cups in a mixture of clear well water and (90%) alcohol (see e.g. [*Sokolow et al.*,

Table 4.1 – Occurrence and habitat preferences of snail intermediate host species of human schistosomes in Burkina Faso. Species relative occurrence is indicated by (+++) most common, (++) common, (+) rare. Qualitative habitat preference is given by (***) preferred, (**) very common, (*) recurrent, (-) rare or not observed. Symbols are qualitative interpretation of data from 496 biotopes across the country reported by [*Poda et al.*, 2004a].

Schistosome species	**Snail species**	**Occurrence**	**Habitat preference**				
			reservoir	stream	pond	irrigation canal	lake
Schistosoma haematobium	*Bulinus truncatus*	+++	***	**	**	*	*
	B. senegalensis	+++	**	**	***	-	-
	B. globosus	++	**	***	-	*	*
	B. forskalii	++	**	**	*	-	-
	B. umbilicatus	+	*	*	-	-	-
Schistosoma mansoni	*Biomphalaria pfeifferi*	+++	**	***	-	*	*

2015]). Sampling was undertaken by suitably trained field technicians. Training was provided during one week before the start of the campaign, and feedback was given by bi-weekly contacts (phone calls) and regular on-site visits during the entire sampling campaign. Biological samples were sent every 3 months back to the Microbiology and Biotechnology Laboratory of the *Institut International d'Ingenierie de l'Eau et de l'Environnement* (2iE) in Ouagadougou for recounting and species identification using standard identification keys [*Brown*, 1980; *Sokolow et al.*, 2014, 2015]. The main *Bulinus* species that were collected were *B. truncatus* in the irrigation canal in Tougou and in the ephemeral stream in Lioulgou, *B. senegalensis* in the temporary pond in Lioulgou, and *B. globosus* in the perennial stream in Panamasso. A preliminary survey was carried out along the shores of the reservoir of Tougou, during which no snails were found. Given that this type of habitat had already been covered in previous studies [*Poda et al.*, 1994], regular snail sampling was not performed along the reservoir shores. Note that the irrigation canal was dry from April to June, while intense rainfall events flooded the canal and the surrounding rice fields in August, making the area *de facto* inaccessible during a period of about two weeks. Because of such exceptional environmental conditions, the analysis of the snail dynamics in the canal focuses on the period up to March 2015.

4.2.2 Population dynamics modelling

Density feedback detection in ecological timeseries has received considerable attention in the literature, building on a common framework of relatively simple mechanistic models for population dynamics coupled with statistical methods for discriminating among alternative feedback processes [*Dennis and Taper*, 1994; *Turchin*, 2003; *Brook and Bradshaw*, 2006]. Here, snail population dynamics is simulated by discrete-time demographic models inclusive of extrinsic environmental forcing. Specifically, if N_t denotes the abundance of the snail population in a given habitat at sampling time t, the simplest demographic model reads

$$\mathrm{N}_{t+1} = \lambda \mathrm{N}_t, \tag{4.1}$$

where λ corresponds, whatever its attributes, to the finite instantaneous growth rate of the population between two sampling dates. This simple Malthusian formulation can be extended to incorporate non-linear density feedback as proposed by Ricker in the form

$$\mathrm{N}_{t+1} = \lambda \mathrm{N}_t e^{b\mathrm{N}_t}, \tag{4.2}$$

were b is a parameter that sets the feedback' strength [*Ricker*, 1954]. On taking logarithms, the Ricker model reads:

$$\log\left(\frac{\mathrm{N}_{t+1}}{\mathrm{N}_t}\right) = a + b\mathrm{N}_t, \tag{4.3}$$

where $a = \log\lambda$. Negative density feedback occurs for $b < 0$, i.e., decreased recruitment and/or increased death rates at high population densities. In the following a denotes the instantaneous intrinsic population growth rate. Depending on the values of a and b, the model can produce a wide range of dynamical behaviors including steady states, limit cycles and chaos [*Corani and Gatto*, 2007]. Obviously, one recovers the original Malthusian model by setting $b = 0$.

Exogenous forcing of environmental covariates, their lags, and lagged effects of abundance [*Turchin*, 1990], can be accounted for as:

$$\log\left(\frac{\mathrm{N}_{t+1}}{\mathrm{N}_t}\right) = a + \sum_{\tau_\mathrm{N}=0}^{r_\mathrm{N}} b_{\tau_\mathrm{N}} \mathrm{N}_{t-\tau_\mathrm{N}} + \sum_{i=1}^{m} \sum_{\tau_\mathrm{X}=0}^{r_\mathrm{X}} c_{i\tau_\mathrm{X}} X^i_{t-\tau_\mathrm{X}}, \tag{4.4}$$

where: b_{τ_N} and $c_{i\tau_\mathrm{X}}$ are respectively the weights of the lagged population abundances $N_{t-\tau_\mathrm{N}}$, and the environmental covariate features, $X^i_{t-\tau_\mathrm{X}}$, taken at non-negative integer time lags $\tau_\mathrm{N} \leq r_N$ and $\tau_\mathrm{X} \leq r_X$. Lagged covariate features were taken in all possible combinations for a given maximum number m. Lagged abundance effects were only considered one at a time or all at once. Product interactions of the type $N_{t-\tau_\mathrm{N}} X^i_{t-\tau_\mathrm{X}}$ were not considered.

A second class of models that incorporate density feedbacks is the Gompertz scheme [*Gamito*, 1998], where the feedback is a function of the logarithm of population abundance, $\mathrm{L}_t = \log(\mathrm{N}_t)$, rather than abundance itself. The Gompertz model can be cast in the same form as eq. 4.4, i.e.

$$\log\left(\frac{\mathrm{N}_{t+1}}{\mathrm{N}_t}\right) = a + \sum_{\tau_\mathrm{N}=0}^{r_\mathrm{N}} b_{\tau_\mathrm{N}} \mathrm{L}_{t-\tau_\mathrm{N}} + \sum_{i=1}^{m} \sum_{\tau_\mathrm{X}=0}^{r_\mathrm{X}} c_{i\tau_\mathrm{X}} X^i_{t-\tau_\mathrm{X}}. \tag{4.5}$$

Note that the logarithmic dependence of the rate of increase on abundance implies a milder density feedback process.

The modelled demographic processes were assumed to be subject to multiplicative log-normal white noise, resulting in additive Gaussian for the logarithms of the discrete rates of increase i.e.

$$y_t = \log\left(\frac{\mathrm{N}_{t+1}}{\mathrm{N}_t}\right), \tag{4.6}$$

yielding a linear regression equation

$$y_t \;=\; f(\mathbf{N}, \mathbf{X}, \boldsymbol{\theta}) + \epsilon_t, \tag{4.7}$$

where $f(\cdot)$ is the model structure used for the regression, $\mathbf{N}$ is the time vector of abundance observations, $\mathbf{X}$ is the matrix of environmental covariate features, $\boldsymbol{\theta} \in \mathscr{R}^k$ is the vector of true regression parameters,

$$\epsilon_t \overset{\text{iid}}{\sim} \mathcal{N}(0, \sigma^2) \tag{4.8}$$

are the regression residuals, and σ is the standard deviation of the white noise.

These demographic models were also contrasted with random walk models in the standard form:

$$y_t = \epsilon_t + f(\mathbf{X}, \boldsymbol{\theta}), \tag{4.9}$$

which was also tested against all ecological time series.

4.2.3 Model implementation

The selection of demographic models required calibration via least-square regression of all possible linear combinations of covariate features within the four modelling families described in the text (namely, random walk, Malthusian, Ricker and Gompertz). Continuous environmental covariates consisted of average and standard deviation of the measurements taken over the week preceding snail sampling dates at each site (Table 2.1). Precipitation data covariates consisted of cumulative sums over two different windows (2 weeks and 1 month), and of the number of precipitation events - daily precipitation higher than 20mm - during the week preceding sampling dates. A limit of $r_X = 3$ time lags on the covariates was imposed, which is equivalent to taking into account habitat environmental conditions up to 1 month preceding sampling. Furthermore the maximum number of covariate features was set to $m = 7$ in the face of the relatively limited number of ecological data points (a maximum of 66 weeks of data), and the number of resulting models to be tested. Lags in the effect of population abundance were limited to $r_N = 3$, and density feedback processes were tested either individually (therefore only one lag present for each combination of environmental covariates), or all together. For a given m, all possible combinations of parameters were tested, giving a total number of models to test equal to the sum of the number of lagged covariate combinations, $\sum_{j=0}^{m} \binom{M}{j}$, were M is the total number of available features and their lags (38 in this study), times the number of model structure types (namely, random walk, Malthusian, Gompertz and Ricker) accounting for lagged abundance covariates:

$$(2(\tau_{\text{N}} + 1) + 2) \sum_{j=0}^{m} \binom{38}{j} \approx \mathcal{O}(10^7) \tag{4.10}$$

for $m = 7$. Weeks in which no snails were observed were given an abundance of 1 to be able to compute logarithms. The Gompertz and Ricker models for which the estimated intrinsic rate of increase was negative, $\hat{a} < 0$, or suggesting positive density feedback, $\hat{b}_{\tau_{\text{N}}} > 0$, were rejected as implausible. Indeed, no experimental evidence of positive density feedbacks for any intermediate host species of schistosomiasis emerges from readily accessible litterature sources. The positive constraint on a is necessary to ensure that the modelled dynamics have a positive nontrivial equilibrium abundance [*Corani and Gatto*, 2007]. Multiplicative interactions between variables were not considered. The computations were run in parallel with R (R Core Team (2015). *R: A Language and Environment for Statistical Computing.* R Foundation for Statistical Computing, Vienna, Austria) and the `foreach` package (Revolution Analytics & Weston, S. (2014). *foreach: Foreach looping construct for R*, R package version 1.4.2.) on the CASTOR cluster of the Scientific IT and Application Support Center of EPFL.

4.2.4 Model identification and selection

Statistical tools for the detection of density feedbacks have been extensively studied, for instance through the use of hypothesis testing with bootstrapping [*Dennis and Taper*, 1994], or information-theoretical methods such as the Akaike information criterion (AIC) [*Johnson and Omland*, 2004]. Recently, Structural

Risk Minimization (SRM) has been proposed as a viable alternative as a tool for ecological model selection [*Corani and Gatto*, 2007]. One advantage of SRM is that it does not depend on particular assumptions about the nature of the joint probability distribution of process and measurement errors. It has been shown to yield better density feedback recognition capabilities than widely used compensated Akaike information criteria (AICc) [*Brook and Bradshaw*, 2006; *Corani and Gatto*, 2007]. Within the SRM framework, the selection criterion corresponds to the choice of the model structure and parameter set that minimize the empirical upper bound of the true structural risk (R), given by:

$$\mathrm{R}(\boldsymbol{\theta}) \le \mathrm{R}(\widehat{\boldsymbol{\theta}}) = \frac{1}{q}\,\frac{\sum_{t=1}^{q}\widehat{\epsilon}_t^2}{\left[1-\sqrt{p-p\log(p)+\frac{\log(q)}{2q}}\right]_+}\ , \tag{4.11}$$

where

$$\hat{\epsilon}_t = y_t - f(\mathbf{N},\mathbf{X},\hat{\boldsymbol{\theta}}) \tag{4.12}$$

gives the estimated model residuals associated to the vector $\hat{\boldsymbol{\theta}} \in \mathscr{R}^{k\times 1}$ of optimal parameter estimates for a given model structure $f(\cdot)$, k is the number of parameters, q is the total number of observations, and p is an index of complexity known as the VC-dimension, conveniently equal to k/q in the case of linear models. The denominator is kept if strictly positive [*Corani and Gatto*, 2007].

To assess the actual predictive ability of the models retained by the SRM criterion, leave-one-out cross-validation (LOO-CV) was performed, consisting of sequentially removing one data point, re-fitting the models to the rest of the data, and predicting the values of the ignored observation. The LOO-CV residuals, say $\widetilde{\epsilon_t}$, resulting from this process are used to assess the predictive capacity of each model based on the mean squared cross-validation error [*Turchin*, 2003],

$$\mathrm{MSE}^{\mathrm{cv}} = \sum_{t=1}^{q}\widetilde{\epsilon}_t^2/q. \tag{4.13}$$

The MSE$^{\mathrm{cv}}$ is an unbiased estimator of the true expected model MSE, thus providing a way of comparing models using MSE$^{\mathrm{CV}}$ ratios. Moreover candidate models can be combined using LOO-CV to obtain an optimal average model for prediction by minimizing the weighted sum of the cross-validation residuals of the retained set of models [*Hansen and Racine*, 2012], resulting in the so-called jackknife model average (JMA, see below). Given the large number of tested models, here this technique was applied to a subset of the models retained using the SRM criterion. The same modelling framework was used to validate the results with the available historical ecological data in Burkina Faso gathered from the literature [*Poda et al.*, 1994].

Fig. 4.5 shows that the SRM criterion can rank the models according to their predictive power (i.e. according to the smaller values of MSE^{CV}) . Density feedback processes selected by the SRM criterion were consistent with the ones selected with other commonly used criteria. Fig. 4.6 show results for the AICc criterion [*Brook and Bradshaw*, 2006; *Corani and Gatto*, 2007], formulated as

$$\mathrm{AIC}_C = 2k - 2\log\left(\frac{1}{q}\sum_{t=1}^{q}\widetilde{\epsilon}_t^2\right) + \frac{2k(k+1)}{q-k-1}, \tag{4.14}$$

and the Bayesian information criterion (BIC), given by

$$\mathrm{BIC} = k\log(q) - 2\log\left(\frac{1}{q}\sum_{t=1}^{q}\widetilde{\epsilon}_t^2\right). \tag{4.15}$$

Note that, as opposed to the SRM criterion in eq. 5, k is the number of parameters of the model plus 1 (including the estimation of the noise variance), q is the total number of observations, and the $\widehat{\epsilon_t}$ are the estimated residuals of the model.

Details on lagged density feedback and covariate occurrence in best selected models for the ecology of the snail populations are given in Fig. 4.7, highlighting the distinct roles of hydrologic controls across habitats and climatic regimes.

4.2.5 Abundance prediction through jackknife model averaging

By applying models to intermediate host abundance data two goals are pursued: model identification, to disentangle the ecological processes underpinning snail population dynamics, and evaluating the model predictive capacity in the perspective of building demographic forecasting tools. The proposed model selection process yields a set of models with minimal structural risk that can be combined to build a predictive model that outperforms any single model candidate. Model averaging consists in assigning a weight to each model. Such weight is a function of its score in terms of an information criterion such as the Akaike Information Criterion or the Bayesian Information Criterion (see [*Claeskens et al.*, 2008] for an overview on model averaging techniques). Here, specifically, the so-called Jackknife model averaging technique is used (for the derivations and properties of this technique the reader is referred to [*Hansen and Racine*, 2012]). The jackknife model average (JMA) estimator is asymptotically optimal when dealing with weighted averages of linear regression estimators (with positive weights summing to 1) in terms of minimizing both the in-sample fit, and the expected true error (*sensu* [*Efron*, 1982]) which accounts for un-observed data. Furthermore the JMA method holds also for heteroscedastic errors. Finally it outperforms information-criteria-based model averages on finite-sample simulation benchmark experiments [*Hansen and Racine*, 2012]. In this procedure the JMA ensues directly from the computation of the leave-one-out cross-validation (LOO-CV) mean-squared error statistic used to asses model predictive power, $\mathrm{MSE}^{\mathrm{cv}} = \sum_{t=1}^{q} \widetilde{\epsilon_t}/q$, where the $\widetilde{\epsilon_t}$ are the residuals of the model fit to the dataset removing the data point at time t, and evaluated at time t. In the JMA framework, the aim is to determeine the weight vector $\mathbf{w}$ that minimizes the expected true error of the model average. Let $\widetilde{\boldsymbol{\epsilon}^j}$ indicate the vector of jackknife residuals for model j among N candidate models. The estimate the of expected true error is

$$CV_N(\mathbf{w}) = \frac{1}{N}\mathbf{w}^T\widetilde{\boldsymbol{\epsilon}}^T\widetilde{\boldsymbol{\epsilon}}\mathbf{w} \tag{4.16}$$

where CV_n is the least-square cross-validation criterion, and $\widetilde{\boldsymbol{\epsilon}}$ is the matrix composed of the N LOO-CV residual vectors $\widetilde{\boldsymbol{\epsilon}^j}$. Given the expression of the expected true error, computing the optimal weight vector $\hat{\mathbf{w}}$ to obtain the JMA reduces to solving the quadratic programming problem

$$\begin{array}{ll} \underset{\mathbf{w}}{\text{minimize}} & CV_N(\mathbf{w}) \\ \text{subject to} & \mathbf{w}^T\mathbf{1}_N = 1, \\ & \mathrm{diag}(\mathbf{w})\mathbf{1}_N \geq \mathbf{0}_N, \end{array}$$

where $\mathbf{0}_N, \mathbf{1}_N$ denote $N \times 1$ vectors of 0s and 1s respectively, and $\mathrm{diag}(\mathbf{u})$ denotes a diagonal matrix with main diagonal composed of the elements of $\mathbf{u}$. The constraints force the weights to be non-negative and to sum to 1. The optimization problem can be solved using any quadratic programming tools. The `quadprog` package in R (Weingessel, A. (2013). `quadprog`*: Functions to solve Quadratic Programming Problems.* R package version 1.5-5.) was used in this analysis.

The roles of density feedbacks and environmental covariates are further illustrated in terms of regression coefficients values by species and habitat in Tables S4-S8.The weights of the 500 best models for each habitat and species show that only a reduced number of models are indeed included in the JMA, and that the best SRM models did not systematically appear in the model average (Fig. 4.9).

4.2.6 Historical data and results validation

Only two field studies have specifically focused on the population dynamics of intermediate hosts of schistosomes in Burkina Faso. Both studies were conducted in the 90's and concerned a temporary pond harbouring *Bulinus senegalensis* (12°11′41"N, 2°35′58"W) and a small reservoir in the central part of the country for *Bulinus truncatus* (12°12′54"N, 2°28′36"W) [*Poda et al.*, 1994, 1996] (Fig. 1.3). Ecological data consisted of fortnightly relative abundance counts using a 30-min sampling technique (see Sampling protocol below).

Environmental covariates were measured locally on snail sampling dates, including water temperature, conductivity and pH. Bi-weekly cumulative precipitation was available for a location adjacent to the sampling sites. Significantly, data showed an annual peak of snail abundance during the rainy season in both habitats, followed by subsequent population reduction and snail aestivation in the case of the temporary pond (Fig. 2.4). *B. senegalensis* abundance presented a double-peak in the temporary pond, with an early peak around July at the start of the rainy season and a second one around October. On the other hand, *B. truncatus* was present in the monitored reservoir during a much longer portion of the year, with a peak of population abundance at the end of January. Poda et al. investigated the correlations between snail counts and environmental covariates, reporting as significant the negative correlation with temperature for *B. truncatus*, and a positive association with pH for *B. senegalensis*.

4.3 Results

Burkina Faso experiences pronounced seasonal climatic fluctuations along a South-North gradient. Seasonality, in turn, greatly affects the suitability of snail aquatic habitats [*Poda et al.*, 1996]. Rainfall occurs mainly during the rainy season (July-October), with little or no rain falling during the rest of the year (Fig. 2.6). Temperatures reach 45-50 °C in the dry season [*Mande et al.*, 2015].

Abundance data show that snail populations in different climatic zones and habitats presented distinct seasonal patterns (Fig. 4.1 F,G,H). Of the three villages in which the fieldwork was performed (Fig. 4.1 A), only Panamasso harbored the intermediate host of intestinal schistosomiasis (*B. pfeifferi*) whereas *Bulinus* spp. was found in all sites. Large populations were observed in the irrigation canal in Tougou during normal irrigation operation conditions (Fig. 4.1 F). In the ephemeral habitats of Lioulgou, snails were absent during most of the year, from December to July, and population peaked towards the end of the rainy season between September and October (Fig. 4.1 G). Opposite fluctuations were observed in the permanent stream of Panamasso for both *B. pfeifferi* and *Bulinus* spp., for which the maximum abundance was observed in the middle of the dry season between January and March. Such annual fluctuations are consistent with the ones observed in the historical data in both a temporary pond and a man-made reservoir experiencing climatic conditions similar to the ones in Lioulgou [*Poda et al.*, 1994, 1996].

According to model selection results (Fig. 4.2), density feedbacks were detected across all species and habitats although operating at different strength depending on habitat type, environmental/hydrologic

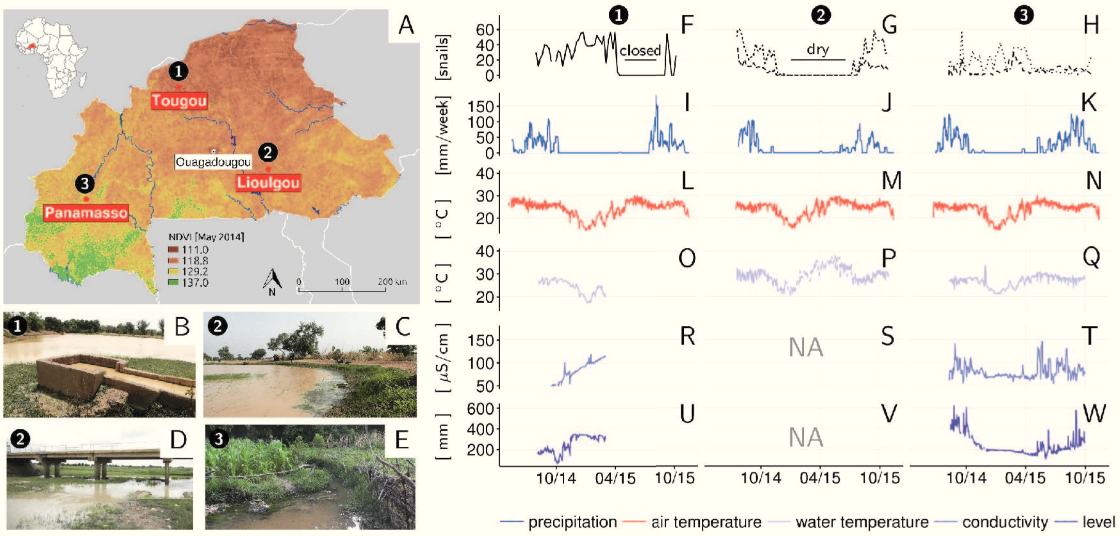

Figure 4.1 – Ecological and environmental field data. A: Situation map of the field sites (black dots) chosen along the South-North climatic gradient in Burkina Faso, here highlighted by values of Normalized Difference Vegetation Index. B-E: Illustrations of the ephemeral or permanent habitats chosen for snail sampling in the experimental sites of Tougou, Lioulgou and Panamasso. F-W: Ecological and environmental data timeseries. Weekly snail relative abundance data are given per species and habitat, *Bulinus* spp. in a canal in Tougou (full line, F), in a pond (short dashed line) and a stream (long dashed line) in Lioulgou (G), and *Biomphalaria pfeifferi* (dashed line) and *Bulinus* spp. (dotted line) in a stream in Panamasso (H). Periods during which the habitat dried out are indicated for Lioulgou and Tougou (canal closed for operational reasons). In column are reported their respective environmental data. Environmental data consists of weekly cumulative precipitation (row I-K), and daily averages of air temperature (L-N), water temperature (O-Q), conductivity (R-T) and water depth (U-W). Empty panels indicate ephemeral habitats.

conditions, and specific snail species. A strong density feedback (i.e. the Ricker model) was consistently selected only for *Bulinus* spp. in the ephemeral stream (Fig. 4.2 W). Weaker density feedbacks (i.e. the Gompertz model) were selected for *Bulinus* spp. in the irrigation canal (Fig. 4.2 U), the temporary pond (Fig. 4.2 V), and the perennial stream (for both *Bulinus* spp. and *B. pfeifferi*, Fig. 4.2 X,V). The strength of density feedbacks also varied across species and habitats in the weak group (4.3), i.e. in decreasing order: *Bulinus* spp./canal > *B. pfeifferi*/stream > *Bulinus* spp./stream > *Bulinus* spp. pond. Density feedback results were fairly consistent for all species for all of the best 100 models, although the model ranked first by structural risk minimization (SRM) for *Bulinus* spp. in the temporary pond corresponds to a random walk model. This could be due to the apparent lack of autocorrelation in the time series of population increments (tested using the Box-Ljung statistics, p-value> 0.05), although a clear pattern of population fluctuation emerges. Results obtained using alternative selection criteria generally agreed with the SRM criterion regarding the presence of density feedback in all habitats (4.3). The analysis of the historical temporary pond data further supports the results described above, although the limited amount of environmental data probably biased the prominent ratings of random walk models (4.10).

Environmental covariates were also found to play different roles in different settings. The importance of exogenous forcing in host population dynamics was quantified in terms of the frequency of occurrence of the monitored covariate types in the features of the 500 best regression models (Fig. 4.2, Figs. S4,S5). Physical and chemical characteristics of the water (including temperature and conductivity) were most important for snail species in both perennial habitats: *Bulinus* spp. in the irrigation canal (Fig. 4.2 F,K); *Bulinus* spp. and *B. pfeifferi* in the perennial stream (Fig. 4.2 J). In both ephemeral habitats (pond and stream, Fig. 4.2 B-C), *Bulinus* spp. were mostly conditioned by the variations in air and water temperatures,

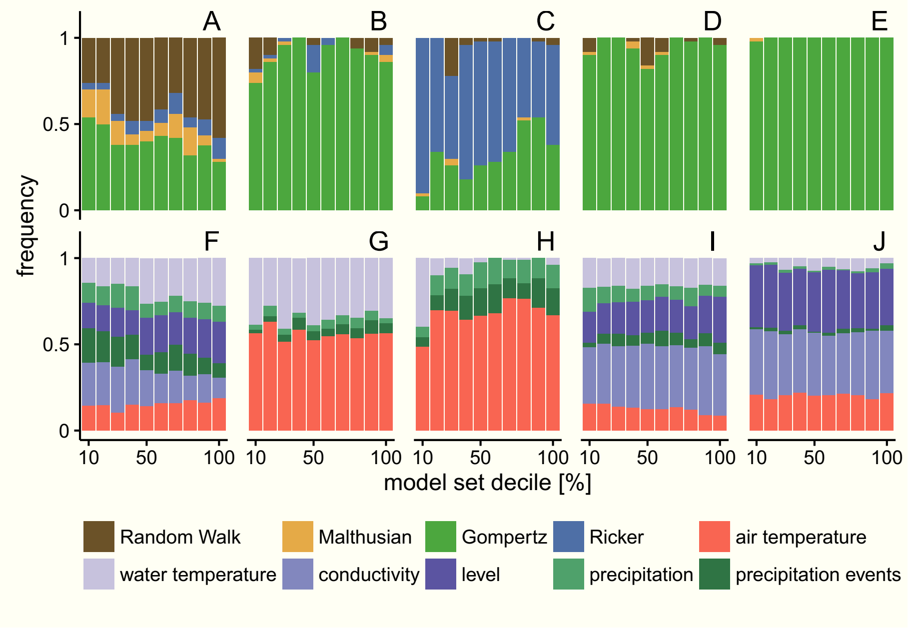

Figure 4.2 – Density feedbacks, environmental covariates, and snail population dynamics. The strength of density feedbacks (row A-E) and of measured environmental covariate features (F-J) is given in terms of the frequency of appearance in the 500 best selected models, summarized by decile (decile 10 corresponds to the top 10% model outcomes). Results are shown by columns for *Bulinus* spp. in the irrigation canal (A-F), in the temporary pond (B-G), in the ephemeral stream (C-H), and for *B. pfeifferi* (D-I) and *Bulinus* spp. (E-J) in the perennial stream.

and much less by precipitation. Water level and conductivity were singled out as important determinants in the perennial stream for both *B. pfeifferi*, and, to an even greater extent, *Bulinus* spp. (Fig. 4.2 N,O). This is in contrast with the snail dynamics in the irrigation canal, a permanent snail habitat. Water temperature did not appear frequently in selected models in the perennial stream habitat for both genera, either in terms of average values or of measures of variability (Fig. 4.4). Precipitation (either cumulative or event-based) seldom appeared in the top 500 models for *Bulinus* spp, and in a slightly larger proportion for *B. pfeifferi*. Finally, air temperature's average and fluctuations were dominant in models for both ephemeral habitats, whereas they were only marginally present in the permanent habitats. Inclusion of lags in both the density feedback and the environmental features was also varied among snail species and habitats, shedding additional light on the biology of snail development on which they possibly intervene (Fig. 4.7). Interestingly, a significant density feedback was singled out only during the week preceding snail sampling date for the Ricker and Gompertz models. This points at increased death rates due to crowding rather than at reduced reproduction, as suggested also by laboratory experiments [*Jobin and Michelson*, 1967]. Environmental covariates had significant effects at different time lags for different habitats and species. Most of the effects were shown at short time lags (1-2 weeks) in the ephemeral habitats (pond and stream), at intermediate lags (2-3 weeks) in the irrigation canal, and at longer ones (3-4 weeks) in the perennial stream. Indeed, water temperature effects were frequently observed at short lags for *Bulinus* spp. in the temporary pond (1 week preceding sampling), and at longer lags in the irrigation canal and the perennial stream (3-4 weeks). Similarly, water conductivity was mainly selected at 3 or 4 weeks lag for both genera in the perennial stream, indicating a connection with the reproduction/development phases of the snail hosts. Water level fluctuations affected *B. pfeifferi* at short lags (1 week), and at longer lags (3-4 weeks) *Bulinus* spp. (Fig. 4.7), a figure suggesting differential susceptibility to hydrologic conditions. In the models where they were selected, precipitation events were only singled out at short time lags both

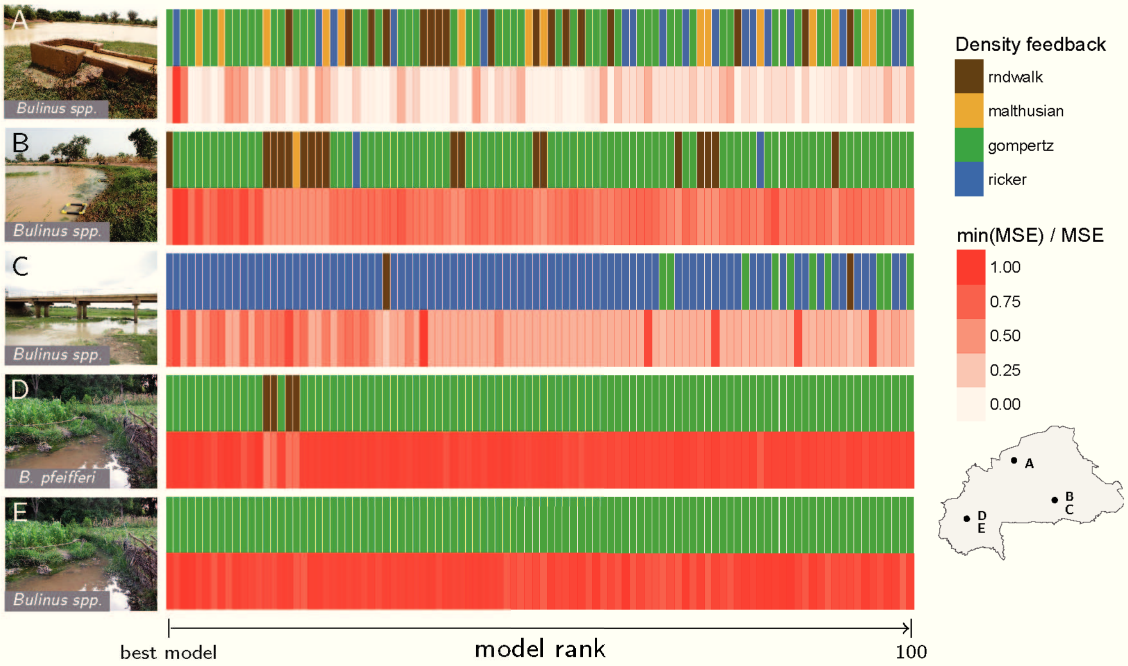

Figure 4.3 – Density feedback detection in snail population dynamics. Model structures selected by the SRM criterion are shown by row for *Bulinus* spp. in the irrigation canal in Tougou (A), the temporary pond (B) and the ephemeral stream (C) in Lioulgou, and in the perennial stream in Panamasso (E), *B. pfeifferi* is only present in the latter (D). Each column represents a model structure, ranked in descending SRM criterion order (first from the left being the best). Density feedback is associated to model type: Malthusian (yellow) correspond to no feedback, Gompertz (green) to mild and Ricker (blue) to strong feedback, and random walk models are indicated in brown. Relative model predictive power is illustrated by the ratio of the smallest cross-validation mean squared error, min($\mathrm{MSE}^{\mathrm{CV}}$), to the model $\mathrm{MSE}^{\mathrm{CV}}$, 1 (red) indicating best relative predictive power among candidate models for a given habitat an species. The inset to the right gives the location of the sampling sites in Burkina Faso.

in temporary habitats and perennial stream.

The use of structural risk minimization (SRM) allows the selection of models suitable for predictions. Their predictive power was generally found to be consistent with model ranking (4.5). This confirms the ability of the SRM criterion to select for adequate levels of ecological complexity, supporting its use as a ranking tool. The SRM rank was therefore used for choosing the subset of all tested models to include in the jackknife model average (JMA) (4.9). Of the $\mathcal{O}(10^7)$ models that were investigated in each site, the best 500 in terms of SRM were averaged to evaluate the prediction capacity of the model set. JMA captured both the trend and local variabilities of the snail abundance time series across habitats (Fig. 4.8), although it included only a fraction of the 500 best SRM-ranked models for each species and habitat (Fig. 4.9). The population dynamics in the canal during the time period were accurately reproduced, in particular the population peak observed in November. Within ephemeral habitats, the JMA reproduced well the seasonal variations of snail abundance with the initial population burst at the beginning of the wet season, a first peak in July and a second peak in October. Snail dynamics in the perennial stream were well predicted for *Bulinus* spp., with a population reduction during the rainy season from June onward and high abundance in March-April. For *B. pfeifferi* the prediction of the seasonal variation was slightly worse, with the March peak not as marked as in the field data. Remarkably, for both species single models overshoot the prediction of snail abundance in August and July because of the strong variability

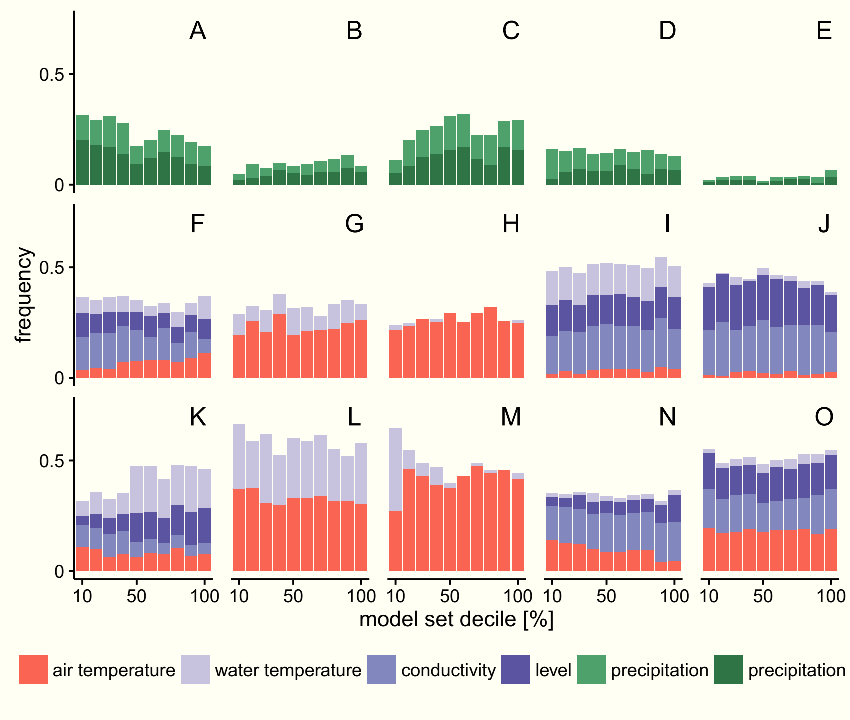

Figure 4.4 – Environmental covariates and snail population dynamics. The importance of measured environmental covariate features is given in terms of the frequency of appearance in the 500 best selected models, summarized by decile (decile 10 corresponds to top 10% model rankings). Results are shown by columns for *Bulinus* spp. in the irrigation canal (A-K), in the temporary pond (B-L), in the ephemeral stream (C-M), and for *B. pfeifferi* (D-N) and *Bulinus* spp. (E-O) in the perennial stream. Results are partitioned by row by the type of covariate feature, including cumulative sums for precipitation (row A-E), and weekly average (F-J) and standard deviation (K-O) for air temperature and water conductivity, level and temperature.

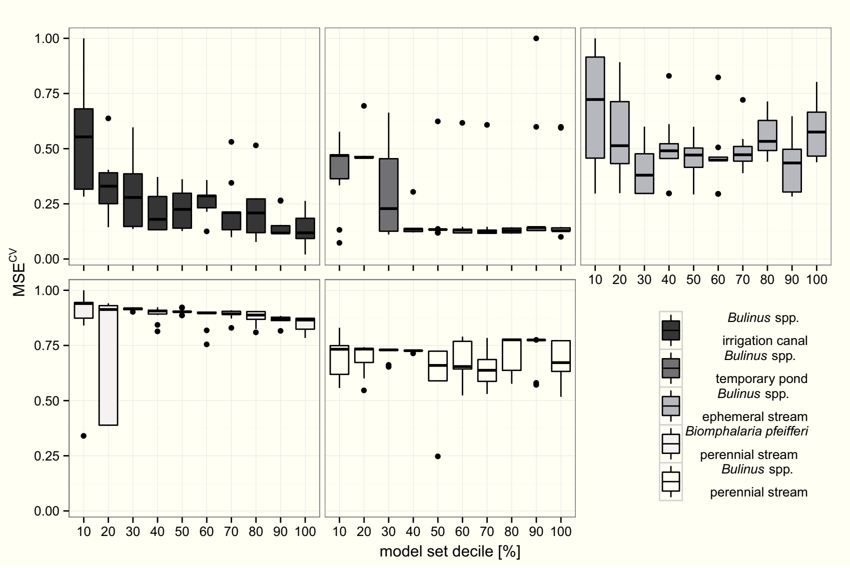

Figure 4.5 – SRM criterion rank and predictive capacity. Cross-validation error boxplots are given for each decile for the top 100 models selected by the SRM criterion. Results are partitioned by species and habitat.

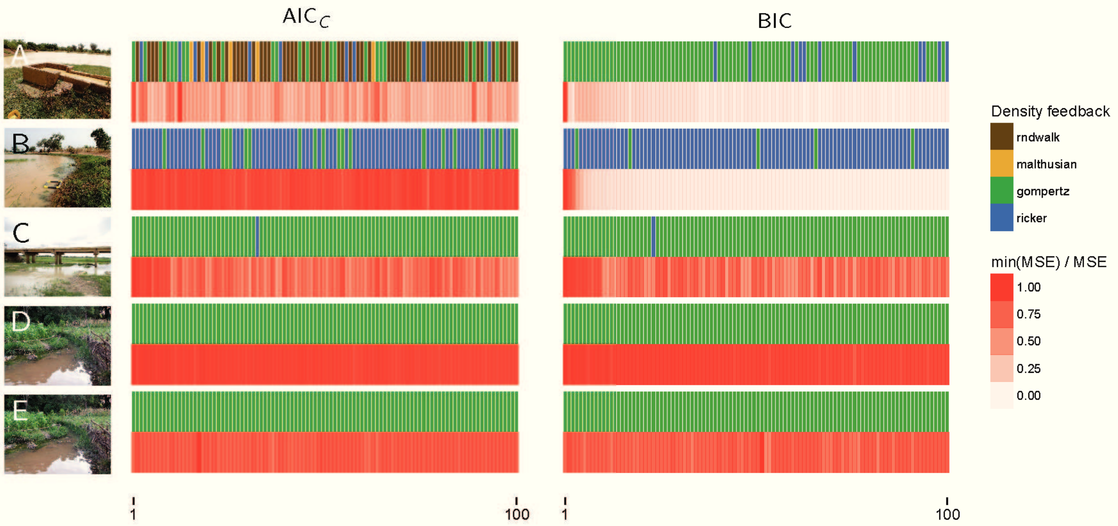

Figure 4.6 – Model identification and cross-validation error with the AICc and BIC criteria. Results are given in the same order and using the same colorcoding as Fig. 4.8, for *Bulinus* spp. in the irrigation canal in Tougou (A), in the ephemeral pond (B) and stream (C) of Lioulgou, and in the perennial stream of Panamasso for *B. pfeifferi* (D) and *Bulinus* spp. (E).

in the environmental covariates, especially water level and conductivity, while the JMA offers reliable out-of-sample predictive ability. It is to be noted that the JMA performed remarkably well on historical data (at bi-weekly intervals) despite the lack of continuous environmental measurements (Figs. 4.10). This is encouraging towards the extension of the approach presented in this Chapter to settings where scarce environmental and ecological data are available.

The modelling framework used to analyze the field observations presented here was also applied to the historical data available for Burkina Faso. Continuously monitored environmental signals were used in this study, whereas only point data (on the dates of snail sampling) were available in the historical studies, thus containing less information about the environmental conditions impacting snail development and reproduction. Interestingly, density feedbacks were consistently found by contrasting Poda's reservoir data via the SRM criterion. Most of the 100 best SRM models selected for the temporary pond, however, corresponded to the random walk model, indicating that the upper bound of the structural risk does not support any ecological modelling (Fig. 4.10 A). It seems likely that this result stems from the limited amount of available environmental data in the 1990-1992 time series, but no proof can be provided. Nevertheless, AICc, BIC, and LOO-CV MSE favored the Gompertz model type, i.e. a mild density feedback (Fig. 4.10 B). This less clear-cut model identification is speculated to be a direct consequence of the lack of continuous environmental data, specifically for the temporary pond during the dry season.

The JMA was able to satisfactorily capture the multi-annual dynamics of *Bulinus* spp. in both habitats. It may be noted that the best selected models overestimate the initial population rate of increase in the reservoir whereas the JMA adequately smooths them out (Fig. 4.10 C). Interestingly, a density feedback in the reservoir was found to be correlated to the snail population one month before snail sampling dates, in contrast with the feedbacks identified in the habitats studied in the fieldwork of this Thesis. Models for both habitats were mainly driven by water temperature (particularly in the temporary pond), with pH, cumulative precipitation and conductivity appearing less frequently (Fig. 4.10 B). The performance of the JMA is encouraging despite the lack of continuously measured environmental data for the potential

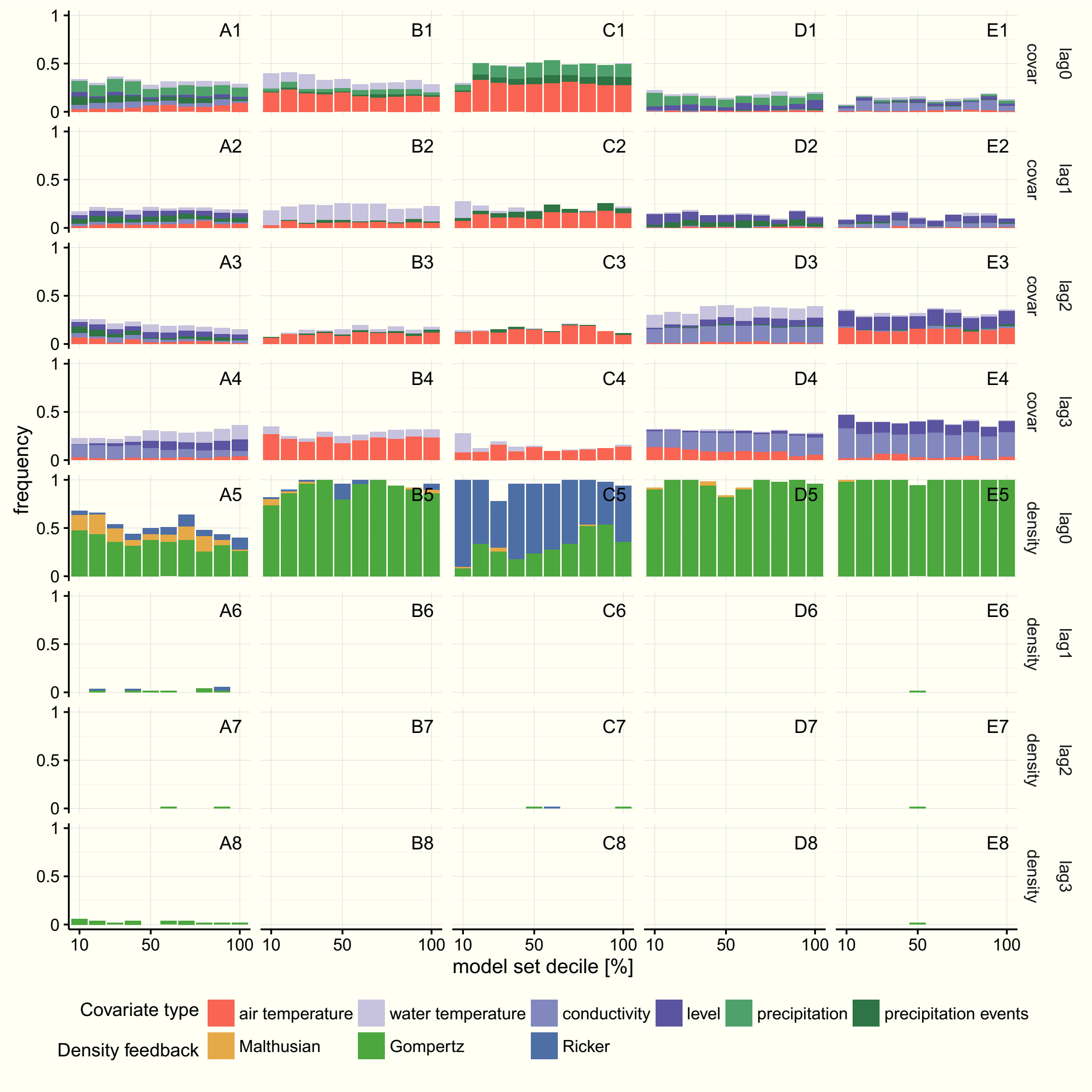

Figure 4.7 – Lags in the effects of exogenous forcing and density dependence on snail population dynamics. Data is given by column for *Bulinus* spp. in the irrigation canal (column A), in the temporary pond (B), in the ephemeral stream (C), and for *B. pfeifferi* and *Bulinus* spp. in the perennial stream (D, E). Data is partitioned by row in terms of lags: no lag (rows 1,5), 1 week lag (2,6), 2 weeks lag (3,7) and 3 weeks lag (4,8). Note that all environmental covariates are measured during the week preceding sampling, thus meaning that the 3 week lagged value of mean water temperature corresponds to the weekly average of water temperature on 4 weeks before collection. Environmental covariates and density feedback mechanisms are given in the color legend.

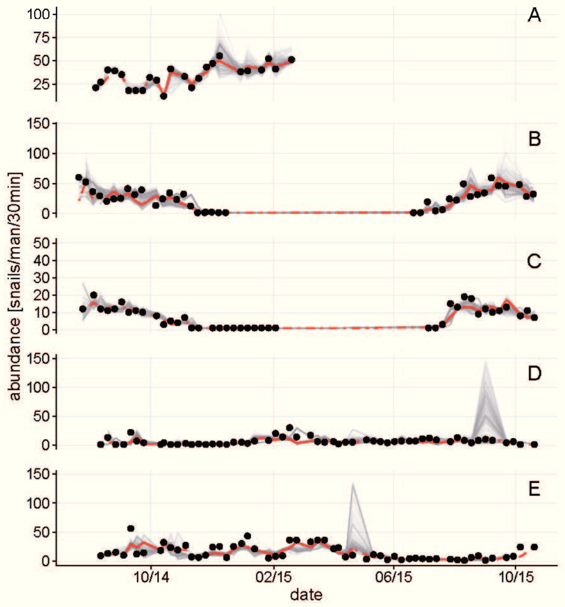

Figure 4.8 – Observed and predicted snail abundances. Abundance (dots), leave-one-out cross-validation (LOO-CV) prediction of the 500 best models (grey lines, increasing transparency indicating lower SRM performance) and jackknife model average (JMA) of the set (red line) are given for *Bulinus* spp. in the irrigation canal (A), the temporary pond (B), and the ephemeral stream (C), an for *B. pfeifferi* (D) and *Bulinus* spp (E) in the perennial stream. Average predictions in the case of partial model averages due to missing data are also shown (dash-dotted red line).

of extending the ecohydrological approach presented here to settings with more sparse and episodic environmental and ecological data.

4.4 Discussion

This study on the ecology of the intermediate hosts of schistosomes highlights the key role of hydrological drivers on parasite transmission dynamics. The findings presented in this Chapter have direct implications on the design of effective disease control programs. In fact, the improved understanding of snail ecology implied by the prediction of their population abundances can directly improve spatially explicit disease transmission models by relaxing the key assumptions of stationary snail populations [*Gurarie and Seto*, 2009; *Perez-Saez et al.*, 2015]. By providing empirical and theoretical evidence for discriminating ecological processes across climatic zones and habitat types, the ecohydrological framework developped here accounts for the relevant environmental drivers, especially the kinds of climatic seasonality and habitat ephemerality typical of the Sahelian ecotone.

The study present in this Chapter encompasses multiple intermediate host species, habitats and climatic zones through their individual roles and mutual interactions in affecting snail population fluctuations. In particular, the results show how snail abundances fluctuate during the dry and the rainy seasons, with opposite phases in the ephemeral habitats in the North and the perennial habitats in the South of Burkina Faso. Climatic conditions obviously determine the ephemerality of surface waters, resulting in the periodic disappearance of suitable habitats for *Schistosoma*'s intermediate hosts during the dry season (note that seasonality is survived through aestivation by *Bulinus* spp. but possibly not by *Biomphalaria* spp). Population abundances peaked during the rainy season (July-September), as observed in Lioulgou

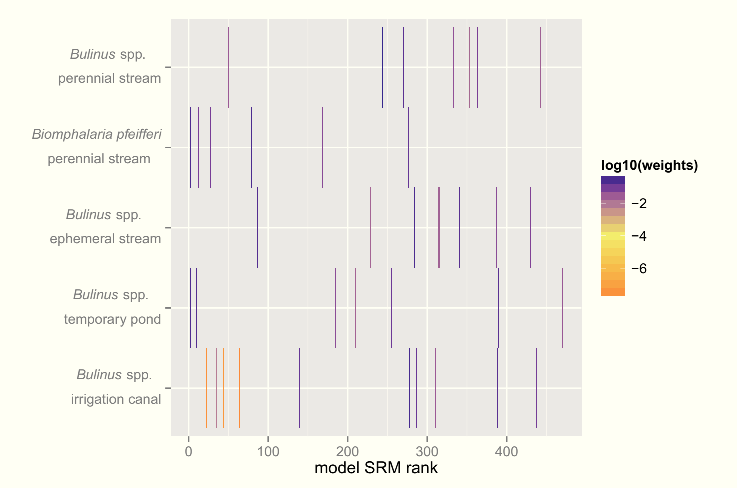

Figure 4.9 – Jackknife model averaging weights. Model average weights are given for each species and habitat, weights sum 1 over the rows.

(in both the stream and the pond) and in the historic ecological data for the country at large (2.4). On the other hand, the perennial stream in the Sudanian climatic region (Panamasso) presented opposite abundance fluctuations (for both *Bulinus* spp. and *B. pfeifferi*) with peaks during the dry season (March-April) and low population levels during the rainy season. This has nontrivial consequences on the determinants of snail abundance and denies the feasibility of all-purpose stationary and homogeneous reference population sizes to be used in large-scale disease pattern identification. Formal methods (e.g. [*Mari et al.*, 2014a]) are available to quantify the impact of seasonality in snail fluctuations on disease persistence and prevalence, which will extend directly existing spatially explicit approaches to the geography of the disease [*Gurarie and Seto*, 2009; *Perez-Saez et al.*, 2015]. Population fluctuations in the perennial habitat of the South appeared to be in synchrony with snail abundance in the man-made reservoir located in the Sudano-Sahelian center of the country where early ecological studies took place (2.4). The phase shift between the different types of habitats (permanent vs ephemeral and natural vs man-made) in the different seasonal climates of the country could have profound consequences on the logistics of national programs for schistosomiasis control due to the regional climatic conditions [*Cecchi*, 2007]. Throughout the historical data (2.4), *Bulinus* spp. displayed a double annual peak in the temporary pond, while the reservoir showed snail presence during longer periods. Such results provide insight into the potential impact of water resources development in the seasonal climate of Burkina Faso on the sustained transmission of schistosomiasis. In fact, the presence of small reservoirs can extend the period of the year in which intermediate hosts are present in the waterpoints used for daily socio-economic activities, with a peak of *Bulinus* spp. abundance in man-made habitats that occurs as the temporary ponds dry out. Moreover, the annual peak in man-made reservoirs was similar to the one observed in the perennial stream of Panamasso except for the disappearance of snail population during aestivation (April and June).

Ecological modelling suggests that snail population dynamics is determined by habitat type and hydrologic conditions, and that quantitative relationships rule such dependence. Negative density feedbacks were detected in all habitats. The strongest feedback was found in the ephemeral streams, while weaker effects were found, in decreasing order of intensity, in the irrigation canal, the perennial stream and in the temporary pond. In the light of the results of this Chapter, the debate about snail demographic determinants [*Shiff*, 1964c; *Jobin and Michelson*, 1967] is still germane today, in particular in countries presenting strong climatic seasonality. In Burkina Faso, results from the model identification process

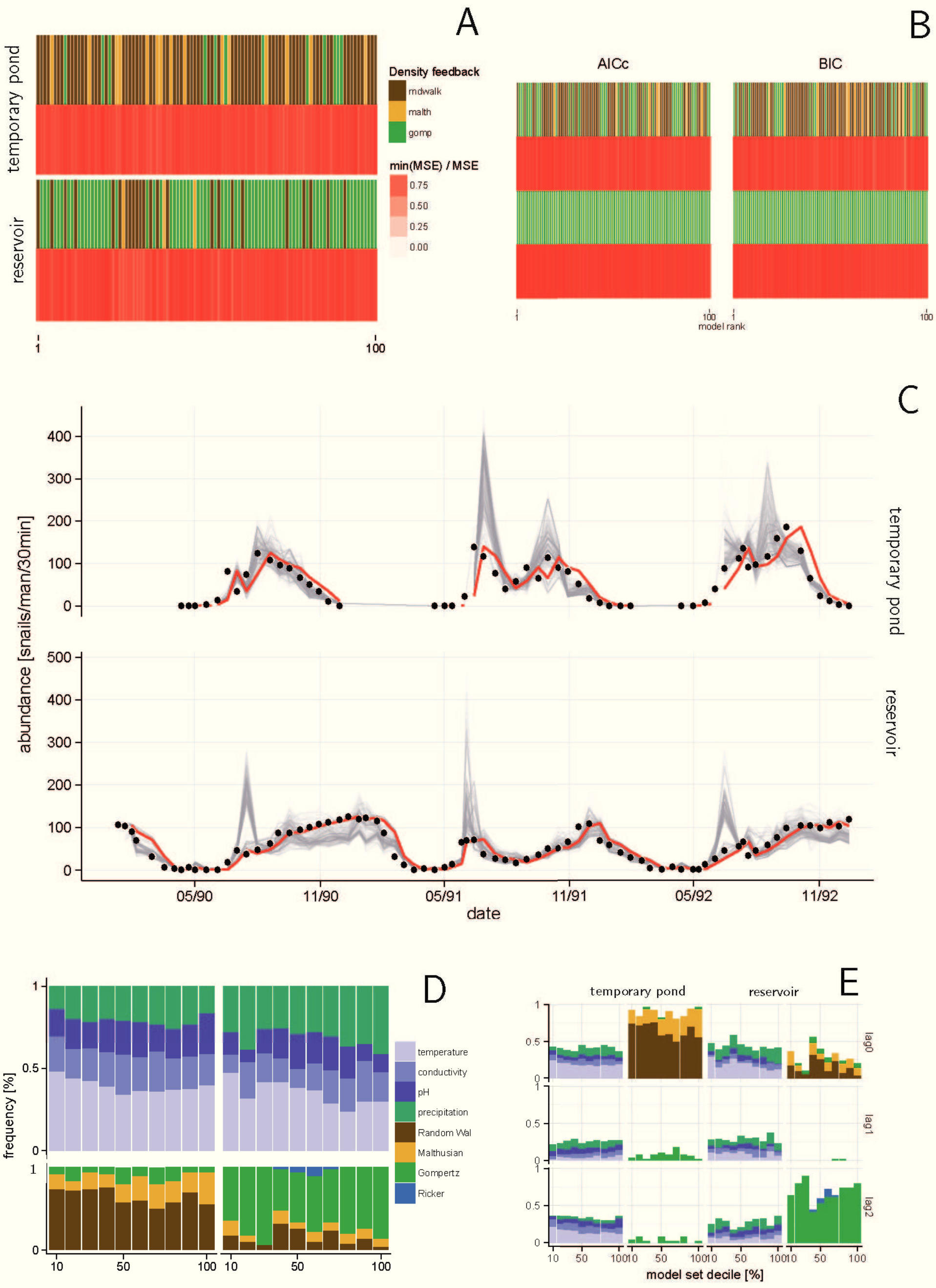

Figure 4.10 – Ecological modelling results of historical snail sampling in Burkina Faso. Results are shown for model selection (using SRM in panel A and AICc and BIC in panel B, legend as Fig. 4.8), population dynamics prediction (C, legend as Fig. 5), overall covariate occurrence (D, legend as Fig. 4), and lagged covariate occurrence (E, legend as Fig. 4.7), for *B. senegalensis* in a temporary pond (top rows in panels A, B and C, left columns in panels D and E) and *B. truncatus* in a small reservoir (bottom rows in panels A , B and C, right columns in panels D and E). Environmental covariates correspond to the ones in Fig. 2.4. In panel C models with predictions larger than 350 snails/man/30min were removed for plotting purposes, all removed models were in the bottom 500 models selected by the SRM criterion.

support the view [*Jobin and Michelson*, 1967] that negative density feedback is necessary to explain seasonal bursts and decay of snail populations. Evidence from this Chapter does not support the hypothesis of density vague dynamics as some form of density dependence was always detected in the field observations presented here. Hydrological conditions that characterize the dry and rainy seasons were found to be fundamental controls for all studied habitats and species. For instance, the variability of water level, conductivity, and temperature were singled out for both *Bulinus* spp. and *B. pfeifferi* in the perennial stream in the Sudanian climate of Panamasso, and in the irrigation canal in the Sahelian village of Tougou. As a matter of fact, measuring conductivity proved valuable because it is not only an important determinant of snail growth rates [*Poda et al.*, 1994], but also a viable proxy of stream discharge in running waters [*Weijs et al.*, 2013]. Fluctuations of air and water temperatures are indicators of the transition between dry and rainy seasons (thus also signaling habitat contraction/expansion), and prove the main control of *Bulinus* spp. in the ephemeral habitats of Lioulgou (both stream and pond).

Statistical methods based on model averaging are shown to provide reliable snail abundance projections. The consistency of the results of this Chapter for a large set of best-ranking models suggest the use of specific models of snail demography depending on habitat type (say, natural vs man-made) and hydrologic characteristics (say, ephemeral vs permanent). ecohydrological approaches thus prove necessary to adequately encompass the determinants of the abundance of the intermediate hosts of schistosomiasis, and as a consequence of the entire life-cycle of the parasite. Notably, the proposed approach could be relevant to other vector-borne diseases driven by environmental factors and ecological feedbacks. Predicting snail abundance fluctuations and their spatial heterogeneity is of prime interest for space-time modelling of schistosomiasis transmission and for timely application of mollusc control measures or optimization of preventive chemotherapy [*Utzinger et al.*, 2011]. Extension and upscaling of the approach presented here would be possible through the use of remotely-sensed data on the hydrological drivers of snail abundance (Table 4.2), in the perspective of providing predictions of control interventions effectiveness. The approach complements ecological range inference methods, e.g. maximum entropy modelling [*Stensgaard et al.*, 2013] or transmission suitability indices incorporating snail biology [*Walz et al.*, 2015a], in assessing seasonal variations of snail abundance and their hydrologic controls, yielding potential insight on the impacts of climate change on schistosomiasis transmission at regional scales [*Perez-Saez et al.*, 2015; *Simoonga et al.*, 2009].

Indeed, extending the forecasting capacity of the JMA for each type of habitat to other regions of Burkina Faso could provide a valuable tool for planning the application of snail control measures and for the distribution of preventive chemotherapy and MDA. Since all models rely on climatic and hydrological variables for which monitoring stations such as the ones installed in the experimental sites equiped in the framework of this Thesis are not widely available in the country, a list of remote-sensing data sources which could be used as substitutes to field data is proposed. Needless to say, the bias (if any) and quality of remotely-sensed data could hinder the model predictive capacity, but they are deemed them valuable nonetheless for locating the most common habitats in which snails can be found, and capturing seasonality and peaks of intermediate host population abundance. Examples of remotely sensed data that are freely accessible are given in Table S3. In a first stage these data can be used to determine the spatial distribution of habitat types on large scales based on the physical and hydrological characteristics of the country. Flow accumulation rasters derived from Digital Terrain Models (DTMs), evapo-transpiration data and multi-seasonal satellite imagery can be used to determine the location and ephemerality of waterbodies at the national scale. Furthermore, existing databases on water resources infrastructure provide the localisation of man-made reservoirs and valuable information on irrigation works [*Cecchi*, 2007]. The development of a robust methodology to perform this task is the object of ongoing work. Snail abundance fluctuations can then be inferred by feeding spatio-temporal remotely sensed data

Table 4.2 – Proposition of remote-sensing data sources for upscaling hydro-ecological forecasting

Data type	Purpose	Data source	Resolution		Web
			space	time	
Water bodies	Habitat identification by extracting of water surfaces from satellite imagery	Landsat [a]	30m	16 days	http://earthexplorer.usgs.gov/
		NASA MODIS [b]	250m	8 days	https://lpdaac.usgs.gov/dataset_discovery/modis/modis_products_table/mod09q1
Evapo-transpiration	Quantification of habitat ephemerality	NASA MODIS [c]	1km	8 days	ftp://ftp.ntsg.umt.edu/pub/MODIS/NTSG_Products/MOD16/
River network	Habitat identification	Hydro-SHEDS [d]	100m	-	http://hydrosheds.cr.usgs.gov/dataavail.php
Land surface temperature	Environmental covariate for demographics modelling	NASA MODIS [e]	1km	1day	https://lpdaac.usgs.gov/dataset_discovery/modis/modis_products_table/mod11a1
Precipitation	Precipitation estimates	NASA TRMM [f]	25km	3 hours	http://gcmd.nasa.gov/records/GCMD_GES_DISC_TRMM_3B42_daily_V6.html

---

[a] http://landsat.usgs.gov//landsat_level_1_standard_data_products.php

[b] http://modis.gsfc.nasa.gov/data/dataprod/mod16.php

[c] http://modis.gsfc.nasa.gov/data/dataprod/mod16.php

[d] http://www.worldwildlife.org/hydrosheds

[e] http://modis.gsfc.nasa.gov/data/dataprod/mod16.php

[f] http://trmm.gsfc.nasa.gov/

on precipitation and air, surface and water temperature into the modelling framework developed in this study. The approach presented in this Chapter has the unique feature of not only yielding the possible locations of the intermediate hosts of schistosomiasis, but also providing estimates of seasonal population fluctuations. Both of these aspects represent important insights this type of approach could give to disease surveillance-response mechanisms.

The results of this Chapter stress the importance of tailoring snail control measures to local ecological conditions, and provide a framework for forecasting snail population fluctuations based on habitat type and dominant hydrological controls. Dam constructions and expansions of water resources development infrastructure like irrigation canals, pursued to meet increasing demand and shirking supply in sub-Saharan Africa, raise preoccupations about increased incidences of schistosomiasis [*Barbier et al.*, 2009; *Steinmann et al.*, 2006]). The quantitative representation of the related dynamics of the parasite's intermediate hosts upgrades risk control and disease modelling capabilities ultimately leading to what could be a minimal set of information required to forecast with confidence likely effects of interventions or control measures on the prevalence of schistosomiasis.

5 Classification and prediction of river network ephemerality

The present Chapter furthers the study of hydrologic controls on schistosomiasis, in particular by characterizing the ephemeral characters that might impede intermediate host to survive in natural ecosystems. In fact, the transmission of water-based diseases hinges on the interactions between hydrology and ecology of hosts, vectors and parasites, with the long-term absence of water constituting a strict lower bound. However, the link between spatio-temporal patterns of hydrological ephemerality and water-borne disease transmission is poorly understood and difficult to account for. The use of limited biophysical and hydroclimate information from otherwise data scarce regions is therefore needed to characterize, classify, and predict river network ephemerality in a spatially explicit framework. This Chapters develops a novel large-scale ephemerality classification and prediction methodology based on monthly discharge data, water and energy availability, and remote-sensing measures of vegetation, that is relevant to epidemiology, and maintains a mechanistic link to catchment hydrologic processes. Using predicted ephemerality classes, a gradient-boosted tree-based prediction yielded three distinct geographic regions of ephemerality. Importantly, a strong epidemiological association between predictions of hydrologic ephemerality and the known spatial patterns of schistosomiasis is observed. The general nature of the approach developed here and its relevance for predicting the hydrologic controls on schistosomiasis occurrence provides a pathway for the explicit inclusion of hydrologic drivers within epidemiological models of water-borne disease transmission[2].

5.1 Introduction

Hydrology underlies water-borne disease outbreaks through its direct impact on the pathogenic agent's survival and ecology (or of primary and intermediate hosts) and through their (mostly) downstream transport, prompting infections to spread within and across human communities, such as in the case of cholera [*Gatto et al.*, 2012; *Mari et al.*, 2012a; *Rinaldo et al.*, 2017]. Hydrology also plays a key role in the endemicity of parasitic diseases by determining habitat presence and suitability for the parasite's vectors, as for malaria [*Bomblies et al.*, 2008; *Bomblies and Eltahir*, 2009] and onchocerciasis (river blindness) [*Servat et al.*, 1990], or for intermediate hosts in the case of schistosomiasis [*Remais et al.*, 2007, 2008; *Perez-Saez et al.*, 2016].

River network ephemerality is an especially important hydrological characteristic. It affects water-borne

---

[2] The content of this chapter has been adapted from *Perez-Saez et al.* [2017]: Perez-Saez, J., Mande, T., Larsen, J., Ceperley, N. and Rinaldo, A., 2017. Classification and prediction of river network ephemerality and its relevance for water-borne disease epidemiology. *Advances in Water Resources.* https://doi.org/10.1016/j.advwatres.2017.10.003

diseases owing to its direct and indirect effects at different stages of the transmission cycle, including pathogen spread and survival, intermediate host ecology, human exposure to the pathogens, and the contamination pathways of water supply sources. Indirectly, the changing connectivity of intermittent river networks may also play a role in the meta-population dynamics of hosts, vectors, pathogens, and humans [*Mari et al.*, 2014a]. Intestinal and uro-genital schistosomiasis are excellent examples of such diseases. Although both genera of snail intermediate hosts are capable of surviving periods of desiccation through aestivation, *Biomphalaria* snails are much less adapted than *Bulinus* to prolonged dry spells which can severely increase snail mortality [*Rubaba et al.*, 2016]. Laboratory estimates of the mean lifespan of *Biomphalaria pfeifferi* under aestivation are about 40 days [*Badger and Oyerinde*, 1996], whereas the species within the *Bulinus* genus have evolved to survive beneath temporary ponds and streams which only have water for a couple of months per year [*Brown*, 1980]. Hydrologic ephemerality thus determines, among other factors, habitat suitability for the snail intermediate hosts, in particular for intestinal schistosomiasis, and also to condition human exposure/contamination by limiting the temporal window and the number of locations in which human-water contacts can occur.

The observed ecological range of *Biomphalaria* snails, and thus of intestinal schistosomiasis, is generally found to coincide with the presence of quasi-permanent rivers and waterbodies in countries with otherwise strongly seasonal climates and ephemeral flow regimes [*Poda*, 1996; *Zongo et al.*, 2013], within a suitable temperature range [*Stensgaard et al.*, 2013; *McCreesh and Booth*, 2014a]. Notably, the development of water reservoirs for irrigation is associated with higher schistosomiasis risk throughout SSA, in particular in the Sahel [*Steinmann et al.*, 2006]. The hydrologic regime (e.g: permanent vs. ephemeral) is a key determinant for the seasonal fluctuations of freshwater snail abundance [*Perez-Saez et al.*, 2016], thus dam construction can have important consequences in the presence and abundance of these species and the parasites [*Perez-Saez et al.*, 2015; *Diakité et al.*, 2017].

On the other hand, construction of man-made reservoirs, often in response to water scarcity [*Barbier et al.*, 2009], can dramatically change local population densities and human water-contact patterns by fostering new economic activities such as market gardening in the dry season, fishing, or cattle herding [*Cecchi*, 2007; *Ayantunde et al.*, 2017]. The new behaviors may prompt heterogeneous exposure and contamination leading to increases in the overall disease burden in the community [*Chandiwana and Woolhouse*, 1991; *Mari et al.*, 2017a].

Hydrologic ephemerality is therefore a risk factor in the case of uro-genital schistosomiasis because intermediate hosts of *S. haematobium* can survive even in extremely dry areas and because it promotes the concentration of human activities around a few long-lasting water contact points, whether they are man-made reservoirs, lakes, or large temporary ponds [*Kloos et al.*, 1997; *Hunter*, 2003; *Poda et al.*, 2003]. This last point is also validated by the observed increase schistosomiasis risk with increasing water-resources development in a global meta-analysis [*Steinmann et al.*, 2006]. Seasonal hydrologic connectivity may also play an important role in the dispersal of the snail intermediate hosts between different habitats, with potential implications for the focal control of snail populations [*Clennon et al.*, 2007], and for the coevolution of snails and schistosomes [*Prugnolle et al.*, 2006]. Although the importance of hydrologic ephemerality has already been identified separately by ecologists, sociologists and epidemiologists, it has yet to be quantitatively implemented. This is possibly due to the lack of an amenable approach for the spatial evaluation of river network ephemerality at regional scales. A better understanding of the hydrological underpinnings of large-scale ephemerality, including the likely extent of dry channels occurrences, is therefore crucial to spatially-explicit predictions of schistosomiasis (and other waterborne disease) transmission dynamics, with implications on disease control and elimination strategies [*Heinrich et al.*, 2017; *Rinaldo et al.*, 2017].

The determinants of stream ephemerality span multiple spatio-temporal scales across the climatic, vegetation, soil and topographic features that characterize each river network [*Costigan et al.*, 2016]. Given the importance of feedbacks between these variables for streamflow generation, the ability to predict the frequency and duration of 0-flow events (discharge $Q = 0$, thus also defining the relative amount of drybed time within a hydroperiod) poses important methodological challenges, particularly in ungauged or data scarce regions [*D'Ambrosio et al.*, 2016]. Determining ephemerality has typically been a component of hydrologic regime classification studies that rely on the extraction of hydrological indices from stream-flow data [*Sivakumar et al.*, 2015]. This is also the case for the exact determination of the atom of probability at the origin, i.e. the frequency of $Q = 0$ events, from flow duration curves [*Botter et al.*, 2007]. In such approaches the classification of ungauged rivers mostly relies upon the prediction of relevant indices of hydrological regimes using remotely-sensed catchment characteristics such as contributing area and slope, and climatic information such as precipitation and temperature [*Oueslati et al.*, 2015]. Although index clustering-prediction methods have proved successful in a number of cases [*Moliere et al.*, 2009; *Zhang and Chiew*, 2012; *Olden et al.*, 2012; *Oueslati et al.*, 2015], they usually require long time series of daily discharge data which seldom exist in SSA and in other developing countries which bear most of the water-borne disease-related health burden [*Gebrehiwot et al.*, 2011]. Other approaches have directly linked multiple environmental covariates to hydrologic regime class membership using decision tree-like classifiers in case studies in Europe [*Snelder et al.*, 2009] and Australia [*Kennard et al.*, 2010; *Trancoso et al.*, 2016]. The success of these approaches builds on the strong mechanistic link between first order climatic drivers and their modulation by catchment biophysical characteristics to produce a spectrum of hydrologic regimes, or, in other words, on the interplay between water and energy availability and other drivers such as vegetation, topography, and geology [*Donohue et al.*, 2006; *Gentine et al.*, 2012; *Troch et al.*, 2015; *Trancoso et al.*, 2016]. Applying this approach to ephemeral catchments in France, [*Snelder et al.*, 2013] highlighted the importance of small-scale (sub-catchment) controls, particularly in temperate climates, and the consequent challenges for large-scale predictions across ungauged catchments. Though encouraging, such studies considered multiple hydrologic regime classes extracted from a large set of long-term observed time series (more than 300 catchments per study with more than 15 years of data), and a rich set of locally-developed remote-sensing products used to extract catchments covariates. These requirements thus hinder their applicability to data-scarce regions and to the needs of spatial context where water-borne diseases typically occur. These reasons could explain the limited number of studies concerning catchment classification in SSA [*Ogunkoya*, 1988; *Gebrehiwot et al.*, 2011; *Berhanu et al.*, 2015], despite its importance for water resources, ecological, and disease management [*McDonnell and Woods*, 2004; *Hughes*, 2005; *Wagener et al.*, 2007].

This Chapter proposes a spatially explicit approach for classifying stream ephemerality across data-scarce regions. The approach may be applied to large-scale modelling of water-borne disease transmission, and is based on an an analysis of hydrologic processes. This study focuses on the seasonality of 0-flows, which exert a first-order control on the life-cycle of water-borne parasites by restricting the possible habitat of their aquatic intermediate hosts, and by constraining human-water contact patterns. The country of Burkina Faso is an interesting case study, with its strong South-to-North gradients in precipitation, temperature, and available water resources. Stream ephemerality is classified in three steps: 1) clustering the available hydrological data into different degrees of ephemerality, 2) building classification-relevant catchment characteristics, and 3) finally predicting ephemerality for the whole river. The spatially-explicit predictions of ephemerality is then used in the analysis of the epidemiology of schistosomiasis both in terms of the ecological range of the intermediate hosts and relevant socio-economic factors. Ultimately, the scope of the present Chapter is to set the stage for a specific utilization of the spatially explicit modelling described in Chapter 5 by incorporating hydrological and ecological insight into transmission dynamics. The generalization of the approach developed in this Chapter is therefore discussed under this light.

5.2 Methods

5.2.1 Hydrologic data

The river network used in this work was extracted from the STRM void-filled digital elevation model with 90m resolution [*Jarvis et al.*, 2008], using the standard hydrology libraries in GRASS [*GRASS Development Team*, 2016], and all network processing and analysis done using PostGIS/PostgreSQL [*PostgreSQL Global Development Group*, 2006; *PostGIS Project Steering Committee*, 2015]. The hydrologic data used in this study consists of mean monthly discharge timeseries from the Global Runoff Data Center that were freely accessed upon the project acceptance by the center [*Grabs et al.*, 1996]. Data was requested for all gauging stations in Burkina Faso and along the river network into neighbouring Niger, Ghana and Côte d'Ivoire, for a total of 68 stations. The available hydrologic data mainly covered the period between the 60's and the 90's, with a median of 12 years with full data (12 months of discharge values) per station. For subsequent clustering analysis only 58 stations with at least 3 years of full data were retained. The characteristics of the gaging stations were found to be representative of the national situation both in terms of spatial coverage and watershed size (Fig. 5.1).

5.2.2 Ephemerality clustering

An unsupervised clustering approach was used to determine the number of ephemerality classes that can be realistically defined by the data, which is more precise than deriving an arbitrary discharge-related threshold and to reduce bias from the strong variations in discharge patterns during the drought of the 191970s. Ephemerality was quantified in terms of the number of months with a mean discharge of 0 in each year for those years where all 12 months of data where available (Fig. 5.1). The histograms of 0-flow months for each station then served as the basis for the extraction of distinct ephemerality classes. Following a methodology proposed for phylogenetic analysis [*Arumugam et al.*, 2011], a hierarchical clustering algorithm is applied using the Jensen-Shannon divergence between the observed probability distributions of 0-flow months as distance metric, and the average distance among clusters for the linkage criterion [*Xu and Wunsch*, 2005]. To account for the impact the long lasting drought in the 1970s and 1980s has on the clustering of classes [*Descroix et al.*, 2009; *Lodoun et al.*, 2013; *Mahe et al.*, 2013] (Fig. 5.1), the analysis was performed twice by dividing the dataset into the years before 1975, and between 1975 and 1985, and then studying the station transition between ephemerality classes. The year 1975 was retained to distinguish the pre-drought (or "normal") and drought periods from the perspective of river ephemerality as it is the first year displaying moderate drought conditions based on the standardized precipitation index (Fig. 5.2 a), and is the median of the distribution of change-point years in the timeseries of 0-flow months per year across stations (Fig. 5.2 b). The detection of changes in hydrologic regimes, more paricularly in the number of dry months per year, was performed using a Gaussian change-point model with the GLR statistic to test for a shift in mean and variance with the `cpm` package in R [*Ross*, 2015]. The median of the year of change in the 26/58 stations for which a change was significant is 1975. The final number of clusters in each period was determined based on a significance cutoff estimated through multiscale bootstrapping using the `pvclust` package in R [*Suzuki and Shimodaira*, 2015].

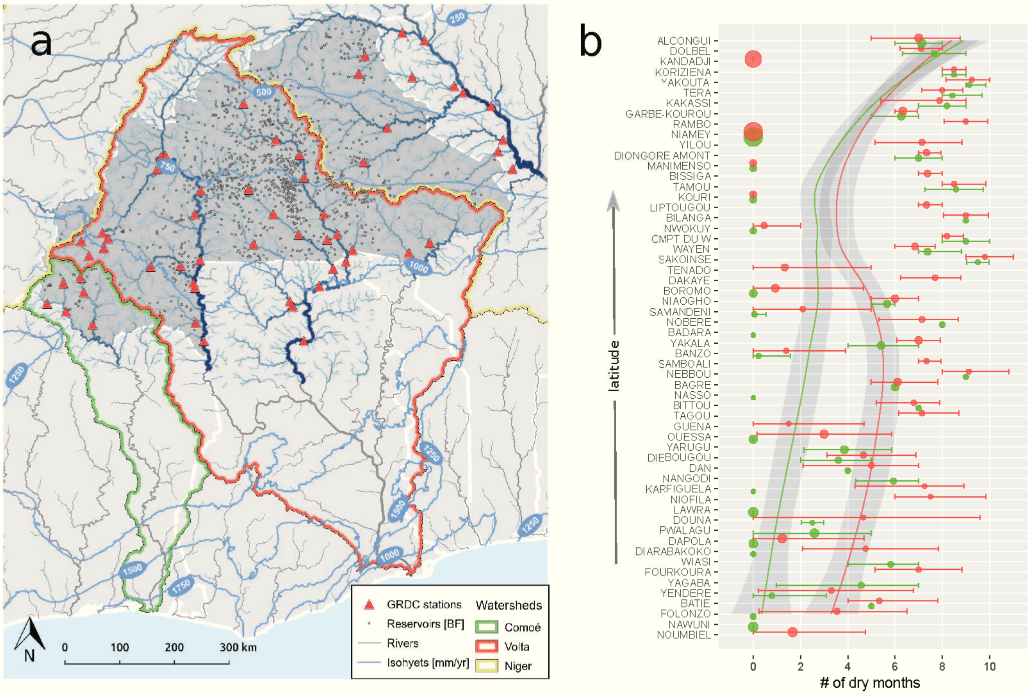

Figure 5.1 – Case study location and available hydrologic data. a) Map of Burkina Faso (dark grey) with the available GRDC stations, the location of small reservoirs, the major watersheds, the HydroSHEDS river network [*Lehner et al.*, 2008] (grey lines, ≈ 500m resolution) in addition to the river network extracted for this study (dark blue lines, 90m resolution, width proportional to contributing area). Isohyets (light blue lines) were extracted from the Worldclim gridded precipitation estimates for the period 1960-1990 [*Hijmans et al.*, 2005]. b) Observed hydrologic ephemerality in the GRDC dataset in terms of the median number of dry months per year (dots) and the 95% interquantiles (bars) before (green) and during (red) the historical drought in the 191970s-1980s. Ordering stations by increasing latitude (Alcongui being the North-most station), suggests a generally increasing trend in the number of dry months along the South-to-North climatic gradient (lines and 95% CI obtained by local weighted least-squares smoothing of the raw counts of dry months).

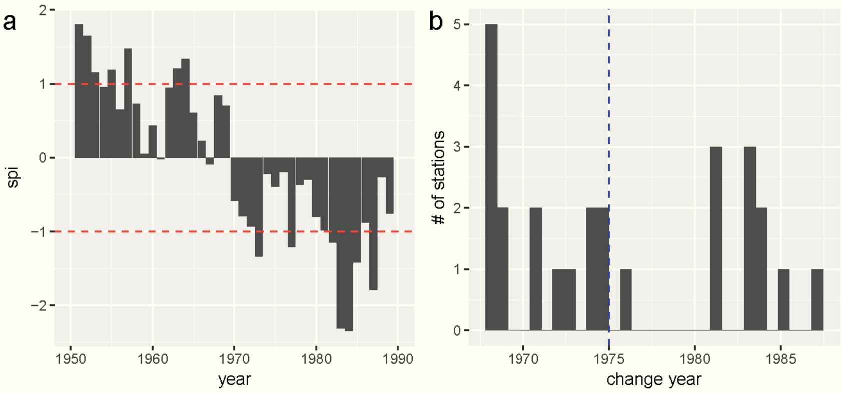

Figure 5.2 – Precipitation and ephemerality regime shift during the long-lasting West-African drought. a) The standard precipitation index computed from mean annual precipitation in Burkina Faso (dotted red lines at the 1 and -1 absciss indicate significantly wet and dry years respectively). Data from the Climate Change Knowledge Platform, http://sdwebx.worldbank.org/climateportal/. b) Distribution of the year of change in the timeseries of 0-flow months and median (dotted blue line).

5.2.3 Controls on ephemerality

In an effort to overcome the limited amount of hydrologic data, a set of hydrologically-relevant covariates was built to predict river ephemerality at the country scale. Aridity (potential evapotranspiration / precipitation), runoff estimates, and remote-sensing based vegetation characteristics are included in the analysis.

Climate and the Budyko curve

Climate constitutes the main first-order control on ephemerality, represented in the Budyko framework as the long term average mass and energy balances [*Budyko and Miller*, 1974]. Indeed, hydrologic regimes have been found to align with Budyko's theoretical relationship relating the ratio of evapotranspiration over precipitation to the ratio of potential evapotranspiration over precipitation (i.e. the aridity index) [*Budyko and Miller*, 1974]:

$$\left.\frac{ET}{P}\right|_{Budyko} = \sqrt{\frac{\overline{ET_0}}{\overline{P}}\tanh\left(\frac{\overline{P}}{\overline{ET_0}}\right)\left(1-\exp\left(\frac{\overline{ET_0}}{\overline{P}}\right)\right)}, \tag{5.1}$$

where $\overline{ET}(\overline{ET_0})$ designates the mean yearly (potential) evapotranspiration, and $\overline{P}$ the mean yearly precipitation. Moreover, a strong link has been suggested to exist between the aridity index and many factors such as runoff generating processes and streamflow regimes [*Trancoso et al.*, 2016], and both the normalized baseflow and the permanent fraction of the drainage density [*Wang and Wu*, 2012]. In this analysis, the aridity index was computed for the whole river network using remote-sensing estimates of precipitation (PERSIANN-CDR product, daily estimates at 0.25° (≈ 30km) resolution [*Ashouri et al.*, 2015]), and potential evapotranspiration (MOD16 product, monthly estimates at 1 km resolution [*Mu et al.*, 2013]).

Annual runoff estimation

Hydrological ephemerality can vary longitudinally along rivers, with flow persistence changing in a non-linear manner with the distance to/from the catchment's outlet [*Larned et al.*, 2011]. Indeed, rivers with sufficient temperate headwater contributing area can sustain permanent flow regimes even if the majority of their flow length is through arid areas [*Snelder et al.*, 2013]. The Niger river is a good example of this, as it flows through extremely arid zones, and thus direct surface evaporation may not be compensated by intermediary inputs. However, the more temperate Guinean highlands are within the upstream runoff-generating area and produce enough streamflow to support permanent water, despite strong decadal variations of precipitation patterns [*Amani and Nguetora*, 2002]. Catchment-scale annual runoff is estimated using the Budyko framework by accounting for the role of vegetation in runoff production. Vegetation strongly modulates catchment response to precipitation through dynamical relations between soil moisture in the rooting zone, the evapotranspiration rates, and the fraction of rainfall interception, thus modulating Budyko's original energy-based prediction of the evaporative fraction [*Porporato et al.*, 2004; *Donohue et al.*, 2006; *Gentine et al.*, 2012], especially when integrated at the annual scale [*Donohue et al.*, 2010]. Fu's equation [*Fu*, 1981], an alternative to the deterministic Budyko curve is used to capture the relationship between vegetation and evaporation fraction. Fu's equation reads:

$$\left.\frac{ET}{P}\right|_{FU} = 1+\frac{\overline{ET_0}}{\overline{P}}-\left(1+\left(\frac{\overline{ET_0}}{\overline{P}}\right)^{\omega}\right)^{\frac{1}{\omega}}, \tag{5.2}$$

where $\omega > 1$ is a free parameter accounting for all non-climate related factors affecting runoff production. Following [*Li et al.*, 2013], instead of having a single estimation $\hat{\omega}$ for the whole dataset a parameter was fit separately to the observed evaporative fraction of each of the available discharge stations and then independently tested the relationship between $\hat{\omega}$ and vegetation cover using a linear regression between ω and the mean annual fraction of absorbed photosynthetically active radiation (*fpar*) over each catchment (MODIS FPAR 8-day product at 500m resolution [*Myneni et al.*, 2015]). The mean annual runoff was predicted for each watershed by multiplying the remotely-sensed average annual precipitation and the estimated runoff coefficients. The uncertainty in runoff estimation was accounted-for through a probabilistic framework [*Greve et al.*, 2015]. The approached consisted in finding a probability distribution for both $\hat{\omega}$ and the corresponding discharge estimates following the methodology proposed by [*Greve et al.*, 2015]. The probabilistic Budyko curves were computed for each river strech i by perturbing ω_i $1'000$ times by adding a random number drawn from a normal distribution fit to the residuals of the linear regression of ω against *fpar* (Fig. 5.7). The resulting distribution of the values of ω (constrained to $\omega \geq 1$) were then used to quantify the variability in the predicted evaporative fraction (5.8). The final estimated runoff for each river stretch was computed by subtracting the storage capacity of reservoirs to all downstream edges of the river network, thus assuming that all water stored in a reservoir is withdrawn either through evaporation or consumption. This is the worst-case scenario estimate given that the specific hydrological dynamics in each reservoir is beyond the scope of this work. The geo-location and storage capacity of small and large dams in Burkina Faso was obtained from the governmental water resources agency database of Burkina Faso (Fig. 5.1, [*Cecchi et al.*, 2007]).

Vegetation-based characteristics

Neither the aridity index nor the estimation of annual runoff take into account the strongly seasonal nature of precipitation and temperature in Burkina Faso which generates observed hydrological fluctuations. Indeed phase differences between seasonally varying potential evapo-transpiration and precipitation characterize distinct soil moisture dynamics. Vegetation activity is uniquely adapted to these dynamics as it is both a response and a determinant of water availability [*Gerrits et al.*, 2009]. Vegetation response thus can be used as an indicator of transpiration, and the corresponding partitioning of precipitation between the different fluxes of the hydrologic cycle, particularly in water-limited regions [*Liu et al.*, 2006; *Rodríguez-Iturbe and Porporato*, 2007; *Souza et al.*, 2016]. Seasonality is therefore accounted for through the analysis of the annual precipitation-vegetation hysteresis. More specifically, the average monthly co-variation between *fpar* and precipitation is examined by using 10 years (2005-2015) of remote-sensing data and extract characteristics of the hysteresis that most distinguish the different classes of ephemeral rivers.

5.2.4 Classification of whole river networks

The classification of whole river networks into the retained classes of ephemerality was performed by using gradient-boosted trees (GBTs) with aridity, estimated runoff, mean *fpar* and precipitation-vegetation hysteresis characteristics as inputs covariates. GBTs are tree-based classification algorithms that use boosting to sequentially fit single trees to re-weighted versions of the training data. The weights given to the elements of the training data are an increasing function to the residuals (or missclassification loss) from the previous iteration, and the final classifier is a weighted average of the single classifiers obtained at each boosting iteration [*Hastie et al.*, 2009]. It has proved to have high predictive capacity both for classification and regression in comparison to other tree-based approaches [*Hastie et al.*, 2009]. GBTs also have the advantage of presenting an interpretable set of decision rules to extract the relative importance of covariates in building the classifier. The gradient boosting algorithm implemented in the `xgboost` package in R is used in this analysis [*Chen and Guestrin*, 2016; *Chen et al.*, 2017]. The algorithm parameters were tuned using leave-one-out cross-validation (LOO-CV) over a grid of parameter ranges for the maximum tree depth, the learning rate and data and feature sub-sampling (SM Table 1). For the classification are excluded from the training set the two stations along the Niger river since this study area did not cover their whole upstream catchment, thus impeding the computation of the associated covariates. Are also included in the training set three smaller scale experimental sites presented in Chapter 2 (Fig. 5.13). Given the built-in random sub-sampling of data and covariates to limit overfitting during training, the classifier was trained 100 times, and for each training iteration class membership was predicted for 100 realizations of annual discharge using the probabilistic Budyko framework for a total of $10,000$ class membership outcomes.

5.2.5 Schistosomiasis and hydrologic ephemerality

The link between hydrological ephemerality and the epidemiology of schistosomiasis was analyzed both in terms of its relevance for predicting the ecological range of the intermediate host in rivers across the country, and for its significance in explaining the observed epidemiological patterns.

Ecological range of the snail intermediate hosts

The relevance of hydrological ephemerality in understanding and predicting the ecological range of the intermediate host of intestinal schistosomiasis was quantified through the use of ecological model selection, comparing models with and without ephemerality as a covariate. The dataset consisted of presence/absence records of *Biomphalaria pfeifferi*, the only known intermediate host of *S. mansoni* in the country, collected by [*Poda et al.*, 1994] throughout Burkina Faso. The dataset was filtered for samples collected in streams and rivers (176 out of 637 points). A first exploratory analysis of the locations of sampling points showed a clustering of samples and uneven distribution of points between the different ephemerality zones (Fig. 5.3). Biased spatial sampling has been shown to limit the performance of spatial ecological models in particular in terms of overfitting [*Kramer-Schadt et al.*, 2013]. The `spThin` package in R [*Aiello-Lammens et al.*, 2015] was used to correct for the spatial clustering of sampling locations. A minimal inter-point distance of 40km and 1000 thinning replicas were used. For each replica i, the null hypothesis that the thinned sampling locations came from a hardcore point process with minimal inter-point distance of 40km (same as the parameter of the thinning algorithm) was tested using a Monte Carlo one-sided Diggle-Cressie-Loosmore-Ford (DCLF) statistics on Besag's L function [*Baddeley et al.*, 2014]:

$$t^i_{DCLF} = \int_0^R \left(L^i_{obs}(r) - \bar{L}^i(r)\right)^2 dr, \tag{5.3}$$

where $L(r) = \sqrt{K(r)/\pi}$ is a variance-stabilized version of Ripley's K-function at interaction distance r [in meters], L^i_{obs} is the observed value of the L-function of thinning replica i, $R = 150$km is the maximal inter-point interaction distance here chosen to be approximately half of the geographical span of Burkina Faso, and $\bar{L}^i(r) = 1/(m+1)\left[L_{obs} + \sum_{j=i}^{m} L_j\right]$ is the average of the m Monte Carlo realizations of the hardcore process and the replica's L-function value (for details on the use of simulation envelopes for tests on spatial patterns see [*Baddeley et al.*, 2014]). A significance level $\alpha = 0.05$ with $m = 199$ Monte Carlo simulations was retained, the null hypothesis was thus rejected for replica i if $t^i_{DCLF} > k(t^{sim}_{DCLF})_k$, where the subscript k denotes the k'th largest value of simulated statistics corresponding of the Monte Carlo

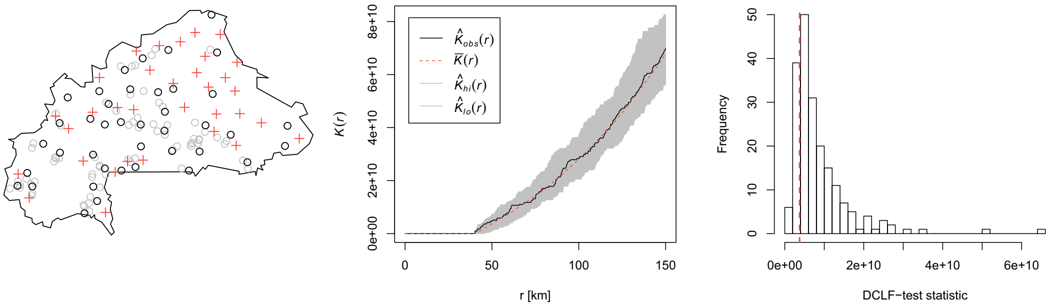

Figure 5.3 – a) Map of the whole sampling location dataset (gray circles) with the ones retained by a run of the thinning algorithm (black circles) and a realization of a hardcore point process with the same intensity and minimal inter-point distance as the thinned replica. b) The value of Rippley's K-function for the thinned replica ($\hat{K}_{obs}(r)$, black line) and simulated hard core process (mean, $\bar{K}(r)$ red line, and higher and lower critical values of the simulation envelop, gray ribbon). Note that $K(r) = 0$ for $r < 40$km since it is the parameter of the thinning algorithm. c) Histogram of the DCLF statistic of the simulated hardcore processes and of the thinned replica (red dotted line). Since the latter is smaller than the 10^{th} simulated DCLF statistic, the null hypothesis that this thinned replica was produced by a harcorde point process at significance level $\alpha = 0.05$ (for 199 simulations) cannot be rejected. This procedure was repeated 1000 times.

simulations of the DCLF statistic under the assumption of a hardcore point process over Burkina Faso to obtain the desired level of significance (here $k = 10$). The intensity parameter β of the hardcore process was fit for each thinning replica using the `spatstat` package in R [*Baddeley et al.*, 2005]. The test was not rejected for any of the thinned replicas, which means that none of the thinning replicas was significantly different from a random sampling of the country with a minimal inter-point distance. An illustration of the spatial statistic testing is given in Fig. 5.3.

A gradient-boosted trees classifier was used for the evaluation of the importance of river ephemerality in predicting snail occurrence. The covariates consisted of the 19 Worldclim 1km spatial resolution environmental data product [*Fick and Hijmans*, 2017], the season (rainy vs. dry) in which the sampling was done, the ephemerality class and the flow accumulation of the river stretch closest to the GPS coordinates of this village in which the sampling was done. Tow GBT models for each of the replicas of thinned spatial sampling locations were trained, one with the ephemerality covariate, flow accumulation, season and 3 Worldclim variables related to temperature (mean temperature of warmest quarter, mean temperature of coldest quarter, and temperature seasonality), and one without ephemerality but with all covariates with a cross-correlation smaller than 0.8 with all other covariates. The optimal number of boosting iterations was chosen by maximizing the area under the ROC curve (AUC) of the predicted probabilities of presence of all the datapoints which were not retained in the replica. The training and evaluation procedure was done for all 1000 thinned replicas using the `xgboost` package in R [*Chen et al.*, 2017].

Epidemiological analysis

The importance of ephemerality in explaining disease prevalence was quantified within a logistic regression framework using odds ratios with the `epiDisplay` package in R [*Chongsuvivatwong*, 2015]. A Generlized Linear Model (GLM) with a logit link function was fit to the intestinal and uro-genital schistosomiasis prevalence data from respectively 178 and 312 villages in Burkina Faso. The parasitological data was

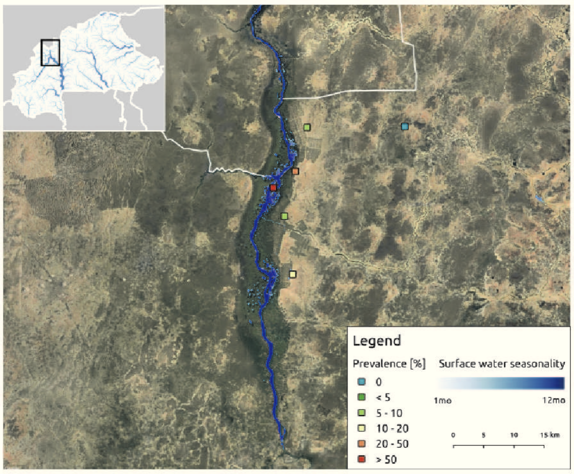

Figure 5.4 – Hotspot of intestinal schistosomiasis around the Léry dam in the North of Burkina Faso. Waterbody persistence is estimated as the number of months per year when water is present [*Pekel et al.*, 2016]. Satellite imagery: ©2017 Google, TerraMetrics

mainly extracted from the Global Neglected Tropical Diseases Database (GNTD, http://www.gntd.org), and complemented with a dataset collected by the Institut de Recherche en Sciences de la Santé of Burkina Faso (IRSS, Ouagadougou, Burkina Faso). Since the prediction of the probability of presence of *B. pfeifferi* did not account for the modifications of the local hydrological regime by dams, all datapoints closer than 3km from permanent man-made reservoirs at the time where the parasitological survey was done were excluded, including the villages around the Léry dam in the North-East (Fig. 5.4). To overcome the temporal miss-match between the prevalence data and socio-economic covariates from the Demographic Health Surveys (DHS, see Table 5.1 for the complete list of covariates), only prevalence data from 1990 on-wards was retained. For each parasitological sampling location, the average of the the DHS data points within 40km of the DHS survey year closest to the year in which the parasitological sampling took place was taken, differentiating between rural and urban locations. Since some villages had been sampled multiple times within the allowed time-window, only the maximum observed prevalence in each village for the epidemiological analysis in the period before, and after the start of Mass Drug Administration (MDA) campaigns against schistosomiasis in 2004 were retained [*Touré et al.*, 2008]. The population of each village in the year of parasitological sampling was projected from the National Census in 2006 using national yearly annual population growth data (Recensement général de la population et de l'habitation au Burkina Faso (RGPH) en 2006, Institut National de la Statistique et de la Démographie, Ouagadougou, Burkina Faso). In terms of the ecological ranges of the intermediate hosts of each form of the disease, the predicted probability of presence of *Biomphalaria pfeifferi* as described in the previous section for intestinal schistosomiasis was used, whereas it was assumed that at least one species of *Bulinus spp.* that transmit uro-genital schistosomiasis can be found throughout Burkina Faso (see Fig. 5.19) [*Poda*, 1996].

5.3 Results

5.3.1 Ephemerality classes

The rivers for which data were available in the GRDC dataset present distinct patterns of ephemerality in terms of the number of 0-flow months per year (Fig. 5.1b). Although hydrological ephemerality generally increases with latitude, which is a proxy of climate, the large variability in the number of 0-flow months

Table 5.1 – Covariates used in epidemiological study. The data from the Demographic Health Surveys (DHS) correspond to geographical clusters of surveyed habitations.

Covariate	Units	Resolution	Source
Socio-economic			
use of surface water for drinking	%	DHS cluster	INSD 1993; INSD 1999; INSD 2003; INSD 2010
open defecation	%	DHS cluster	INSD 1993; INSD 1999; INSD 2003; INSD 2010
population	-	village	IGB*
Ecology			
B. pfeifferi presence	probability	river	computed
Hydrology			
distance to closest river	meters	-	extracted from DEM
distance to closest lake or dam	meters	-	IGB*
river ephemerality class	categorical	river	computed

* National Geographical Institute of Burkina Faso

per year across stations highlights the importance of watershed-specific processes. A regime shift during the drought period is clearly visible as an increase in the number of dry months per year (Fig. 5.1b), with 26 stations presenting a significant change-point in their timeseries of 0-flow months per year (Fig. 5.2 b). By applying a hierarchical clustering algorithm on the Jensen-Shannon divergence between histograms of 0-flow months 4 distinct clusters were obtained in the pre-drought and 5 during the drought periods using a threshold probability value of 0.85. (Fig. 5.5 a,b).

The clusters determined in each period follow the same patterns with very similar 0-flow duration histograms: two clusters of increasing ephemerality with more than 6 months of 0-flow on average, a cluster mainly composed of year-round (perennial) discharge, and finally one (two) clusters in the pre-drought (drought) period characterized by more erratic behavior with a very variable number of dry months from permanent to highly seasonal (Fig. 5.5c). The overall classes of ephemerality of each river was defined in terms of the ephemerality cluster in which it was assigned to both before and during the drought, thus accounting for changes in hydrologic regime caused by the drought (Fig. 5.5d). The permanent flow cluster in the pre-drought period experienced most changes, with many of its members experiencing an increase in the number of dry months and transitioning to the erratic, mid and strongly ephemeral classes. Five final ephemerality classes were thus defined based on the classes in both the pre-drought and drought conditions, as well as the transition between classes:

1. *permanent*: permanent rivers both in normal and drought conditions;
2. *permanent with low variability*: permanent rivers in normal conditions that became erratic during the drought;
3. *permanent with high variability*: rivers that where either already erratic in the pre-drought period or permanent rivers in the pre-drought period which became mid or strongly ephemeral during the drought;
4. *mid ephemeral*: rivers which never experienced full-year flow with an average of 7 dry months per year;
5. *strongly ephemeral*:rivers which never experienced full-year flow with an average of 9 dry months per year.

Half of the monitored rivers (29/58) in the country were classified as ephemeral overall, with most strongly

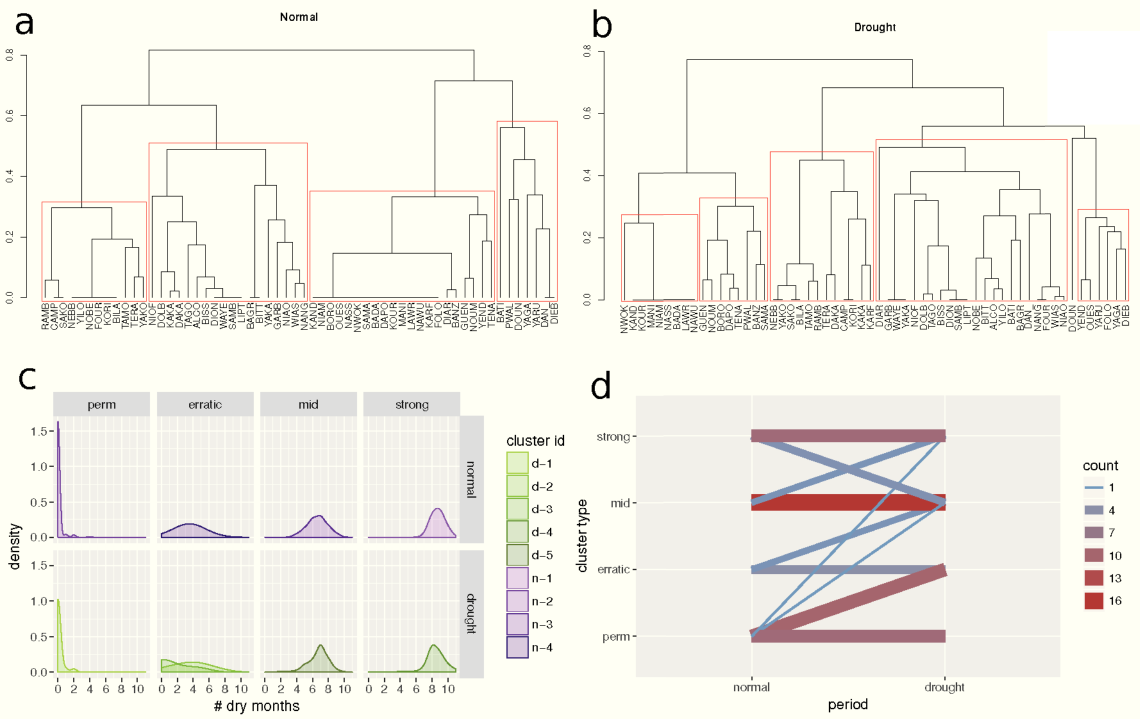

Figure 5.5 – Ephemerality clustering analysis. a) Hirearchical clustering dendogram of stations (abbreviated to first 4 letters) and significant cluster (red lines, probability value of 0.85) before 1975 (year retained as the start of the long-lasting drought in the West Africa). b) Same as a) for discharge data after 1975 (drought period). c) Density plots of the number of dry months per year for each of the ephemerality clusters for the pre-drought and drought periods. Note that 5 clusters were identified in the drought period vs. 4 in the normal period. d) The transition between ephemeratliy classes during the drought shows the the sensitivity of certain regions to reduction in precipitation.

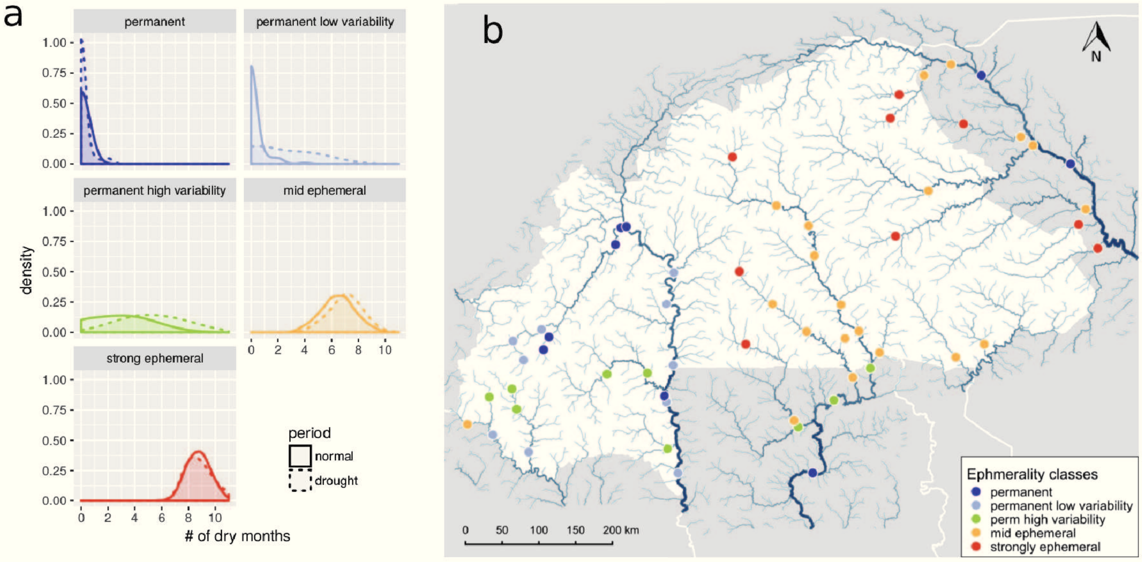

Figure 5.6 – Ephemerality clustering analysis. a) Density plots of the number of dry months per year for each of the ephemerality classes defined by hierarchical clustering using the Jensen-Shannon divergence as distance metric. Epehemerality classes account for the sensitivity to the long-lasting drought in the 1970s - 1980s. b) Map of ephemerality classes of the GRDC stations.

ephemeral streams located in the Sahelian climatic zone to the North (Fig. 5.6b). Rivers in the different permanent classes are mainly located in the South-West and in the downstream sections of the large tributaries of the Volta. Interestingly, the tributaries to the Comoe river in the South-West exhibit a strong drought sensitivity and have a large increase in the duration of the dry spells during this period.

5.3.2 Evaporation and precipitation-vegetation hysteresis

Most of the monitored catchments have high (water limited) aridity indices with high evaporative fraction (Fig. 5.7). Furthermore, most catchments tend to plot above the (non-parameterised) Budyko curve, leaving only the extremely arid catchments (aridity index >5) below it. Interestingly, the position of the ephemerality clusters is non-trivial along the Budyko-curve (Fig. 5.7). Although the most ephemeral class tends to have a higher aridity index as espected, the other classes co-occur at intermediate levels of aridity thus suggesting that controls other than aridity are influencing this aspect of the hydrologic regime. Fitting Fu's equation (eq. 5.2) to each catchment separately reveals a strong positive linear relationship between ω and vegetation photosynthetic activity in terms of the mean yearly *fpar* (Fig. 5.7c, p-value $< 10^{-5}$), in agreement with results from similar studies at the global level [*Li et al.*, 2013; *Xu et al.*, 2013]. Catchments with more photosynthetically active vegetation, indicated by a high value of *fpar*, transpire a larger fraction of the input precipitation compared to more sparsely vegetated areas. This feedback demonstrates that vegetation is both a response and a determinant of moisture availability and hydrologic conditions. Given the significance of the relationship, it was included in the prediction of annual discharge $\bar{Q}_i$ in all catchments as:

$$\overline{Q}_i = \overline{P}_i \cdot \left(1+\left(\frac{\overline{ET_{0}}_i}{\overline{P}_i}\right)^{\omega_i}\right)^{\frac{1}{\omega_i}} - \overline{ET_{0}}_i, \tag{5.4}$$

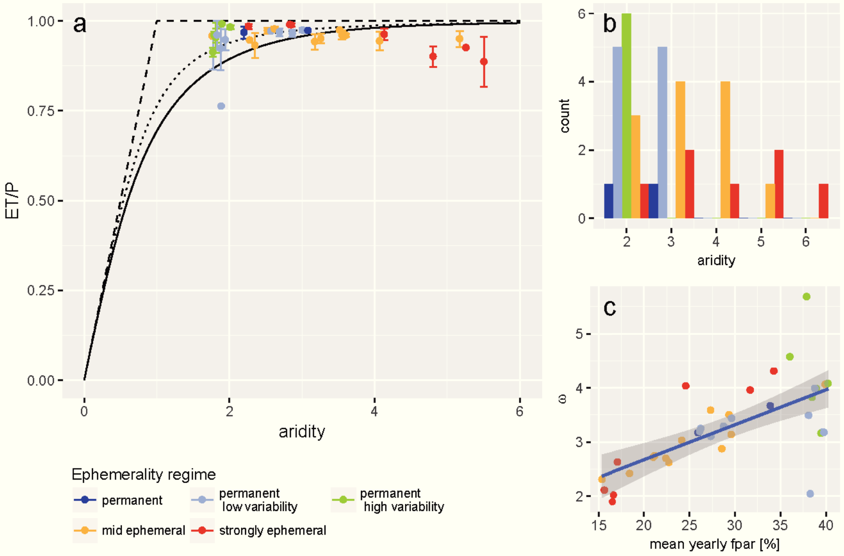

Figure 5.7 – Rivers of Burkina Faso in the Budyko-Fu framework. a) Position along the Budyko curve. The aridity index was computed by using remotely-sensed estimates of potential evapotranspiration and precipitation in the contributing area of each river stretch for the period 2005-2015. The observed evaporative fraction was computed through annual cumulates of discharge and precipitation for the years in which hydrologic data was available (error bars indicate one standard deviation) by ephemeraliy class (point color), and compared to the Budyko curve (full line), and Fu's curve fitted to all the data (one single value of $\hat{\omega}$, dotted line). b) Histograms of aridity by ephemerality class. c) Relationship between vegetation and the evapotranspirative fraction in the Budyko framework. Vegetation is expressed as the yearly average fraction of photosynthetically active radiation (fpar) in the upstream contributing area, and its effect on the evapotranspirative fraction in terms of the value of the free parameter in Fu's equation (ω) fitted to each individual river stretch, showing a clear positive linear relation between $\overline{fpar}$ and ω.

with $\omega_i = \max(1, a + b \times \overline{fpar_i})$ where $a = 1.32(\mathrm{CI}[0.68-2.02]$ and $b = 0.067[\mathrm{CI}0.043-0.090]$ are respectively the intercept and the slope of the regression line in Fig. 5.7c.

The regression between ω and *fpar* was used within the probabilistic Budyko framework by fitting a normal distribution to the residuals of the regression (Fig. 5.8 a, $\hat{\mu} = -2 \times 10^{-16}$ and $\hat{\sigma} = 0.576$) and computing the probability distribution of evaporative fraction for a given aridity index by adding $1'000$ random values drawn from the residuals distribution to the linear regression of ω vs. *fpar*. The net result can be seen in Fig. 5.8 b, whereby lower values of *fpar* yield lower values of ω, leading to lower evaporative fraction and higher runoff variability for intermediate values of aridity.

The hysteresis of monthly precipitation and vegetation (*fpar*) presents a counter-clockwise loop shape for all studied catchments in Burkina Faso. In general, an initial increase in photosynthetic activity was observed as soon as rainfall starts in late April or May with a steady increase over the course of the rainy season extending into the month of September, ending with a rapid decline in activity, or senescence that lasts from from November to March (Fig. 5.9). This general pattern responds to rainy season start, magnitude, and duration. Differences in land-cover and plant type, for example agricultural or naturally occurring vegetation could modify this pattern, although the analysis of these factors is beyond the scope of this study. More specifically, the hysteresis of the ephemerality clusters differ both in the duration of vegetation activity increases during the wet season, and in the speed of the recession as precipitation decreases. When partitioned by the size of the catchment, permanently flowing rivers had a slower recession of catchment vegetation at the end of the rainy season, and higher overall

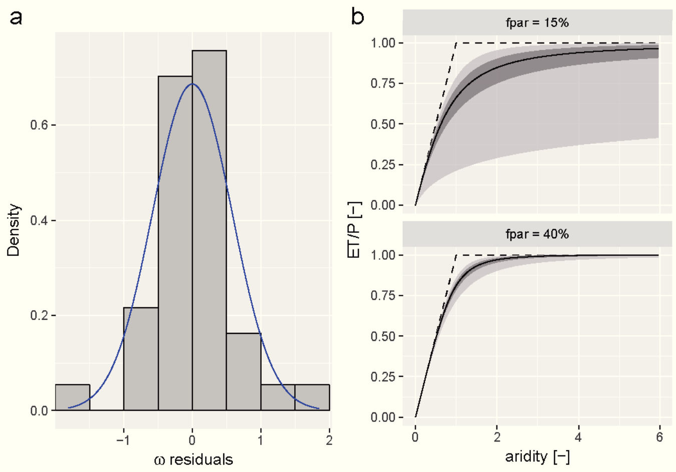

Figure 5.8 – Probabilistic Budyko framework. a) Distribution of the residuals of the linear regression of ω against *fpar* (bars) and fitted normal distribution (blue line). b) Probabilistic Budyko curves resulting from perturbing ω (eq. 5.2) $1'000$ times yielding the mean (black line), 50% (dark gray) and 95% (light gray) confidence intervals, here illustrated for the minimum and maximum observed values of *fpar*.

vegetation activity throughout the year. On the other hand the permanent rivers in smaller catchments with higher sensitivity to changes in precipitation conditions were distinguished by a decrease in the fraction of absorbed photosynthetically active radiation at the peak of the rainy season in August, a stronger seasonal increase in October and November, and slower recession at the end of the year. Highly sensitive permanent rivers presented stronger August decay and faster recession than the lower sensitivity permanent rivers. The small and stable permanent rivers presented a more circular hysteresis with no August decrease in *fpar*. These hysteresis differences were quantified in terms of two metrics: the angle between the July-August and August-September segments of the hysteresis, and the slope of the October-November segment (Fig. 5.9 inset). The first captures the difference between the total amount of precipitation in the different catchments and the corresponding vegetation increase. The slope of the recession quantifies the speed at which vegetation retracts after the end of the rainy season. The final set of covariates used for the classification of the entire river network are given in Fig. 5.10.

5.3.3 River network classification

The best performing GBT model under LOO-CV obtained a cross-validation accuracy of 66% over all 5 ephemerality classes and up to 88.5% when distinguishing between permanent and ephemeral classes (the best parameter set is shown in Table 5.2). All the top-five best-fitting GBT models were relatively shallow (low number of branches), and significant sub-sampling of both the data and the covariates which both are mechanisms that limit over-fitting [*Hastie et al.*, 2009; *Chen and Guestrin*, 2016]. The relative importance of the four covariates in the best-performing GBT model shows that the mean annual discharge has a preponderant role in distinguishing ephemerality classes. The aridity index, the two precipitation-vegetation hysteresis metrics and the mean annual value of *fpar* had similar relative importance in the classifier training (Fig. 5.11).

The classification results had limited sensitivity to the subset of data and covariates used for training and to the probabilistic prediction of annual discharge, with little change in class assignment subject to different values of the predicted discharge and classifier training (Fig. 5.12).

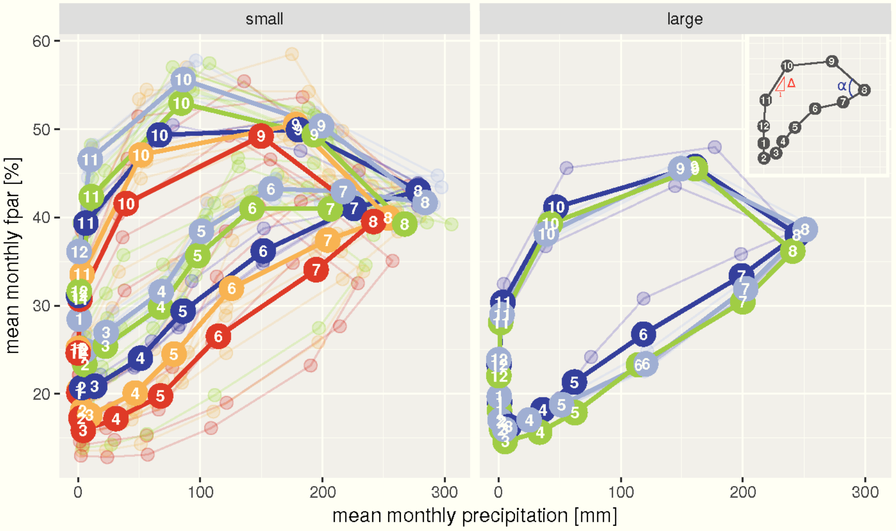

Figure 5.9 – Monthly precipitation-vegetation hysteresis in Burkina Faso by ephemerality class and watershed size. Ephemerality class colors as in Fig. 5.6. Watersheds are considered large if they are larger than 10^4km^2. The hysteresis points are plotted for the mean monthly precipitation and *fpar* in the upstream contributing areas for the period 2005-2015. The inset represents a hysteresis sketch with an indication of the two characteristics that were extracted, the angle (α) and the slope (Δ).

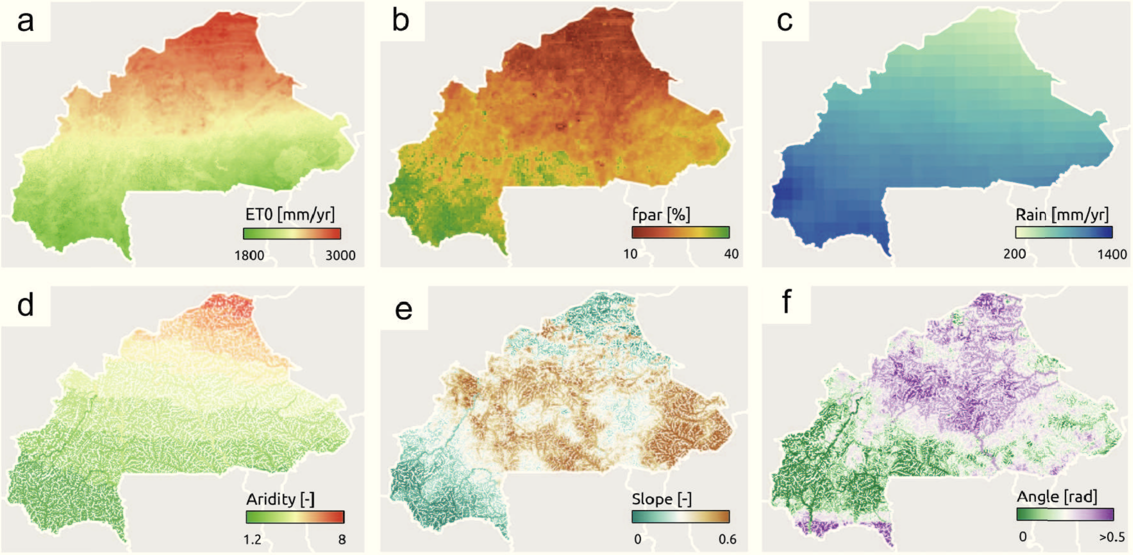

Figure 5.10 – Covariates used in the gradient-boosted trees classification of river network ephemerality. Remote sensing gridded inputs are the mean yearly potential evapotranspiration (a), mean yearly fraction of absorbed photosynthetically active radiation (*fpar*) (d), and the mean yearly precipitation (d). Indices computed for each river stretch over the upstream contributing area are: the aridity index (d), and characteristics of the precipitation-vegetation hysteresis, the slope of the October-November edge (e, α in Fig. 5.9), and angle between the July-August and the August-September edges (f, Δ in Fig. 5.9).

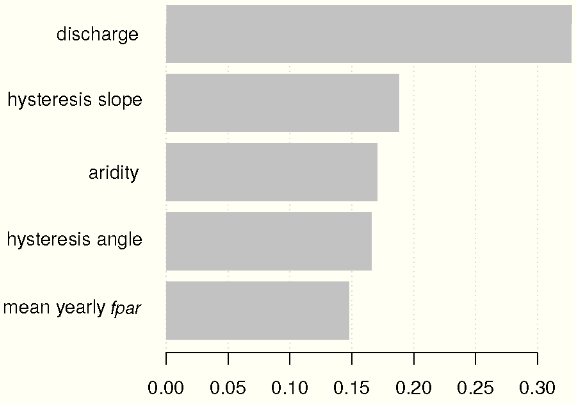

Figure 5.11 – Relative importance of the covariates in the gradient-boosted trees classification of river network ephemerality. Annual discharge was estimated using the vegetation-specific Fu's equation and accounting for additional evaporative losses in man-made reservoirs.

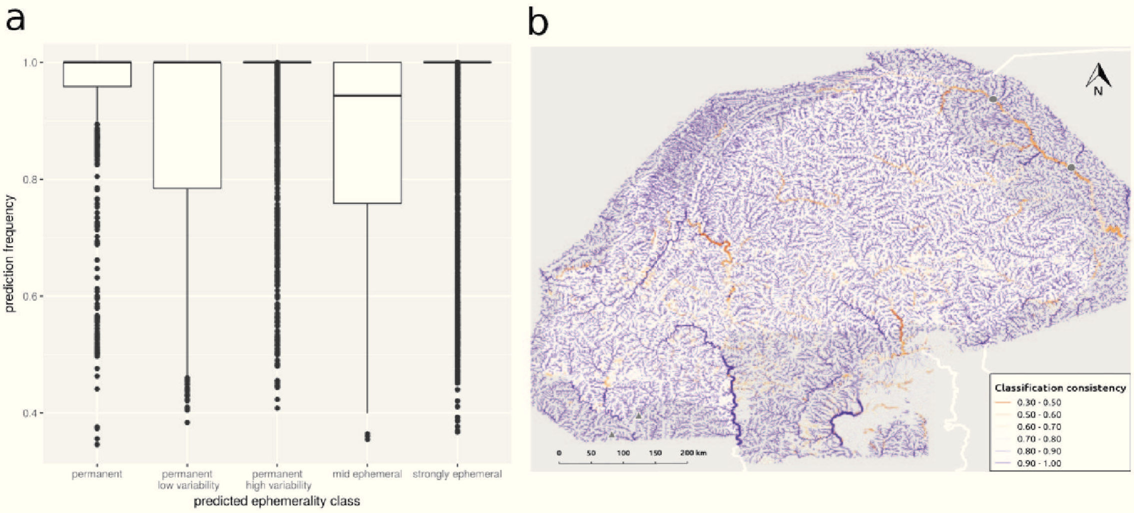

Figure 5.12 – Sensitivity of class membership prediction to classifier training and probabilistic discharge prediction. The robustness of the classification approach is expressed in terms of the frequency of classification outcomes (out of 10,000 repetitions) which are the same as the final class assigned determined by the majority of outcomes (consistent prediction). a) Box-plots of consistent prediction frequency with all classes presenting a median classification frequency larger than 99% and inter-quantile ranges above 80% except for the permanent low variability class, b) Map of consistent prediction frequency.

Table 5.2 – Tuning of the gradient-boosted trees classification parameters. Parameters include the learning rate (η), the depth of the random trees, the number of boosting iterations (n), and the sub-sampling fraction of training datapoints (ρ_{data}) and covariates (ρ_{cov}). Parameter sets were evaluated in terms of the mean LOO-CV error (ϵ) over 10 repetitions of random data and covariates samplings.

rank	η	depth	n	ρ_{data}	ρ_{cov}	ϵ
1	0.10	4	79	0.8	0.8	0.34
2	0.10	3	96	0.8	0.8	0.36
3	0.10	3	73	0.8	0.8	0.36
4	0.10	3	61	0.8	0.8	0.36
5	0.10	5	88	0.8	0.8	0.36

At the large scale, the classification of river ephemerality is marked by the South-to-North climatic gradient that characterizes Burkina Faso (Fig. 5.13). Indeed, North of ≈ 12° latitude all streams are predicted to be strongly ephemeral except for the main rivers with large flow accumulation. To the South of that limit a West-to-East gradient comes into play with small rivers predicted to be permanent to the West of the country with differing levels of variability and sensitivity to drought conditions. Interestingly, streams are predicted to be permanent but with high variability in the very South-Western regions despite high annual precipitations. This prediction is supported by data from two gauging stations in Northern Côte d'Ivoire which were not included in the training set due to the lack of full records (Fig. 5.14). The stable permanent river stretches were predicted to be the ones with a very large predicted annual discharge either due to the size of the contributing area (e.g.: the downstream parts of the Volta River) and/or the high runoff generated upstream.

In order to further verify the accuracy of this classification the predicted classes of hydrologic regimes were compared to the observed ephemerality of reservoir waterbodies in the country. The seasonality of water presence in the country's reservoirs was extracted from remote sensing estimates of water presence in [*Pekel et al.*, 2016], and a reservoir was considered ephemeral if it did not contain at least one pixel covered by water year-round. Of the 558 reservoirs for which water seasonality information was available, around 80% were found to be ephemeral. Of these, ≈ 95% were correctly classified in the predictive ephemerality map, i.e. intercepting river stretches of either the mid ephemeral or strongly ephemeral classes (Fig. 5.15), and only 3 were predicted to be on permanent rivers.

Based on these results, three ephemerality regions were delineated in the country, namely: 1) strongly ephemeral to the North of the 12° latitude, 2) intermediate ephemerality in the center and eastern parts of the country South of the 12th parallel, and 3) permanent in the West and South-west encompassing all classes with permanent flow (Fig. 5.18). The boundaries of the ephemerality regions were extracted using an automatic procedure that aggregates the rasterized ephemerality class values using the mode of a circular window with a width of 75 km and 150 km. The mean of the two aggregated maps was used to define the ephemerality class of each pixel within the study area.

5.3.4 Ephemerality and the geography of schistosomiasis

The following analysis focus on the use of the ephemerality classification for epidemiological studies on both intestinal and uro-genital schistosomiasis. Mapping the known occurrence of the aquatic snail *B. pfeifferi* in Burkina Faso highlights a Northern limit to its ecological range (Fig. 5.18). The association between hydrological ephemerality and snail occurrence was supported by the fact that the GBT models taking hydrological ephemerality into account outperformed their counterparts in most cases in terms

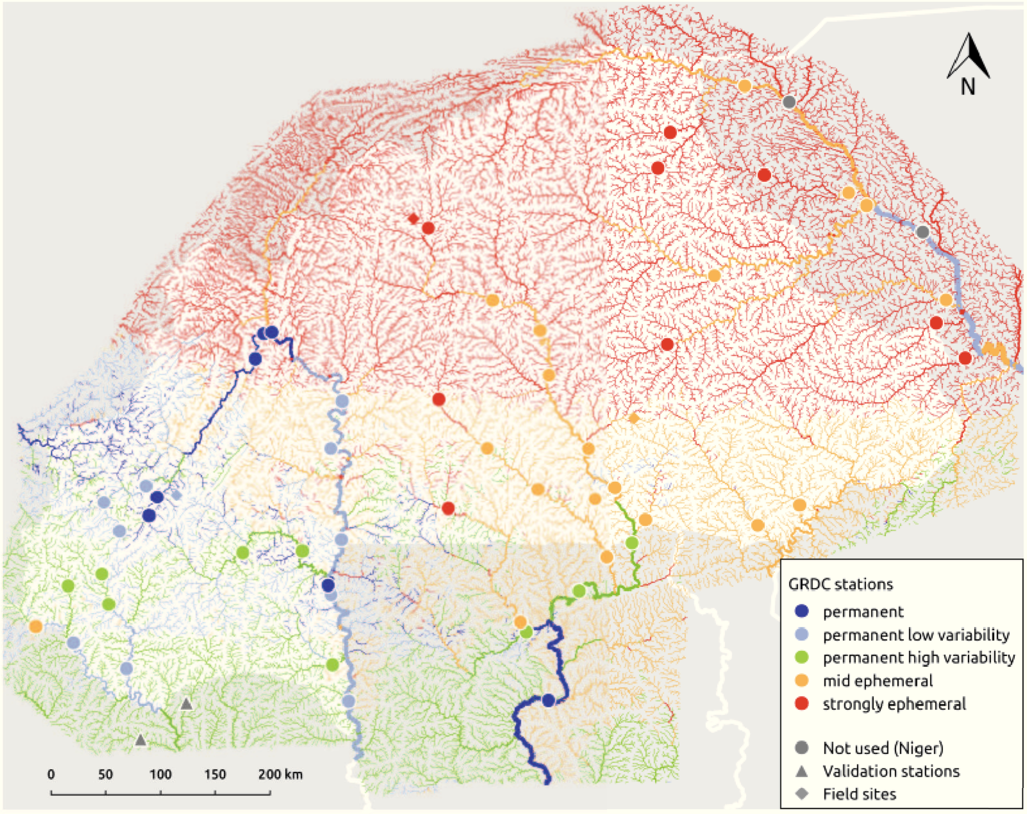

Figure 5.13 – Predicted ephemerality classes in Burkina Faso. Predicted classes correspond to the most frequent class outcome from the GBT classifier accounting for sub-sampling in the training process and uncertainty in the annual discharge estimates within the probabilistic Budyko framework.

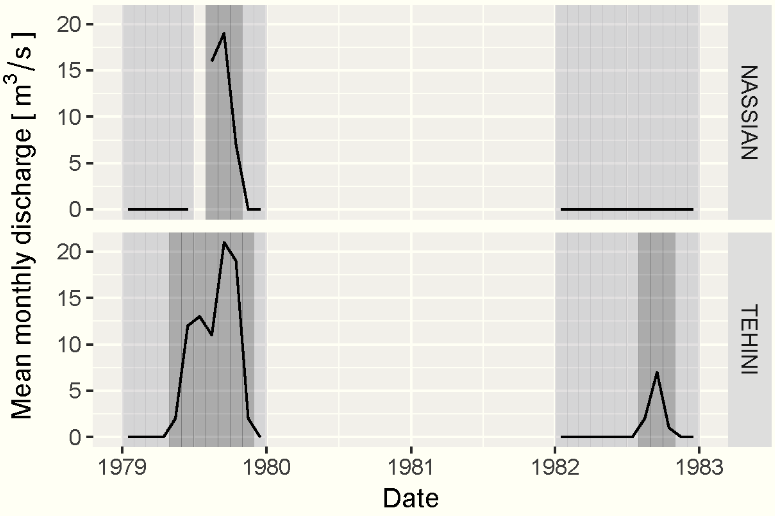

Figure 5.14 – Discharge data from the two GRDC stations not included in the training set. The predicted class of both stations was permanent with strong variability which is compatible with the length 0-flow periods (dark grey shading) observed in the discharge timeseries (data availability indicated by light grey shading).

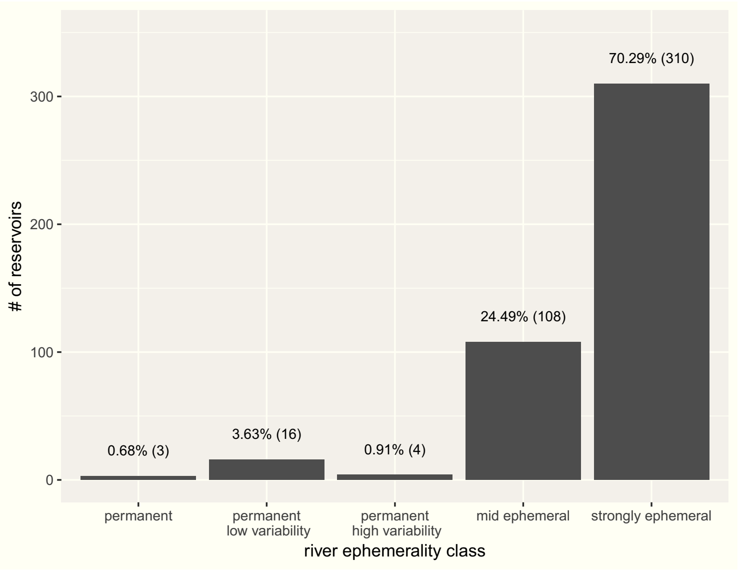

Figure 5.15 – Predicted ephemerality classes for reservoir waterbodies. Reservoirs were considered to be non-permanent if they did not contain at least one pixel covered by water year-round in the dataset by [*Pekel et al.*, 2016]. Predicted reservoir ephemerality is given in terms of the percentage of the total and counts (in parenthesis).

of AUC (82.6% of training-testing replicas). Such associations had a significantly broader validation in terms of classification accuracy (p-value< 0.001, Fig. 5.16). An ensemble model combining the best GBT classifier of each training-testing replica yielded a prediction accuracy over the whole dataset of 85.3% [CI 77.3-91.4] and an AUC of 0.916, both larger than any single model candidate (Fig. 5.16).

The predicted ecological range of *B. pfeifferi* was obtained by applying the ensemble model to the whole river network in the country (Fig. 5.17). This is thought to be the first attempt to predict the ecological range of intermediate hots of schistosomiasis in rivers that explicitly includes the structure and hydrological characteristics of the network.

In the logistic regression of intestinal schistosomiasis prevalence, both the predicted snail probability of presence and hydrological ephemerality class were present and significant (p-value< 0.001) in the best-fitting model along with socio-economic covariates (Table 5.3). Indeed, villages in the mid- and strong ephemerality class had much lower risk of intestinal schistosomiasis with respect to villages along permanent rivers, and snail probability of presence had dominant effect on the odds of contracting the disease (Table 5.4). It is recalled that the ORs correspond to 1 unit increase of continuous variables, and w.r.t. the baseline category (permanent river) for the ephemerality class, therefore the OR of 11006 for snail presence in Table 1 corresponds to the ratio of the odds of schistosomiasis between a village with probability 0 and probability 1 of *B. pfeifferi* presence. The analysis excluded known disease hotspots located around the Léry dam on the border with Mali (Fig. 5.4). Indeed the damming of the Sourou river in the mid 1970s created a permanent water body which favored the establishment of *B. pfeifferi* snails that migrated from the South-West, and ultimately led to the emergence of intestinal schistosomiasis in previously disease-free villages around the reservoir in a region with otherwise ephemeral rivers [*Poda et al.*, 2004a]. On the other hand, in the case of uro-genital schistosomiasis (whose intermediate host snails are ubiquitous in the area), stronger hydrological ephemerality was associated with larger disease odds with respect to permanent rivers (mid ephemerality: OR 4.6 [3.77 -5.61], strong ephemerality: OR 7.6 [6.29-9.18]). This differs from intestinal schistosomiasis fro which the mid and strong ephemerality classes

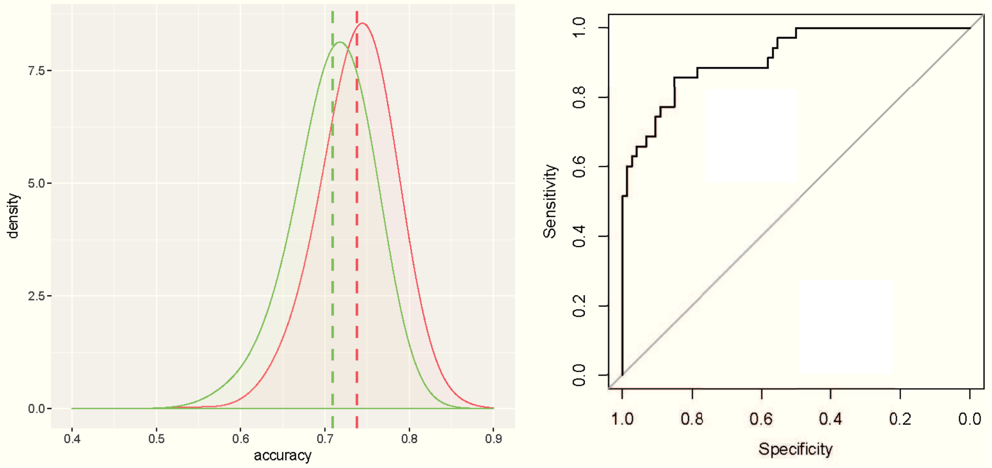

Figure 5.16 – a) Density plots of the evaluation prediction accuracy of the GBTs models with hydrological ephemerality (red) or without it (green) and their respective means (73.8% vs. 70.9%). b) Receiver Operator Characteristic curve of the mean ensemble of best-fitting models (accuracy: 85.3% [CI 77.3%-91.4%], AUC = 0.916).

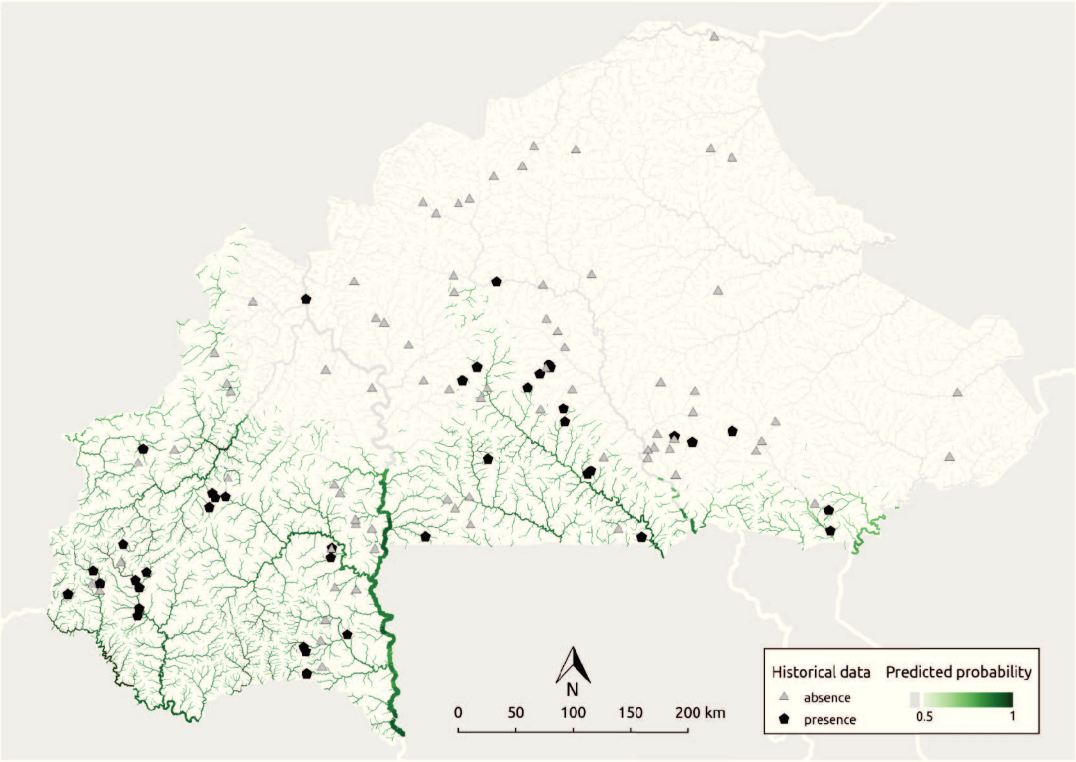

Figure 5.17 – Predicted ecological range of *B. pfeifferi* in rivers in Burkina Faso. Predictions are the result of a ensemble of 1000 GBTs models trained on spatially-thinned subsets of the historical data using environmental covariates and the predicted hydrological ephemerality class. The threshold of 0.5 is retained for classifying predicted snail presence/absence (accuracy of 85.3% [CI 77.3-91.4]).

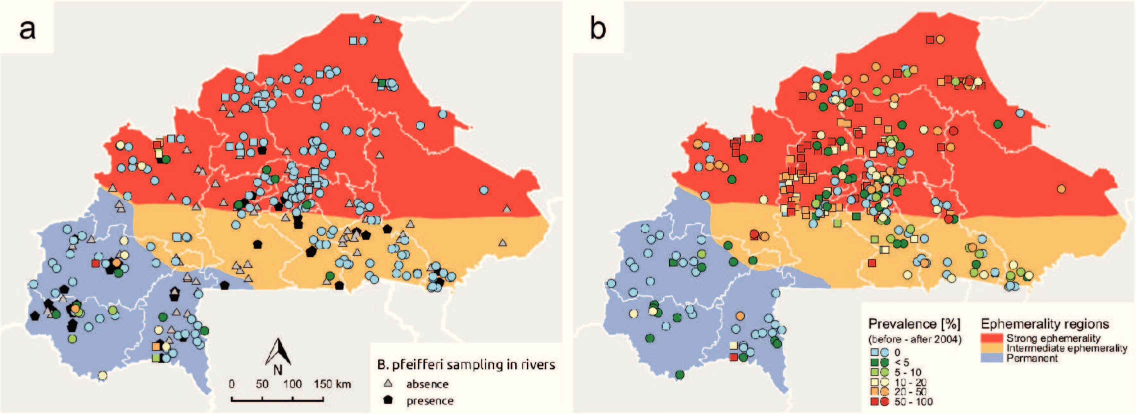

Figure 5.18 – River network ephemerality and the geography of schistosomiasis. a) Map of predicted ephemerality regions corresponding to the most common ephemerality classes found within them along with the locations of historical malacological and parasitological data for before (squares) and after (circles) the start of MDA in the coutry (white lines indicate the 13 administrative regions). b) Same as a) but for uro-genital schistosomiasis. The intermediate hosts of *S. haematobium* can be found throughout the country (Fig. 5.19) and are therefore not shown.

had similar odd-ratios. Furthermore proximity to quasi-permanent waterbodies including man-made dams and natural lakes was associated to higher odds of schistosomiasis (Table 5.4). Interestingly, this effect as significant along side socio-economic covariates, such as the use of surface water for drinking purposes, and population density (Table 5.1). The difference between the two forms of the disease with respect to socio-economic covariates is that open air defecation was only present in the case of intestinal schistosomiasis, whereas use of surface water for drinking purposes was retained for the uro-genital form.

5.4 Discussion

The methodology proposed in this Chapter addresses the fundamental problem of how to classify river network ephemerality in data-scarce regions. A classification methodology of such kind can also be used for estimating habitat suitability for intermediate hosts of schistosomiasis and disease transmission. Indeed, in terms of discharge data the novel metric that were proposed for the clustering of river ephemerality only requires the histogram of the number of 0-flow months per year and can be easily generalized to other regions using to the GRDC database. Moreover, the methodology based on the Jensen-Shannon divergence could be valuable in characterizing hydrologic ephemerality over a wide spectrum of streamflow intermittency by using the probability distribution of the duration of 0-flow events at the daily or even hourly scales where this type of data exist, with further potential applications to stream ecology affected by highly intermittent hydrological drivers [*Datry et al.*, 2014; *Costigan et al.*, 2016].

The main limitation of this approach is that the hydrologic and remotely sensed data used here do not overlap in time – the former cease in the mid 1980s during the historical drought whereas the latter cover the period 2000-2015. A recent study of long-term re-analysis data suggests that yearly precipitation is recovering from the drought period in many regions of Burkina Faso especially in the center and Northern regions [*De Longueville et al.*, 2016]. This could imply a reduction of 0-flow months to pre-drought levels in those streams that changed of ephemerality class during the drought, which would support the relevance of the historical discharge data contained in this study. Nevertheless, the evolution of landcover over the past 40 years may also have played an important role in observed changes in runoff generation in the

Table 5.3 – Best-fitting logistic model of intestinal and uro-genital schistosomiasis prevalence in Burkina Faso. Variable types are boolean [bool], percentage [%], numerical [num], probability [prob], and categorical [cat]. Regression coefficients are given along with their standard error (in parethesis). The baseline for the ephemerality class is permanent rivers.

	Intestinal	Uro-genital
Baseline		
Intercept [num]	$-10.44\ (0.96)^{***}$	$-2.40\ (0.10)^{***}$
Socio-economic		
MDA [bool]	$-2.06\ (0.15)^{***}$	$-1.98\ (0.04)^{***}$
open defecation [bool]	$2.14\ (0.40)^{***}$	
drinking surface water [fraction]		$1.53\ (0.12)^{***}$
population $\times 10^{-4}$ [num]	$1.48\ (0.55)^{**}$	
small city [num]		$1.18\ (0.18)^{***}$
large city [num]		$-0.62\ (0.10)^{***}$
Ecology		
snail presence [prob]	$9.31\ (1.02)^{***}$	
Hydrology		
reservoir or lake at < 1500m [bool]		$0.48\ (0.04)^{***}$
mid ephemerality [cat]	$-1.82\ (0.43)^{***}$	$1.53\ (0.10)^{***}$
strong ephemerality [cat]	$-1.77\ (0.46)^{***}$	$2.03\ (0.10)^{***}$
AIC	528.91	4663.85
Log Likelihood	-257.45	-2323.92
Num. obs.	178	312

$^{***}p < 0.001$, $^{**}p < 0.01$, $^{*}p < 0.05$

Table 5.4 – Odd-ratios and 95% CI of intestinal and urogenital schistosomiasis with respect to socio-economic, ecological and hydrological factors in Burkina Faso. The OR were derived from the coefficients of a logistic regression model (SM Table 3). Variable types are boolean [bool], percentage [%], numerical [num], probability [prob], and categorical [cat]. The OR correspond to 1 unit increase of continuous variables, and w.r.t. the baseline category (permanent river) for the ephemerality class.

	Intestinal	Uro-genital
Socio-economic		
MDA^{i} [bool]	0.127 [0.0944 – 0.171]	0.137 [0.127 – 0.149]
open defecation^{ii} [bool]	8.46 [3.87 – 18.5]	-
drinking surface water [fraction]	-	4.6 [3.63 – 5.85]
population $\times 10^{-4}$ [num]	4.4 [1.49 – 13]	-
small city^{iii} [num]	-	3.25 [2.29 – 4.61]
large city [num]	-	0.54 [0.445 – 0.656]
Ecology		
snail presence [prob]	11006 [1477 – 82039]	-
Hydrology		
reservoir or lake at < 1500m [bool]	-	1.62 [1.5 – 1.76]
mid ephemerality [cat]	0.161 [0.069 – 0.377]	4.6 [3.77 – 5.61]
strong ephemerality [cat]	0.171 [0.0698 – 0.419]	7.6 [6.29 – 9.18]

^{i}Mass Drug Administration campaigns, ^{ii}more than 50%, ^{iii}defined as less than 5,000 inhabitants last decades in SSA [*Mahe et al.*, 2013]. Further validation of the results presented here with more recent hydrological records requires additional nation-specific data sources, which is the subject of ongoing work. The five covariates used in the prediction step (predicted annual discharge, aridity index, mean annual *fpar* and two characteristics of the precipitation-vegetation hysteresis) were chosen according to their relevance for hydrologic process, in this case runoff production and precipitation-vegetation hysteresis, and the availability of data for Burkina Faso. In applying this approach to other contexts, alternative sets of covariates, or some modification of the covariates used here (e.g.: the preciptiation - vegetation hysteresis) might prove more relevant in other study areas, and the design and pre-selection of covariates will require a sound conceptual understanding of the hydrological drivers. That being said, even without modification this Chapter's approach is easily transferred to the large tracts of the globe with limited hydrological measurements. The main result of this Chapter is the definition of five ephemerality classes based on the duration of 0-flow and the sensitivity of these classes to the extreme drought in the 1970s and 1980s. Strongly ephemeral rivers are characterized by very high aridity indices and small or moderate flow accumulations and are not sensitive to drought conditions. Large contributing areas and flow accumulations enable rivers located in very arid environments to maintain flow for longer periods of time and thus are classified within the intermediate ephemerality class. Although some stations in the intermediate ephemerality class transitioned to strongly ephemeral during the drought, the most significant effect of the drought was the loss of permanent flow in medium and small sized rivers in the South-West of the country (Fig. 5.5d). Sensitivity to the drought and erratic ephemerality were associated with particular precipitation-vegetation hysteresis characteristics, i.e. a peak rainy season decrease in photosynthetically active radiation (*fpar*) and the rate of decline in photosynthetic activity following the cessation in wet season rainfall.

It is important to note that the area of study, Burkina Faso, spans multiple endemic vegetation zones (Sahelian and Sudanian mainly), land covers (various forests, woodlands, scrublands, grasslands), and land uses (diverse agriculture, pastures, and urban) [*White*, 1983]. Each zone is characterized by plant assemblages with varying water use strategies, photosynthetic adaptations, and phenologies. Since the photosynthetic activity, expressed as *fpar*, is both a determinant and a response to water availability, functional plant characteristics can be non-negligible [*Xu et al.*, 2015b; *Diémé et al.*, 2017]. Deciduousness, which would be visible as a rapid decline in photosynthetic activity and *fpar* following the end of the wet season, is a clear adaptation to a tropical seasonally dry climate [*Vico et al.*, 2015]. Deciduouness is often accompanied by an efficient soil water extraction capacity, which in exceptionally dry years such as the during the 1970s West African drought could result in lower average soil moisture, on top of reductions due to lack of precipitation, and a reduction in river discharge relative to vegetation water use. Indeed eddy-covariance measurements in South-Eastern Burkina Faso demonstrate a positive correlation between seasonal vegetation cover, soil moisture and evaporative fraction [*Ceperley*, 2014; *Ceperley et al.*, 2017]. Moreover, the small reduction in *fpar* at the peak of the rainy season in permanent catchments can be attributed to reductions in energy availability associated with high levels of cloud cover, thus reducing relative photosynthetic activity. Overall, the sensitivity of catchments with permanent flow and high levels of vegetation cover to drought demonstrates the intricate relationship between climate, soil moisture, vegetation and discharge, especially in already water limited catchments [*Porporato et al.*, 2004; *Donohue et al.*, 2006]. Hydrological ephemerality provides a new lens that could improve how resilience is observed, defined, and managed with important implications for meeting Sustainable Development Goals, particularly related to water resources management, agriculture and public health in arid climates [*Falkenmark and Rockström*, 2008].

As an illustration of the epidemiological relevance that ephemerality has for water-borne diseases, the predicted ephemerality class was used both for the study of the ecological range of the intermediate hosts of intestinal schistosomiasis, and as an explanatory factor for contracting the disease. Indeed, hydrologic ephemerality significantly improved the predictive capacity of ecological models for the distribution of *B. pfeifferi* in rivers, which is the first attempt of including network topology explicitly with respect to to existing approaches using maximum entropy and gridded covariates [*Stensgaard et al.*, 2013]. As expected, stronger ephemerality decreases the probability that the intermediate snail hosts are present. The logistic modelling results of the prevalence of schistosomiasis in Burkina Faso highlighted the distinct ways in which ephemerality has an effect on disease transmission. In the case of intestinal schistosomiasis, the probability of snail occurrence had a dominant effect on disease risk along with socio-economic covariates. Ephemerality was further significantly associated to lower. One possible explanation is that although *Biomphalaria spp.* snails can be found in mildly ephemeral habitats, the limited suitability of the environment in combination with *Schistosoma* parasite infection strongly limits the probability of snails surviving the pre-patent period (about 15-40 days for *S. mansoni* depending on water temperature [*Anderson and May*, 1979]), particularly during aestivation [*Badger and Oyerinde*, 1996]. Laboratory experiments have shown, however, that environmental stress may increase parasite fecundity in snails once the latter start shedding [*Gleichsner et al.*, 2016].

The strong association between the probability of snail presence and intestinal schistosomiasis risk is a clear example of the hydrologically-driven ecological underpinnings of disease transmission. A natural extension of this analysis would be to account for the ecology of *B. pfeifferi* in small reservoirs for which high spatial and temporal resolution data are becominb increasingly available through advances in remote sensing technology [*Amitrano et al.*, 2017]. The opposite pattern was observed for uro-genital schistosomiasis with hydrological ephemerality being associated to higher risk of (OR 7.6 [6.29-9.18] for the strong ephemerality class), and even more so in villages located close to man-made reservoirs or natural lakes (OR 1.61 [1.5-1.76]) in agreement with previous meta-analysis [*Steinmann et al.*, 2006]. Moreover, ephemerality dominated the other socio-economic covariates except for the protective effect of MDA. It is hypothesized that the higher risk in ephemeral regions, in addition to prompting the construction of dams and other water resource engineering, is due to the constraints water presence impose on the location of human-water contacts, potentially causing more human-water contacts/day/m^2 of water in fewer water contact points as the dry season advances, which in turn increases the circulation of parasites from the human to the snail hosts and back [*Chandiwana*, 1987; *Kloos et al.*, 1997]. Indeed, the analysis of models which account for spatial heterogeneities indicates that reducing (increasing) the number of water contact points increases (decreases) the strength of schistosomiasis transmission quantified in terms of a generalization of the basic reproduction number used in epidemiology for connected systems [*Mari et al.*, 2017a]. This interpretation of the multivariate epidemiological analysis relies on five hypothesis made about potential confounding factors that could correlate with hydrological ephemerality:

H1 at least one species of *Bulinus* spp. snails is present in the water contact points of all prospected villages

H2 variations of the species-dependent infectivity and susceptibility in the *Bulinus-S. haematobium* system do not drive the geography of uro-genital schistosomiasis at the country scale

H3 substitution of *S. haematobium* by *S. mansoni*, if existent, is limited to specific regions and does not determine larges-scale patterns of uro-genital schistsosomiasis

H4 spatially un-correlated residual variance in human exposure to infection with respect to the chosen covariates (hydrological conditions, distance to rivers, dams and lakes, population density, use of surface water for drinking purposes, and open defecation)

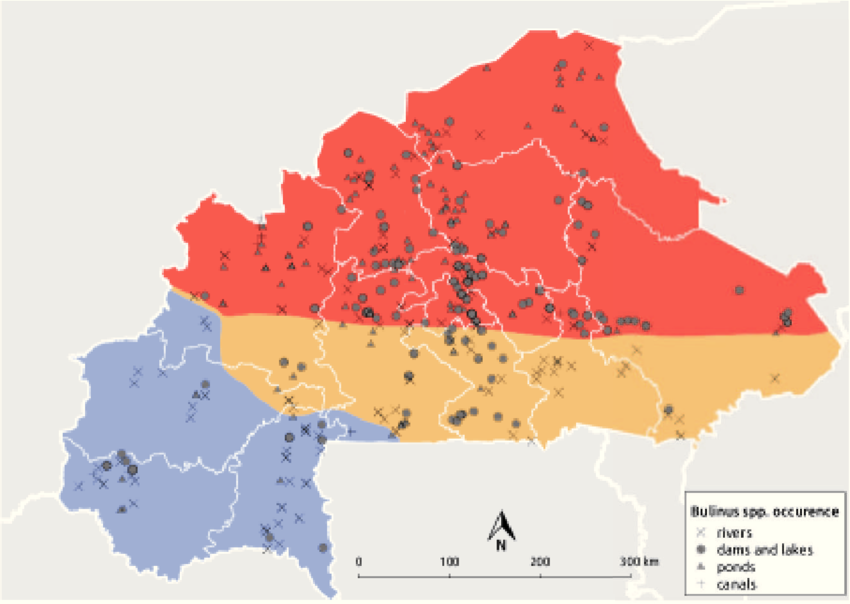

Figure 5.19 – Occurrence of *Bulinus* spp. snails in Burkina Faso. Presence data is shown by sampled habitat [*Poda et al.*, 1994]. The *Bulinus* species found in Burkina Faso are: *B. truncatus*, *B. globosus*, *B. senegalensis* and *B. forskalii*.

H5 there is no significant spatial autocorrelation in human individual-based susceptibility/resistance to schistosomal infection.

The results of the country-wide sampling by [*Poda*, 1996] support H1 in that species of *Bulinus* were found in almost all sampling dates and sites with *B. pfeifferi* being the only present species in only one occasion out of 308 samplings (Fig. 5.19). In this analysis the seasonal variations of snail abundance were only indirectly taken into account by the hydrologic ephemerality class, although population fluctuations can differ largely between different habitats (natural vs. man made) with the same climatic forcing [*Perez-Saez et al.*, 2016]. Taking this aspect into account would therefore require a dynamical modelling framework, which is the matter of ongoing work.

The coevolution of snails and schistosomes and the resulting variations of compatibility between the parasite and its host have been shown in laboratory experiments [*Webster and Davies*, 2001], with particular emphasis on the varying compatibility between snails and schistosomes from distinct spatial locations [*Southgate et al.*, 2000], and across strains of schistosomes and species of snails [*Theron et al.*, 2014]. Furthermore it has been suggested that different levels of morbidity in humans are associated to specific schistosome strains, with genetic variation influencing infectivity and virulence [*Rollinson et al.*, 2009]. Although there is evidence for the spatial genetic structuring of the snail intermediate hosts along habitats (rivers and lakes) [*Davies et al.*, 1999], structuring of schistosomes in human hosts tends to be lower or absent at the village [*Davies et al.*, 1999], or local scale [*Sire et al.*, 2001] (< 150km in the case of Lake Victoria shown in [*Standley et al.*, 2010]), and only be significant at very large distances (> 300km) [*Betson et al.*, 2013]. The absence of structuring has been suggested to owe to the higher dispersal of schistosomes due to human mobility and migration with respect to passive transport of snails along waterways [*Davies et al.*, 1999], which could explain the observed absence of local adaptation in some settings [*Prugnolle et al.*, 2006]. Although these hypothesis would need to be verified in Burkina Faso at the national scale, it is deemed that H2, re-stated as the absence of regions of snail genetic resistance to schistosome infection, as a reasonable working hypothesis. On a different level, snail species-dependent cercarial production (the schistosome larva infective to humans) have been reported with a significantly larger maximum daily production of cercariae by *Bulinus globosus* w.r.t *B. senegalensis* and *B. truncatus* and little difference between the later two [*Fryer and Probert*, 1988]. Since the ecological range of *B. globosus* is similar to that of *Biomphalaria pfeifferi*, i.e. the permanent rivers and waterbodies in the Center and South of the country, and the highest *S. haematobium* infections are in the North, it is reasonable to assume that species-dependent cercarial production is not an important factor [*Poda et al.*, 2004a].

One possible confounding factor for the lower prevalence of uro-genital schistosomiasis in the permanent ephemerality region could be the replacement of *S. haematobium* by *S. mansoni* in areas of historical co-endemicity which has been reported in the South-West [*Colette et al.*, 1982; *Poda et al.*, 2004a], and to a lesser extent around the Léry dam in the North-West [*Poda et al.*, 2004a]. One explanation proposed by these studies is the out-competition of *Bulinus* spp. by *Biomphalaria* spp. in areas suitable to both species as seen in other settings [*Abdel-Wahab et al.*, 1993; *Ernould*, 1996], although recent malacological samplings in the country do not seem to validate this hypothesis in the case of Burkina Faso [*Perez-Saez et al.*, 2016]. Another invoked argument is the larger per capita production of *S. mansoni* cercariae by *Biomphalaria* spp. than *S. haematobium* cercariae by *Bulinus* spp. [*Colette et al.*, 1982]. The corollary of this interpretation is that some form of in-host (human) competition is involved in the substitution. A very well documented case of inter-species competition is that of the replacement of *S. intercalatum* by *S. haematobium* and *S. mansoni* in Cameroon through competitive mating interactions and asymmetrical immunological protection [*Tchuem Tchuenté et al.*, 2003]. Experimental evidence however suggest that *S. haematobium* is dominant over *S. mansoni* in terms of mating competition between the two species [*Webster et al.*, 1999], which would imply that other factors are involved such as population dynamics over the whole schistosome lifecycle, immunological responses in the human host, or the ecology of the snail intermediate hosts [*Webster et al.*, 1999, 2008], although the specific pathways of this substitution are far from having been elucidated as clearly as for *S. intercalatum*. The in-host dynamics of both species are certainly altered by MDA campaigns due to reported differential sensitivity to praziquantel by the two species [*Garba et al.*, 2013; *Knowles et al.*, 2015]. Because the understanding of the extent and mechanisms of *S. mansoni* substitution is limited in Burkina Faso, H3 assumes that it is limited to intestinal schistosomiasis transmission pockets, and correlates but is not at the origin of the observed association between ephemerality and uro-genital schistosomiasis. Moreover, even if this phenomenon occur in the areas of *S. mansoni* endemecity, the significance of the difference of uro-genital risk between the intermediate and strong ephemerality regions would remain unchanged since neither are associated to high intestinal schistosomiasis prevalence. This assumption is tested by including the probability of presence of *Biomphalaria pfeifferi* as a (pessimistic) proxy of intestinal schistosomiasis transmission in the logistic regression. The results show that although the addition was significant ($p\text{-value} < 0.05$) and with the expected negative slope, the ephemerality effects remained significant and ($p\text{-value} < 0.001$) and there was little improvement in terms of AIC (5.5).

Important heterogeneities in human-water contact patterns have been observed even at small spatial scales [*Chandiwana and Woolhouse*, 1991; *Kloos et al.*, 1997], and varying contact duration, frequency and types have been associated to exposure to schistososmiasis infection [*de Moira et al.*, 2010], although not directly to infection intensity in all settings [*Scott et al.*, 2003; *Sow et al.*, 2011]. Although the spatial prediction of water contacts on a village base is beyond the scope of this work [*Kulinkina et al.*, 2016; *Perez-Saez et al.*, 2015], access to water, sanitation, and hygiene (WASH) have been shown to be relevant factors in predicting schistosomiasis risk [*Soares Magalhães et al.*, 2011]. This motivated the use of socio-economic variables in the logistic regression analysis as a proxy of human exposure to infection. Furthermore, the issue of confounding in the context of interpreting the link between ephemerality and

Table 5.5 – Additional risk factors of uro-genital schistosomiasis in Burkina Faso.

	With *B. pfeifferi*	With Temperature
Baseline		
Intercept [num]	$-1.86\ (0.27)^{***}$	$-24.86\ (1.82)^{***}$
Socio-economic		
MDA [bool]	$-1.98\ (0.04)^{***}$	$-2.00\ (0.04)^{***}$
drinking surface water [fraction]	$1.53\ (0.12)^{***}$	$1.25\ (0.13)^{***}$
small city [num]	$1.22\ (0.18)^{***}$	$1.23\ (0.18)^{***}$
large city [num]	$-0.60\ (0.10)^{***}$	$-0.39\ (0.10)^{***}$
Ecology		
snail presence [prob]	$-0.75\ (0.34)^{*}$	
Hydrology		
reservoir or lake at < 1500m [bool]	$0.48\ (0.04)^{***}$	$0.30\ (0.04)^{***}$
mid ephemerality [cat]	$1.38\ (0.12)^{***}$	$0.97\ (0.11)^{***}$
strong ephemerality [cat]	$1.83\ (0.13)^{***}$	$1.18\ (0.12)^{***}$
Climate		
mean annual temperature [num]		$0.82\ (0.07)^{***}$
AIC	4661.07	4511.92
Log Likelihood	-2321.54	-2246.96
Num. obs.	312	312

$^{***}p < 0.001$, $^{**}p < 0.01$, $^{*}p < 0.05$

disease patterns would arise if the degree of exposure and contamination which is independent from hydrological ephemerality and unaccounted-for by the socio-economic covariates varied systematically across the country resulting in the spatial patterns of uro-genital schistosomiasis prevalence. H4 therefore relates to the spatial auto-correlation in water-contact patterns related to exposure and contamination rather than to the actual prediction of water contact patterns with the socio-economic covariates. On the other hand the analysis presented here did not include any hypothesis on the link between air temperature and human-water contacts as it has been suggested in the case of recreational bathing of children in Burkina Faso [*Traoré et al.*, 2016] since no direct relationship has been quantified on a large spatial scale (the cited study only included one village). Interestingly, when accounting for mean annual air temperature in the logisitic regression higher air temperature was indeed significantely associated to greater risk, but both the association between intermediate and strong ephemerality regions and schistosomiasis risk remained significant (p-value< 0.001) (5.5).

Spatially-autocorrelated patterns of individual immunological resistance to schistosome infection would bear a strong mark on the geography of the disease. One specific cause could be ethnic-specific susceptibility or resistance to schistosomiasis, as it has been shown for tuberculosis [*Delgado et al.*, 2002], and malaria in Burkina Faso [*Modiano et al.*, 1996]. A study on *S. mansoni* in an Ugandan fishing community associated variation to re-infection to differences in cercarial exposure during human-water contacts rather than to ethnic-specific immunological response [*de Moira et al.*, 2010]. Based on these conclusions, and assuming that H4 is true, this analysis assumes homogeneous individual susceptibility to schistosomiasis in the country.

In the context of these results, this suggests that increasingly ephemeral conditions can also create disease hotspots in arid regions by both creating a higher dependence on reservoirs for water resources, and a highly isolated habitat for intermediate hosts. Indeed, the construction of reservoirs, and their associated irrigation waterways, not only creates suitable habitats for the intermediate hosts by expanding the water surface and changing the hydrology of the tributary river stretch and its upstream contributors, but also alters the socio-economic activities in the villages they serve, thus modifying population density and human-water contact patterns in ways that can further strengthen transmission [*Boelee et al.*, 2009; *Ayantunde et al.*, 2017]. Although these observations cannot be directly extended without additional evidence from fieldwork in Burkina Faso and other settings, the results for intestinal and urinary schistosomiasis suggest a direct (and non-linear) feedback between disease transmission and hydrological ephemerality. Disease risk outcomes could therefore depend on both the ecological (snail) and human response to drought according to the sensitivity of disease transmission to decreased habitat suitability on one hand, and variations in water contact patterns and/or water resources development on the other, as suggested by the disease odd-ratios analysis performed here. Addressing these hydrological ephemerality-related issues within a dynamical modelling framework constitutes an important yet largely unexplored avenue into studying the effects of climate change on schistosomiasis, as current studies have manly focused on the effects of temperature on snail ecology and parasite biology [*McCreesh and Booth*, 2013, 2014a]. This is important since climate change is predicted to have a growing impact on baseflow discharge in water limited environments as increasing atmospheric CO_2 encourages an increase in catchment leaf area and seasonal transpiration, in addition to ongoing changes in precipitation and atmospheric water demand [*Trancoso et al.*, 2017]. In the light of these considerations, the observed correspondences between hydrological ephemerality and schistosomiasis prevalence support the relevance of the ephemerality classification approach used here as it enables the inclusion of hydrology as a key ingredient in the development of national-scale spatially-explicit models of disease transmission for the spatio-temporal prediction of both snail abundance and seasonality [*Gurarie et al.*, 2017; *Perez-Saez et al.*, 2016], and human-water contact [*Perez-Saez et al.*, 2015]. If the importance of understanding and accounting for the socio-ecological factors that support schistosomiasis transmission when designing and implementing control and elimination programs is now acknowledged [*Utzinger et al.*, 2011], it is important to highlight the role of hydrology (here identified in terms of ephemerality) as a first-order control of both human-water contact patterns and snail ecology in what could be termed the socio-ecohydrological matrix of disease transmission. The importance of hydrological ephemerality for water-borne diseases largely depends on the nature of the water-borne disease and spatial scale considered. Disease-specific ephemerality indices could therefore be designed depending on the available hydrological data and pathogen life-cycle. For instance, the flow duration within the rainy season or the size of the hydrologically connected components of the network could be of interest for other water-borne diseases in other settings. Indeed, the choice of the number of dry months was largely driven by the available hydrological data, and this simple index could be modified according to length and flow threshold, including as an ecological constraint for long-lasting free-living pathogens. By relying only on openly accessible data, the approach proposed in this Chapter is repeatable in, and adaptable to, other contexts where hydrologic ephemerality is also an important driver of water-borne disease transmission [*Heinrich et al.*, 2017; *Rinaldo et al.*, 2017].

5.5 Conclusion

This Chapter develops an approach for the large-scale classification of river network ephemerality based on openly accessible data, and tested it within Burkina Faso, in sub-Saharan Africa. This novel methodology shows promise for the generalization to other data-scarce settings where water-borne diseases are a public health issue. The regions with different degrees of ephemerality that were defined strongly matched historical prevalence of intestinal schistosomiasis, the disease being present almost exclusively around permanent rivers. On the other hand, an opposite pattern was observed for uro-genital schistosomiasis with higher risk associated to stronger ephemerality, possibly due to the concentration of socio-economic and domestic activities around a limited number of human-water contact points in which compatible aquatic snail hosts can be found throughout the country. The exposed nonlinear links between ephemerality and disease risks support for the use of the proposed ephemerality prediction methodology for other regions and builds a case for the appraisal of water-borne diseases from a socio-ecohydrological perspective.

6 Spatio-temporal prediction of snail ecology

Leveraging the ecological insight gathered from the three experimental sites in the spatially explicit modelling framework presented in Chapter 3 requires the spatio-temporal prediction of snail abundance whose fluctuations depend not only on environmental covariates, but also on habitat hydrology (permanent vs. ephemeral). This Chapter presents a methodology for regionalizing the ecological modelling framework developed in Chapter 4. The approach utilizes remote sensing data and is applied spatially by habitat type based on the national-scale hydrological ephemerality predictions of Chapter 5. Although the national-level simulation results are preliminary and require further analysis and model refinement, they are encouraging with respect to the capacity to produce reliable predictions of snail population dynamics to be incorporated into spatially explicit models of schistosomiasis transmission.

6.1 Introduction

Spatio-temporal modelling of the ecology of intermediate hosts or vectors of infectious diseases of humans has principally been applied to malaria and other mosquito-borne diseases, in particular in terms of temperature suitability for *Anopheles* spp. [*Weiss et al.*, 2014, 2015], and to also the effects of rainfall on seasonal variations of mosquito densities [*Bomblies et al.*, 2008; *Bomblies and Eltahir*, 2009; *Rumisha et al.*, 2014]. For instance *Diboulo et al.* [2015] use a rich set of entomological data in a Bayesian geo-statistical approach to model the seasonal variations in mosquito density as a function of remotely-sensed environmental covariates (rainfall, vegetation indices, and temperature). Mosquito densities were then used to infer the resulting number of infected bites per person at a 250m pixel resolution over an entire health district in Burkina Faso. Hydrology has also been explicitly incorporated into mosquito models, for instance to track water levels in ponds affecting population of the mosquito vectors of Rift Valley Fever at a daily timestep in Senegal *Soti et al.* [2012], or of *Anopheles* spp. in an integrated model of malaria which accounts for pool water availability for larval reproduction *Tompkins and Ermert* [2013].

As noted in section 1.2.2, spatial studies on the intermediate hosts of *S. mansoni* and *S. haematobium* have principally focused on the determination of their ecological range using historical presence/absence in species distribution models [*Stensgaard et al.*, 2013, 2016]. Using the same tools but with recent temporally-resolved malacological surveys, *Manyangadze et al.* [2016] took into account seasonal variation in snail occurrence in South Africa by partitioning the the modelling process by season (cold/dry, hot/dry, rainy, post-rainy), thus producing season-dependent suitability maps. The inclusion of seasonality in spatial estimations of snail occurrence is an innovative step, however their approach does not account for variations in snail abundance - only presence and absence - and does not incorporate temporal auto-correlation in snail abundance from one season to the other. On the other hand, past temporal studies on the ecology of the snail intermediate hosts have focused on local population dynamics which already require considerable fieldwork (cf. section 1.2.2), but without a perspective a view on predictionting them at larger spatial scales.

This Chapter presents a methodology aimed at bridging the gap in spatio-temporal predictions of snail population dynamics for their use in schistosomiasis risk mapping, and their incorporation into spatially-explicit models of disease transmission. More particularly, the the issue of the regionalization of discrete-time ecological models with remote sensing estimates of key environmental covariates is addressed building on three complete years of ecological data from the experimental sites presented in Chapter 2.

6.2 Materials and methods

6.2.1 Data and ecological models

The protocols for the collection of field ecological and environmental data have been described in Chapter 4, with the difference that in this Chapter the timeseries of snail counts and covariates extended up to July 2017. Given the objective of applying the models of snail demography to the whole country, all data were aggregated at a monthly timestep. Sampling was interrupted in the irrigation canal in Tougou in 2016 due to external factors. This Chapter thus focuses on the natural habitats in Lioulgou (temporary pond and ephemeral river), and in Panamasso (permanent river).

Following the methods in Chapter 4, thee Malthusian, Ricker and Gompertz discrete time models are used to describe snail population dynamics, this time also allowing for piece-wise linear effects of the covariates on the natural rate of increase [*Toms and Lesperance*, 2003]. The use of piece-wise linear models was motivated by the need to account for sharp changes in population growth and collapse that characterize snail ecological dynamics in the absence of environmental data gathered at high temporal resolution, as the ones available in the experimental sites presented in Chapter 2 (refered to as "the experimental sites" hereafter). Indeed the regionalization of the predictions to the rest of the country needs to rely upon the use of remote sensing estimates of environmental variables (cf. section 6.2.2). In particular, the aim is to capture the abrupt changes in the ephemeral habitats at the beginning and the end of the rainy seasons, and in the permanent stream in Panamasso during the cold dry season (Fig. 6.3). Specifically, the change of the relative snail abundance N_t between time t and $t+1$, with a Ricker-type density feedback, is modelled as:

$$\log\left(\frac{\mathrm{N}_{t+1}}{\mathrm{N}_t}\right) = a + b\mathrm{N}_t + \sum_{i=1}^{m_i}\sum_{j=0}^{m_j}\sum_{\tau_{\mathrm{x}_i}=0}^{r_{\mathrm{x}}}\sum_{\tau_{\mathrm{x}_j}=0}^{r_{\mathrm{x}}} c_{i,\tau_{\mathrm{x}_i},\tau_{\mathrm{x}_j}} \cdot X^i_{t-\tau_{\mathrm{x}_i}} \cdot I\left(X^j_{t-\tau_{\mathrm{x}_j}} > \mathscr{T}_{j,\tau_{\mathrm{x}_j}}\right), \tag{6.1}$$

where: $b < 0$ is the negative density-feedback parameter, and $c_{i,\tau_{\mathrm{x}_i},\tau_{\mathrm{x}_j}}$ denotes the coefficient of environmental covariate feature $X^i_{t-\tau_{\mathrm{x}_i}}$ multiplied by the indication function $I(\cdot)$ of covariate $X^j_{t-\tau_{\mathrm{x}_j}}$ being larger than the covariate- and lag-specific threshold $\mathscr{T}_{j,\tau_{\mathrm{x}_j}}$, taken at non-negative integer time lags $\tau_{\mathrm{x}_i}, \tau_{\mathrm{x}_j} \leq r_X$. Given the monthly timestep, only lags of 1 month were considered. Lagged covariate features were taken in all possible combinations up to a maximum of $m_i + m_j = 5$, yielding a total of $\approx 500'000$ models to test for each habitat/species combination. The thresholds $\mathscr{T}_{j,\tau_{\mathrm{x}_j}}$ were fit for each covariate combination using the subplex algorithm, a more efficient extension of the Nelder-Mead derivatives-free simplex algorithm, using the `subplex` package in R [*King*, 2015]. Product interactions of the type $N_{t-\tau_{\text{N}}} X^{i}_{t-\tau_{\text{X}}}$ were not considered. As in Chapter 4, the Gompertz-type density feedback where N_t is substituted by $\log(N_t)$ on the RHS of eq. 6.1, and the Malthusian model ($b = 0$) were also tested.

6.2.2 Remote sensing data

Remote sensing data was used for the regionalization of the predictions the population dynamics of snail intermediate hosts throughout the country. The choice of the covariates to include in the spatial models of snail ecology took into consideration both model identification results from Chapter 4, and the availability of relevant remote sensing products providing estimates at suitable spatial and temporal resolutions. Among the 6 environmental covariates investigated in this Thesis' experimental sites (air temperature, water temperature, conductivity, level, precipitation amounts and number of intense rainfall events), only precipitation and air temperature were retained due to their systematic appearance in the model identification process and the availability of corresponding remote sensing products. For both covariates, available remote sensing products were selected among possible candidates, corrected against ground measurements, and their uncertainty characterized by fitting appropriate error models. Following common approaches in hydrology for rainfall-runoff models [*Hong et al.*, 2006; *Moradkhani and Sorooshian*, 2009], the latter step is necessary to account for the propagation of uncertainty in measured and estimated environmental covariates into the outputs of snail demography models. Covariate extraction and aggregation to monthly steps was done using the Googl EarthEngine API. Given different temporal coverage of the remote sensing products, the extraction was made for the period from January 2003 to December 2016.

Precipitation

Among possible remote sensing products of precipitation the Rainfall Estimate version 2.0 of the Climate Prediction Center (REFV2 product, dekadal estimate at ≈ 10km spatial resolution [*Xie and Arkin*, 1997]) was retained. The latter has been single out as the product with the highest correlation with rain gauge measurements over Burkina Faso [*Dembélé and Zwart*, 2016]. Indeed the estimates of monthly precipitation correlate well ($R^2 = 0.92$) to ground measurements obtained from 10 stations of Meteorological agency of Burkina Faso (Direction Générale de la météo, Ouagadouguo, Burkina Faso) for the period 2006-2016. The agreement between the data observed at station i, and satellite data was further evaluated in terms of the average monthly bias $B_m(i)$:

$$B_m(i) = \frac{1}{n_m} \sum_{t \in \gamma_m} \left(P_{obs,i}(t) - P_{est,i}(t) \right), \tag{6.2}$$

where $m \in [1, 12]$ is the month index, γ_m the set of dates t that have month m, $P_{obs,i}$ and $P_{est,i}$ the observed and estimated monthly precipitation sums at station i, and n_m the number of non-missing datapoints in γ_m. The bias correction was extended to the rest of the dataset by geographical differentiation analysis (GDA) [*Cheema and Bastiaanssen*, 2012]. The estimated monthly bias $B^*_m(i)$ in the precipitation estimates at each pixel i was computed through inverse distance weighting (IDW) of the observed biases $B_m(j)$ at each gauging stations j as:

$$B^*_m(i, p) = \sum_{j=1}^{n_s} d_{ij}^{-p} \cdot \left(\sum_{j=1}^{n_s} d_{ij}^{-p} \right)^{-1} \cdot B_m(j), \tag{6.3}$$

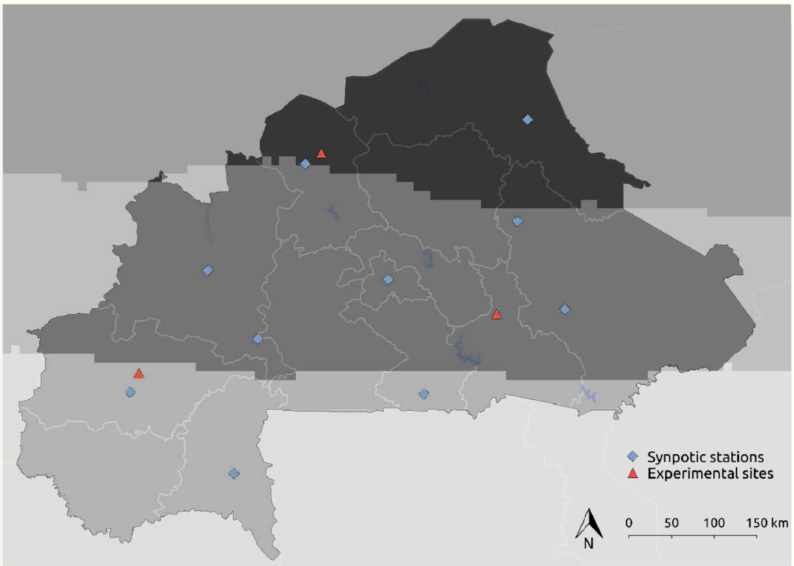

Figure 6.1 – Map of precipitation gauging stations used for the ground-truthing of remote sensing estimates. Were included the 10 synoptic (measuring multiple variables) stations of the Meteorological Agency of Burkina Faso (blue diamonds), and the data from the three experimental sites presented in Chapter 2 (red triangles). Gray tones indicate the latitude and precipitation clusters used for the partitioning of stations for error model fitting.

where p is a parameter, $n_s = 10$ is the number of available gauging stations, and d_{ij} is the euclidean distance between pixel i and station j [*Babak and Deutsch*, 2009]. Parameter p was calibrated through leave one out cross-validation by minimizing the sum of squared differences between the observed and IDW-predicted biases at each station $\frac{1}{n_s}\sum_{j=1}^{n_s}\left(B_m(j) - B^*_m(j,p)\right)^2$.

The uncertainty in the satellite precipitation estimates was quantified by fitting candidate probability density function to the observed monthly errors. Due to climate-dependent differences in estimation errors, the available rain gauge stations were subdivided into three latitude regions accounting for the South-to-North precipitation gradient by performing a k-means clustering on both the latitude and mean annual precipitation of each pixel (Fig. 6.1). For each month (January through December), and each latitude region, the normal and the asymmetric Laplace (ASL) distributions were fit to the precipitation estimation errors by maximum likelihood estimation, and the one with the best (smallest) AIC retained. Initially proposed for quantile regression, the ASL distribution reads:

$$f(x;\mu,\sigma,p) = \frac{p(1-p)}{\sigma}\exp\left(-\frac{x-\mu}{\sigma}\left[p - I(x \leq \mu)\right]\right), \tag{6.4}$$

where $\mu \in (-\infty, +\infty)$ is the location parameter, $\sigma > 0$ the scale, $p \in (0,1)$ the skew, and $I(\cdot)$ is the indication function [*Yu and Zhang*, 2005]. As opposed to the normal distribution, it is suitable for describing data that present more peaked and skewed distribution than the former would assume [*Yu and Zhang*, 2005]. Errors whose absolute values were further than 4 empirical standard deviations from the mean in each month and latitude region were considered as outliers and removed prior to fitting the error models.

Air temperature

Results in Chapter 4 highlighted the link between air and water temperature for the ecological dynamics of both genera of snails across habitats. More particularly, air temperature was systematically selected

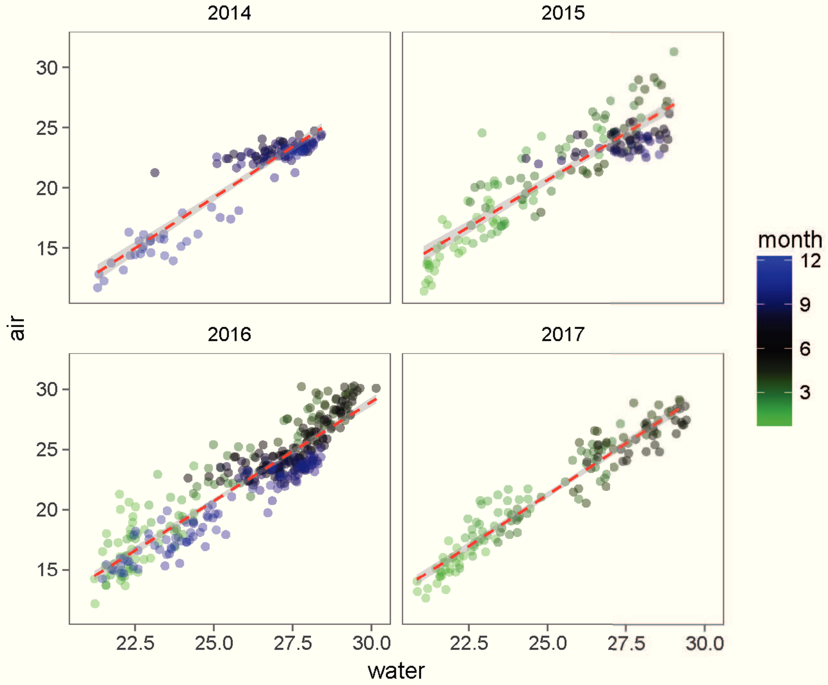

Figure 6.2 – Correlation between nighttime air temperature and daily water temperature in the stream in Panamasso. Nighttime temperature shows a strong correlation with daily water temperature (dashed red lines represent best fitting regression lines, overall $R^2 = 0.84$), here shown partitioned by year. Each point corresponds to one daily mean measurement, and the annual temperature cycle is illustrated in terms of point colouring by month.

in the ephemeral habitats, whereas water temperature was more often retain in the permanent habitat, especially for *B. pfeifferi* (Fig. 4.2). Given the national scale of the analysis, predicting water temperature in then whole river network is well beyond the scope of this work. Instead, the strong correlation between the average monthly water temperature and nighttime (6PM-6AM) air temperature (Fig. 6.2, adjusted $R^2 = 0.84$) in the stream in Panamasso is exploited, and include both day and night temperatures as separate covariates in eq. 6.1.

Different global scale modelling estimates of temperature at daily to monthly resolutions are available, including the MODIS Aqua/Terra temperature products (MYD11A2, 8-day composites at 1km spatial resolution, [*Wan*, 2015]), and the 3-hour state variable outputs of the Global Land Data Assimilation system (GLDAS-1, 3-hour model output at 0.25° resolution [*Rodell et al.*, 2004]). Given the discrepancies between the field measurements and remote sensing estimates of both day and night temperature (Fig. 6.6), a temperature correction process was applied following methods applied to mapping of malaria transmission suitability at national and continental scales. Indeed, the spatio-temporal estimation of daily maximal and minimal air temperature based on remote sensing data has been the subject of numerous studies in the field of malaria given its importance for in the ecology of the mosquito vector (*Anopheles* spp.), and for the development of the parasite within it [*Garske et al.*, 2013; *Weiss et al.*, 2014]. This Chapter follows the methods proposed by *Garske et al.* which consist in a multivariate regression analysis allowing for random slopes and intercepts, using the air temperature data from this Thesis' three experimental sites as reference. More specifically the day and night observed temperatures (T^o_{day}, T^o_{night}) are first modelled as a linear combination with random slopes of the timeseries of MODIS (T^M) and GLDAS-1 (T^G) monthly estimates, the mean daily temperature range ($T_{day} - T_{night}$), the enhanced vegetation index (EVI, MODIS Terra daily product at 1km resolution [*Huete et al.*, 2002]), the estimated daylight hours (from [*Forsythe et al.*, 1995]), and precipitation (cf. preceding section). All covariate combination were tested and the best one selected using the AIC separately for day and night temperatures. In a second step, the random slopes and intercepts in these best fitting models were estimated as a function of all possible combinations of fixed (non-temporal) covariates, which included longitude, latitude, mean annual EVI and mean annual precipitation (for details the reader is referred to [*Garske et al.*, 2013]). The models from step 2 with the lowest AIC were retained for the prediction of monthly day and night temperature.

The same approach for quantifying the uncertainty in the errors in the estimated precipitation was applied to the residuals of the multivariate temperature regression models, except that the error models were fit per station and separately for the rainy (June through September) and dry seasons (October through May), instead than in a monthly basis as done for the precipitation data.

6.2.3 Model implementation and regionalization of predictions

The ecological model fitting procedure was analogous to the one presented in Chapter 4, testing for all combinations of covariates and using information criteria for model selection. Model fitting was done for the data up to December 2016 for the ephemeral habitats in Lioulgou, date at which sampling was interrupted due to external factors, and up to July 2017 in the permanent habitat in Panamasso. It is recalled that the ecological models were fit to the field-measured environmental covariates, and subsequently predictions made using remote sensing estimates of the same covariates (precipitation and temperature). Ecological models were ranked using the compensated Akaike information criterion (cf. Chapter 4), and combined into an ensemble model using a weighted sum of model outcomes, where the weight w_i assigned to model i is a function of the difference between its AICc score and the smallest one obtained in the model set, ΔAIC_i, as [*Burnham and Anderson*, 2002]:

$$w_i = \frac{e^{-0.5\Delta\text{AIC}_i}}{\sum_j e^{-0.5\Delta\text{AIC}_j}}. \tag{6.5}$$

Model ensemble predictions were realized by performing 1000 simulations of model outcomes using perturbed remote sensing estimates of rainfall and temperature drawn from their respective error models, which depended on climatic region (Fig. 6.1) and season (for temperature) or month (for precipitation). Here, simulations were run between January 2015 and December 2016 to cover 2 whole successions of rainy/dry seasons. Initial conditions for the simulation were drawn from a uniform distribution whose bounds correspond to the minimum and maximal sampled snail density in the month of January in each species/habitat dataset.

After comparison with observed ecological timeseries in the experimental sites, the simulation methodology was applied to the pixel-based prediction of snail abundance at the national scale as a proof-of-concept of the capabilities of the framework. For *Biomphalaria pfeifferi*, the hydrological ephemerality regions delineated in Chapter 5 were used as a simple mask for snail presence, thus only prediction within the permanent and intermediate regions were retained. On the other hand *Bulinus* spp. can be present in both permanent and ephemeral rivers, which each have their corresponding ecological model ensemble (i.e. the models fits to the ephemeral stream in Lioulgou, and the permanent stream in Panamasso). The two model ensemble were applied each to their respective hydrological ephemerality region (strongly ephemeral and permanent). In pixels falling in the intermediate ephemerality region, a weighted mean of the permanent and ephemeral model sets was used, with weights proportional to the distance to each ephemerality region and summing to 1. As done in the epidemiological analysis in

5, it is here assumed that at least one species of *Bulinus* can be present in all hydrological ephemerality conditions in Burkina Faso (see section 6.4 for justifications). On the other hand, the predictions for snail ecology in temporary ponds are shown for all the country, thus assuming that these can be found in the permanent ephemerality region (Fig.5.19).

6.3 Results

6.3.1 Observed seasonal variations of snail populations

The full timeseries of abundance counts highlight the same seasonal pattern as the one observed in the 2014-2015 subset used in the ecological analysis in Chapter 4 (Fig. 6.3). The populations of *Bulinus* spp. in the ephemeral habitats in Lioulgou experience population bursts at the start of the rainy season, attaining peak abundance in August-September and subsequently decreasing sharply in November-December prior to the complete drying out of the habitats. Both *Bulinus* spp. and *Biomphalaria pfeifferi* follow opposite seasonal fluctuations with maximal abundance during the dry season in March and April, with population dips during the rainy season. Interestingly, both snail genera in Panamasso present inter-annual variability. The high densities of *Bulinus* spp. which were observed in 2014 did not occur again in the following years. On the other hand, *B. pfeifferi* populations maintained at high densities during the 2016 rainy season, which resulted in unusually high densities in early 2017 after which population collapsed again as the rainy season started. Overall however, seasonal patterns of snail populations emerge clearly throughout the sampling period (Fig. 6.4).

6.3.2 Uncertainty models for remotes-sensing covariates

Precipitation The REFV2 precipitation product shows a systematic bias in rainfall estimates, generally over-estimating rainfall during the dry season and under-estimating it during the wet season (Fig. 6.5). Of importance for snail population dynamics is the general over-estimation of rainfall in the month of May which could lead to erroneous predictions of snail population bursts. The bias correction methodology successfully reduced bias as excepted, but also slightly reduced the overall error between observed an estimated precipitation (Fig. 6.5). The normal (ASL) distribution was retained in 5/36 (31/36) month/latitude error partitions, and captured adequately the distribution of precipitation estimation errors (Fig. C.1).

Temperature The best fitting temperature models were in good agreement with observed day and night temperature at all three monitoring stations (R^2>0.95, Fig. 6.6). Interestingly, both the GLDAS and MODIS temperature estimates were retained in the best-fitting models. As for the precipitation estimates, both the normal and the ASL distribution were retained (respectively in 9 and 3 of 12 data partitions by day/night and season), and represent well the observed error distributions (Fig. C.2).

6.3.3 Predicting snail population dynamics

The population dynamics models incorporating remote sensing covariates as surrogates of locally measured ones were in good agreement with observed seasonal fluctuations (Fig. 6.7). The simulations reproduced well the seasonal dynamics of *Bulinus* spp. in the temporary pond and ephemeral stream, and their population bursts during the rainy season. The variability in the predicted onset of snail population is well captured by the temprature and precipitation error models, with some models greatly

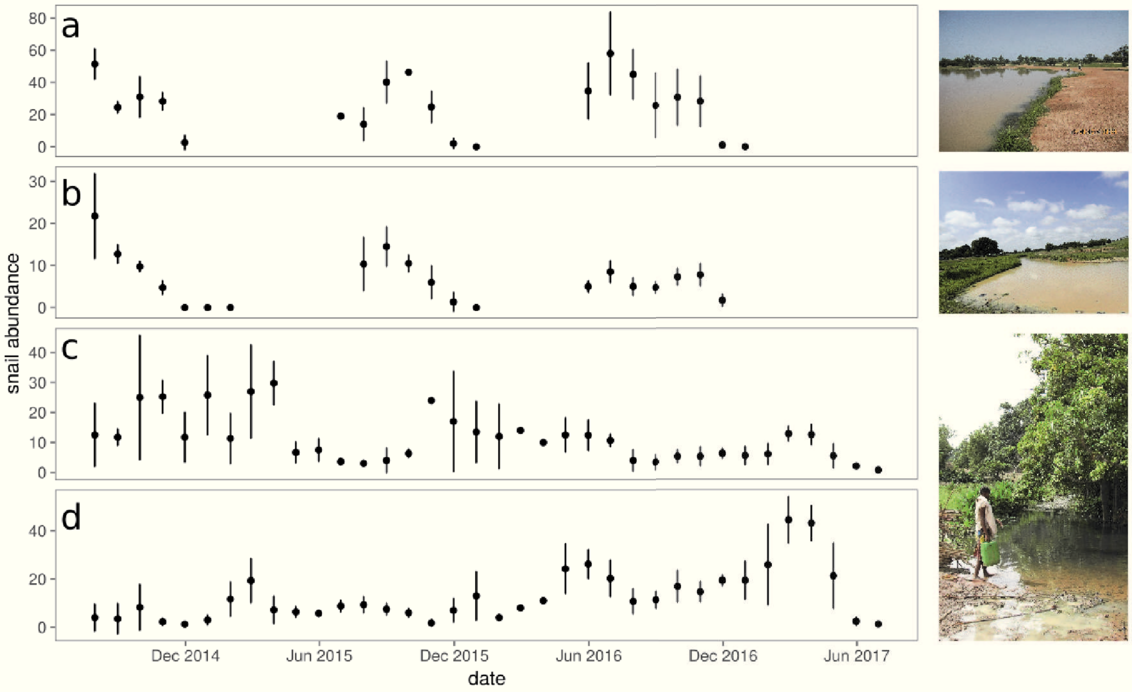

Figure 6.3 – Snail abundance fluctuations throughout the duration of the experiments. Mean monthly counts [snails/30min sampling effort] (points, error bars span 1 standard deviation) of *Bulinus* spp. in a) Lioulgou's temporary pond, and b) ephemeral river (b); and *Bulinus* spp. (c) and *Biomphalaria pfeifferi* (d) in Panamasso's permanent river. Note that the absence of points in a) and b) up to December 2016 indicate periods when the habitat dried out, and not missing data. Sampling was subsequently interrupted due to external factors.

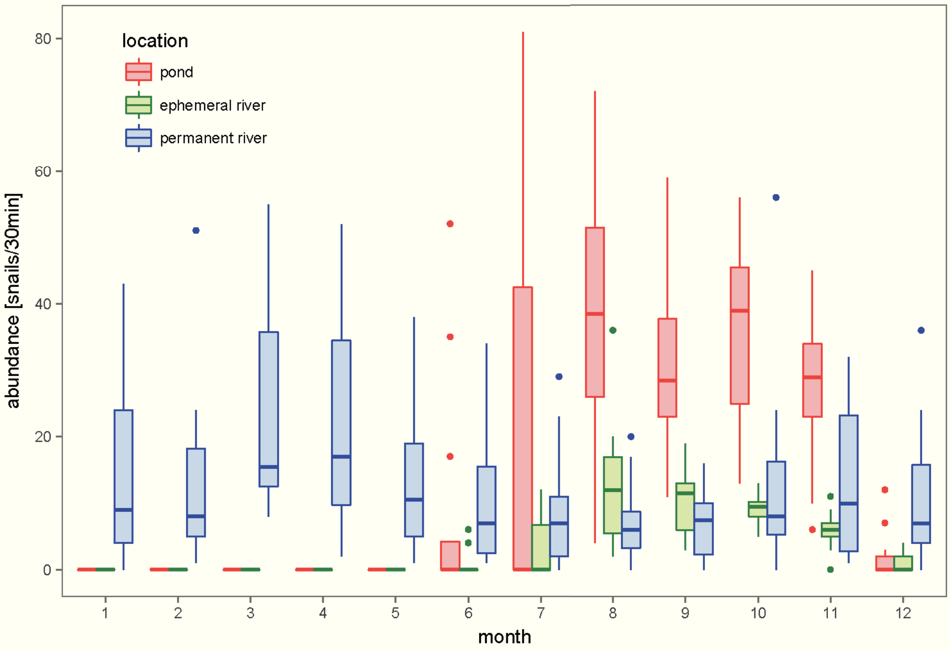

Figure 6.4 – Seasonal fluctuations of snail abundance. Relative abundance counts for the period May 2014 - July 2017 are represented in terms of monthly boxplots per habitat (*Bulinus globosus* and *Biomphalaria pfeifferi* counts are combined in the permanent stream in Panamasso).

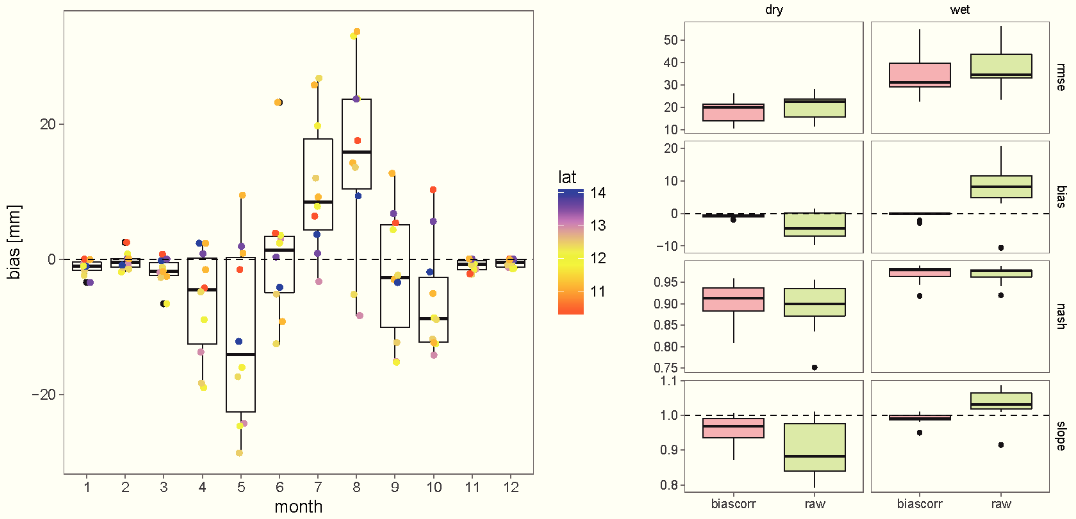

Figure 6.5 – Bias correction of precipitation remote sensing estimates. *Left)* Monthly bias of remote sensing precipitation estimates are non-stationary, with systematic over-estimation in the dry season (October through Mays), and over-estimation in the rain season (June-August). No systematic relationship can be drawn between bias and latitude (point color). *Right* Agreement between the estimated and observed precipitation in terms of root mean squared error (rmse), bias, Nash–Sutcliffe coefficient, and the linear regression slope with 0 intercept (slope) before (green), and after (red) bias correction, partitioned by season (rainy vs. wet). Bias correction successfully reduces bias as expected, but also slightly reduces the estimation error.

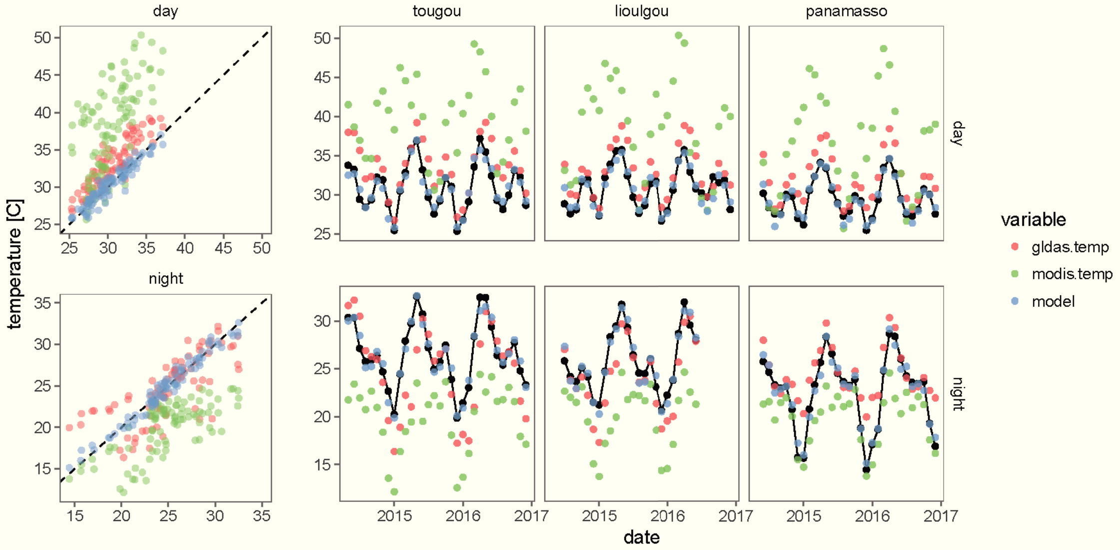

Figure 6.6 – Multivariate regression of day and night temperatures. Day and night temperatures are modeled as a function of time-varying (precipitation, vegetation indices, daylight hours) and fixed (latitude, longitude, covariate means) covariates.

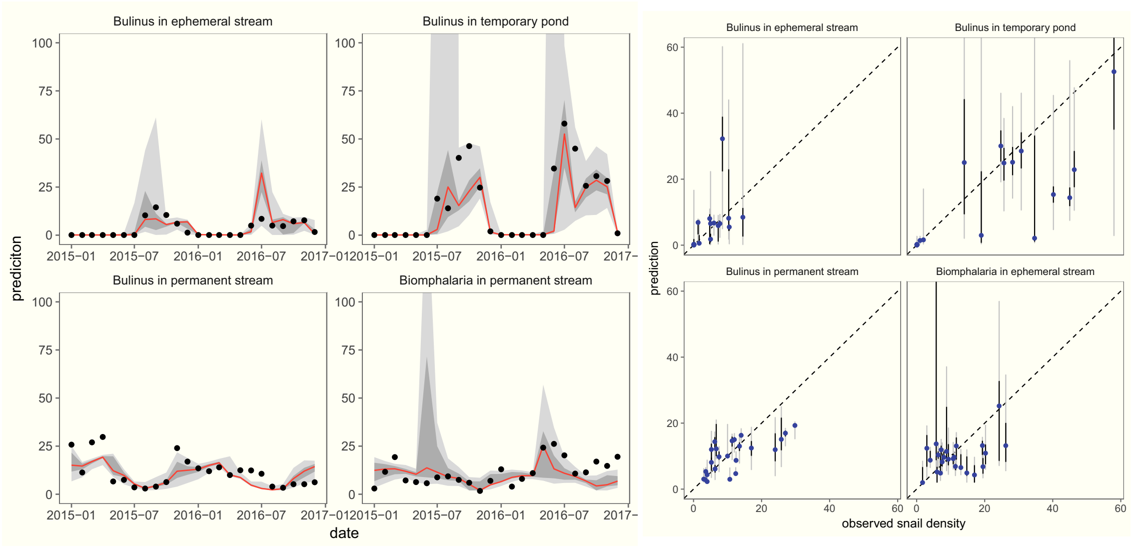

Figure 6.7 – Ecological predictions using remote-sensing covariates. *Left)* Comparison between observed (points) and simulated (median: red line, dark shading: 50% simulation envelops (SE), light shading: 95% SE of 1000 simulations) monthly population dynamics using remote sensing covariates in substitution of ground measurements. *Right)* Scatterplots between observed and simulated mean monthly abundances (median: points, dark gray: 50% SE, light gray: 95% SE of 1000 simulations).

overshooting and some under-estimating the initial population growth in June after the first rains for in the temporary ponds. Although the median simulation tends to under-estimate initial growth, the latter falls within the 50% simulation envelops (Fig. 6.7). The dry-season peak in the permanent river in Panamasso is also well followed by the median simulations. The marked wet season dips in the abundance of *Bulinus* spp. are very well simulated with little sensitivity to uncertainty in precipitation and temperature. On the other hand models of *B. pfeifferi* are more sensible to covariate variations, in particular in the March - April population increase, although the median simulation tracks well the observed population fluctuations. Overall the median simulations are in good agreement with the observed monthly abundance counts (Fig. 6.7, $R^2 > 0.7$), in particular when considering simulation envelops in addition to the median simulation.

Having verified the accordance between observed snail population dynamics and remote sensing-based simulations, the analysis proceeds to the application of the ecological model ensembles at the national scale. It is recalled that simulations were run for the years 2015 and 2016, and results are mapped here only the predictions of 2016 as an illustrative example. The predicted spatio-temporal patterns for *Bulinus* spp. reproduce well the seasonal variations in snail abundance observed in Lioulgou and Panamasso, i.e. a marked population increase in strongly ephemeral region during the rainy season and subsequent crash in the dry season, and more stable population levels in the permanent rivers to the South-West (Fig. 6.8). Patterns worth specific attention are predicted at both latitudinal extremes, with very low *Bulinus* spp. abundance predicted in the Southern regions between 9° and 11°, and very strong population bursts in the Northern parts of the country in July and August. Interestingly, the spatial heterogeneity in precipitation and temperature amounts in the ephemeral region produces marked differences in the onset of initial snail population growth between regions, for instance the late increase in population around 0° longitude and 14° latitude in July 2016. Similarly, the observed seasonal variation of *B. pfeifferi* are matched well by the regionalized predictions, with decreased population densities in the rainy season and subsequent regain from November on (Fig. 6.9). However,the population densities in the

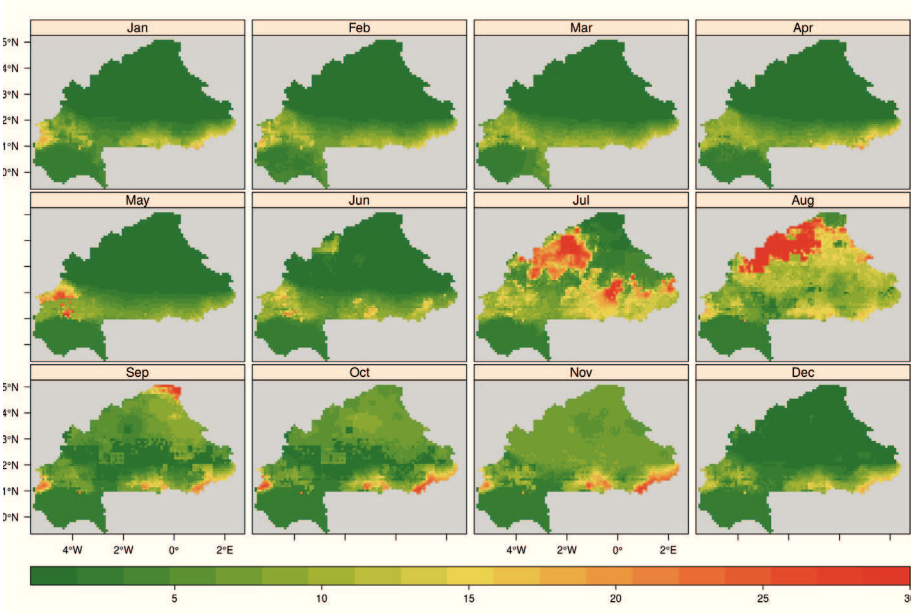

Figure 6.8 – Spatio-temporal predictions of the population dynamics of *Bulinus* spp. in streams for the year 2016 (median of 1000 simulations).

Southern-most part of the country (around 10° latitude) are predicted to have an opposite pattern, with population rise from May throughout the rainy season, and population reduction in the early months of the year. The results in this area require further investigation and are discussed bellow. Finally, the predictions of snail population dynamics in temporary ponds showed similar patterns than the ones in ephemeral streams, with rainfall-driven growth and peak abundances predicted in the months of July and August particular in the Sahelian zone, and population collapse from December on (Fig. 6.10). Later population peaks were predicted in September-November in the South-Western part of the country, although with similar population reductions in from January on.

6.4 Discussion

The aim of this Chapter is to introduce a methodology for the national-scale spatio-temporal prediction of snail abundance fluctuations across the highly seasonal climate of Burkina Faso, building on the data and results from chapters 4 and 5.

The analysis of the full 3-year ecological dataset on the abundance of the snail intermediate hosts confirmed observations made in Chapter 4 which were based on the first 15 months of sampling. The population dynamics of *Bulinus* spp. in the ephemeral habitats in Lioulgou (pond and river) were characterized by strong population bursts at the onset of the rain season, and subsequent population decline into the dry season, disappearing before habitats dry out completely. On the other hand both *Bulinus* spp. and *Biomphalaria pfeifferi* were present year-long at the surveyed water contact point on the permanent stream in Panamasso, with population density maxima towards the end of the dry season in March and April, and reductions in snail populations during the rainy season. Interestingly, inter-annual variability could be observed on top of this seasonal pattern in the permanent stream, in particular in the abundance of *B. pfeifferi* with its population maintaining at intermediate density during the 2016 rainy season to then rebound at densities that had not been observed before in March and April 2017, after

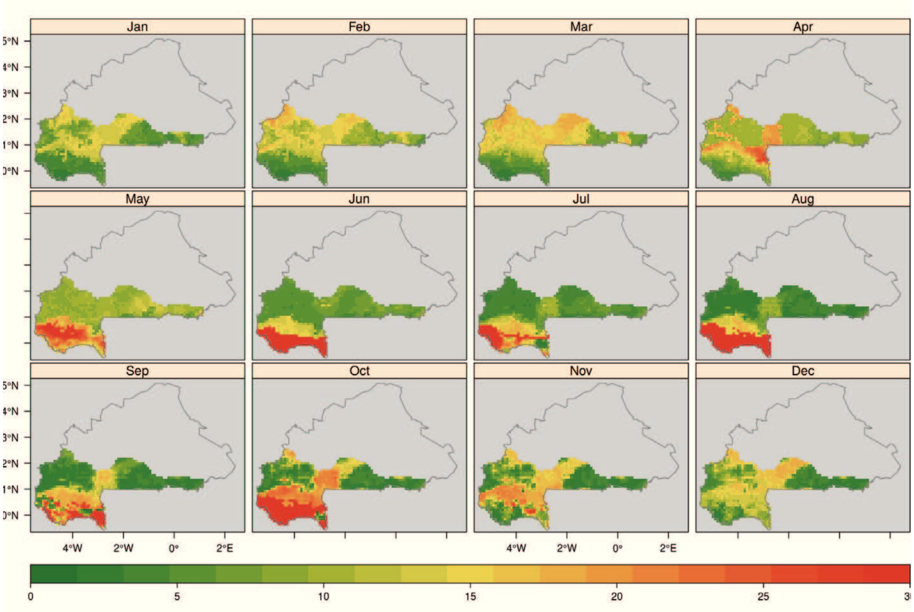

Figure 6.9 – Spatio-temporal predictions of the population dynamics of *Biomphalaria pfeifferi* in permanent streams for the year 2016 (median of 1000 simulations). Results are shown for the permanent and intermediate hydrological ephemerality regions only (Fig. 5.18), as a crude proxy of its ecological range (see Fig. 5.17 for species distribution modelling results along the river network).

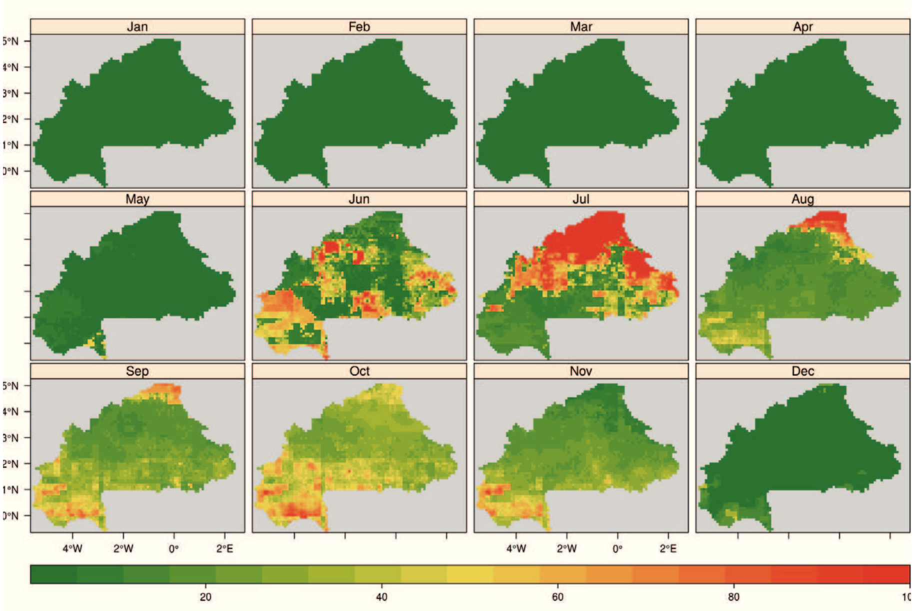

Figure 6.10 – Spatio-temporal predictions of the population dynamics of *Bulinus* spp.temporary ponds for the year 2016 (median of 1000 simulations).

which population crashed once again. A more in depth analysis would be necessary to determine if this anomalous pattern can be assigned to the climatic variables in 2016, which was a strong El Ninõ year, or to natural variability in snail population dynamics. El Ninõ anomalies have been shown to have adverse effects on snail demography in Kenya due to intense rainfall events which characterize East Africa's climate in El Niño years [*Kariuki et al.*, 2013]. On the other hand El Niño tends to produce bellow-average rainfall in West and Central Africa, and has been associated to the disastrous drought of 1972 in the Sahel [*Sonwa et al.*, 2017], and the shift of cholera outbreaks from Western and Southern to Eastern Africa in El Niño years [*Moore et al.*, 2017]. Elucidating the link between El Niño and schistosomiasis transmission through its impact on local weather patterns would be of great value for anticipating shifts in transmission patterns, as it has been done for cholera in SSA [*Finger et al.*, 2014; *Moore et al.*, 2017] and the Bengal region [*Pascual et al.*, 2000]. Another factor which has not been explored here is the possible ecological interaction between *Bulinus* spp. and *Biomphalaria pfeifferi* through inter-species density effects. Indeed, the abundance of each species seem to follow opposite trends (Fig. 6.3), with the dry-season peak population density of the former seeing a decline during the three years, whereas the latter's increased year after year. Competition between the two intermediate hosts has been argued to explain, in part, the substitution of *S. haematobium* by *S. mansoni* in a village 15km East from Panamasso in the 1970's before the widespread use of praziquantel [*Colette et al.*, 1982], it would therefore be of interest to further investigate this hypothesis.

The first necessary step for applying the expanded ecological modelling framework presented in this Chapter (incorporating thresholds in population rates of increase) at the national scale was to verify whether remote sensing estimates of environmental covariates could be used as substitutes for field measurements. It is important to note that the results presented in Fig. 6.7 are "full" simulations, in the sense that they are run for the 2 years of simulation fixing only the initial conditions, as opposed to the 1-step ahead predictions shown in Fig. 4.8. The adequate performance of the approach suggests that the models should behave reasonably well when forced with forecasts of temperature and precipitation, subject of course to their quality (as done for example in the spatially-explicit modelling of cholera by *Pasetto et al.* [2017]). Furthermore, the simulation-based predictions can readily account for uncertainty in environmental covariate forecasts in a similar fashion at it has been done here for errors in past remote sensing estimates of driving covariates.

The regionalization of habitat-specific ecological models, specifically between permanent and ephemeral habitats, was made possible by the use of the whole river-network ephemerality predictions of Chapter 5 to assign the different pixel-base model outcomes to their respective habitats. The underlying assumption is that the intermediate host's ecological dynamics are qualitatively different in permanent and temporary rivers, with Lioulgou and Panamasso being two representative examples at each end of the ephemerality spectrum, in particular for *Bulinus* spp. which is present in both habitat types as opposed to *B. pfeifferi* (Fig. 6.3). The main limitation of the regionalization of snail population dynamics predictions is the application of the models fitted at two locations (Lioulgou and Panamasso) to the rest of the territory with no contemporary validation points. The predicted spatio-temporal patterns seemed reasonable for *Bulinus* spp. at the national scale, however the assumption for the ecological dynamics in the intermediate ephemerality region -i.e. a combination of the ones predicted for the permanent and strongly ephemeral habitats as a function of distance to each ephemerality region- needs to be verified. Ideally this would require additional ecological sampling in rivers within this region, although the effort to maintain such sampling campaigns is significant. Another limitation in the regionalization of predicted snail abundance in rivers at the national scale is linked to the ecological data used for model fitting, which consisted of time-based snail counts [*Poda et al.*, 1994]. Indeed, time-based sampling is considered to be consistent for the analysis of seasonality in terms of relative abundances at given habitat if it is the same person which does the sampling throughout the survey period, thus avoiding possible differences in collector-specific efficiency [*Hairston et al.*, 1958]. The combination of models outputs presented in Fig. 6.8 should therefore be interpreted as relative variations with respect in each ephemerality region with respect to observed snail counts in Lioulgou and Panamasso respectively, rather than in absolute terms. The results in the intermediate ephemerality region combine model ensemble outcomes fit to the two distinct relative abundance counts, and their interpretation at this point is subject to caveats. On another front, a sensitivity analysis would need to be done to investigate whether the low predicted abundances in the South-West (South of 10° latitude) are a result of the temperature modelling methodology developed here, which was only based on data from this Thesis' three experimental sites, and could thus result in inaccurate temperature predictions at the national level. To improve temperature modelling results, a request has been filed for daytime and nighttime temperatures from the 10 synoptic stations of National Meteorological Agency (Fig. 6.1), however the data was not yet available at the time the results were produced. The same analysis would need to be done to verify the counter-intuitive patterns obtained for *B. pfeifferi* in the South-West which are not in phase with the observed seasonal abundance fluctuations in Panamasso. A similar analysis could also be carried out to investigate the shifted population peak of *Bulinus* spp. in ponds in the same area.

Possible extension of the modelling framework could consist in i) incorporating discharge estimates in the ecological models for rivers, and ii) extending the pond models to account for snail ecology in man-made reservoirs and lakes. Both aspects imply a better representation of the hydrological processes underlying transmission. Regarding rivers, incorporating predicted monthly discharge into the ecological models, instead of rainfall alone, would allow to differentiate snail population dynamics between tributaries and the main branches of the Comoé and Volta rivers, thus possibly capturing the adverse effect of flow velocity on snail abundance [*Woolhouse and Chandiwana*, 1989; *Poda*, 1996]. Moreover, building a more direct link between hydrology and snail ecology could lead to the combined fitting of models to both the ephemeral river in Lioulgou and the permanent stream in Panamasso, possibly making extrapolations into the intermediate ephemerality region more robust, conditioned on the difference in population rates between the distinct snail species that occur in different habitat types. Indeed, *B. senegalensis* and *B. truncatus* (the species found in Lioulgou and Tougou) are known to be very well suited to strongly ephemeral habitats, whereas *B. globosus* (the species found in Panamasso) occurs more frequently in permanent habitats (Table 4.1, [*Poda*, 1996]). Incorporating species-dependent population dynamics could be possible by repeating the species distribution modelling done for *B. pfeifferi* (Fig. 5.17), in combination with the ecological modelling approach presented here. National-scale predictions of discharge at the river-stretch level poses non-trivial challenges, in particular due to the issue of data scarcity highlighted in Chapter 5. However, a hydrologic modelling approach based on the Budyko framework has shown good results for monthly discharge predictions [*Zhang et al.*, 2008], and provides a promising solution for discharge prediction in Burkina Faso and other data-scarce regions. Moreover pixel-based predictions of snail population dynamics in rivers could be further combined with network-based species distribution modelling results of Chapter 5 (Fig. 5.17) to have a river stretch-base mask to weigh abundance predictions. Regarding the extension of the ecological modelling framework to man-made reservoirs and lakes, the main factor which needs to be taken into account is the duration of surface water presence which can support snail populations, which typically extends beyond that of temporary ponds in small topographic sinks. This is well illustrated by the historical data presented in the previous Chapter on the population dynamics of *Bulinus senegalensis* and *B. truncatus* in a temporary pond and a small reservoir respectively (Fig. 2.4, [*Poda*, 1996]). Using field data and very high remote sensing imagery, *Soti et al.* [2010] proposed a hydrological model for water level fluctuations in ponds in an area of $\approx 100\text{km}^2$ in Norther Senegal, showing good agreement with data, even when the model was forced with remote sensing estimates of precipitation. Although promising for delimited study-areas, data requirement hinder the application of their methodology at the national scale.

On a larger spatial scale, detailed hydrological modelling of water accumulation and evaporation in reservoirs has been investigated using high-resolution synthetic aperture radar (SAR) remote sensing data in Norther Burkina Faso [*Amitrano et al.*, 2016, 2017], however the extension of the methodology to the national scale is not possible due to limitations in data acquisition capacity. However, empirical relationships between water surface area and reservoir volume established in these approaches could be used to approximate the retention capacity of small reservoirs in the country in combination with recently developed global high-resolution estimates of water surfaces and their seasonality [*Pekel et al.*, 2016]. This information could then be used together with monthly predictions of the evaporative fraction within the Budyko framework to estimate location-specific surface water availability, which would be included as a covariate in the ecological modelling framework developed here. Another approach could consist in following a more conceptual approach along the lines of *Tompkins and Ermert* [2013], which presents the advantage of straightforward regionalization at the expense of hydrological realism. More generally, interesting overlaps with the more well developed field of hydrological modelling for mosquito-borne transmission could provide new tools for the modelling of the population dynamics of the snail intermediate hosts in temporary ponds, which are known to play a key role in schistosomiasis transmission in arid climates [*Poda et al.*, 2004a]. This "water-availability" extension of the modelling framework would bring it closer to the resource-based model proposed by *Gurarie et al.* [2017], however allowing for density feedbacks and temperature effects. The historical data in *Poda et al.* [1994, 1996], along with additional data currently being collected in the reservoir and a temporary pond in Tougou, provide an opportunity for future developments in this direction. On the other hand additional data would need to be collected on the ecology of *B. pfeifferi* in man-made reservoirs in the intermediate ephemerality and permanent hydrological zones.

This Chapter has confirmed the species- and hydrological ephemerality-dependent seasonal variations that characterize snail population dynamics in Burkina Faso. An extended ecological modelling framework using remote sensing estimates of environmental covariates showed promising results in reproducing snail demography at a monthly timestep. The regionalization of the ecological models at the national scale, informed by hydrological ephemerality regions showed promising results in terms of general predictions of spatio-temporal patterns of population dynamics. However, discrepancies between predictions in certain regions, namely the South-West, and the observed seasonal snail variations in the experimental sites underline the need for further model refinement, chiefly in terms of estimated temperatures and the incorporation of more detailed hydrologic processes, including river discharge and water accumulation in reservoirs and lakes. These preliminary results therefore encourage the development of a modelling framework for the hydrology-adapted ecology of the different species of snail intermediate hosts of schistosomiasis, with a view on its incorporation into spatially-explicit model of disease transmission.

7 Discussion and perspectives

7.1 Hydrology and human-water contact patterns

The association between hydrology and schistosomiasis transmission stressed in the Introduction has been principally explored in the previous chapters in terms of its impacts on the snail intermediate hosts' ecology, including its population dynamics (Chapters 4 and 6) and spatial occurrence (Chapters 5 and 6). However, hydrology is also a first order control on where and when surface water is available, and thus of type of water contact-causing activities may take place. Specific water-contact patterns have been directly linked in some settings to individuals variations in infection intensity [*Klumpp and Webbe*, 1987; *Chandiwana*, 1987; *Bundy et al.*, 1990], and can shape disease transmission at the community level (see section 1.2.3). In fact, the works by *Clennon et al.* [2006] and *Mutuku et al.* [2011] discussed in the Introduction of this Thesis (Table 1.1) are compelling examples of the effect of hydrology on spatial micro-epidemiological patterns, even at small spatial scales. Spatial and temporal heterogeneities in water contact patterns ,-both in their origin (communities, neighborhoods) and destination (water contact points)- could exacerbate transmission stability and hinder disease elimination through non-targeted MDA [*Barbour*, 1978; *Woolhouse et al.*, 1998; *Mari et al.*, 2017a]. The spatio-temporal variations of surface water presence at the village scale could therefore be seen as an exogenous driver of transmission dynamics, and their characteristics could yield useful information for control and elimination programmes. Indeed, the results of Chapter 5 highlighted an association, between strong ephemerality and uro-genital schistosomiasis risk, in particular for villages located in close proximity to quasi-perennial waterbodies (Table 5.4). Hydrology-driven variations in the disease's transmission intensity, e.g. quantified by the human-to-snails and snails-to-human forces of infection [*Anderson et al.*, 2016], thus need to be incorporated into national scale spatially-explicit models of disease transmission as the one proposed in Chapter 3. Of particular interest for modelling transmission dynamics is the seasonality of water contact patterns relative to that of the climate- and habitat-specific demography of the snail intermediate hosts [*Mari et al.*, 2017a].

7.1.1 Characterizing human-water contact patterns in the experimental sites

Aiming at addressing the spatial patterns and seasonality of water contacts in the context of the strongly seasonal climate of Burkina Faso, this section presents preliminary results from questionnaires and participatory workshops held in the three experimental sites presented in Chapter 2.

The quantification of water-contact patterns has typically been done either through questionnaires [eg.

Utzinger et al., 2000; *Rudge et al.*, 2008], direct observations at water contact points [eg. *Chandiwana*, 1987; *Sow et al.*, 2008; *Kpoda et al.*, 2013; *Traoré*, 2013], or a combination of both [eg. *Kloos et al.*, 1997; *Krauth et al.*, 2015]. More recent studies have also used wearable GPS tracking devices [*Seto et al.*, 2013; *Traoré*, 2013], although this method presents significant technical challenges [*Traoré*, 2013]. Field observations present the advantage of being more accurate than questionnaires, although they require considerable manpower, in particular for inter-seasonal investigations of water contact patterns in multiple water-contact points [*Sow et al.*, 2008; *Traoré*, 2013]. In Burkina Faso, direct observations of children bathing habits in the Sourou valley suggested that water contacts are strongly correlated to mean daily air temperature, with temperatures above ≈ 25°C characterizing bathing-prone days [*Traoré et al.*, 2016]. Also using direct observations, *Kpoda et al.* [2013] highlighted marked difference between the water contact activities of men and women in South-Western Burkina Faso, the former being more associated to agricultural works and the latter's to domestic chores. The seasonality of water contact patterns has not been investigated in Burkina Faso, although studies from other countries in West Africa suggest that seasonal variations do occur [e.g. *Klumpp and Webbe*, 1987; *Ofoezie et al.*, 1998; *Sow et al.*, 2011].

Given operational constraints linked to the fact that three experimental sites with multiple water points each needed to be covered, a questionnaire-based method was retained to collect information on the seasonal variations in water contacts[1]. The spatial aspect was explored through a participatory mapping activity during workshops organized in each village[2]. More particularly, the water contacts consisted in the form of one-to-one interviews focusing on adults and covered socio-economic activities, mobility outside of the village, knowledge on the disease cycle (contamination-consequences-transmission), and water contacts. Interviews were made so as to cover all village neighborhoods, and to include approximately the same number of men and women. Interviews were made either in Moore, Bobo or Dioula depending on the village and with the help of a translator. Water contact questions investigated the type, duration, frequency and body exposure of water contacts with explicit differentiation between the dry (taken as June-October) and wet (November-May) seasons. The participatory workshops in each village spanned three days with the local community and authorities. The workshops were organized in three phases: understanding local perceptions of schistosomiasis (mode of contamination, pathology, epidemiology, treatment and prevention), information exchange on the disease, and participatory mapping of water contacts points and activities in the village. About 35 inhabitants in each village were enrolled for the participatory workshop. Participants were chosen so as to represent all primary economic occupations (fishery, agriculture, cattle farming), ethnic groups (Mossi, Peul, Bobo, Dioula), age classes (young, adults and elders), neighborhoods, and gender. Participatory mapping has been extensively used in the framework of Participatory Rural Appraisal (PAR) for empowering local communities to sustainably manage their natural resources [*Chambers*, 1994; *Rambaldi et al.*, 2006]. Here participatory mapping was used in complement to the water contact surveys to identify water contact activities and their locations in the villages (Fig. 7.1). The participatory mapping activities were based on high-resolution satellite images of the area, on which transparent sheet were laid for annotation. Participants were divided by gender into small groups (≈6 people), and the activities started by an orientation game in which each participant had to identify her/his home in the village. Once the participants were familiar with the satellite image,

---

[1] Results presented here ensue from the master projects of Anna Faes who performed the questionnaires in Tougou, assisted by David Yaméogo and Laure Borgeaud, helped in the participatory workshop, and performed initial data analysis; and Charles Marmy who performed data cleaning and analysis of the whole dataset. Fabrizzio Gonzales Zurita contributed to the cleaning and analysis of data from Lioulgou during a semester project. Their contributions are gratefully acknowledged.

[2] The participatory workshops were made possible by Théophile Mande (ECHO-EPFL), and supported by Dr. Dakouré-Sou, Dr. Bologo, and M. Compaoré at the *International Institute d'Ingénierie de l'Eau et de l'Environnement* (Ougadougou, BF), and M. Bagayan and Dr. Zongo at the *Institut de Recherche en Sciences de la Santé* (Ouagadougou, BF). Their contributions are gratefully acknowledged. All three village's inhabitants and traditional and administrative authorities are also warmly thanked for their collaboration.

Figure 7.1 – Participatory mapping of human-water contact points. Participatory mapping activities were done during workshops organized in Panamasso (a), Lioulgou (b) and Tougou (c) (one per village) aiming at gathering local perception and knowledge about schistosomiasis, informing about the disease, and determining the location of human-water contacts and their seasonality.

guided questions led the group to agree on the main socio-economic activities that lead to water contact, to locate each activity on the map, and to indicate the months during which each activity took place in each location. The participatory workshops were all concluded by a public presentation during a closing ceremony in the presence of the village's traditional and administrative authorities, including when possible departmental, provincial and regional representatives. Both the water contact surveys and participatory workshop protocols were approved by the EPFL Human Research Ethics Committee (# HREC 014-2016), and the Health Research Ethics Committee in Burkina Faso (# 2016-11-128). Results are only discussed here for the water contact parts of the surveys and participatory workshops.

7.1.2 Spatial and temporal variability of human-water contacts

The questionnaires and participatory mappings revealed strong spatial and temporal heterogeneities in water contact-causing activities, and the locations in which they took place in the three villages. First of all, questionnaire results suggest that in the presence of quasi-perennial waterbodies as in Panamasso (river) and Tougou (reservoir), more water-contact causing activities occur during the dry season than during the wet season (Fig. 7.2). Domestic chores (laundry, dish washing, gathering water for the household) and agriculture were the most common reported activities, women being typically associated to the former and men to the latter [*Kpoda et al.*, 2013]. Seasonal water contacts patterns, with more activities during the dry season in the presence of long-lasting or permanent waterbodies echo similar findings in Senegal [*Sow et al.*, 2008], and elsewhere in SSA [e.g. *Klumpp and Webbe*, 1987; *Chandiwana*, 1987]. Moreover, the questionnaires show a strong heterogeneity in exposure to water, here expressed in terms of the frequency-duration-body surface adjusted (FBD) index [*Rudge et al.*, 2008], both between individuals at the village level, and between different neighborhoods (Fig. 7.2).

Regarding the locations in which water contact-causing activities occured, results from participatory mapping highlighted important differences between the three villages in terms of the spatial configuration of water-contact points both within and between seasons (Fig. 7.4). The neighborhoods in Panamasso are all in direct proximity to the stream (< 500m), and most water-contact points which supported domestic, recreational and agricultural activities are located in a within a 500m stretch of the stream. In Lioulgou water contact activities are only possible during the wet season, and mainly concern rice culture along the river North of the village. Importantly, a pond (the same in which the malacological sampling for Chapter 4 took place) is located in very close proximity of the village's schools, and various activities take place including domestic chores and recreational bathing (as illustrated in Fig. 2.7). Lioulgou's

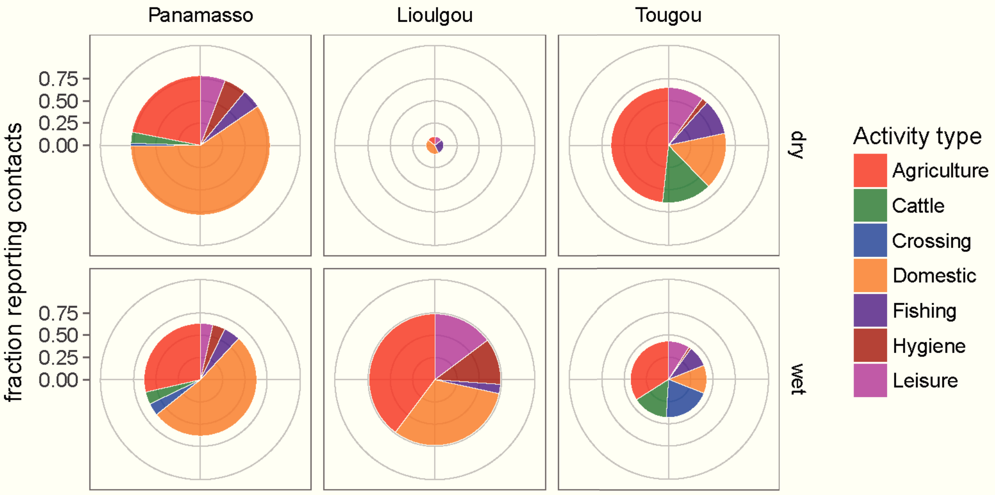

Figure 7.2 – Reported human water contacts in the three experiment sites. Pie charts give the partitioning of questionnaire answers to water contact-causing activity type, village, and season (circle width indicates percentage of interviewees reporting at least one water contact-causing activity).

neighborhoods are more spread out than Panamasso's, and located further away from waterbodies. Finally Tougou is the largest study area, composed of different neighborhoods surrounding the reservoir. Activities leading to water contacts occur both along the reservoir shores, and in different temporary ponds scattered in the study area. The latter support domestic and recreational activities during the wet season, in the dry season the remaining water supports herding and the extraction of clay to make bricks for construction. The reservoir itself supports a wide range of activities including fishing, herding, agriculture, and domestic and recreational bathing, exemplifying small reservoirs throughout Burkina Faso and West Africa [*Cecchi*, 2007; *Ayantunde et al.*, 2017; *Diakité et al.*, 2017]. As in the case of Lioulgou, the location of water contacts was reported to vary significantly between seasons due to the area's strong hydrological ephemerality, depending on the type of activity and the nature of water contact points. For instance, domestic chores were reported to be done in the temporary ponds only during the wet season, whereas the reservoir shores were used in both seasons due to the prolonged presence of water. The spatial configuration of neighborhoods and reported activities also suggests heterogeneous intensities of water contacts in different water access points. For example, wide range of activities are reported by the participants along the reservoir shores in proximity to the northernmost neighborhood in Tougou (called Tambeguede), both during the wet and the dry seasons. Although the descriptions here are made in terms of seasons, it is clear that the water surfaces evolve continuously throughout the year[1], coupling the seasonal dynamics of the number of water contacts suggested by the questionnaires with physical constraints on their spatial distribution as the dry season progresses.

The interpretation of the survey and participatory mapping results thus suggest the existence of distinct risk categories of individual exposure, structured at the neighborhood level, with the amount and spatial distribution of water contacts varying seasonally, depending on the availability of surface water. Although only three villages of different spatial extents were considered here, these observations echo results from water contact surveys throughout SSA [*Klumpp and Webbe*, 1987; *Chandiwana*, 1987; *Clennon*

---

[1] The seasonal expansion and contraction of Tougou's reservoir water surface has been monitored using high-resolution remote sensing radar data by *Amitrano et al.* [2014], showing a clear seasonal pattern of rapid filling at the beginning of the rainy season, and gradual contraction throughout the dry season down to two disconnected small waterbodies in the northernmost and southernmost parts of the reservoir.

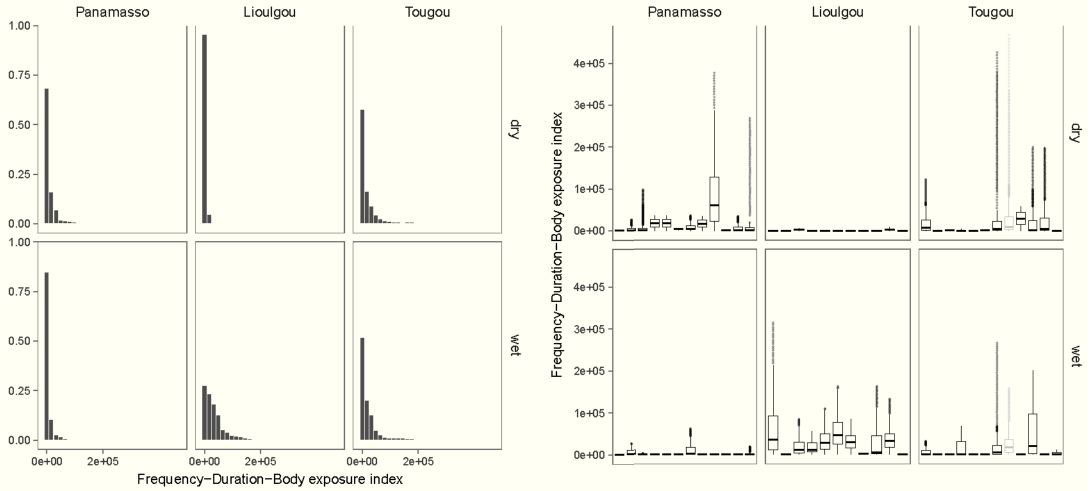

Figure 7.3 – Individual and spatial heterogeneity in exposure to surface water. Individual exposure to water is expressed in terms of the frequency-duration-body surface adjusted index (FDB) [*Rudge et al.*, 2008] as $FDB = \sum_i f_i \times d_i \times bsa_i$, where f_i is the frequency [month^{-1}] of the individual's reported activity i, d_i its duration [min], and bsa_i the coefficient [-] associated to the amount body surface exposed [*Livingston and Lee*, 2000]. Since possible answers to the questionnaires included ranges (for instance the duration of 5-15min), the minimum and maximum index values were computed for each individual, and used to define uniform distributions from which the values for plotting were drawn. *Left)* Distribution of individual FDB values by village and season. *Right)* Boxplots of FDB values by neighborhood (12 in Panamasso, 11 in Lioulgou and 12 in Tougou). Indicated in gray is the neighborhood in Tougou presenting significant adult schistosomiasis prevalence (Tambeguede) discussed in the text.

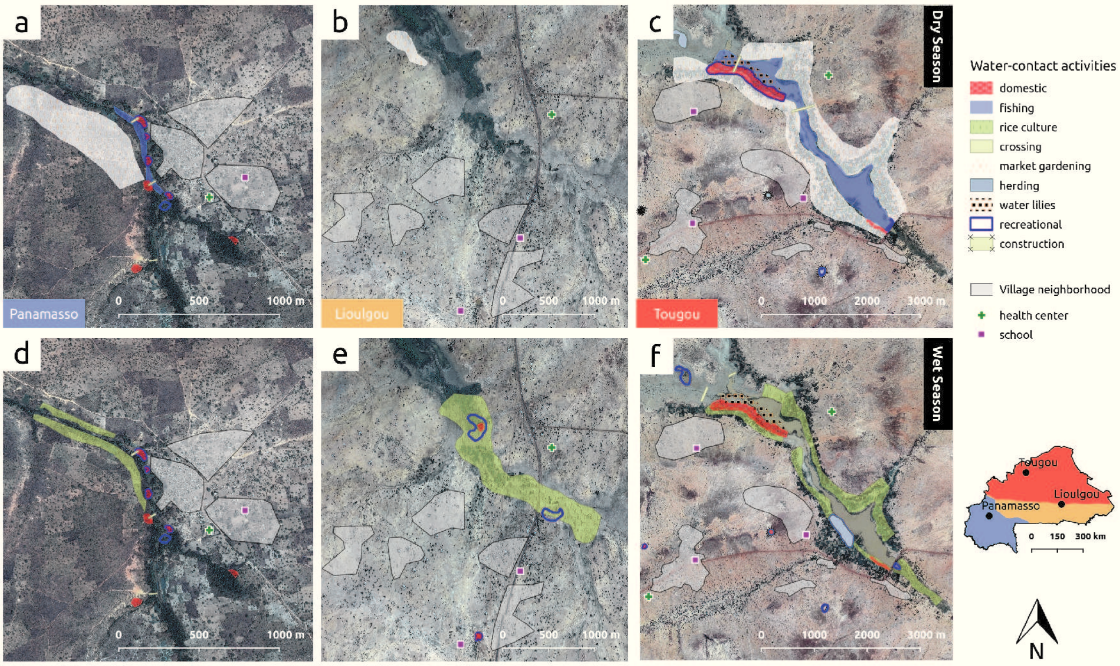

Figure 7.4 – Map of the locations of water contact points and their seasonality. Water contact points, the activities that occur in them and the months in which these occur were determined through participatory mapping activities in each village. Market gardening includes the cultivation of tomatoes, onions, peppers and the likes, and construction the extraction of clay bricks from ponds. The location of the three villages in Burkina Faso, and the hydrologic ephemerality region in which they fall into (cf. Chapter 5) are shown in the inset. Map data: Google, DigitalGlobe.

et al., 2006; *Mutuku et al.*, 2011; *Kpoda et al.*, 2013; *Meurs et al.*, 2013; *Krauth et al.*, 2015]. A more in-depth understanding of spatio-temporal exposure dynamics in the three experimental sites could be attained through direct observations of water contacts in select access points in different periods of the year, possibly complemented by the investigation of the availability and use of water infrastructure [*Krauth et al.*, 2015; *Kosinski et al.*, 2016]. Moreover, direct observations would strengthen the qualitative information regarding water contact patterns of children which was gathered from discussions during the participatory mapping activities, since only adults were interviewed during the survey. Additional analysis of the data collected here could provide insight into the explanatory power and relative importance of socio-economic and environmental determinants in adult exposure to water, for instance using tools developped for multivariate analayis in ecology [*Legendre and Anderson*, 1999].

7.1.3 Hydrology, water contacts, and schistosomiasis transmission

These preliminary results support the view that hydrology, particularly ephemeraliy, and its anthropogenic alterations, act as first order controls on water contact patterns fueling schistosomiasis transmission. Indeed, activities leading to water contacts were ultimately determined by the presence and duration of neighboring waterbodies, exemplified by the absence of water contacts in Lioulgou during the dry season due to the ephemeral nature of its river, whereas in Panamasso and Tougou most water contact activities were reported in the dry season, supported by the perennial stream and the reservoir's water surface respectively. An overview of the recent evolution of schistosomiasis in the three villages enables to draw an initial interpretative link between hydrology, snail ecology, and disease transmission.

In Panamasso, intestinal schistosomiasis prevalence in school-aged children has remained relatively stable around 25% since 2008 despite quasi-annual MDA rounds targeting this specific age class in the region (Fig. 7.5) [*Ouedraogo et al.*, 2016]. Moreover, a recent parasitological analysis done by the national Health Sciences Research Institute (*Insitut de Recherche en Sciences de la Santé*, BF)[1] has shown a prevalence of 26% (20/76) in adults from a single Kato-Katz thick smear, which is very probably an under-estimation of true prevalence (individuals with at least 1 worm pair) in the population [*de Vlas*, 1996; *Bärenbold et al.*, 2017]. Adults in Panamasso could therefore play a non-negligible role in fueling transmission. Moreover, water contact surveys suggest that adult water contacts are the highest during the dry season, which is also when the population of *Biomphalaria pfeifferi* peak in the river (Fig. 6.4). Mathematical modelling results have suggested that synchrony between seasonally varying human-water contacts and snail abundance greatly favor disease transmission stability [*Mari et al.*, 2017a]. Even if it has not been shown here that children and adults have similar seasonal water contact patterns, evidence from other regions of Burkina Faso suggest that high temperatures are associated to more intense bathing [*Traoré et al.*, 2012], which would therefore contribute to strengthen transmission during the dry season in the few and tightly packed water access points the villagers use in Panamasso (Fig. 7.4a,c).

Uro-genital schistosomiasis prevalence in Lioulgou has varied significantly between years, with a remarkable peak of 56% of infected school-aged children in 2013, a year only after MDA was delivered in the region, which suggests that re-infection occurred rapidly (Fig. 7.5). Lioulgou is at the border of the intermediate hydrological ephemerality region, and water contact points disappear almost completely in the dry season (Fig. 7.4b), and barely an activity leading to water contacts was reported during the survey. However, the presence of a temporary pond in close proximity to the village's school favors the concentration of activities in a well-delimited area while the pond doesn't dry up, in particular recreational bathing of children (Fig 2.7). Indeed, the abundance of *Bulinus* spp. in the temporary pond did not collapse until

---

[1] Unpublished data shared by Dr. Zongo (IRSS, BF), his collaboration is gratefully acknowledged.

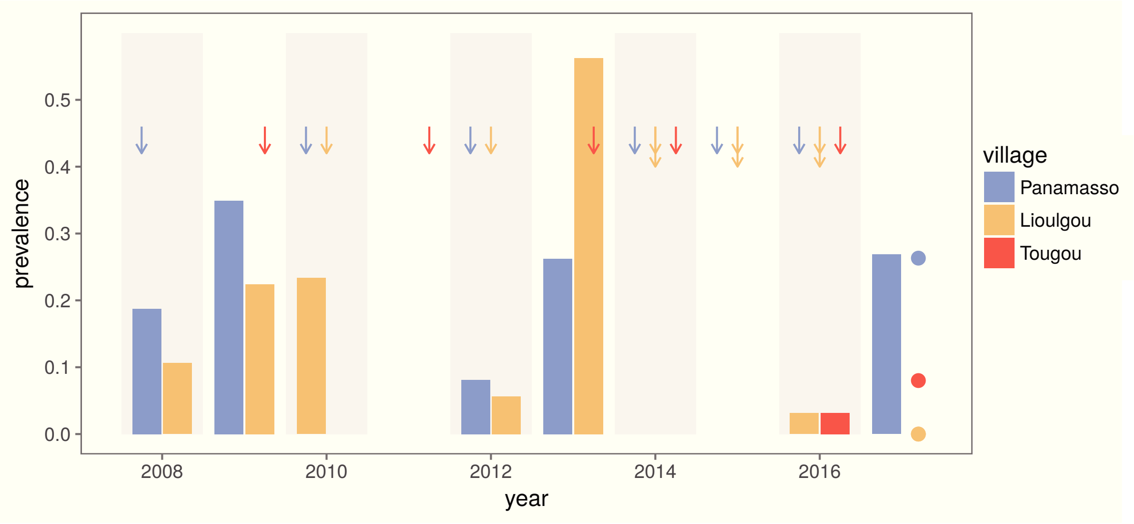

Figure 7.5 – Evolution of schistosomiasis prevalence in the experimental sites. Bars (points) indicate the prevalence of uro-genital schistosomiasis in Tougou and Lioulgou, and the intestinal form in Panamasso, in school-aged children (adults). Years in which MDA rounds targeting school children (the whole community) took place in the village's region are indicated by single (double) arrows[1] [from *Ouedraogo et al.*, 2016]. Lioulgou and Panamasso are part of the sentinel sites of the national schistosomiasis control program. Parasitological surveys in Tougou and among adults were conducted by the IRSS.

December (Fig. 6.4), thus providing a 6-month time window for transmission to occur between the snail population bursts following the start of the rainy season in July, and the onset of snail aestivation. The concentration of water contacts in limited numbers of available waterbodies in ephemeral landscapes, here that of children in a temporary pond inhabited by the intermediate snail hosts, could therefore strongly favor parasite circulation. This effect has also been foreseen in the analysis of mathematical models allowing for the spatial structuring of water contacts, in particular highlighting that a possible measure to reduce transmission would be to increase the number of water contact points, in particular if the additions are snail free [*Mari et al.*, 2017a]. On the other hand, prevalence in adults was of 0/83 in the individuals prospected by the IRSS in 2017 (Fig. 7.5). Although the prevalence in adults prior to the initiation of annual community-wide MDA in 2014 [*Ouedraogo et al.*, 2016] is not known, it could be assumed that treating adults was effective in reducing worm burden, and that water contact patterns in adults did not favour re-infection. Indeed, water-contact surveys suggested that no contact occurred during the dry season, and water contact activities during the wet season are distributed between a large number of water contact points, in particular in the rain-fed rice paddies which cover ≈ 100ha North of the village. Although activity-specific exposure indeces would need to be computed to support this hypothesis, it is noteworthy that no *Bulinus* spp. specimens were found in the rice paddies during exploratory samplings in July and August 2014, therefore suggesting that transmission to adults does not occur during rice culture. A more comprehensive malacological sampling is necessary to verify this observation.

Information on schistosomiasis prevalence in Tougou was more limited than in the other two villages, with only one sampling done by the IRSS in 2016 for children (performed in the South-Western school in Fig. 7.4), and one in 2017 involving adults (covering all neighborhoods) (Fig. 7.5). Prevalence in

---

[1] According to *Ouedraogo et al.* [2016], from 2004 to 2008 MDA took place in average biannually in all regions in the country. Information on the relative timing of parasitological surveys in years in which praziquantel was distributed by health authorities was not available from accessible reports.

school-children was around 5%, similar to that of Lioulgou, and also observed in schools in the central part of the country [*Savadogo et al.*, 2015; *Ouedraogo et al.*, 2016]. On the other hand, the village-level prevalence in adults was of 8% (6/75), with most egg-positive individuals (5/6) coming from Tambeguede (northernmost neighborhood in Fig. 7.4), for which prevalence was of about 20% (5/26). Interestingly, numerous water contact-causing activities both during the wet and the dry seasons were reported to take place along the reservoir shores in close proximity to this neighborhood (Fig. 7.4c,f), although the neighborhood-level FDB exposure index estimated from questionnaires did not particularly stand out from the others (Fig. 7.3). To draw specific conclusions regarding schistosomiasis micro-epidemiology in the village, a more detailed analysis of the association between prevalence -both in children and adults- and water contact patterns in Tougou is warranted, using complementary parasitological, malacological, and observational data [*Rudge et al.*, 2008; *Stothard et al.*, 2011; *Meurs et al.*, 2013; *Krauth et al.*, 2015]. However, these preliminary results strongly support the hypothesis that the reservoir plays a key role in transmission by enabling a wide scope of water-contact causing activities in well-defined areas, including recreational bathing by children but also agricultural activities. As stressed by others, the construction of reservoirs thus not only expand suitable habitat for the snail intermediate hosts in irrigation canals and along reservoir shores and its tributaries, but can also have an impact on socio-economic and recreational activities, leading to increased levels of human-water contacts and ensuing disease transmission [*Poda et al.*, 2003; *Steinmann et al.*, 2006; *Boelee et al.*, 2009].

Pursuing the conclusions broached in Chapter 5, the preliminary results presented here cast light on the role of hydrology, in particular ephemerality, in schistosomiasis transmission in Burkina Faso. Indeed, spatial and temporal seasonal aggregation of water contacts in ephemeral landscapes are possibly at the origin of intense parasite circulation between human and snail hosts. This effect is exemplified here by the remarkable increase in school-aged children prevalence in 2013 in Lioulgou -where a single pond attracts important recreation bathing by children from the neighboring schools- and the adult prevalence in observed in Tambeguede -where adjacent reservoir shores support a wide range of activities year round. Water contact aggregation in the perennial stream in Panamasso is due to the close proximity of the few well-defined access points used in the village, possibly accentuated by seasonal variations in water-contact causing activities, also highlighted in Tougou anournd its reservoir. From a theoretical standpoint, the association between spatio-temporal heterogeneities and schistosomiasis transmission stability is well understood [*Barbour*, 1976; *Woolhouse et al.*, 1991, 1998; *Gurarie and King*, 2005; *Mari et al.*, 2017a]. Bearing in mind the habitat-dependent seasonality of snail ecology highlighted in Chapters 4 and 6, the survey and participatory mapping results presented here substantiate this association along two axis: on one hand the synchrony between snail abundance fluctuations and human-water contact-causing activities, and on the other the spatio-temporal aggregation of human-water contacts foster by ephemeral hydrologic conditions. This Thesis has provided evidence for the hydrological underpinning of both aspects, although additional analysis are needed to confirm and strengthen the interpretations presented here. Importantly, mechanistically linking hydrology and schistosomiasis provides a promising path to a process-based appraisal of transmission dynamics at the national scale through the use of spatially-explicit mathematical models ensuing from Chapter 3.

7.2 Modelling and the ecohydrology of schistosomiasis

7.2.1 Expanding the modelling framework

Two main aspects of the spatially-explicit mathematical modelling framework developed in Chapter 3 could be expanded based on the ecohydrologic insight brought forward by this Thesis in the view of supporting control and elimination decisions. The first one, which was the primary focus of the fieldwork in Burkina Faso, is to account for the ecology of the snail intermediate hosts, both in terms of snail occurrence and seasonal population dynamics. A first step towards the regionalization of the local ecological models developed in Chapter 4 has been proposed in Chapter 6 using remote sensing covariates, and possible ways forward to better account for hydrological drivers of snail demography have been discussed in detail in the latter. The collection of the type of data necessary to the building of the ecological models presented in Chapter 4 (multiple sites during multiple years) requires significant effort and means, thus hindering the replication of the results obtained here in other endemic countries in SSA. However, the literature review presented in the Introduction (section 1.2.2) stressed a need for this type of work in the face of the constant decline in multiannual ecological studies on snail population dynamics in SSA (Fig. 1.3). A possible way to bridge this gap while new studies are undertaken would be to perform a systematic analysis of the historical timeseries data gathered from the review, possibly following methods similar to that of Chapter 4 depending on the availability of suitable environmental covariates, to determine general patterns of snail abundance seasonal fluctuations across habitat types and ecozones (illustrated in Fig. 1.3). This would complement existing snail spatial occurrence data analyzed through species distribution models in SSA [*Stensgaard et al.*, 2013]. The second aspect of the spatially-explicit modelling framework which requires improvements ensues from the preliminary results from the surveys and participatory workshops in the preceding section, and concerns the spatio-temporal aggregation of human-water. Indeed, both the contamination and exposure parameters linked to human-water contacts, which were assumed constant and population density-dependent in eq. 3.8, should be made time-varying. More particularly, these parameters could be defined as a function of site-dependent hydrological ephemerality of rivers and streams, in combination with remotely-sensed presence of waterbodies. It is clear that widespread access to water infrastructure will reduce the strength of the association between hydrology and water contact patterns, in particular regarding domestic chores [*Krauth et al.*, 2015; *Kosinski et al.*, 2016]. However, beyond the issue of access to and use of water infrastructure and its actual impact on reduction water contacts [*Grimes et al.*, 2015], coverage is still low in Burkina Faso (only 43% of the rural population has access to at least basic water as defined in *World Health Organization and UNICEF* [2017]), and it is reasonable to assume that reductions in agricultural activities requiring water contacts, and recreational bathing by children in warm climates, are unlikely to occur through infrastructure interventions alone. Albeit additional analysis on water contact patterns in the three experimental sites is warranted, the hypothesis that hydrology (i.e. distance to the closest waterbody) is a first order control on the seasonality and spatial configuration of human-water contacts under the strongly seasonal climate of Burkina Faso has been highlighted. Moreover, the relationship between hydrological ephemerality and schistosomiasis prevalence drawn in Chapter 5 and in the previous section may also explain the greater negative effect of dam construction in the Sahel with respect to other regions highlighted by *Steinmann et al.* [2006], thus encouraging the extension of the approach proposed in this Thesis to other areas in SSA.

7.2.2 Seasonality and schistosomiasis transmission dynamics

Expanding the ecohydrological aspects mentioned above could enable to account for the seasonality of both snail abundance and exposure/contamination patterns within a spatially explicit framework, shedding new light into their importance for schistosomiasis transmission. Indeed, seasonal variations in environmental drivers of transmission occur in numerous infectious disease systems, many of witch have received significant attention from a theoretical points of view (see *Altizer et al.* [2006] for a review). Despite the extensive description of seasonal variations in the abundance of the snail intermediate hots since the early 1950's (see section 1.2.2), and in human-water contact patterns (see the previous section), seasonality has only very recently been incorporated explicitly into mathematical models of diseases transmission, most of which with a focus on the control of *S. japonicum* using simulation studies [*Liang et al.*, 2007; *Remais et al.*, 2009; *Remais*, 2010; *Gao et al.*, 2013, 2017], and fewer aiming at a qualitative understanding the dynamical behavior of the snail-human-schistosome system [e.g. *Ciddio et al.*, 2015; *Mari et al.*, 2017a]. Using simple, but analytically tractable models, the latter have illustrated how complex dynamics may arise when seasonality is incorporated into *Macdonald*'s model, and how the phase shifts (relative timings) and amplitudes of seasonal components may produce qualitatively distinct dynamics, the most relevant from a control point of view being that of the stability or instability of the disease-free equilibrium (see Appendix A). Additional sources of transmission seasonality not contemplated in these mathematical models may also include the temperature-dependent development of patency and onset of cercarial shedding in snails [*Pitchford et al.*, 1969; *Shiff et al.*, 1979; *Woolhouse and Chandiwana*, 1990b]. The evidence from the literature, and from the work in this Thesis, thus suggest that seasonality is the norm, rather than the exception, in schistosomiasis-endemic setting throughout SSA, owing to the specificities of the socio-ecohydrological system in which transmission is embedded. Moreover, the amplitude and phases of seasonal forcings vary spatially at the national level, mainly as a function of climate and hydrology, and potentially interacting with the spatial dynamics of disease transmission due to human mobility and hydrological connectivity [*Gurarie and Seto*, 2009; *Ciddio et al.*, 2016; *Mari et al.*, 2017b, and Chapter 3 of this Thesis].

The importance of seasonality suggested here may have implications for the way schistosomiasis transmission is conceived and implemented in (spatially-implicit) mathematical models currently used to investigate the feasibility and requirements of transmission interruption in endemic countries in SSA [*Anderson et al.*, 2015; *Gurarie et al.*, 2015; *French et al.*, 2015; *Truscott et al.*, 2017]. Indeed, these approaches have typically assumed constant transmission parameters which are fit to parasitological data assuming that the system is at a stable endemic equilibrium (except for the the Case-Western-Reserve model in *Truscott et al.* [2017]), incorporating the effect of MDA through a reduction of the worm burden in the population, and simulations subsequently compared against follow-up infection data. This procedure precludes the models from disentangling seasonally varying transmission patterns, and can lead to the conclusion that parasite accumulation in the population occurs throughout the year through an "average" rate of infection (what *Barbour* [1996] denotes the "trickling" hypothesis in *Macdonald*'s model, to which he contends against). Although point-prevalence data assumed to correspond to an endemic equilibrium can be reproduced by simple models with time-constant or time-varying parameters[1], their dynamic response to external forcing (for instance MDA) can be radically different, yielding either slow or fast re-infection patterns depending on parameter values. This concern has been raised by *Gurarie et al.* [2017], which have attempted to correct for it by including (non-seasonal) snail population dynamics, and a saturating human-to-snail force of infection (eq. 9 in the above-cited article) which in turn forces the model parameters to produce stronger snail-to-human transmission (this is well illustrated in Fig. 5 of *Truscott et al.* [2017]). As argued by *Gurarie et al.* [2017], a consequence-heavy corollary of not assuming constant transmission parameters through year-round "trickling" accumulation of worms, but rather a strong but varying snail-to-human force of infection, is that gains attained with MDA are inherently precarious since the potential for disease transmission (cf. the notion of "internal potential" discussed below) remains high, and if materialized can yield very rapid re-infection. Although they expressed this mathematically with the saturating human-to-snail force of infection, another natural formulation would be in terms of seasonal (and potentially synchronous) drivers of transmission as discussed above. It is clear however that re-infection will only occur if parasites are re-introduced into the snail population,

---

[1] As a matter of fact, a simple transmission model allowing for time-invariant snail population dynamics has been shown to be able to produce complex dynamical behaviors, including stable fixed points and limit cycles, which expanded to a seasonal time-varying form can yield period doubling bifurcations and chaotic dynamics [*Ciddio et al.*, 2015].

which can be seen as a highly stochastic process [*Barbour*, 1976, 1996], and thus does not systematically happen. The evolution of school-children prevalence in Lioulgou can be seen as a compelling example of this process, with the strong re-infection patterns observed in 2013, but not in 2009. What could be seen as a mathematical technicality could therefore have important consequences in terms of the accuracy of the projected long-term evolution of schistosomiasis at national levels as the one attempted by *Anderson et al.* [2015]; *Gurarie et al.* [2015], and the strategic decisions that are made based on them[1].

Following this line of thought, incorporating seasonality into mainstream mathematical models, both in terms of snail ecology and exposure/contamination processes as discussed above, could be a new and fecund path in the representation of schistosomiasis transmission dynamics. This could not only potentially "save" the mean-worm-burden approach by yielding more adequate estimation of the basic reproduction number[2] which had been criticized by *Barbour* [1996] (cf. section 3.2), but could also provide important insight into the ways to reach and maintain transmission interruption by allowing for the existence of "windows" of intense transmission which are known to strongly affect the efficacy of chemotherapy [*Augusto et al.*, 2009; *Ahmed et al.*, 2012; *Tchuem Tchuenté et al.*, 2013; *Senghor et al.*, 2015]. This stance echoes the approach followed by *Liang et al.* [2007] who expressed the importance of local environmental, behavioral and socio-economic factors in the concept of the "internal potential" of *S. japonicum* transmission, with well-defined temporal windows in which it occurs, denoted as "gating effects", depending on the relative seasonal variations of the incorporated forcings. This approach was made possible by a rich set of data on the factors affecting transmission in the three villages the modelling framework was applied to, yielding a comprehensive appreciation of the distinct dynamics of schistosomiasis transmission in each site, and identifying potential measures to curb it. Nevertheless, its application to a regional or national scale is unclear, and possibly hindered by the very data requirements that rendered its tailored results so insightful.

Transposing this experience to SSA may help to better define control and elimination strategies in endemic countries. However this will require the re-definition of key seasonal social-ecological drivers of schistosomiasis specific to the *Bulinus*-*S. haematobium* and *Biomphalaria*-*S. mansoni* systems across endemic countries in the sub-continent, with the challenges it entails, among other, in terms of data collection. Nevertheless, the association between hydrology and these drivers that has been highlighted in this Thesis in the case of Burkina Faso is encouraging in the possibility to successfully incorporate them into a full ecohydrological spatially-explicit mathematical model of disease transmission at the national scale.

7.2.3 A wider view on schistosomiasis ecohydrology

Taking a further step back, the appraisal of the spatio-temporal ecohydrological drivers of schistosomiasis transmission through mathematical modelling brought to the fore in this Thesis could be seen as a first step towards developing a comprehensive ecohealth approach to the disease. Ecohealth is a relatively new discipline that fosters the creation and synthesis of inter- and transdisciplinary knowledge at the ecology-health nexus [*Parkes*, 2011], which has been strongly advocated for the apprehension of health issues

---

[1] Thinking through the conception of schistosomiasis as driven by very intense parasite circulation events with variable duration, rather than through the prism of the "trickling" hypothesis could lead to conceptualize the disease's transmission as seasonally recurring epidemics, rather than one with slow dynamics. Interestingly, the term "epidemic" has been used in some occasions for schistosomiasis [e.g. *Talla et al.*, 1990; *Cunin et al.*, 2000; *Wang et al.*, 2004; *Appleton et al.*, 2008], although always in cases where the disease was not present before or in areas with rapid resurgence.

[2] As mentioned previously, the aggregation of human-water contacts, heterogeneity in individual exposure/contamination risk, and synchrony in seasonal variations in snail abundance and exposure have all been shown to strengthen transmission, yielding a stable endemic equilibrium for sub-threshold values of the equivalent homogeneous basic reproduction number [*Mari et al.*, 2017a].

and neglected tropical diseases in Africa [*Bergquist et al.*, 2017]. Indeed, the field and theoretical work undertaken in this Thesis with respect to schistosomiasis has addressed different aspects of the social-ecological system (cf. *Utzinger et al.* [2011]), using tools of and building on collaborations with experts from different disciplines. At the village scale were explored chiefly the ecology of the snail intermediate hosts through ecological sampling, environmental monitoring, and mathematical modelling; and the seasonality of water contact-causing activities and their spatial configuration through questionnaire surveys and participatory mapping activities. At the national scale were investigated the role of water resource development in conjunction with human mobility through stability analysis of spatially explicit models of transmission; and the role of ephemerality on the geography of the disease owing to the ecological range of the intermediate hosts and speculated patterns of human-water contacts through hydrological modelling and epidemiological analysis. Interestingly, hydrology has served as the common denominator in all these analysis, and is thought to hold the key for bridging the local and national scales of analysis through the incorporation of the seasonal drivers of disease transmission discussed in the preceding section into a national-scale spatially explicit model of disease transmission. It is clear however that the approach is not comprehensive, indeed the participatory workshops in the three villages were not held at the very onset of the research project, and the research agenda had already been defined, and thus could not take into account the specific needs and interests of the population. However, these workshops yielded important insight into the socio-economic and behavioral component of transmission, fueling much of the results and interpretations in section 7.1. Mathematical models that incorporate the type of hydro-socio-ecological drivers as the ones discussed in this Thesis can be seen as an important component of the appraisal of the complexity of schistosomiasis through and ecohealth approach, which can be usefully expressed and studied in terms of dynamical systems [*Michael and Madon*, 2017; *Ngonghala et al.*, 2017]. This methodological approach could be applicable to other waterborne and vector-borne disease presenting environmental transmission pathways [*Garchitorena et al.*, 2017]. Ecohydrological approaches to schistosomiasis must therefore strive to benefit both from the insight from ecology regarding host-pathogen system dynamics [*Cable et al.*, 2017], in particular for causal inference [*Plowright et al.*, 2008] and model-guided fieldwork [*Restif et al.*, 2012]; and from the multi-scale modelling and parameter estimation methodologies from hydrology (as discussed in *King and Caylor* [2011] with a focus on plant ecohydrology).

7.3 A frame of action for surveillance-response

If the process of establishing the most appropriate path towards schistosomiasis elimination is still ongoing [*Lo et al.*, 2017; *Tchuem Tchuenté et al.*, 2017; *Sokolow et al.*, 2017], there is a strong consensus with respect to the need for appropriate surveillance-response systems (SRS) to secure transmission interruption once it is attained [*Zhou et al.*, 2013; *Rollinson et al.*, 2013; *Tambo et al.*, 2014; *Manyangadze et al.*, 2015; *Bergquist et al.*, 2015; *Xu et al.*, 2016; *Malone et al.*, 2017; *Stothard et al.*, 2017]. It is here argued that a spatially-explicit mathematical modelling framework ensuing from the expansions proposed in section 7.2.1 could be a key ingredient in such systems in endemic countries in SSA.

Surveillance is defined as *"the continuous, systematic collection, analysis and interpretation of health-related data needed for the planning, implementation, and evaluation of public health practice"*[*World Health Organization*, 2012b]. Data, its collection, analysis and interpretation, are thus at the core of surveillance response systems (SRS) for both epidemic and endemic diseases [*Choi*, 2012]. Indeed SRSs are implemented at the national scale, therefore requiring the assimilation of geographically embedded epidemiological data [*Bergquist et al.*, 2015]. Computational tools are essential to the operation of SRSs for database management and the development of statistical/mathematical models to process, extract and predict the spatio-temporal characteristics of the surveyed disease [*Zhou et al.*, 2013; *Feng et al.*, 2016]. The blossoming of remotely-sensed spatial datasets has had a profound impact on the discipline of spatial epidemiology, in particular in the direction of statistical mapping tools for the prediction of pathogen/vector/reservoir species' ecological ranges as a proxy of infection risk [*Ostfeld et al.*, 2005] (see *Manyangadze et al.* [2015] and *Walz et al.* [2015a] for reviews regarding schistosomiasis). Furthermore statistical modelling has been at the core of a large number of surveillance systems proposed for water-borne [*Lleo et al.*, 2008], snail-borne [*Malone et al.*, 2001, 2017], and arthropod vector-borne diseases [*Kalluri et al.*, 2007; *Eisen and Lozano-Fuentes*, 2009; *Kelly et al.*, 2011; *Yang et al.*, 2012a], with a particular emphasis on NTDs [*Bergquist et al.*, 2015; *Tambo et al.*, 2017]. Indeed, disease mapping permits the identification of high risk areas and the prediction of the effect of future changes in climatic and abiotic factors on disease hotspots [*Zhou et al.*, 2013; *Bergquist et al.*, 2015] (see *Lai et al.* [2015] for a compelling example). These functionalities are meant to support the design of active and passive surveillance sampling startegies of the territory for the compilation of the *minimal essential database* (MEB) which constitutes the cornerstone of any SRS [*Zhou et al.*, 2013; *Bergquist et al.*, 2015]. A major challenge for SRSs for NTD elimination is the operationally-meaningful definition of the MEB, and the spatio-temporal sampling scheme it entails, encompassing the choice of diagnostic tools (classical or rapid) and the sampling locations, timing and objects (humans, vectors, environmental concentrations of the pathogen). In the face of these considerations, statistical mapping approaches may fall short in answering the *minimal essential data* question because of the difficulty for these tools to adequately take the dynamical nature of infectious disease transmission into account [*Kalluri et al.*, 2007]. Regarding SRSs, process-based approaches that are spatially resolved on national scales have been featured for evaluating the cost-effectiveness of alternative intervention scenarios [*Zhou et al.*, 2013]. Indeed, the explicit formulation of the mechanisms behind disease transmission provides a framework for comparing control options based on their costs and dynamical effects on disease burden on various spatial and temporal scales [eg. *Guyatt and Tanner*, 1996; *Williams et al.*, 2002; *Lo et al.*, 2015, 2016]. Both statistical and mathematical models have been incorporated into the Chinese schistosomiasis surveillance-response system, building on the process-based temporal capabilities of mathematical models and the spatial capabilities of statistical methods [*Feng et al.*, 2016]. Furthermore, the appraisal of infectious disease transmission as spatially explicit dynamical systems is relevant for the formulation of pathogen (re)invasion conditions which extend the fundamental concept of the basic reproduction number to connected spaces [*Gatto et al.*, 2012], as proposed for schistosomiasis in Chapter 3 of this Thesis (see Appendix A). In this framework, pathogen invasion and spread are inherent characteristics of disease transmission dynamics that can be expressed in terms of the dynamical stability of the system accounting for spatial connectivity [*Gatto et al.*, 2013], and seasonal variability [*Mari et al.*, 2014b]. A spatially-explicit modelling framework expanding the one developed in Chapter 3, accounting for the ecohydrological drivers of disease transmission could therefore be valuable in assessing the optimal deployment of surveillance resources, in particular the choice of sentinel sites and the frequency at which parasitological sampling needs to take place with respect to the spatially-varying seasonality of transmission. Moreover, models allowing for hydrological connectivity could leverage data from novel environmental surveillance methods such as eDNA [*Stothard et al.*, 2017], as it has been successfully done for an infectious disease of freshwater fish in rivers [*Carraro et al.*, 2017]. Echoing the utility of ecozones for the inference of schistosomiasis transmission across large spatial scales voiced by *Brooker et al.* [2002], the developments proposed here for surveillance would be directly supported by ecohydrological insight, possibly resulting in an increased efficiency of the use of the often limited resources at the disposal of the ministries of health in endemic countries.

Regarding response, a spatially-explicit model of schistosomiasis could readily allow for the testing and optimization of control strategies. First and foremost would be the exploration of the effect of tailoring the timing of MDA to the ecohydrological seasonality of disease transmission. Indeed, the observed importance of seasonal disease transmission for the efficacy of MDA [*Augusto et al.*, 2009] has not yet been addressed by mathematical models in SSA, and could provide key information on the optimization of available praziquantel supplies in the view of transmission interruption. Moreover, the explicit incorporation of snail ecology into the modelling framework allows for the investigation of the optimal timing of snail control measures as a function of hydrology and habitat types. For instance the central role played by the temporary pond in Lioulgou in schistosomiasis infection in schoolchildren could very well justify targeted mollusciciding, however the shores of Tougou's reservoir seem like a less suitable target. The nature and spatial configuration of waterbodies sustaining transmission therefore needs to be taken into account, which could be done thanks to growing availablity of remote sensing products with increasing spatial and temporal resolutions [*Malone et al.*, 2017]. Importantly, the spatially-explicit nature of the transmission model could also allow for the determination of optimal space-time allocation of resources drawing from optimal-control theory [*Sokolow et al.*, 2017].

8 Conclusion

The fascinating complexity of *Schistosoma* spp.' lifecycle is rooted in the interplay between climatic, environmental, ecological, and socio-economic factors affecting the snail-human-schistosome system. This Thesis aimed at addressing this complexity through the development of a mathematical modelling framework grounded in a field-based ecohydrological approach which permits a predictive appraisal of the spatio-temporal determinants of disease transmission.

The latitudinal climatic gradient in Burkina Faso, combined with the presence of both the uro-genital and intestinal forms of the disease, provided a representative experimental setting in which to investigate the link between hydrology and schistosomiasis. A spatially-explicit mathematical model of transmission was applied for the first time at the national scale, allowing for connectivity through human mobility inferred from population density maps, and spatially-varying parameters of transmission. The relevance of expressing disease transmission in terms of spatial dynamical systems was addressed in by the theoretical analysis of the effect of mobility and water resources development on parasite (re-)invasion of the connected space. An analytic expression of the stability of disease spatial spread, the generalized reproduction number, was used to explore wide ranges of uncertain model parameter values, focusing on human mobility and water contact rates, along with the effect of dam construction in terms of altered snail probability of presence. On one hand, the appraisal of schistosomiasis transmission through this national-scale spatially-explicit model brought additional evidence to the relationship between water resources development and schistosomiasis risk. On the other hand, it also shed light on the interplay between the local and larger-scale effects of water resources development due to the likelihood of parasite dispersal through human mobility, in particular if it occurs in highly connected locations. Importantly, the development of the national-scale model highlighted the limitations of its underlying assumptions, chiefly regarding snail ecology -assumed constant-, and human-water contact patterns -assumed a function of population density. Hydrology can be seen as a first order control of both processes. For the former by regulating the presence and quality of snail habitat and conditioning ecological dynamics therein. For the latter by constraining the occurrence and spatial configuration of the waterbodies supporting human-water contacts.

The hydrological underpinning of the socio-ecological drivers of schistosomiasis transmission was highlighted in this Thesis both at the local and national scales. Field and modelling ecological studies in three experimental sites along Burkina Faso's climatic gradient revealed a habitat- (natural vs. man-made) and hydrology- (permanent vs. ephemeral) dependent seasonality in snail population dynamics. Opposite phases were observed in the abundance fluctuations of *Bulinus* spp. in ephemeral ponds and rivers which undergo population burst and crash during the rainy season, with respect to permanent rivers harbouring perennial populations of both *Biomphalaria pfeifferi* and *Bulinus* spp. who's population decreased during the rainy season and peaked at the end of the dry season. Interestingly, snail demography in man-made habitats resembled that of the sampled permanent stream although located in otherwise ephemeral landscapes. Moreover, statistical model comparison and averaging techniques helped identify controversial density-feedbacks in all habitats, and provides an approach for the prediction of snail population dynamics using environmental covariates. At the national scale, the link between hydrology and snail ecology was substantiated through the classification and prediction of hydrological ephemerality of Burkina Faso's whole river network. This allowed for the incorporation of hydrological characteristics, subsumed in discrete classes of ephemerality, into species distribution modelling of the occurrence of the snail intermediate hosts. The predicted ecological range of *B. pfeifferi* along the country's river network was identified as the dominant risk factor associated to intestinal schistosomiasis in a statistical analysis of the disease's geography. The possibility to bridge from the local to a national scale appraisal of snail population dynamics was suggested by preliminary results from a combined national scale model of snail demography driven by remote-sensing estimates of precipitation and temperature, although further model refinement is warranted. Shedding new light into national-scale patterns of uro-genital schistosomiasis, the observed association between hydrological ephemerality and disease prevalence was interpreted as a consequence of the spatio-temporal aggregation of human-water contacts driven by the (contracted) availability of surface water. This interpretation was supported by the analysis of preliminary results from water-contact surveys and participatory workshops held in the three experimental sites. These suggest strong seasonal variations both in the frequency of water contact-causing activities in all three villages, and the spatial configuration of the water contact points in which they occur, especially in ephemeral landscapes. Additional data, especially regarding children water contacts, and analysis are both required to validate and better quantify these findings. Despite of this the observed association between hydrology and schistosomiasis risk through its hypothesized effect on the aggregation water contacts is encouraging for the development of a future appraisal of exposure and contamination patterns in spatially-explicit models of disease transmission.

The results in this Thesis support the stance that ecohydrology offers a promising angle from which to look into the complex transmission cycle of schistosomiasis in SSA, potentially yielding useful insight into how best to control it. The ecological studies of the snail intermediate hosts along Burkina Faso's climatic gradient, supported by on-site monitoring of environmental and hydrological covariates, are at odds with the previously-noted decreasing trend of attention drawn to snail population dynamics in the literature. Moreover, the novel incorporation of hydrology in snail species distribution models improved their predictive accuracy, thus warranting its more systematic appraisal in ecological range studies. Hydrology was also directly linked to disease transmission through the odd-ratio analysis of schistosomiasis prevalence against ephemerality and socio-economic covariates. The results suggested a non-linear relationship between ephemerality and the epidemiology of schistosomiasis resulting from the ecological constraints it imposes on snail occurrence on the one hand, and possibly favouring the concentration of human-water contact on the other. Even if the latter point remains to be further substantiated, it strongly supports the thesis that hydrology is not only a determinant of the ecology of the intermediate hosts, but also that of the human host by conditioning the type, seasonality, and spatial configuration of livelihood-supporting activities through which water contacts occur. This can be often seen in most rural areas with seasonal climates like that of Burkina Faso. The successful incorporation of both these aspects into the spatially-explicit modelling framework proposed in this Thesis could have important implications for the way national schistosomiasis elimination programs are operated in endemic countries in SSA. First of all, the revealed phase shifts between permanent and ephemeral habitats in the seasonal fluctuations of snail abundance could help determine climate- and hydrology-specific windows of intense transmission. These could have important implications for the optimization of the timing of MDA in Burkina Faso. Countries with strong geographical climatic gradients in SSA could also benefit from this type of knowledge. It is recognized that looking beyond MDA optimization is needed. In this context, the spatially-explicit modelling framework proposed in this Thesis could provide an important tool for the design and implementation of adequate surveillance-response systems (SRSs) which are deemed necessary for the elimination of schistosomiasis and NTDs in general. Such framework could help answering the question of the *minimal essential database* needed to be collected through active and passive channels to adequately survey the state of a disease in a country. Spatially-explicit mathematical models, such as the one developed in this Thesis, are uniquely equipped to answer this inherent spatial challenge for better understanding and controlling schistosomiasis. Moreover, the issue of parasite re-introduction through human mobility or other transport mechanisms becomes increasingly important when approaching elimination, which can be taken into account as demonstrated in this Thesis. Finally, the proposed mathematical modelling framework herewith developed could be used to tailor response packages combining MDA, snail control and other measures to specific socio-ecohydrological settings. It is foreseen that the framework could also accomodate cost-efficiency analysis of measures being implemented.

The findings presented here can be seen as a first step in the ecohydrological appraisal of schistosomiasis in SSA through mathematical modelling, noting that numerous points deserve further research. Though an initial methodology has been proposed for the regionalization of the ecological models of snail population dynamics, further investigation is required to verify the validity of the predictions beyond the range covered by the three experimental sites. Additional ecological sampling across habitat types and hydrologic regimes could also strengthen the approach, despite the operational challenges and financial costs they imply. Applying similar methods as proposed in this Thesis to timeseries of snail abundance across SSA gathered from the literature could provide a continental scale perspective on the seasonal characteristics of snail population dynamics. This could be particularly useful for countries in which schistosomiasis is a public health concern and where there are scarce historical malacological datasets. Moreover, the extension of the proposed methodology for the classification and prediction of hydrological ephemerality to the continental-scale river network would be valuable for updating snail ecological range maps in SSA, and could also be useful for ecohydrological research beyond schistosomiasis. Key to the implementation of the spatially-explicit modelling framework is the development of a more in-depth research of the association between hydrological characteristics and the exposure resulting from water-contact patterns, and its subsequent translation into a functional form within the model. Another promising improvement consists of the incorporation of human mobility fluxes extracted from mobile phone data which has already been leveraged in the analysis of other infectious diseases in SSA, and which could be an important component of model-informed surveillance-response systems. Last but not least, fitting the final model to parasitological data is a crucial step. Even though this has not been addressed in this Thesis, it is recognized the pose non-negligible challenges associated to the choice of the spatial scale on which to model transmission, to the definition of the likelihood and error models, as well as to the optimization of parameter sets. In this context, it is noteworthy to mention the potential support that the inclusion of these aspects could bring to schistosomiasis elimination.

More than 150 years have passed since the discovery of human schistosomiasis by Bilharz in Egyptian workers in 1851 [*Bilharz*, 1853], however the disease still causes severe morbidity in millions of people today. For more than 150 years scientists have been awed by *Schistosoma*'s multifaceted lifecycle, who's intricacy has often been thought of as an obstacle to control and elimination efforts due to the remarkable stability it confers to disease transmission. Nevertheless, it can also be seen as an opportunity, due to the multiple points through which the cycle can be broken, if they can be properly identified and exploited. The findings and perspectives brought forward by this Thesis are thought to contribute to the overcoming of this duality, paving the way for the development of tools leveraging ecohydrological insigh for supporting schistosomiasis elimination in Burkina Faso and elsewhere in sub-Saharan Africa.

A Derivation of the stability criteria for the connected schistosomiasis model

A.1 The local model

Let[2] us start with the analysis of the parasite invasion condition in MacDonald's (1965) spatially implicit model. We recall that the model can be written as

$$\begin{aligned}
\frac{dW}{dt} &= a\theta C - \gamma W \\
\frac{dY}{dt} &= bM(1-Y) - \nu Y \\
\frac{dC}{dt} &= \frac{\Pi_C}{V} NY - \mu_C C \\
\frac{dM}{dt} &= \frac{\Pi_M}{V} \theta' H \frac{W}{2} - \mu_M M\,.
\end{aligned}$$

As the model is a positive system (namely its state variables can never become negative if the system is initialized at generic non-negative conditions), the bifurcation from stable to unstable of the disease-free equilibrium (DFE) $\mathbf{X_0} = [0,0,0,0]^T$, i.e. a state of the system characterized by the absence of the parasite, can only occur via an exchange of stability. This implies that the DFE switches from being a stable equilibrium to being a saddle (i.e. an equilibrium with one unstable manifold) through a so-called transcritical bifurcation *Kuznetsov* [1995]. The condition for the bifurcation to occur (hence for parasite invasion) is thus determined by the stability properties of the Jacobian of the system evaluated at the DFE, i.e.

$$\mathbf{J_0} = \begin{bmatrix} -\gamma & 0 & a\theta & 0 \\ 0 & -\nu & 0 & b \\ 0 & \frac{\Pi_C}{V}N & -\mu_C & 0 \\ \frac{\Pi_M}{V}\theta'\frac{H}{2} & 0 & 0 & -\mu \end{bmatrix}.$$

Specifically, the DFE is asymptotically stable (thus precluding parasite invasion) if and only if the dominant eigenvalue of $\mathbf{J_0}$ is strictly negative. In this case the determinant of $\mathbf{J_0}$ is positive, because the Jacobian is a matrix of even order. The change of stability for $\mathbf{X_0}$ is thus obviously associated to the condition

---

[2] This Annex corresponds to Supplementary Text 1 in *Perez-Saez et al.* [2015], developed by principally by L. Mari and presented here for completeness.

$\det(\mathbf{J_0}) = 0$, i.e.

$$\begin{aligned}\det(\mathbf{J_0}) &= -\gamma \det\left(\begin{bmatrix} -\nu & 0 & b \\ \frac{\Pi_C}{V}N & -\mu_C & 0 \\ 0 & 0 & -\mu_M \end{bmatrix}\right) - a\theta \det\left(\begin{bmatrix} 0 & -\nu & b \\ 0 & \frac{\Pi_C}{V}N & 0 \\ \frac{\Pi_M}{V}\theta' \frac{H}{2} & 0 & -\mu_M \end{bmatrix}\right) = \\ &= -\gamma\nu\mu_C\mu_M + \frac{ab\theta\theta'\Pi_c\Pi_M HN}{2V^2} = 0\,.\end{aligned}$$

The previous condition can be equivalently written in terms of the basic reproduction number R_0 as

$$R_0 = \frac{ab\theta\theta'\Pi_C\Pi_M HN}{2\gamma\nu\mu_C\mu_M V^2} = 1\,,$$

and the parasite can invade a disease-free community if and only if $R_0 > 1$.

A.2 The spatially explicit network model

A spatially explicit version of Macdonald's model, accounting for human mobility and hydrological transport of the intermediate larval stages of the parasite (and neglecting snail mobility) proposed by *Gurarie and Seto* [2009] is formulated as follows:

$$\begin{aligned}\frac{dW_i}{dt} &= a\left[(1-m_i)\theta_i C_i + m_i \sum_{j=1}^{n} Q_{ij}\theta_j C_j\right] - \gamma W_i \\ \frac{dY_i}{dt} &= bM_i(1-Y_i) - \nu Y_i \\ \frac{dC_i}{dt} &= \frac{\Pi_C}{V_i}N_i Y_i - \mu_C C_i - l_i^C C_i + \sum_{j=1}^{n} l_j^C P_{ji} S_{ji}^C \frac{V_j}{V_i} C_j \\ \frac{dM_i}{dt} &= \frac{\Pi_M}{V}\theta'_i\left[(1-m_i)H_i\frac{W_i}{2} + \sum_{j=1}^{n} m_j H_j \frac{W_j}{2} Q_{ji}\right] - \mu_M M_i - l_i^M M_i + \sum_{j=1}^{n} l_j^M P_{ji} S_{ji}^M \frac{V_j}{V_i} M_j\,.\end{aligned}$$

Analogously to the spatially implicit case, the condition for parasite invasion in the network model is determined by the stability properties of the Jacobian matrix of the system linearised at the disease-free equilibrium. Switching to matrix notation, we have

$$\mathbf{J_0^*} = \begin{bmatrix} \mathscr{A} & \mathscr{B} \\ \mathscr{C} & \mathscr{D} \end{bmatrix},$$

where

$$\mathscr{A} = \begin{bmatrix} -\gamma\mathbf{I} & 0 \\ 0 & -\nu\mathbf{I} \end{bmatrix} \qquad \mathscr{B} = \begin{bmatrix} a(\mathbf{I}-\mathbf{m}+\mathbf{mQ})\boldsymbol{\theta} & 0 \\ 0 & b\mathbf{I} \end{bmatrix}$$

$$\mathscr{C} = \begin{bmatrix} 0 & \Pi_C\mathbf{V}^{-1}\mathbf{N} \\ \frac{\Pi_M}{2}\mathbf{V}^{-1}\boldsymbol{\theta}'(\mathbf{I}-\mathbf{m}+\mathbf{Q}^T\mathbf{m})\mathbf{H} & 0 \end{bmatrix} \qquad \mathscr{D} = \begin{bmatrix} -\mu_C\mathbf{I}+\mathbf{T_C} & 0 \\ 0 & -\mu_M\mathbf{I}+\mathbf{T_M} \end{bmatrix}.$$

In the previous expressions $\mathbf{I}$ is the identity matrix; $\mathbf{m}$, $\boldsymbol{\theta}$, $\mathbf{V}$, $\mathbf{N}$, $\boldsymbol{\theta}'$ and $\mathbf{H}$ are diagonal matrices whose non-zero elements are made up by the parameters m_i, θ_i, V_i, N_i, θ'_i and H_i, respectively; $\mathbf{Q} = [Q_{ij}]$ is the connectivity matrix for human mobility; $\mathbf{T_C} = \left(\mathbf{V}^{-1}\mathbf{P_C}^T\mathbf{V}-\mathbf{I}\right)\mathbf{l_C}$ and $\mathbf{T_M} = \left(\mathbf{V}^{-1}\mathbf{P_M}^T\mathbf{V}-\mathbf{I}\right)\mathbf{l_M}$, where $\mathbf{P_C} = [P_{ij}S_{ij}^C] = \mathbf{P}\circ\mathbf{S_C}$ and $\mathbf{P_M} = [P_{ij}S_{ij}^M] = \mathbf{P}\circ\mathbf{S_M}$ are transport matrices accounting for hydrological connectivity and larval survival during transport, and $\mathbf{l_C}$ and $\mathbf{l_M}$ are diagonal matrices whose non-zero elements are the local values of l_i^C and l_i^M, respectively.

Let us preliminary note that the off-diagonal entries of $\mathbf{J_0^*}$ are all nonnegative and at least one diagonal entry is negative, thus $\mathbf{J_0^*}$ is a proper Metzler matrix *Farina and Rinaldi* [2011] and its eigenvalue with maximal real part (dominant eigenvalue) is real. If the union of graphs associated with matrices **P** and **Q** is strongly connected, then the graph associated with $\mathbf{J_0^*}$ is also strongly connected. Therefore we can apply Perron-Frobenius theorem for irreducible matrices *Gantmacher* [1959] and state that the dominant eigenvalue of $\mathbf{J_0^*}$ is the maximum simple real root of the characteristic polynomial. The condition for the transcritical bifurcation of the DFE is that the dominant eigenvalue crosses the imaginary axis at zero, namely that the determinant of $\mathbf{J_0^*}$ is zero *Kuznetsov* [1995]. When the DFE is stable (sufficient condition to prevent parasite invasion), all the eigenvalues of $\mathbf{J_0^*}$ have negative real parts and $\det(\mathbf{J_0^*})$ is positive because $\mathbf{J_0^*}$ is a matrix of order $4n$. The DFE becomes unstable (necessary condition for parasite invasion) when $\det(\mathbf{J_0^*})$ switches from positive to negative, or equivalently when the dominant eigenvalue of $\mathbf{J_0^*}$ switches from negative to positive.

Noting the block structure of $\mathbf{J_0^*}$ and that $\mathscr{A}$ is a piece-wise scalar matrix (thus $\mathscr{A}\mathscr{B} = \mathscr{B}\mathscr{A}$), the determinant of $\mathbf{J_0^*}$ can be computed as *Silvester* [2000]

$$\begin{aligned}
\det(\mathbf{J_0^*}) &= \det(\mathscr{D}\mathscr{A} - \mathscr{C}\mathscr{B}) = \\
&= \det\left(\begin{bmatrix} \gamma(\mu_C \mathbf{I} - \mathbf{T_C}) & -b\Pi_C \mathbf{V}^{-1}\mathbf{N} \\ -\frac{a\Pi_M}{2}\mathbf{V}^{-1}\boldsymbol{\theta}'(\mathbf{I} - \mathbf{m} + \mathbf{Q}^T\mathbf{m})\mathbf{H}(\mathbf{I} - \mathbf{m} + \mathbf{m}\mathbf{Q})\boldsymbol{\theta} & \nu(\mu_M \mathbf{I} - \mathbf{T_M}) \end{bmatrix}\right) = \det(\mathbf{J_0^{**}})\,.
\end{aligned}$$

Writing $\mathbf{J_0^{**}}$ as

$$\mathbf{J_0^{**}} = \begin{bmatrix} \mathscr{U} & \mathscr{W} \\ \mathscr{X} & \mathscr{Z} \end{bmatrix}$$

it is possible to show [see again *Silvester*, 2000] that

$$\det(\mathbf{J_0^{**}}) = \det(\mathscr{U}\mathscr{Z} - \mathscr{W}\mathscr{Z}^{-1}\mathscr{X}\mathscr{Z})\,,$$

obviously provided that matrix $\mathscr{Z}$ is invertible. With straightforward algebraic manipulations the right-hand side of the previous equation can be written in a form that is more amenable to further analysis, i.e.

$$\det(\mathscr{U}\mathscr{Z} - \mathscr{W}\mathscr{Z}^{-1}\mathscr{X}\mathscr{Z}) = \det(\mathscr{W})\det(\mathscr{Z}\mathscr{W}^{-1}\mathscr{U} - \mathscr{X}) = \det(\mathscr{W})\det(\mathbf{J_0^{***}})\,,$$

which additionally requires matrix $\mathscr{W}$ to be invertible. If the conditions on matrices $\mathscr{Z}$ and $\mathscr{W}$ are verified, the bifurcation condition $\det(\mathbf{J_0^*}) = 0$ corresponds to $\det(\mathbf{J_0^{***}}) = 0$. The determinant of $\mathbf{J_0^{***}}$ can be written as

$$
\begin{aligned}
&\det(\mathbf{J_0^{***}}) = \\
&\quad = \det\left(\nu(\mu_M\mathbf{I}-\mathbf{T_M}) \left(-\frac{1}{b\Pi_C}\mathbf{V}\mathbf{N}^{-1}\right) \gamma(\mu_C\mathbf{I}-\mathbf{T_C}) + \right. \\
&\quad \left. + \frac{a\Pi_M}{2}\mathbf{V}^{-1}\boldsymbol{\theta}'(\mathbf{I}-\mathbf{m}+\mathbf{Q}^T\mathbf{m})\mathbf{H}(\mathbf{I}-\mathbf{m}+\mathbf{m}\mathbf{Q})\boldsymbol{\theta} \right) = \\
&\quad = \det\left(\frac{a\Pi_M}{2}\mathbf{V}^{-1}\boldsymbol{\theta}'(\mathbf{I}-\mathbf{m}+\mathbf{Q}^T\mathbf{m})\mathbf{H}(\mathbf{I}-\mathbf{m}+\mathbf{m}\mathbf{Q})\boldsymbol{\theta} - \frac{\gamma\nu}{b\Pi_C}(\mu_M\mathbf{I}-\mathbf{T_M})\mathbf{V}\mathbf{N}^{-1}(\mu_C\mathbf{I}-\mathbf{T_C}) \right) = \\
&\quad = \det\left(\frac{ab\Pi_C\Pi_M}{2\gamma\nu\mu_C\mu_M}\mathbf{N}\mathbf{V}^{-1}\boldsymbol{\theta}'[(\mathbf{I}-\mathbf{m})\mathbf{H}(\mathbf{I}-\mathbf{m}) + (\mathbf{I}-\mathbf{m})\mathbf{H}\mathbf{m}\mathbf{Q} + \mathbf{Q}^T\mathbf{m}\mathbf{H}(\mathbf{I}-\mathbf{m}) + \mathbf{Q}^T\mathbf{m}\mathbf{H}\mathbf{m}\mathbf{Q}]\boldsymbol{\theta}\mathbf{V}^{-1} + \right. \\
&\quad \left. - \frac{1}{\mu_C\mu_M}\mathbf{N}(\mu_M\mathbf{I}-\mathbf{T_M})\mathbf{V}\mathbf{N}^{-1}(\mu_C\mathbf{I}-\mathbf{T_C})\mathbf{V}^{-1} \right) \left(\frac{b\Pi_C}{\gamma\nu\mu_C\mu_M}\right)^n \det\left(\mathbf{N}^{-1}\right)\det(\mathbf{V}) = \\
&\quad = \det(\mathbf{J_0^{****}}) \left(\frac{\gamma\nu\mu_C\mu_M}{b\Pi_C}\right)^n \det\left(\mathbf{N}^{-1}\right)\det(\mathbf{V})\,.
\end{aligned}
$$

The condition $\det(\mathbf{J_0^{***}}) = 0$ is thus clearly equivalent to $\det(\mathbf{J_0^{****}}) = 0$, where

$$
\begin{aligned}
&\det(\mathbf{J_0^{****}}) = \\
&\quad = \det\left(\frac{ab\Pi_C\Pi_M}{2\gamma\nu\mu_C\mu_M}\mathbf{N}\left(\mathbf{V}^{-1}\right)^2\boldsymbol{\theta}'(\mathbf{I}-\mathbf{m})^2\mathbf{H}\boldsymbol{\theta} + \right. \\
&\quad + \frac{ab\Pi_C\Pi_M}{2\gamma\nu\mu_C\mu_M}\mathbf{N}\mathbf{V}^{-1}\boldsymbol{\theta}'\left[(\mathbf{I}-\mathbf{m})\mathbf{m}\mathbf{H}\mathbf{Q} + \mathbf{Q}^T\mathbf{H}\mathbf{m}(\mathbf{I}-\mathbf{m}) + \mathbf{Q}^T\mathbf{m}^2\mathbf{H}\mathbf{Q}\right]\boldsymbol{\theta}\mathbf{V}^{-1} + \\
&\quad \left. - \mathbf{N}\left(\mathbf{I} - \frac{1}{\mu_M}\mathbf{T_M}\right)\mathbf{V}\mathbf{N}^{-1}\left(\mathbf{I} - \frac{1}{\mu_C}\mathbf{T_C}\right)\mathbf{V}^{-1} \right) = \\
&\quad = \det\left(\frac{ab\Pi_C\Pi_M}{2\gamma\nu\mu_C\mu_M}\mathbf{N}\left(\mathbf{V}^{-1}\right)^2\boldsymbol{\theta}'(\mathbf{I}-\mathbf{m})^2\mathbf{H}\boldsymbol{\theta} + \right. \\
&\quad + \frac{ab\Pi_C\Pi_M}{2\gamma\nu\mu_C\mu_M}\mathbf{N}\mathbf{V}^{-1}\boldsymbol{\theta}'\left[(\mathbf{I}-\mathbf{m})\mathbf{m}\mathbf{H}\mathbf{Q} + \mathbf{Q}^T\mathbf{H}\mathbf{m}(\mathbf{I}-\mathbf{m}) + \mathbf{Q}^T\mathbf{m}^2\mathbf{H}\mathbf{Q}\right]\boldsymbol{\theta}\mathbf{V}^{-1} + \\
&\quad \left. - \mathbf{I} + \frac{1}{\mu_C}\mathbf{V}\mathbf{T_C}\mathbf{V}^{-1} + \frac{1}{\mu_M}\mathbf{N}\mathbf{T_M}\mathbf{N}^{-1} - \frac{1}{\mu_C\mu_M}\mathbf{N}\mathbf{T_M}\mathbf{V}\mathbf{N}^{-1}\mathbf{T_C}\mathbf{V}^{-1} \right)\,.
\end{aligned}
$$

If we introduce a diagonal matrix $\mathbf{R_0}$, whose non-zero elements are the local values R_{0i} of the basic reproduction number, i.e.

$$
R_{0i} = \frac{ab\theta_i\theta_i'\Pi_C\Pi_M H_i N_i}{2\gamma\nu\mu_C\mu_M V_i^2}\,,
$$

a matrix

$$
\mathbf{R_0^M}(\mathbf{m},\mathbf{Q}) = \frac{ab\Pi_C\Pi_M}{2\gamma\nu\mu_C\mu_M}\mathbf{N}\mathbf{V}^{-1}\boldsymbol{\theta}'\left[(\mathbf{I}-\mathbf{m})\mathbf{m}\mathbf{H}\mathbf{Q} + \mathbf{Q}^T\mathbf{H}\mathbf{m}(\mathbf{I}-\mathbf{m}) + \mathbf{Q}^T\mathbf{m}^2\mathbf{H}\mathbf{Q}\right]\boldsymbol{\theta}\mathbf{V}^{-1}
$$

accounting for the effects of human mobility on disease transmission, and another matrix

$$
\mathbf{T}(\mu_C,\mathbf{T_C},\mu_M,\mathbf{T_M}) = \frac{1}{\mu_C}\mathbf{V}\mathbf{T_C}\mathbf{V}^{-1} + \frac{1}{\mu_M}\mathbf{N}\mathbf{T_M}\mathbf{N}^{-1} - \frac{1}{\mu_C\mu_M}\mathbf{N}\mathbf{T_M}\mathbf{V}\mathbf{N}^{-1}\mathbf{T_C}\mathbf{V}^{-1}
$$

describing the effects of pathogen hydrological transport, it is possible to define a generalized reproduction matrix

$$\mathbf{G_0} = (\mathbf{I} - \mathbf{m})^2 \mathbf{R_0} + \mathbf{R_0^M}(\mathbf{m}, \mathbf{Q}) + \mathbf{T}(\mu_C, \mathbf{T_C}, \mu_M, \mathbf{T_M}) \, .$$

The original bifurcation condition $\det(\mathbf{J_0^*}) = 0$ can thus be written as

$$\det(\mathbf{I} - \mathbf{G_0}) = 0 \, .$$

Let λ_i ($i = 1..n$) be the eigenvalues of $\mathbf{G_0}$ and $g_0 = \max_i(\lambda_i)$. Then

$$\det(\mathbf{I} - \mathbf{G_0}) = \prod_{i=1}^{n} (1 - \lambda_i) \, .$$

Therefore, the determinant of $\mathbf{J_0^*}$ switches from positive to negative when g_0, the dominant eigenvalue of $\mathbf{G_0}$, switches from being smaller to being larger than one. It follows that the condition for the instability of the DFE (hence for parasite invasion) is $g_0 > 1$.

We note that in the absence of hydrological dispersal ($l_i^C = l_i^M = 0$ for all i) and human mobility ($m_i = 0$ for all i), i.e. in the case of completely isolated communities, the condition for parasite invasion becomes

$$\det(\mathbf{I} - \mathbf{R_0}) = 0 \, ,$$

which is obviously satisfied when the largest of the R_{0i} values is equal to one – which corresponds to the classical criterion obtained in a spatially implicit context. However, the introduction of human mobility and hydrological connections makes the condition $g_0 > 1$ for parasite invasion absolutely nontrivial. This criterion synthesizes the intertwined effects of local epidemiological processes, human mobility and hydrological transport on parasite invasion. As a matter of fact, $\mathbf{G_0}$ is the sum of three matrices: one depending on local dynamics only, the other two (non-linearly) on spatial coupling mechanisms. The dominant eigenvalue of $\mathbf{G_0}$ is not simply deducible from the eigenvalues of these three addenda. Therefore, human mobility and hydrological networks interplay in a complex manner to determine parasite invasion and spread.

A.3 Spatial patterns of disease spread

Because of the assumption of strong connectivity made in the previous section, the condition under which the parasite can invade an initially disease-free community corresponds to that for the spatial spread of the disease. The spatial localization of the sites that are colonized by the parasite in the early phases following its introduction in a metacommunity is determined by the dominant eigenvector of the Jacobian matrix $\mathbf{J_0^*}$. In fact, if the DFE is unstable, the dominant eigenvector of matrix $\mathbf{J_0^*}$ pinpoints the directions in the state space along which the system trajectories, after a transient period related to initial conditions, will diverge from the equilibrium. The dominant eigenvector is characterized by strictly positive components [according to Perron-Frobenius theorem applied to Metzler matrices; see again *Gantmacher*, 1959], each corresponding – in this case – to the parasite burden in human hosts, the prevalence of infected snails, and the abundances of cercariae and miracidia in different nodes of the network.

The dominant eigenvector of $\mathbf{J_0^*}$ can be computed by solving

$$\mathbf{J_0^*}\begin{bmatrix}\mathbf{W}\\ \mathbf{Y}\\ \mathbf{C}\\ \mathbf{M}\end{bmatrix} = \lambda' \begin{bmatrix}\mathbf{W}\\ \mathbf{Y}\\ \mathbf{C}\\ \mathbf{M}\end{bmatrix},$$

where λ' is the dominant eigenvalue of $\mathbf{J_0^*}$, and $\mathbf{W}$, $\mathbf{Y}$, $\mathbf{C}$ and $\mathbf{M}$ are the components of the dominant eigenvector corresponding, respectively, to parasite burden, prevalence of infected snails, and abundances of cercariae and miracidia. Recalling that close to the transcritical bifurcation through which the DFE loses stability the dominant eigenvalue of $\mathbf{J_0^*}$ is equal to zero, the previous matrix equation becomes

$$\begin{aligned}
&-\gamma\mathbf{W} + a(\mathbf{I}-\mathbf{m}+\mathbf{mQ})\boldsymbol{\theta}\mathbf{C} = 0\\
&-\nu\mathbf{Y} + b\mathbf{M} = 0\\
&\Pi_C\mathbf{V}^{-1}\mathbf{NY} - (\mu_C\mathbf{I}-\mathbf{T_C})\mathbf{C} = 0\\
&\frac{\Pi_M}{2}\mathbf{V}^{-1}\boldsymbol{\theta}'(\mathbf{I}-\mathbf{m}+\mathbf{Q}^T\mathbf{m})\mathbf{HW} - (\mu_M\mathbf{I}-\mathbf{T_M})\mathbf{M} = 0\,.
\end{aligned}$$

From the first two equations we get

$$\mathbf{W} = \frac{a}{\gamma}(\mathbf{I}-\mathbf{m}+\mathbf{mQ})\boldsymbol{\theta}\mathbf{C}$$

and

$$\mathbf{Y} = \frac{b}{\nu}\mathbf{M}\,.$$

If we plug these two expressions into the third and fourth equations of the linear system above we find

$$\frac{b\Pi_C}{\nu}\mathbf{V}^{-1}\mathbf{NM} - (\mu_C\mathbf{I}-\mathbf{T_C})\mathbf{C} = 0$$

and

$$\frac{a\Pi_M}{2\gamma}\mathbf{V}^{-1}\boldsymbol{\theta}'(\mathbf{I}-\mathbf{m}+\mathbf{Q}^T\mathbf{m})\mathbf{H}(\mathbf{I}-\mathbf{m}+\mathbf{mQ})\boldsymbol{\theta}\mathbf{C} - (\mu_M\mathbf{I}-\mathbf{T_M})\mathbf{M} = 0\,.$$

Solving for $\mathbf{M}$ the first of these two equations

$$\mathbf{M} = \frac{\nu}{b\Pi_C}\mathbf{VN}^{-1}(\mu_C\mathbf{I}-\mathbf{T_C})\mathbf{C}$$

and substituting into the second we get

$$\left[\frac{a\Pi_M}{2}\mathbf{V}^{-1}\boldsymbol{\theta}'(\mathbf{I}-\mathbf{m}+\mathbf{Q}^T\mathbf{m})\mathbf{H}(\mathbf{I}-\mathbf{m}+\mathbf{mQ})\boldsymbol{\theta} - \frac{\gamma\nu}{b\Pi_C}(\mu_M\mathbf{I}-\mathbf{T_M})\mathbf{VN}^{-1}(\mu_C\mathbf{I}-\mathbf{T_C})\right]\mathbf{C} = 0\,,$$

which corresponds (see previous section) to

$$\mathbf{J_0^{***}}\mathbf{C} = 0\,.$$

Because we already know that

$$\mathbf{J_0^{***}} = \frac{\gamma\nu\mu_C\mu_M}{b\Pi_C}\mathbf{N}^{-1}\mathbf{J_0^{****}}\mathbf{V} = \frac{\gamma\nu\mu_C\mu_M}{b\Pi_C}\mathbf{N}^{-1}(\mathbf{G_0}-\mathbf{I})\mathbf{V}\,,$$

combining the two previous expressions we have

$$(\mathbf{G_0}-\mathbf{I})\mathbf{C} = 0\,.$$

If we remember that close to the transcritical bifurcation of the DFE the dominant eigenvalue g_0 of matrix $\mathbf{G_0}$ is equal to one we can write

$$\mathbf{G_0}\mathbf{C} = \mathbf{C} = g_0\mathbf{C}\,.$$

We can thus conclude that close to the bifurcation through which the DFE loses stability the dominant eigenvector $\mathbf{g_0}$ of matrix $\mathbf{G_0}$ corresponds to the cercarial components of the dominant eigenvector of $\mathbf{J_0^*}$, while the other components of $\mathbf{J_0^*}$ can be found as linear combinations of $\mathbf{g_0}$, i.e.

$$\begin{aligned}
\mathbf{W} &= \frac{a}{\gamma}(\mathbf{I}-\mathbf{m}+\mathbf{mQ})\boldsymbol{\theta}\mathbf{g_0}\\
\mathbf{Y} &= \frac{1}{\Pi_C}\mathbf{V}\mathbf{N}^{-1}(\mu_C\mathbf{I}-\mathbf{T_C})\mathbf{g_0}\\
\mathbf{C} &= \mathbf{g_0}\\
\mathbf{M} &= \frac{\nu}{b\Pi_C}\mathbf{V}\mathbf{N}^{-1}(\mu_C\mathbf{I}-\mathbf{T_C})\mathbf{g_0}\,.
\end{aligned}$$

Note that these simple relationships between the dominant eigenvectors of $\mathbf{J_0^*}$ and $\mathbf{G_0}$ hold only close to the transcritical bifurcation of the DFE. In general, for parameter combinations for which $g_0 \gg 1$, the study of the geography of disease spread requires the computation of the eigenvalues and eigenvectors of matrix $\mathbf{J_0^*}$.

B Additional tables of ecology models

Table B.1 – Regression coefficents of the 8 best SRM-ranked models for *Bulinus* spp. in an irrigation canal. Coefficients are color-coded for significant (p-value< 0.05) positive (green) and negative (red) effects on snail abundance variantions. Standard error at 95% CI is given in bellow coefficient values (light gray, in parenthesis). Environmental covariate names are color-coded by type as in Fig. 3. Table produced using the R `texreg` package (Leifeld, P. (2013). *texreg: Conversion of Statistical Model Output in R to LaTex and HTML Tables*, J. Stat. Softw., 55, 1-24).

	model1	model2	model3	model4	model5	model6	model7	model8
a	0.435	**10.24*****	**8.152*****	0.747	**−4.654*****	**5.719*****	**1.201***	**−4.862*****
	(0.230)	(0.732)	(0.816)	(0.421)	(0.495)	(0.536)	(0.355)	(0.519)
L_t			**−1.974*****	**−1.446*****		**−1.140*****	**−1.346*****	
			(0.118)	(0.092)		(0.089)	(0.078)	
$L_t.lag3$	**−0.394*****							
	(0.051)							
N_t		**−0.031*****						
		(0.002)						
air.temp.sd.lag1	**−0.426*****							
	(0.047)							
air.temp.sd.lag2	**0.475*****				**0.330*****			**0.386*****
	(0.048)				(0.050)			(0.052)
air.temp.sd.lag3			**0.293*****					
			(0.039)					
conductivity.mean.lag1		**−0.052*****						
		(0.004)						
conductivity.mean.lag3	**0.015*****		**−0.031*****					
	(0.002)		(0.005)					
conductivity.sd.lag2		**−0.116*****						
		(0.011)						
conductivity.sd.lag3				0.024	−0.008	**−0.048***	**0.047****	−0.005
				(0.013)	(0.014)	(0.018)	(0.013)	(0.015)
precip.14	**−0.045*****	**0.119*****						**−0.024*****
	(0.002)	(0.009)						(0.003)
precip.30		**−0.017*****						
		(0.001)						
precip.7				**−0.096*****			**−0.089*****	**0.053*****
				(0.017)			(0.013)	(0.006)
precip.events.14		**−3.367*****	**0.456*****		**−0.618*****			
		(0.262)	(0.048)		(0.065)			
precip.events.30	**0.441*****				**0.824*****			**0.845*****
	(0.042)				(0.073)			(0.076)
precip.events.7	**2.418*****			**3.598*****	**1.462*****	**0.770*****	**3.522*****	
	(0.134)			(0.513)	(0.158)	(0.110)	(0.383)	
water.level.mean					**0.007*****			**0.007****
R^2	0.984	0.992	0.982	0.973	0.970	0.969	0.987	0.967
Adj. R^2	0.968	0.983	0.964	0.949	0.943	0.943	0.972	0.938
Num. obs.	17	16	17	16	16	16	16	16
MSE	0.062	0.050	0.067	0.080	0.084	0.084	0.059	0.088

$^{***}p < 0.001$, $^{**}p < 0.01$, $^{*}p < 0.05$

Continued on next page

Table B.1 – continued

	model1	model2	model3	model4	model5	model6	model7	model8
					(0.001)			(0.001)
water.level.mean.lag1			**0.012*****	**0.008*****		**0.008*****	**0.007*****	
			(0.001)	(0.001)		(0.001)	(0.001)	
water.level.mean.lag2	**−0.002****		**−0.004*****			**−0.005*****		
	(0.000)		(0.001)			(0.001)		
water.level.sd					**0.023*****			**0.024*****
					(0.003)			(0.003)
water.level.sd.lag2				**−0.011*****			**−0.013*****	
				(0.002)			(0.002)	
water.level.sd.lag3						**0.012****		
						(0.002)		
water.temp.mean				**0.106*****			**0.090*****	
				(0.015)			(0.013)	
water.temp.mean.lag1			**0.071*****					
			(0.012)					
water.temp.mean.lag3		**−0.191*****	**−0.174*****			**−0.114*****		
		(0.016)	(0.019)			(0.017)		
water.temp.sd.lag1							**−0.740***	
							(0.272)	
water.temp.sd.lag3		**1.992*****						
		(0.218)						
R^2	0.984	0.992	0.982	0.973	0.970	0.969	0.987	0.967
Adj. R^2	0.968	0.983	0.964	0.949	0.943	0.943	0.972	0.938
Num. obs.	17	16	17	16	16	16	16	16
MSE	0.062	0.050	0.067	0.080	0.084	0.084	0.059	0.088

$^{***}p < 0.001$, $^{**}p < 0.01$, $^{*}p < 0.05$

Table B.2 – Regression coefficents of the 7 best SRM-ranked models for *Bulinus* spp. in a temporary pond. Legend as in B.1.

	model1	model2	model3	model4	model5	model6	model7
a	4.404	5.638	**2.203*****	**2.628*****	2.105	**2.962*****	**2.579*****
	(2.662)	(3.487)	(0.541)	(0.661)	(2.500)	(0.656)	(0.555)
L_t	**−0.650*****	**−0.744*****	**−0.409*****	**−0.425*****	**−0.662*****	**−0.486*****	**−0.469*****
	(0.109)	(0.133)	(0.101)	(0.105)	(0.112)	(0.105)	(0.100)
air.temp.mean	**0.786*****	**0.737*****			**0.714*****		
	(0.184)	(0.191)			(0.188)		
air.temp.mean.lag2	**−0.405***				**−0.406***		
	(0.156)				(0.165)		
air.temp.mean.lag3		**−0.379***					
		(0.182)					
air.temp.sd			**−0.282*****			−0.184	**−0.288*****
			(0.078)			(0.091)	(0.079)
air.temp.sd.lag3	**−0.674*****	**−0.684*****		**−0.399****	**−0.573*****	−0.250	
	(0.154)	(0.161)		(0.112)	(0.151)	(0.131)	
water.temp.mean	**−0.352****	**−0.363****			**−0.376****		
	(0.108)	(0.114)			(0.114)		
water.temp.mean.lag3					0.176		
					(0.090)		
water.temp.sd	**0.502****	**0.484****			**0.441****		**0.358***
	(0.146)	(0.154)			(0.146)		(0.140)
water.temp.sd.lag1	**−0.626*****	**−0.657*****			**−0.552*****		**−0.425****
	(0.146)	(0.152)			(0.140)		(0.121)
water.temp.sd.lag3	**0.275***	**0.318***					
	(0.116)	(0.135)					
R^2	0.737	0.716	0.334	0.327	0.721	0.397	0.509
Adj. R^2	0.656	0.628	0.297	0.289	0.635	0.345	0.448
Num. obs.	35	35	39	39	35	39	37
MSE	0.484	0.503	0.663	0.666	0.498	0.640	0.597

$^{***}p < 0.001$, $^{**}p < 0.01$, $^{*}p < 0.05$

Table B.3 – Regression coefficents of the 7 best SRM-ranked models for *Bulinus* spp. in an ephemeral stream. Legend as in B.1.

	model1	model2	model3	model4	model5	model6	model7
a	**1.229****	**1.026***	**1.298****	**1.340***	2.783	3.935	1.610
	(0.361)	(0.358)	(0.371)	(0.491)	(2.453)	(4.247)	(0.734)
N_t	**−0.129*****	**−0.132*****	**−0.137*****	**−0.122*****	**−0.132*****	**−0.133*****	**−0.132*****
	(0.020)	(0.019)	(0.021)	(0.023)	(0.021)	(0.021)	(0.021)
air.temp.mean.lag3						−0.110	
						(0.173)	
air.temp.sd.lag1							−0.120
							(0.200)
precip.30		0.003					
		(0.002)					
precip.events.30			0.106				
			(0.115)				
water.temp.mean.lag1					−0.049		
					(0.076)		
water.temp.sd				**−0.501****			
				(0.157)			
water.temp.sd.lag1	**−0.616****	**−0.554****	**−0.592****		**−0.587****	**−0.514***	**−0.555***
	(0.146)	(0.141)	(0.150)		(0.157)	(0.219)	(0.182)
water.temp.sd.lag3	**0.678*****	**0.603*****	**0.596****	**0.466*****	**0.616****	**0.644*****	**0.625****
	(0.111)	(0.113)	(0.144)	(0.092)	(0.150)	(0.126)	(0.145)
R^2	0.856	0.886	0.867	0.804	0.861	0.861	0.861
Adj. R^2	0.816	0.841	0.813	0.750	0.806	0.806	0.805
Num. obs.	15	15	15	15	15	15	15
MSE	0.247	0.229	0.248	0.287	0.254	0.254	0.254

$^{***}p < 0.001$, $^{**}p < 0.01$, $^{*}p < 0.05$

Table B.4 – Regression coefficents of the 7 best SRM-ranked models for *Biomphalaria pfeifferi* in a perennial stream. Legend as in B.1.

	model1	model2	model3	model4	model5	model6	model7
a	1.013	1.410	1.499	1.448	2.738	1.257	2.807
	(1.913)	(2.026)	(1.986)	(2.069)	(2.230)	(2.002)	(2.654)
L_t	**−0.911*****	**−1.045*****	**−1.036*****	**−0.939*****	**−0.993*****	**−0.900*****	**−1.060*****
	(0.137)	(0.144)	(0.141)	(0.137)	(0.147)	(0.141)	(0.150)
air.temp.mean							0.227
							(0.143)
air.temp.sd.lag3	**0.385****	**0.360****	**0.412*****	**0.300****	**0.288***	**0.386****	**0.470*****
	(0.110)	(0.102)	(0.105)	(0.097)	(0.114)	(0.114)	(0.101)
conductivity.mean.lag2	**0.068*****	**0.053*****	**0.059*****	**0.044****	**0.058*****	**0.064*****	**0.060*****
	(0.013)	(0.013)	(0.013)	(0.012)	(0.013)	(0.014)	(0.013)
conductivity.mean.lag3	**−0.039****				−0.017	−0.020	
	(0.013)				(0.012)	(0.012)	
conductivity.sd.lag3	**0.279*****	**0.250*****	**0.282*****	**0.251*****	**0.248*****	**0.271*****	**0.279*****
	(0.063)	(0.063)	(0.065)	(0.064)	(0.062)	(0.065)	(0.065)
precip.14	**0.019*****	**0.016*****	**0.017*****		**0.015*****	**0.017*****	**0.017*****
	(0.004)	(0.004)	(0.004)		(0.004)	(0.004)	(0.004)
precip.events.14				**0.599*****			
				(0.141)			
water.level.mean.lag1		**−0.006*****	**−0.006*****	**−0.006****	**−0.007*****	**−0.005****	**−0.006*****
		(0.002)	(0.002)	(0.002)	(0.002)	(0.002)	(0.002)
water.level.sd.lag1	**−0.019*****						
	(0.005)						
water.temp.mean	**−0.198*****		−0.123			**−0.222*****	**−0.528***
	(0.055)		(0.076)			(0.058)	(0.205)
water.temp.mean.lag2		**−0.225*****	−0.142	**−0.194****	**−0.225*****		
		(0.059)	(0.077)	(0.059)	(0.059)		
R^2	0.644	0.606	0.631	0.589	0.624	0.623	0.623
Adj. R^2	0.570	0.535	0.553	0.515	0.545	0.544	0.543
Num. obs.	47	47	47	47	47	47	47
MSE	0.657	0.683	0.670	0.698	0.676	0.677	0.677

$^{***}p < 0.001$, $^{**}p < 0.01$, $^{*}p < 0.05$

Table B.5 – Regression coefficents of the 8 best SRM-ranked models for *Bulinus* spp. in a perennial stream. Legend as in B.1.

	model1	model2	model3	model4	model5	model6	model7	model8
a	1.178 (0.948)	0.105 (0.855)	**3.567*** (1.492)	1.599 (0.999)	1.323 (1.008)	0.889 (0.975)	0.184 (0.404)	2.394 (1.429)
L_t	**−0.871***** (0.115)	**−0.836***** (0.124)	**−0.895***** (0.114)	**−0.845***** (0.116)	**−0.815***** (0.121)	**−0.871***** (0.115)	**−0.741***** (0.118)	**−0.903***** (0.118)
air.temp.sd.lag2	**0.305***** (0.071)		**0.222**** (0.078)	**0.281***** (0.073)	**0.274***** (0.075)	**0.300***** (0.071)	**0.308***** (0.066)	**0.272**** (0.077)
air.temp.sd.lag3		**0.334***** (0.067)						
conductivity.mean		**−0.019*** (0.008)	**−0.020*** (0.010)					−0.009 (0.008)
conductivity.mean.lag3	**−0.020*** (0.009)		**−0.029**** (0.010)	**−0.020*** (0.009)	**−0.027**** (0.010)	**−0.019*** (0.009)		**−0.023*** (0.010)
conductivity.sd			0.094 (0.046)					
conductivity.sd.lag1		**−0.111*** (0.043)						
conductivity.sd.lag3	**−0.123*** (0.049)		**−0.133**** (0.048)	**−0.149**** (0.052)		**−0.135**** (0.049)	**−0.141**** (0.052)	**−0.114*** (0.049)
water.level.mean.lag1		**0.009***** (0.002)						
water.level.mean.lag2				−0.005 (0.004)				
water.level.mean.lag3	**0.005**** (0.002)		**0.005**** (0.001)	**0.008**** (0.003)	**0.005**** (0.002)	**0.005**** (0.002)		**0.005**** (0.002)
water.level.sd.lag2	**0.014**** (0.005)		**0.016**** (0.005)	**0.020**** (0.006)	**0.011*** (0.005)	**0.015**** (0.005)	**0.023***** (0.005)	**0.015**** (0.005)
water.temp.sd						0.248 (0.212)		
R^2	0.628	0.556	0.676	0.643	0.567	0.641	0.518	0.640
Adj. R^2	0.571	0.502	0.606	0.577	0.513	0.575	0.471	0.574
Num. obs.	46	47	46	46	46	46	46	46
MSE	0.541	0.577	0.519	0.537	0.577	0.539	0.601	0.539

$^{***}p < 0.001$, $^{**}p < 0.01$, $^{*}p < 0.05$

C Uncertainty models of remote sensing covariates

Error models fit to the errors between remote sensing estimates of precipitation and temperature and field measurements for the regionalization of the models of snail ecology.

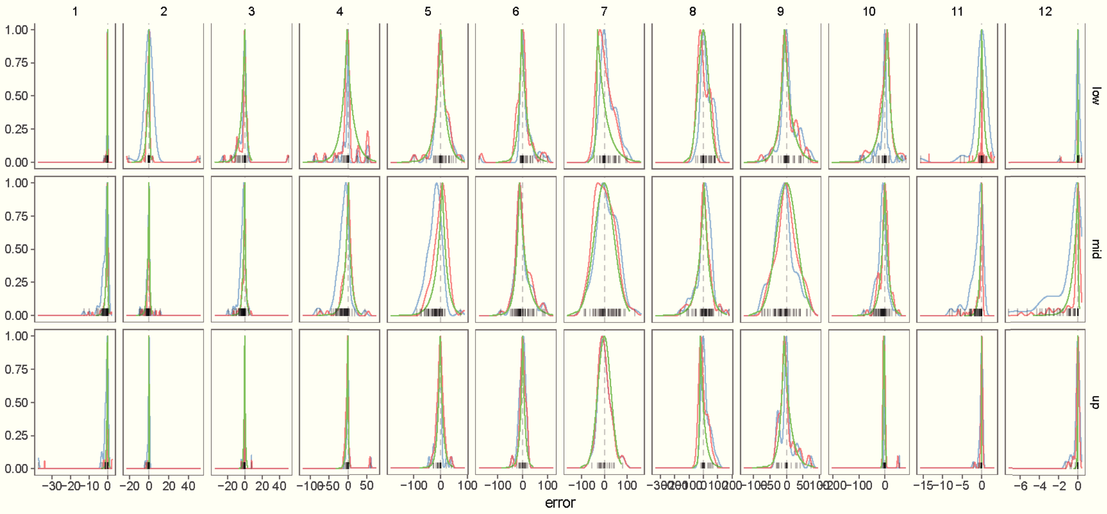

Figure C.1 – Error models of remote sensing precipitation estimates. The frequency distribution of the errors in the raw dataset (black ticks and blue density lines) are shown against the normalized density of the bias-corrected dataset (red), and best-fitting error model (blue, either the normal or ASL distributions), by latitude/precipitation zone (low ≈ latitude < 13, mid = 13 < latitude < 14, high = latitude > 14).

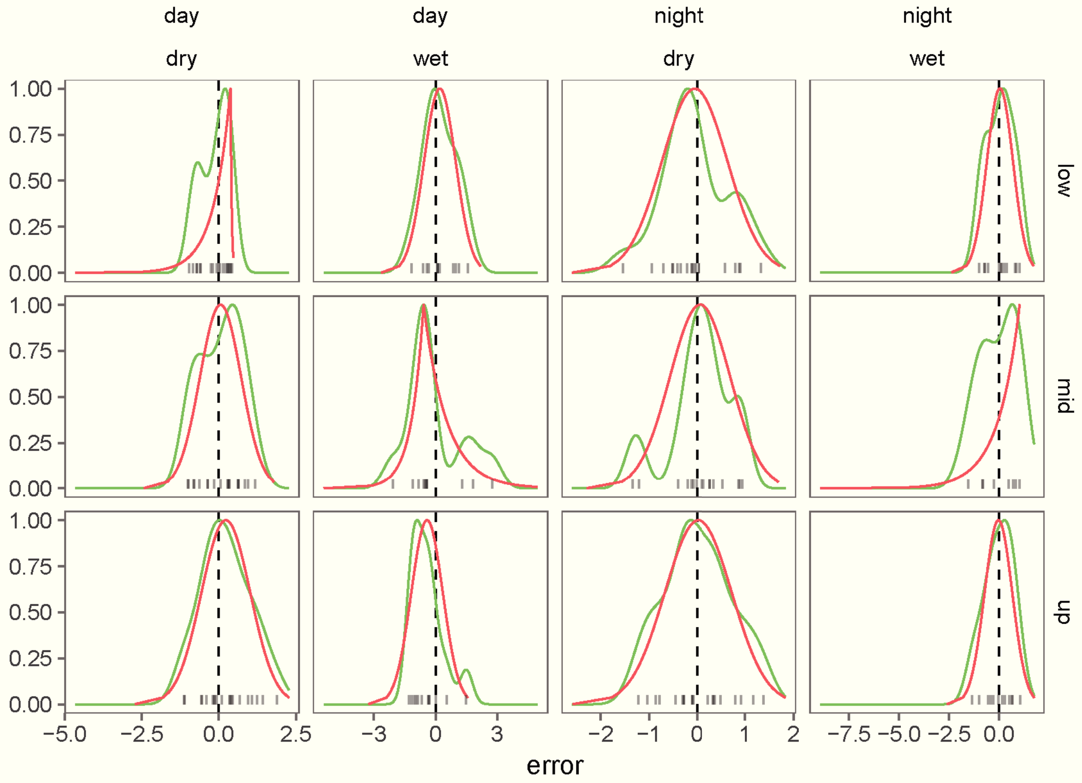

Figure C.2 – Error models of temperature regression estimates. The frequency distribution of the errors of the multivariate linear regression model (black ticks and green density lines) are shown against the best-fitting error model (red), by latitude zone (low = Panamasso, mid = Lioulgou, high = Tougou) and season (wet vs. dry).

Bibliography

Aagaard-Hansen, J., J. R. Mwanga, and B. Bruun. Social science perspectives on schistosomiasis control in Africa: past trends and future directions. *Parasitology*, 136(13):1747–58, 2009. doi: 10.1017/S0031182009006404.

Abdel-Wahab, M. F., A. Yosery, S. Narooz, G. Esmat, S. El Hak, S. Nasif, and G. T. Strickland. Is *Schistosoma mansoni* replacing *Schistosoma haematobium* in the Fayoum? *American Journal of Tropical Medicine and Hygiene*, 49(6): 697–700, 1993.

Abdelhak, S., J. Sulaiman, and S. Mohd. The missing link in understanding and assessing vulnerability to poverty: a conceptual framewwork. *Trends in Applied Sciences Research*, 7(4):256–272, 2012. doi: 10.3923/tasr.2012.

Ahmed, A. M., H. Abbas, F. A. Mansour, G. I. Gasim, and I. Adam. *Schistosoma haematobium* infections among schoolchildren in central Sudan one year after treatment with praziquantel. *Parasites & Vectors*, 5(1):108, 2012. doi: 10.1186/1756-3305-5-108.

Aiello-Lammens, M. E., R. A. Boria, A. Radosavljevic, B. Vilela, and R. P. Anderson. `spThin`: an R package for spatial thinning of species occurrence records for use in ecological niche models. *Ecography*, 38(5):541–545, 2015. doi: 10.1111/ecog.01132.

Akullian, A. N., D. Lu, J. Z. McDowell, G. M. Davis, R. C. Spear, and J. V. Remais. Modeling the combined influence of host dispersal and waterborne fate and transport on pathogen spread in complex landscapes. *Water Quality, Exposure, and Health*, 4(3):159–168, 2012. doi: 10.1007/s12403-012-0074-y.

Altizer, S., A. Dobson, P. Hosseini, P. Hudson, M. Pascual, and P. Rohani. Seasonality and the dynamics of infectious diseases. *Ecology Letters*, 9:467–484, 2006.

Amani, A., and M. Nguetora. Evidence d'une modification du regime hydrologique du fleuve Niger a Niamey. In Lanen, H. A. J. v., and F. Conference, editors, *FRIEND 2002: Regional Hydrology : Bridging the Gap Between Research and Practice*, number 274 in IAHS publication, page 449. International Assn of Hydrological Sciences, 2002. ISBN 1-901502-82-3.

Amitrano, D., F. Ciervo, G. Di Martino, M. N. Papa, A. Iodice, Y. Koussoube, F. Mitidieri, D. Riccio, and G. Ruello. Modeling watershed response in semiarid regions with high-resolution synthetic aperture radars. *IEEE Journal of Selected Topics in Applied Earth Observations and Remote Sensing*, 7(7):2732–2745, 2014.

Amitrano, D., G. Di Martino, A. Iodice, F. Mitidieri, M. N. Papa, D. Riccio, and G. Ruello. Water resource monitoring in semi-arid environment through the synergic use of sar data and hydrological models. In *Remote Sensing for Agriculture, Ecosystems, and Hydrology XVIII*, volume 9998, page 99980U. International Society for Optics and Photonics, 2016.

Amitrano, D., G. Di Martino, A. Iodice, F. Mitidieri, M. N. Papa, D. Riccio, and G. Ruello. Mapping small reservoirs in semi-arid regions using multitemporal sar: methods and applications. In *9th International Workshop on the Analysis of Multitemporal Remote Sensing Images (MultiTemp), 2017*, pages 1–4. IEEE, 2017.

Anderson, R., H. Turner, S. Farrell, J. Yang, and J. Truscott. What is required in terms of mass drug administration to interrupt the transmission of schistosome parasites in regions of endemic infection? *Parasites & Vectors*, 8(1):553, 2015. doi: 10.1186/s13071-015-1157-y.

Anderson, R. M. The role of mathematical models in helminth population biology. *International Journal of Parasitology*, 17(2):519–529, 1987. doi: 10.1016/0020-7519(87)90128-7.

Anderson, R. M., and R. M. May. Prevalence of schistosome infections within molluscan populations: observed patterns and theoretical predictions. *Parasitology*, 79(01):63–94, 1979. doi: 10.1017/S0031182000051982.

Anderson, R. M., and R. M. May. Helminth infections of humans: mathematical models, population dynamics, and control. *Advances in Parasitology*, 24:1–101, 1985.

Anderson, R. M., J. G. Mercer, R. A. Wilson, and N. P. Carter. Transmission of *Schistosoma mansoni* from man to snail: experimental studies of miracidial survival and infectivity in relation to larval age, water temperature, host size and host age. *Parasitology*, 85(02):339–360, 1982. doi: 10.1017/S0031182000055323.

Anderson, R. M., H. C. Turner, S. H. Farrell, and J. E. Truscott. Studies of the transmission dynamics, mathematical model development and the control of schistosome parasites by mass drug administration in human communities. *Advances in Parasitology*, 94:199–246, 2016. doi: 10.1016/bs.apar.2016.06.003.

Andreasen, V., and A. Pugliese. Pathogen coexistence induced by density-dependent host mortality. *Journal of Theoretical Biology*, 177(2):159–166, 1995.

Appleton, C. C. The influence of stream geology on the distribution of the bilharzia host snails, *Biomphalaria pfeifferi* and *Bulinus (Physopsis) sp.* *Annals of Tropical Medicine and Parasitology*, 69(2):241–255, 1975. doi: 10.1080/00034983.1975.11687007.

Appleton, C. C., S. M. Ngxongo, L. E. Braack, and D. le Sueur. *Schistosoma mansoni* in migrants entering South Africa from Moçambique – a threat to public health in north-eastern KwaZulu-Natal? *South African Medical Journal*, 86 (4):350–353, 1996.

Appleton, C. C., W. N. Ellery, J. Byskov, and S. S. Mogkweetsinyana. Epidemic transmission of intestinal schistosomiasis in the seasonal part of the Okavango Delta, Botswana. *Annals of Tropical Medicine and Parasitology*, 102(7):611–623, 2008. doi: 10.1179/136485908X311867.

Arumugam, M., J. Raes, E. Pelletier, D. Le Paslier, T. Yamada, D. R. Mende, G. R. Fernandes, J. Tap, T. Bruls, J.-M. Batto, et al. Enterotypes of the human gut microbiome. *Nature*, 473(7346):174–180, 2011. doi: 10.1038/nature09944.

Asaolu, S., and I. Ofoezie. The role of health education and sanitation in the control of helminth infections. *Acta Tropica*, 86(2-3):283–294, 2003. doi: 10.1016/S0001-706X(03)00060-3.

Ashouri, H., K.-L. Hsu, S. Sorooshian, D. K. Braithwaite, K. R. Knapp, L. D. Cecil, B. R. Nelson, and O. P. Prat. PERSIANN-CDR: daily precipitation climate data record from multisatellite observations for hydrological and climate studies. *Bulletin of the American Meteorological Society*, 96(1):69–83, 2015. doi: 10.1175/BAMS-D-13-00068.1.

Auger, P., S. Charles, M. Viala, and J.-C. Poggiale. Aggregation and emergence in ecological modelling: integration of ecological levels. *Ecological Modelling*, 127(1):11–20, 2000. doi: 10.1016/S0304-3800(99)00201-X.

Augusto, G., P. Magnussen, T. K. Kristensen, C. C. Appleton, and B. J. Vennervald. The influence of transmission season on parasitological cure rates and intensity of infection after praziquantel treatment of *Schistosoma haematobium*-infected schoolchildren in Mozambique. *Parasitology*, 136(13):1771–1779, 2009. doi: 10.1017/S0031182009006210.

Ayantunde, A., M. Karambiri, V. Yameogo, and O. O. Cofie. *Multiple uses of small reservoirs in crop-livestock agro-ecosystems of the Volta River Basin with an emphasis on livestock management.* International Water Management Institute (IWMI), 2017.

Babak, O., and C. V. Deutsch. Statistical approach to inverse distance interpolation. *Stochastic Environmental Research and Risk Assessment*, 23(5):543–553, 2009.

Baddeley, A., R. Turner, and Others. Spatstat: an R package for analyzing spatial point patterns. *Journal of Statistical Software*, 12(6):1–42, 2005.

Baddeley, A., P. J. Diggle, A. Hardegen, T. Lawrence, R. K. Milne, and G. Nair. On tests of spatial pattern based on simulation envelopes. *Ecological Monographs*, 84(3):477–489, 2014. doi: 10.1890/13-2042.1.

Badger, L. I., and J. P. O. Oyerinde. *Schistosoma mansoni* : effect of aestivation on the intra-molluscan stages and the survival rate of infected *Biomphalaria pfeifferi*. *Annals of Tropical Medicine and Parasitology*, 90(6):617–620, 1996. doi: 10.1080/00034983.1996.11813091.

Barbier, B., H. Yacouba, H. Karambiri, M. Zoromé, and B. Somé. Human vulnerability to climate variability in the Sahel: farmers' adaptation strategies in northern Burkina Faso. *Environmental Management*, 43(5):790–803, 2009. doi: 10.1007/s00267-008-9237-9.

Barbour, A. D. A stochastic model for the transmission of bilharzia. *Mathematical Biosciences*, 38(3):303–312, 1976. doi: 10.1016/0025-5564(78)90051-2.

Barbour, A. D. Macdonald's model and the transmission of bilharzia. *Transactions of the Royal Society of Tropical Medicine and Hygiene*, 72(1):6–15, 1978. doi: 10.1016/0035-9203(78)90290-0.

Barbour, A. D. Modeling the transmission of schistosomiasis: an introductory view. *American Journal of Tropical Medicine and Hygiene*, 55(5_Suppl):135–143, 1996.

Bärenbold, O., G. Raso, J. T. Coulibaly, E. K. N'Goran, J. Utzinger, and P. Vounatsou. Estimating sensitivity of the Kato-Katz technique for the diagnosis of *Schistosoma mansoni* and hookworm in relation to infection intensity. *PLoS Neglected Tropical Diseases*, 11(10):e0005953, 2017.

Basáñez, M.-G., J. S. McCarthy, M. D. French, G.-J. Yang, M. Walker, M. Gambhir, R. K. Prichard, and T. S. Churcher. A research agenda for helminth diseases of humans: Modelling for control and elimination. *PLoS Neglected Tropical Diseases*, 6(4):e1548, 2012. doi: 10.1371/journal.pntd.0001548.

Bella, H., T. de C. Marshall, A. Omer, and J. Vaughan. Migrant workers and schistosomiasis in the Gezira, Sudan. *Transactions of the Royal Society of Tropical Medicine and Hygiene*, 74(1):36–39, 1980. doi: 10.1016/0035-9203(80)90008-5.

Bergquist, R., and D. P. McManus. Schistosomiasis vaccine development: the missing link. *Schistosoma: Biology, Pathology and Control*, page 462, 2017.

Bergquist, R., G.-J. Yang, S. Knopp, J. Utzinger, and M. Tanner. Surveillance and response: Tools and approaches for the elimination stage of neglected tropical diseases. *Acta Tropica*, 141(Pt B):229–34, 2015. doi: 10.1016/j.actatropica.2014.09.017.

Bergquist, R., N. W. Brattig, M. J. Chimbari, J. Zinsstag, and J. Utzinger. Ecohealth research in africa: where from-where to? *Acta Tropica*, 175:1–8, 2017. ISSN 0001-706X. doi: https://doi.org/10.1016/j.actatropica.2017.07.015. URL http://www.sciencedirect.com/science/article/pii/S0001706X17308598. Ecohealth: An African Perspective.

Berhanu, B., Y. Seleshi, S. S. Demisse, and A. M. Melesse. Flow regime classification and hydrological characterization: A case study of Ethiopian rivers. *Water*, 7(6):3149–3165, 2015. doi: 10.3390/w7063149.

Bertuzzo, E., A. Maritan, M. Gatto, I. Rodriguez-Iturbe, and A. Rinaldo. River networks and ecological corridors: Reactive transport on fractals, migration fronts, hydrochory. *Water Resources Research*, 43(4):n/a–n/a, 2007. doi: 10.1029/2006WR005533. W04419.

Bertuzzo, E., M. Gatto, A. Maritan, I. Rodriguez-Iturbe, and A. Rinaldo. On the space-time evolution of a cholera epidemic. *Water Resources Research*, 44(1):W01424, 2008.

Bertuzzo, E., R. Casagrandi, M. Gatto, I. Rodriguez-Iturbe, and A. Rinaldo. On spatially explicit models of cholera epidemics. *Journal of the Royal Society Interface*, 7(43):321–333, 2010. doi: 10.1098/rsif.2009.0204.

Bertuzzo, E., L. Mari, L. Righetto, M. Gatto, R. Casagrandi, M. Blokesch, I. Rodriguez-Iturbe, and A. Rinaldo. Prediction of the spatial evolution and effects of control measures for the unfolding Haiti cholera outbreak. *Geophysical Research Letters*, 38(6), 2011. doi: 10.1029/2011GL046823.

Betson, M., J. C. Sousa-Figueiredo, N. B. Kabatereine, and J. R. Stothard. New insights into the molecular epidemiology and population genetics of *schistosoma mansoni* in ugandan pre-school children and mothers. *PLoS Neglected Tropical Diseases*, 7(12), 2013. doi: 10.1371/journal.pntd.0002561.

Bhaduri, B., E. Bright, P. Coleman, and M. L. Urban. LandScan USA: a high-resolution geospatial and temporal modeling approach for population distribution and dynamics. *GeoJournal*, 69(1-2):103–117, 2007. doi: 10.1007/s10708-007-9105-9.

Bieri, F. A., D. J. Gray, G. M. Williams, G. Raso, Y.-S. Li, L. Yuan, Y. He, R. S. Li, F.-Y. Guo, S.-M. Li, et al. Health-education package to prevent worm infections in Chinese schoolchildren. *New England Journal of Medicine*, 368(17):1603–1612, 2013.

Bilharz, T. Further observations concerning *Distomum haematobium* in the portal vein of man and its relationship to certain pathological formations with brief notes by seibald. *Zeitschrift für wissenschaftliche Zoologie*, 4:72, 1853.

Boelee, E., and H. Madsen. *Irrigation and Schistosomiasis in Africa: Ecological Aspects*. International Water Management Institute (IWMI), Colombo, Sri Lanka: International Water Management Institute., 2006. ISBN 9789290906315. 39p . (IWMI Research Report 99).

Boelee, E., P. Cecchi, and A. Koné. *Health impacts of small reservoirs in Burkina Faso*. International Water Management Institute (IWMI), 2009. ISBN 9290907177.

Bomblies, A., and E. A. B. Eltahir. Assessment of the impact of climate shifts on malaria transmission in the sahel. *EcoHealth*, 6(3):426–437, 2009. doi: 10.1007/s10393-010-0274-5.

Bomblies, A., J.-B. Duchemin, and E. A. B. Eltahir. Hydrology of malaria: Model development and application to a sahelian village. *Water Resources Research*, 44(12):n/a–n/a, 2008. doi: 10.1029/2008WR006917.

Botter, G., A. Porporato, E. Daly, I. Rodriguez-Iturbe, and A. Rinaldo. Probabilistic characterization of base flows in river basins: roles of soil, vegetation, and geomorphology. *Water Resources Research*, 43(6):n/a–n/a, 2007. doi: 10.1029/2006WR005397. W06404.

Brook, B. W., and C. J. A. Bradshaw. Strength of evidence for density dependence in abundance time series of 1198 species. *Ecology*, 87(6):1445–1451, 2006. doi: 10.1890/0012-9658(2006)87[1445:SOEFDD]2.0.CO;2.

Brooker, S. Schistosomes, snails and satellites. *Acta Tropica*, 82(2):207–214, 2002. doi: 10.1016/S0001-706X(02)00012-8.

Brooker, S., S. I. Hay, and D. A. Bundy. Tools from ecology: useful for evaluating infection risk models? *Trends in Parasitology*, 18(2):70–74, 2002. doi: 10.1016/S1471-4922(01)02223-1.

Brown, D. *Freshwater snails of Africa and their medical importance*. Taylor & Francis, London, UK, 1980.

Brown, D. *Freshwater snails of Africa and their medical importance*. Taylor and Francis, London, UK, 1994. 2nd edition.

Brown, K. M., K. R. Carman, and V. Inchausty. Density-dependent influences on feeding and metabolism in a freshwater snail. *Oecologia*, 99(1-2):158–165, 1994. doi: 10.1007/BF00317097.

Bruun, B., and J. Aagaard-Hansen. *The social context of schistosomiasis and its control: an introduction and annotated bibliography*. World Health Organization, 2008. ISBN 978-92-4-159718-0.

Buckee, C. O., A. Wesolowski, N. N. Eagle, E. Hansen, and R. W. Snow. Mobile phones and malaria: modeling human and parasite travel. *Travel Medicine and Infectious Disease*, 11(1):15–22, 2013. doi: 10.1016/j.tmaid.2012.12.003.

Budyko, M. I. M. I., and D. H. Miller. *Climate and life*. Academic Press, 1974. ISBN 9780121394509.

Bundy, D. A. P., U. J. Blumenthal, C. J. Barnard, and J. M. Behnke. *Parasitism and Host Behaviour*, chapter Human behaviour and the epidemiology of helminth infections: the role of behaviour in exposure to infection., pages 264–289. Taylor & Francis Ltd, 1990. ISBN 0-85066-490-5.

Burnham, K. P., and D. R. Anderson. *Model selection and multimodel inference: a practical information-theoretic approach*. Springer Science & Business Media, 2002.

Bustinduy, A., C. King, J. Scott, S. Appleton, J. C. Sousa-Figueiredo, M. Betson, and J. R. Stothard. HIV and schistosomiasis co-infection in African children. *Lancet Infectious Diseases*, 14(7):640–9, 2014. doi: 10.1016/S1473-3099(14)70001-5.

Bustinduy, A. L., J. R. Stothard, and J. F. Friedman. Paediatric and maternal schistosomiasis: shifting the paradigms. *British medical bulletin*, pages 1–11, 2017.

Cable, J., I. Barber, B. Boag, A. R. Ellison, E. R. Morgan, K. Murray, E. L. Pascoe, S. M. Sait, A. J. Wilson, and M. Booth. Global change, parasite transmission and disease control: lessons from ecology. *Philosophical Transactions of the Royal Society of London B: Biological Sciences*, 372(1719):20160088, 2017.

Campbell, S. J., N.-K. Biritwum, G. Woods, Y. Velleman, F. Fleming, and J. R. Stothard. Tailoring water, sanitation, and hygiene (WASH) targets for soil-transmitted helminthiasis and schistosomiasis control. *Trends in Parasitology*, xx: 1–11, 2017. doi: 10.1016/j.pt.2017.09.004.

Cao, C.-l., Z.-p. Bao, S.-z. Li, W.-y. Wei, P. Yi, Q. Yu, H.-q. Zhu, J. Xu, J.-g. Guo, and Z. Feng. Schistosomiasis in a migrating population in the lake region of china and its potential impact on control operation. *Acta Tropica*, 145: 88–92, 2015.

Carraro, L., E. Bertuzzo, L. Mari, I. Fontes, H. Hartikainen, N. Strepparava, H. Schmidt-Posthaus, T. Wahli, J. Jokela, M. Gatto, et al. Integrated field, laboratory, and theoretical study of PKD spread in a Swiss prealpine river. *Proceedings of the National Academy of Sciences of the United States of America of the United States of America*, 114 (45):11992–11997, 2017.

Cecchi, P. *L'eau en partage*. Institut de Rercherche pour le Développement (IRD), 2007. ISBN 978-2-7099-1615-8.

Cecchi, P., A. Meunier-Nikiema, N. Moiroux, B. Sanou, and F. Bougaire. Why an atlas of lakes and reservoirs in Burkina Faso? Technical Report iii, Small Reservoirs Project, 2007.

Ceperley, N. C. *Ecohydrology of a Mixed Savanna-Agricultural Catchment in South-East Burkina Faso, West Africa*. PhD thesis, Ecole Polytechnique Fédérale de Lausanne, Switzerland, 2014.

Ceperley, N. C., T. Mande, N. van de Giesen, S. Tyler, H. Yacouba, and M. B. Parlange. Evaporation from cultivated and semi–wild Sudanian Savanna in west Africa. *Hydrology and Earth System Sciences*, 21:4149–4167, 2017. doi: 10.5194/hess-21-4149-2017.

Cetron, M. S., L. Chitsulo, J. J. Sullivan, J. Pilcher, M. Wilson, J. Noh, V. C. Tsang, A. W. Hightower, and D. G. Addiss. Schistosomiasis in Lake Malawi. *Lancet*, 348(9037):1274–1278, 1996. doi: 10.1016/S0140-6736(96)01511-5.

Chambers, R. The origins and practice of participatory rural appraisal. *World development*, 22(7):953–969, 1994.

Chan, M. S., H. L. Guyatt, D. A. P. Bundy, M. Booth, A. J. C. Fulford, and G. F. Medley. The development of an age structured model for schistosomiasis transmission dynamics and control and its validation for *Schistosoma mansoni*. *Epidemiology and Infection*, 115(02):325, 1995. doi: 10.1017/S0950268800058453.

Chandiwana, S. How *Schistosoma mansoni* eggs reach natural waterbodies. *Transactions of the Royal Society of Tropical Medicine and Hygiene*, 80(6):963–964, 1986. doi: 10.1016/0035-9203(86)90273-7.

Chandiwana, S. K. Community water-contact patterns and the transmission of *Schistosoma haematobium* in the highveld region of Zimbabwe. *Social Science and Medicine*, 25(5):495–505, 1987. doi: 10.1016/0277-9536(87) 90173-0.

Chandiwana, S. K., and M. E. Woolhouse. Heterogeneities in water contact patterns and the epidemiology of *Schistosoma haematobium*. *Parasitology*, 103(3):363–370, 1991. doi: 10.1017/S0031182000059874.

Chao, D. L., M. E. Halloran, and I. M. Longini. Vaccination strategies for epidemic cholera in Haiti with implications for the developing world. *Proceedings of the National Academy of Sciences of the United States of America*, 108(17): 7081–7085, 2011. doi: 10.1073/pnas.1102149108.

Cheema, M. J. M., and W. G. Bastiaanssen. Local calibration of remotely sensed rainfall from the TRMM satellite for different periods and spatial scales in the Indus Basin. *International Journal of Remote Sensing*, 33(8):2603–2627, 2012. doi: 10.1080/01431161.2011.617397.

Chen, T., and C. Guestrin. Xgboost: A scalable tree boosting system. In *Proceedings of the 22Nd ACM SIGKDD International Conference on Knowledge Discovery and Data Mining*, pages 785–794. ACM, 2016. doi: 10.1145/ 2939672.2939785.

Chen, T., T. He, M. Benesty, V. Khotilovich, and Y. Tang. `xgboost`*: Extreme Gradient Boosting*, 2017. R package version 0.6-4.

Chiyaka, E. T., and W. Garira. Mathematical analysis of the transmission dynamics of schistosomiasis in the human-snail. *Journal of Biological Systems*, 17(03):397–423, 2009. doi: 10.1142/S0218339009002910.

Chlyeh, G., P.-Y. Henry, P. Sourouille, B. Delay, K. Kahalaayoune, and P. Jarne. Population genetics and dynamics at short spatial scale in *Bulinus truncatus*, the intermediate host of *Schistosoma haematobium*, in Morocco. *Parasitology*, 125(4):349–357, 2002. doi: 10.1017/S0031182002002123.

Choi, B. C. K. The past, present, and future of public health surveillance. *Scientifica*, 2012:e875253, 2012. doi: 10.6064/2012/875253.

Chongsuvivatwong, V. `epiDisplay`*: Epidemiological Data Display Package*, 2015. R package version 3.2.2.0.

Ciddio, M., L. Mari, M. Gatto, A. Rinaldo, and R. Casagrandi. The temporal patterns of disease severity and prevalence in schistosomiasis. *Chaos: An Interdisciplinary Journal of Nonlinear Science*, 25(3):036405, 2015.

Ciddio, M., L. Mari, S. H. Sokolow, G. A. De Leo, R. Casagrandi, and M. Gatto. The spatial spread of schistosomiasis: A multidimensional network model applied to Saint-Louis region, Senegal. *Advances in Water Resources*, 0:1–10, 2016. doi: 10.1016/j.advwatres.2016.10.012.

Claeskens, G., N. L. Hjort, et al. *Model selection and model averaging*, volume 330. Cambridge University Press Cambridge, 2008.

Clennon, J. A., P. L. Mungai, E. M. Muchiri, C. H. King, and U. Kirton. Spatial and temporal variations in local transmission of *Schistosoma haematobium* in Msambweni, Kenya. *American Journal of Tropical Medicine and Hygiene*, 75(6):1034–1041, 2006.

Clennon, J. A., C. H. King, E. M. Muchiri, and U. Kitron. Hydrological modelling of snail dispersal patterns in Msambweni, Kenya and potential resurgence of *Schistosoma haematobium* transmission. *Parasitology*, 134(Pt 5): 683–93, 2007. doi: 10.1017/S0031182006001594.

Colette, J., B. Sellin, G. Garrigue, and E. Simonkovich. Etude épidémiologique de la substitution de *Schistosoma haemobium* par *Schistosoma mansoni* dans une zone d'endémie bilharzienne d'Afrique de l'Ouest (Haute-Volta). *Médecine et Santé Tropicales*, 42(3):289–296, 1982.

Colley, D. G., A. L. Bustinduy, W. E. Secor, and C. H. King. Human schistosomiasis. *Lancet*, 383(9936):2253–2264, 2014. doi: 10.1016/S0140-6736(13)61949-2.

Compaoré, G., and I. Kaboré. Gestion urbaine et environnement: l'exemple de Ouagadougou (Burkina Faso). *Villes du Sud et Environnement*, pages 80–99, 1997.

Corani, G., and M. Gatto. Structural risk minimization: a robust method for density-dependence detection and model selection. *Ecography*, 30(3):400–416, 2007. doi: 10.1111/j.2007.0906-7590.04863.x.

Costigan, K. H., K. L. Jaeger, C. W. Goss, K. M. Fritz, and P. C. Goebel. Understanding controls on flow permanence in intermittent rivers to aid ecological research: integrating meteorology, geology and land cover. *Ecohydrology*, 1153 (February):1141–1153, 2016. doi: 10.1002/eco.1712.

Cridland, C. C. Ecological factors affecting the numbers of snails in temporary bodies of water. *Journal of Tropical Medicine and Hygiene*, 60(12):287–93, 1957.

Cridland, C. C. Ecological factors affecting the numbers of snails in a permanent stream. *Journal of Tropical Medicine and Hygiene*, 61(1):16–20, 1958.

Criscione, C. D., J. D. Anderson, D. Sudimack, J. Subedi, R. P. Upadhayay, B. Jha, K. D. Williams, S. Williams-Blangero, and T. J. C. Anderson. Landscape genetics reveals focal transmission of a human macroparasite. *PLoS Neglected Tropical Diseases*, 4(4):e665, 2010. doi: 10.1371/journal.pntd.0000665.

Cunin, P., A. Griffet, B. Poste, K. Djibrilla, and P. M. V. Martin. Epidemic *Schistosoma mansoni* in a known *S. haematobium* area. *Transactions of the Royal Society of Tropical Medicine and Hygiene*, 94(6):657–660, 2000.

Dalton, P. R. A socioecological approach to the control of *Schistosoma mansoni* in St Lucia. *Bulletin of the World Health Organization*, 54(5):587–95, 1976.

D'Ambrosio, E., A. M. De Girolamo, E. Barca, P. Ielpo, and M. C. Rulli. Characterising the hydrological regime of an ungauged temporary river system: a case study. *Environmental Science and Pollution Research*, pages 1–17, 2016. doi: 10.1007/s11356-016-7169-0.

Danso-Appiah, A., and S. J. de Vlas. Interpreting low praziquantel cure rates of *Schistosoma mansoni* infections in Senegal. *Trends in Parasitology*, 18(3):125–129, 2002.

Datry, T., S. T. Larned, and K. Tockner. Intermittent rivers: a challenge for freshwater ecology. *BioScience*, 64(3): 229–235, 2014. doi: 10.1093/biosci/bit027.

Davies, C. M., J. P. Webster, O. Krüger, A. Munatsi, J. Ndamba, and M. E. J. Woolhouse. Host-parasite population genetics: a cross-sectional comparison of *Bulinus globosus* and *Schistosoma haematobium*. *Parasitology*, 119(03): 295–302, 1999.

Dazo, B. C., N. G. Hairston, and I. K. Dawood. The ecology of *Bulinus truncatus* and *Biomphalaria alexandrina* and its implications for the control of bilharziasis in the Egypt-49 project area. *Bulletin of the World Health Organization*, 35(3):339–56, 1966.

De Longueville, F., Y.-C. Hountondji, I. Kindo, F. Gemenne, and P. Ozer. Long-term analysis of rainfall and temperature data in Burkina Faso (1950-2013). *International Journal of Climatology*, 36(13):4393–4405, 2016. doi: 10.1002/joc.4640.

de Moira, A. P., A. J. C. Fulford, N. B. Kabatereine, J. H. Ouma, M. Booth, and D. W. Dunne. Analysis of complex patterns of human exposure and immunity to *Schistosomiasis mansoni*: the influence of age, sex, ethnicity and IgE. *PLoS Neglected Tropical Diseases*, 4(9), 2010. doi: 10.1371/journal.pntd.0000820.

De Oliveira Duarte, H., E. L. Droguett, M. d. C. Moura, E. C. de Souza Gomes, C. Barbosa, V. Barbosa, and M. Araújo. An ecological model for quantitative risk assessment for schistosomiasis: The case of a patchy environment in the coastal tropical area of Northeastern Brazil. *Risk Analysis*, 34(5):831–846, 2014. doi: 10.1111/risa.12139.

de Vlas, S. J. *Modelling human Schistosoma mansoni infection : the art of counting eggs in faeces.* PhD thesis, Erasmus Universiteit Rotterdam, 1996.

Dejong, R. J., J. A. T. Morgan, W. L. Paraense, J.-p. Pointier, M. Amarista, P. F. K. Ayeh-kumi, A. Babiker, S. Barbosa, P. Canese, C. P. D. Souza, C. Dominguez, S. File, A. Gutierrez, R. N. Incani, T. Kawano, F. Kazibwe, J. Kpikpi, N. J. S. Lwambo, R. Mimpfoundi, F. Njiokou, J. Noe, M. Sene, M. Yong, C. M. Adema, B. V. Hofkin, G. M. Mkoji, and E. S. Loker. Evolutionary relationships and biogeography of *Biomphalaria* (Gastropoda: Planorbidae) with implications regarding its role as host of the human bloodfluke, *Schistosoma mansoni*. *Molecular Biology and Evolution*, pages 2225–2239, 2001.

Delgado, J. C., A. Baena, S. Thim, and A. E. Goldfeld. Ethnic-specific genetic associations with pulmonary tuberculosis. *Journal of Infectious Diseases*, 186(10):1463–1468, 2002.

Dembélé, M., and S. J. Zwart. Evaluation and comparison of satellite-based rainfall products in burkina faso, west africa. *International Journal of Remote Sensing*, 37(17):3995–4014, 2016.

Dennis, B., and M. L. Taper. Density dependence in time series observations of natural populations: estimation and testing. *Ecological Monographs*, 64(2):205–224, 1994.

Descroix, L., G. Mahé, T. Lebel, G. Favreau, S. Galle, E. Gautier, J. C. Olivry, J. Albergel, O. Amogu, B. Cappelaere, R. Dessouassi, A. Diedhiou, E. Le Breton, I. Mamadou, and D. Sighomnou. Spatio-temporal variability of hydrological regimes around the boundaries between Sahelian and Sudanian areas of West Africa: a synthesis. *Journal of Hydrology*, 375(1-2):90–102, 2009. doi: 10.1016/j.jhydrol.2008.12.012.

Diakité, N. R., M. S. Winkler, J. T. Coulibaly, N. Guindo-Coulibaly, J. Utzinger, and E. K. N'Goran. Dynamics of freshwater snails and *Schistosoma* infection prevalence in schoolchildren during the construction and operation of a multipurpose dam in central Côte d'Ivoire. *Infectious Diseases of Poverty*, 6(1):93, 2017.

Diamond, J. M. Biogeographic kinetics: estimation of relaxation times for avifaunas of southwest Pacific islands. *Proceedings of the National Academy of Sciences of the United States of America*, 69(11):3199–3203, 1972.

Diboulo, E., A. Sié, D. A. Diadier, D. A. K. Voules, Y. Yé, and P. Vounatsou. Bayesian variable selection in modelling geographical heterogeneity in malaria transmission from sparse data: an application to Nouna Health and Demographic Surveillance System (HDSS) data, Burkina Faso. *Parasites & Vectors*, 8(1):118, 2015.

Diémé, J. S., M. Diouf, C. Armas, G. M. Rusch, and F. I. Pugnaire. Functional groups of Sahelian trees in a semiarid agroforestry system of Senegal. *Journal of Plant Ecology*, page rtw140, 2017. doi: 10.1093/jpe/rtw140.

D'Odorico, P., F. Laio, A. Porporato, L. Ridolfi, A. Rinaldo, and I. Rodriguez-Iturbe. Ecohydrology of terrestrial ecosystems. *BioScience*, 60(11):898–907, 2010. doi: 10.1525/bio.2010.60.11.6.

Doenhoff, M. J., D. Cioli, and J. Utzinger. Praziquantel: mechanisms of action, resistance and new derivatives for schistosomiasis. *Current Opinion in Infectious Diseases*, 21(6):659–667, 2008.

Donohue, R., M. Roderick, and T. R. McVicar. Can dynamic vegetation information improve the accuracy of Budyko's hydrological model? *Journal of Hydrology*, 390(1):23–34, 2010. doi: 10.1016/j.jhydrol.2010.06.025.

Donohue, R. J., M. L. Roderick, and T. R. Mcvicar. On the importance of including vegetation dynamics in Budyko's hydrological model. *Hydrology and Earth System Sciences*, 3(4):1517–1551, 2006. doi: 10.5194/hess-11-983-2007.

Efron, B. *The Jackknife, the Bootstrap and other Resampling Plans*, volume 38. SIAM, 1982.

Egesa, M., K. F. Hoffmann, C. H. Hokke, M. Yazdanbakhsh, and S. Cose. Rethinking schistosomiasis vaccine development: Synthetic vesicles. *Trends in Parasitology*, 2017. doi: 10.1016/j.pt.2017.07.007.

Eisen, L., and S. Lozano-Fuentes. Use of mapping and spatial and space-time modeling approaches in operational control of *aedes aegypti* and dengue. *PLoS Neglected Tropical Diseases*, 3(4):e411, 2009. doi: 10.1371/journal.pntd.0000411.

Eisenberg, J. N. S., M. A. Desai, K. Levy, S. J. Bates, S. Liang, K. Naumoff, and J. C. Scott. Environmental determinants of infectious disease: a framework for tracking causal links and guiding public health research. *Environmental Health Perspectives*, 115:1216–1223, 2007.

Elith, J., S. J. Phillips, T. Hastie, M. Dudík, Y. E. Chee, and C. J. Yates. A statistical explanation of MaxEnt for ecologists. *Diversity and Distributions*, 17(1):43–57, 2011. doi: 10.1111/j.1472-4642.2010.00725.x.

Engels, D., L. Chitsulo, A. Montresor, and L. Savioli. The global epidemiological situation of schistosomiasis and new approaches to control and research. *Acta Tropica*, 82(2):139–146, 2002.

Ernould, J.-C. *Epidémiologie des schistosomoses humaines dans le delta du fleuve Sénégal : phénomène récent de compétition entre Schistosoma haematobium Sambon, 1907 et S. mansoni (Bilharz, 1852).* PhD thesis, Université Paris 12 : Val de Marne, 1996.

Ernould, J. C., A. Kaman, R. Labbo, D. Couret, and J. P. Chippaux. Recent urban growth and urinary schistosomiasis in Niamey, Niger. *Tropical Medicine and International Health*, 5(6):431–437, 2000. doi: 10.1046/j.1365-3156.2000.00577.x.

Esch, G. W., L. a. Curtis, and M. a. Barger. A perspective on the ecology of trematode communities in snails. *Parasitology*, 123(2001):57–75, 2001. doi: 10.1017/S0031182001007697.

Essé, C., V. A. Koffi, A. Kouamé, K. Dongo, R. B. Yapi, H. M. Moro, C. A. Kouakou, M. S. Palmeirim, B. Bonfoh, E. K. N'Goran, J. Utzinger, and G. Raso. "Koko et les lunettes magiques": an educational entertainment tool to prevent parasitic worms and diarrheal diseases in Côte d'Ivoire. *PLoS Neglected Tropical Diseases*, 11(9):e0005839, 2017. doi: 10.1371/journal.pntd.0005839.

Fagan, W. F. Connectivity, fragmentation, and extinction risk in dendritic metapopulations. *Ecology*, 83(12):3243–3249, 2002.

Falkenmark, M., and J. Rockström. Building resilience to drought in desertification-prone savannas in Sub-Saharan Africa: the water perspective. *Natural Resources Forum*, 32(2):93–102, 2008. doi: 10.1111/j.1477-8947.2008.00177.x.

Farina, L., and S. Rinaldi. *Positive linear systems: theory and applications*, volume 50. John Wiley & Sons, 2011.

Feng, Y., L. Liu, S. Xia, J. F. Xu, R. Bergquist, and G. J. Yang. Reaching the surveillance-response stage of schistosomiasis control in The People's Republic of China: a modelling approach. *Advances in Parasitology*, 92:165–196, 2016. doi: 10.1016/bs.apar.2016.02.006.

Feng, Z., C.-C. Li, and F. A. Milner. Schistosomiasis models with density dependence and age of infection in snail dynamics. *Mathematical Biosciences*, 177-178:271–286, 2002. doi: 10.1016/S0025-5564(01)00115-8.

Feng, Z., A. Eppert, F. A. Milner, and D. J. Minchella. Estimation of parameters governing the transmission dynamics of schistosomes. *Applied Mathematics Letters*, 17(10):1105–1112, 2004. doi: 10.1016/j.aml.2004.02.002.

Fenwick, A., L. Savioli, D. Engels, N. R. Bergquist, and M. H. Todd. Drugs for the control of parasitic diseases: current status and development in schistosomiasis. *Trends in Parasitology*, 19(11):509–515, 2003. doi: 10.1016/j.pt.2003.09.005.

Fenwick, A., D. Rollinson, and V. Southgate. Implementation of human schistosomiasis control: challenges and prospects. *Advances in Parasitology*, 61:567–622, 2006. doi: 10.1016/S0065-308X(05)61013-5.

Fick, S. E., and R. J. Hijmans. Worldclim 2: new 1-km spatial resolution climate surfaces for global land areas. *International Journal of Climatology*, 2017.

Finger, F. *Spatially explicit modeling of cholera epidemics.* PhD thesis, Ecole Polytechnique Fédérale de Lausanne - ENAC, Lausanne, 2017.

Finger, F., A. Knox, E. Bertuzzo, L. Mari, D. Bompangue, M. Gatto, I. Rodriguez-Iturbe, and A. Rinaldo. Cholera in the lake kivu region (drc): Integrating remote sensing and spatially explicit epidemiological modeling. *Water Resources Research*, pages 5624–5637, 2014. doi: 10.1002/2014WR015521.

Forsythe, W. C., E. J. Rykiel, R. S. Stahl, H.-i. Wu, and R. M. Schoolfield. A model comparison for daylength as a function of latitude and day of year. *Ecological Modelling*, 80(1):87–95, 1995.

French, M. D., T. S. Churcher, J. P. Webster, F. M. Fleming, A. Fenwick, N. B. Kabatereine, M. Sacko, A. Garba, S. Toure, U. Nyandindi, J. Mwansa, L. Blair, E. Bosqué-Oliva, and M.-G. Basáñez. Estimation of changes in the force of infection for intestinal and urogenital schistosomiasis in countries with schistosomiasis control initiative-assisted programmes. *Parasites & Vectors*, 8(1):558, 2015. doi: 10.1186/s13071-015-1138-1.

Fryer, S. E., and A. J. Probert. The cercarial output from three Nigerian bulinids infected with two strains of *Schistosoma haematobium*. *Journal of Helminthology*, 62(2):133–40, 1988. doi: 10.1017/S0022149X00011378.

Fu, B. On the calculation of the evaporation from land surface. *Scientia Atmospherica Sinica*, 5(1):23–31, 1981.

Fulford, A. J. C., A. E. Butterworth, J. H. Ouma, and R. F. Sturrock. A statistical approach to schistosome population dynamics and estimation of the life-span of *Schistosoma mansoni* in man. *Parasitology*, 110(03):307, 1995. doi: 10.1017/S0031182000080896.

Gamito, S. Growth models and their use in ecological modelling: an application to a fish population. *Ecological Modelling*, 113(1):83–94, 1998.

Gantmacher, F. *Theory of Matrices.* AMS Chelsea publishing, New York (NY), USA, 1959.

Gao, S.-J., Y.-Y. He, Y.-J. Liu, G.-J. Yang, and X.-N. Zhou. Field transmission intensity of *Schistosoma japonicum* measured by basic reproduction ratio from modified Barbour's model. *Parasites & Vectors*, 6:141, 2013. doi: 10.1186/1756-3305-6-141.

Gao, S.-J., H.-H. Cao, Y.-Y. He, Y.-J. Liu, X.-Y. Zhang, G.-J. Yang, and X.-N. Zhou. The basic reproductive ratio of Barbour's two-host schistosomiasis model with seasonal fluctuations. *Parasites & Vectors*, 10(1):42, 2017. doi: 10.1186/s13071-017-1983-1.

Garba, A., S. Touré, R. Dembelé, E. Bosque-Oliva, and A. Fenwick. Implementation of national schistosomiasis control programmes in West Africa. *Trends in Parasitology*, 22(7):322–6, 2006. doi: 10.1016/j.pt.2006.04.007.

Garba, A., M. S. Lamine, N. Barkiré, A. Djibo, B. Sofo, A. N. Gouvras, R. Labbo, H. Sebangou, J. P. Webster, A. Fenwick, and J. Utzinger. Efficacy and safety of two closely spaced doses of praziquantel against *Schistosoma haematobium* and *S. mansoni* and re-infection patterns in school-aged children in Niger. *Acta Tropica*, 128(2):334–344, 2013. doi: 10.1016/j.actatropica.2012.08.008.

Garchitorena, A., S. H. Sokolow, B. Roche, C. N. Ngonghala, M. Jocque, A. Lund, M. Barry, E. A. Mordecai, G. C. Daily, J. H. Jones, J. R. Andrews, E. Bendavid, S. P. Luby, A. D. LaBeaud, K. Seetah, J. F. Guégan, M. H. Bonds, and G. A. De Leo. Disease ecology, health and the environment: a framework to account for ecological and socio-economic drivers in the control of neglected tropical diseases. *Philosophical Transactions of the Royal Society of London B: Biological Sciences*, 372(1722):20160128, 2017. doi: 10.1098/rstb.2016.0128.

Garske, T., N. M. Ferguson, A. C. Ghani, H. van den Berg, and B. Tabashnik. Estimating air temperature and its influence on malaria transmission across Africa. *PLoS ONE*, 8(2):e56487, 2013. doi: 10.1371/journal.pone.0056487.

Gatto, M., L. Mari, E. Bertuzzo, R. Casagrandi, L. Righetto, I. Rodriguez-Iturbe, and A. Rinaldo. Generalized reproduction numbers and the prediction of patterns in waterborne disease. *Proceedings of the National Academy of Sciences of the United States of America*, 109(48):19703–8, 2012. doi: 10.1073/pnas.1217567109.

Gatto, M., L. Mari, E. Bertuzzo, R. Casagrandi, L. Righetto, I. Rodriguez-Iturbe, and A. Rinaldo. Spatially explicit conditions for waterborne pathogen invasion. *American Naturalist*, 182(3):328–346, 2013. doi: 10.1086/671258.

Gazzinelli, A., R. Correa-Oliveira, G.-J. Yang, B. A. Boatin, and H. Kloos. A Research Agenda for Helminth Diseases of Humans: Social Ecology, Environmental Determinants, and Health Systems. *PLoS Neglected Tropical Diseases*, 6 (4):e1603, 2012. doi: 10.1371/journal.pntd.0001603.

Gebrehiwot, S. G., U. Ilstedt, A. I. Gärdenas, and K. Bishop. Hydrological characterization of watersheds in the Blue Nile Basin, Ethiopia. *Hydrology and Earth System Sciences*, 15(1):11–20, 2011. doi: 10.5194/hess-15-11-2011.

Gentine, P., P. D'Odorico, B. R. Lintner, G. Sivandran, and G. Salvucci. Interdependence of climate, soil, and vegetation as constrained by the Budyko curve. *Geophysical Research Letters*, 39(19):n/a–n/a, 2012. doi: 10.1029/2012GL053492.

Gérard, C., and A. Théron. Age/size- and time-specific effects of *Schistosoma mansoni* on energy allocation patterns of its snail host Biomphalaria glabrata. *Oecologia*, 112(4):447–452, 1997. doi: 10.1007/s004420050331.

Gerrits, A. M. J., H. H. G. Savenije, E. J. M. Veling, and L. Pfister. Analytical derivation of the Budyko curve based on rainfall characteristics and a simple evaporation model. *Water Resources Research*, 45(4):1–15, 2009. doi: 10.1029/2008WR007308.

Gleichsner, A. M., J. A. Cleveland, and D. J. Minchella. One stimulus-two responses: Host and parasite life-history variation in response to environmental stress. *Evolution*, 70(11):2640–2646, 2016. doi: 10.1111/evo.13061.

Global Burden of Disease 2013 Collaborators. Global, regional, and national incidence, prevalence, and years lived with disability for 301 acute and chronic diseases and injuries in 188 countries, 1990-2013: a systematic analysis for the Global Burden of Disease Study 2013. *Lancet*, 386(9995):743–800, 2015. doi: 10.1016/S0140-6736(15)60692-4.

Global Burden of Disease Collaborative Network. Global Burden of Disease Study 2016 (GBD 2016) Results. Seattle, United States: Institute for Health Metrics and Evaluation (IHME), 2017.

Gönnert, R., and P. Andrews. Praziquantel, a new broad-spectrum antischistosomal agent. *Parasitology Research*, 52 (2):129–150, 1977.

Gouvras, A. N., F. Allan, S. Kinung'hi, M. Rabone, A. Emery, T. Angelo, T. Pennance, B. Webster, H. Nagai, and D. Rollinson. Longitudinal survey on the distribution of *Biomphalaria sudanica* and *B. choanomophala* in Mwanza region, on the shores of Lake Victoria, Tanzania: implications for schistosomiasis transmission and control. *Parasites & Vectors*, 10(1):316, 2017. doi: 10.1186/s13071-017-2252-z.

Grabs, W., T. de Couet, and J. Pauler. *Freshwater Fluxes from Continents Into the World Oceans Based on Data from the Global Runoff Database*. Fed. Inst. of Hydrology, 1996.

GRASS Development Team. *Geographic Resources Analysis Support System (GRASS GIS) Software*. Open Source Geospatial Foundation, USA, 2016.

Gray, D. J., D. P. McManus, Y. Li, G. M. Williams, R. Bergquist, and A. G. Ross. Schistosomiasis elimination: lessons from the past guide the future. *Lancet Infectious Diseases*, 10(10):733–6, 2010. doi: 10.1016/S1473-3099(10)70099-2.

Greve, P., L. Gudmundsson, B. Orlowsky, and S. I. Seneviratne. Introducing a probabilistic Budyko framework. *Geophysical Research Letters*, 42(7):2261–2269, 2015. doi: 10.1002/2015GL063449.

Grimes, J. E. T., D. Croll, W. E. Harrison, J. Utzinger, M. C. Freeman, and M. R. Templeton. The relationship between water, sanitation and schistosomiasis: a systematic review and meta-analysis. *PLoS Neglected Tropical Diseases*, 8 (12):e3296, 2014. doi: 10.1371/journal.pntd.0003296.

Grimes, J. E. T., D. Croll, W. E. Harrison, J. Utzinger, M. C. Freeman, and M. R. Templeton. The roles of water, sanitation and hygiene in reducing schistosomiasis: a review. *Parasites & Vectors*, 8(1):156, 2015. doi: 10.1186/s13071-015-0766-9.

Grimes, J. E. T., G. Tadesse, K. Mekete, Y. Wuletaw, A. Gebretsadik, M. D. French, W. E. Harrison, L. J. Drake, I. A. Gardiner, E. Yard, and M. R. Templeton. School water, sanitation, and hygiene, soil-transmitted helminths, and schistosomes: National mapping in Ethiopia. *PLoS Neglected Tropical Diseases*, 10(3):e0004515, 2016. doi: 10.1371/journal.pntd.0004515.

Gryseels, B., K. Polman, J. Clerinx, and L. Kestens. Human schistosomiasis. *Lancet*, 368(9541):1106–18, 2006. doi: 10.1016/S0140-6736(06)69440-3.

Gurarie, D., and C. H. King. Heterogeneous model of schistosomiasis transmission and long-term control: the combined influence of spatial variation and age-dependent factors on optimal allocation of drug therapy. *Parasitology*, 130(1):49–65, 2005. doi: 10.1017/S0031182004006341.

Gurarie, D., and E. Y. W. Seto. Connectivity sustains disease transmission in environments with low potential for endemicity: modelling schistosomiasis with hydrologic and social connectivities. *Journal of the Royal Society Interface*, 6:495–508, 2009. doi: 10.1098/rsif.2008.0265.

Gurarie, D., C. H. King, and X. Wang. A new approach to modelling schistosomiasis transmission based on stratified worm burden. *Parasitology*, 137(13):1951–1965, 2010. doi: 10.1017/S0031182010000867.

Gurarie, D., N. Yoon, E. Li, M. Ndeffo-Mbah, D. Durham, A. E. Phillips, H. O. Aurelio, J. Ferro, A. P. Galvani, and C. H. King. Modelling control of *Schistosoma haematobium* infection: predictions of the long-term impact of mass drug administration in Africa. *Parasites & Vectors*, 8(1):529, 2015.

Gurarie, D., C. H. King, N. Yoon, and E. Li. Refined stratified-worm-burden models that incorporate specific biological features of human and snail hosts provide better estimates of *Schistosoma* diagnosis, transmission, and control. *Parasites & Vectors*, 9(1):428, 2016. doi: 10.1186/s13071-016-1681-4.

Gurarie, D., C. King, N. Yoon, X. Wang, and R. Alsallaq. Seasonal dynamics of snail populations in coastal Kenya: Model calibration and snail control. *Advances in Water Resources*, 108:397 – 405, 2017. ISSN 0309-1708. doi: https://doi.org/10.1016/j.advwatres.2016.11.008. URL http://www.sciencedirect.com/science/article/pii/S0309170816306571.

Guyatt, H., and M. Tanner. Different approaches to modeling the cost-effectiveness of schistosomiasis control. *American Journal of Tropical Medicine and Hygiene*, 55(5):159–164, 1996.

Hairston, N. G., B. Hubendick, J. M. Watson, and L. J. Olivier. An evaluation of techniques used in estimating snail populations. *Bulletin of the World Health Organization*, 19(4):661–72, 1958.

Handschumacher, P., R. Dorsainville, O. Diaw, G. Hebrard, M. Niang, and J. Herve. Constraintes climatiques et amenagements hydroliques à propos de l'epidemie de bilharziose intestinale de Richard-Toll (Sénégal) ou la modification des risques sanitaire en milieu Sahelian. *Risques Pathol Rythm Paroxysmes*, 1151:287–295, 1992.

Hansen, B. E., and J. S. Racine. Jackknife model averaging. *Journal of Econometrics*, 167(1):38–46, 2012. doi: 10.1016/j.jeconom.2011.06.019.

Hastie, T., R. Tibshirani, and J. Friedman. Boosting and additive trees. In *The Elements of Statistical Learning*, pages 337–387. Springer, 2009.

Hauswald, A.-K., J. V. Remais, N. Xiao, G. M. Davis, D. Lu, M. J. Bale, and T. Wilke. Stirred, not shaken: genetic structure of the intermediate snail host *Oncomelania hupensis robertsoni* in an historically endemic schistosomiasis area. *Parasites & Vectors*, 4(1):206, 2011. doi: 10.1186/1756-3305-4-206.

Head, J. R., H. Chang, Q. Li, C. M. Hoover, T. Wilke, C. Clewing, E. J. Carlton, S. Liang, D. Lu, B. Zhong, and J. V. Remais. Genetic evidence of contemporary dispersal of the intermediate snail host of *schistosoma japonicum*: movement of an NTD host is facilitated by land use and landscape connectivity. *PLoS Neglected Tropical Diseases*, 10(12): e0005151, 2016. doi: 10.1371/journal.pntd.0005151.

Heinrich, K., M. Bach, and L. Breuer. Infectious disease research - what role is there for hydrologists? *Journal of Water Resource and Protection*, 9(02):139, 2017. doi: 10.4236/jwarp.2017.92011.

Herrando-Pérez, S., S. Delean, B. W. Brook, and C. J. a. Bradshaw. Density dependence: an ecological Tower of Babel. *Oecologia*, 170(3):585–603, 2012. doi: 10.1007/s00442-012-2347-3.

Hijmans, R. J., S. E. Cameron, J. L. Parra, P. G. Jones, and A. Jarvis. Very high resolution interpolated climate surfaces for global land areas. *International Journal of Climatology*, 25(15):1965–1978, 2005. doi: 10.1002/joc.1276.

Hira, P. R. Seasonal population densities of snails transmitting urinary and intestinal schistosomiasis in Lusaka, Zambia. *Tropical and geographical medicine*, 27(1):83–92, 1975.

Hollingsworth, T. D., E. R. Adams, R. M. Anderson, K. Atkins, S. Bartsch, M.-G. Basáñez, M. Behrend, D. J. Blok, L. A. C. Chapman, L. Coffeng, O. Courtenay, R. E. Crump, S. J. de Vlas, A. Dobson, L. Dyson, H. Farkas, A. P. Galvani, M. Gambhir, D. Gurarie, M. A. Irvine, S. Jervis, M. J. Keeling, L. Kelly-Hope, C. King, B. Y. Lee, E. A. Le Rutte, T. M. Lietman, M. Ndeffo-Mbah, G. F. Medley, E. Michael, A. Pandey, J. K. Peterson, A. Pinsent, T. C. Porco, J. H. Richardus, L. Reimer, K. S. Rock, B. K. Singh, W. Stolk, S. Swaminathan, S. J. Torr, J. Townsend, J. Truscott, M. Walker, and

A. Zoueva. Quantitative analyses and modelling to support achievement of the 2020 goals for nine neglected tropical diseases. *Parasites & Vectors*, 8(1):630, 2015. doi: 10.1186/s13071-015-1235-1.

Hong, Y., K. L. Hsu, H. Moradkhani, and S. Sorooshian. Uncertainty quantification of satellite precipitation estimation and Monte Carlo assessment of the error propagation into hydrologic response. *Water Resources Research*, 42(8): 1–15, 2006. doi: 10.1029/2005WR004398.

Hostettmann, K. On the use of plants and plant-derived compounds for the control of schistosomiasis. *Naturwissenschaften*, 71(5):247–251, 1984. doi: 10.1007/BF00441334.

Hu, G.-H., H. Jia, K.-Y. Song, D.-D. Lin, J. Zhang, C.-L. Cao, J. Xu, D. Li, and W.-S. Jiang. The role of health education and health promotion in the control of schistosomiasis: experiences from a 12-year intervention study in the Poyang Lake area. *Acta Tropica*, 96(2):232 – 241, 2005. doi: 10.1016/j.actatropica.2005.07.016.

Hu, H., P. Gong, and B. Xu. Spatially explicit agent-based modelling for schistosomiasis transmission: human-environment interaction simulation and control strategy assessment. *Epidemics*, 2(2):49–65, 2010. doi: 10.1016/j.epidem.2010.03.004.

Huete, A., K. Didan, T. Miura, E. P. Rodriguez, X. Gao, and L. G. Ferreira. Overview of the radiometric and biophysical performance of the modis vegetation indices. *Remote sensing of environment*, 83(1):195–213, 2002.

Hughes, D. A. Hydrological issues associated with the determination of environmental water requirements of ephemeral rivers. *River Research and Applications*, 21(8):899–908, 2005. doi: 10.1002/rra.857.

Hunter, J. M. Inherited burden of disease: agricultural dams and the persistence of bloody urine (*Schistosomiasis hematobium*) in the Upper East Region of Ghana, 1959-1997. *Social Science and Medicine*, 56(2):219–234, 2003. doi: 10.1016/S0277-9536(02)00021-7.

Ibrahim, B. *Characterization of the rainy seasons in Burkina Faso under a climate change condition and hydrological impacts in the Nakanbé basin.* PhD thesis, Université Pierre et Marie Curie - Paris VI, 2012.

Institut National de la Statistique et de la Démographie - INSD/Burkina Faso, and ICF International. Enquête Démographique et de Santé et à Indicateurs Multiples du Burkina Faso 2010. Technical report, Calverton, Maryland, USA: INSD and ICF International, 2012.

Institut National de la Statistique et de la Démographie - INSD/Burkina Faso, and ORC Macro. Enquête Démographique et de Santé et à Indicateurs Multiples du Burkina Faso 2003. Technical report, Calverton, Maryland, USA: INSD and ORC Macro, 2004.

Institut National de la Statistique et de la Démographie (INSD), and ICF Macro International. Enquête Démographique et de Santé et à Indicateurs Multiples du Burkina Faso 1998-1999. Technical report, Calverton, Maryland, USA: INSD and Macro Intertational, 2000.

Izah, S. C., and T. C. Angaye. Ecology of human schistosomiasis intermediate host and plant molluscicides used for control: a review. *Sky Journal of Biochemistry Research*, 5(6):075–082, 2016.

Jamieson, B. G. *Schistosoma: Biology, Pathology and Control.* CRC Press, 2017. ISBN 9781498744256.

Jamiesson, B. G., and W. Haas. Miracidium of *Schistosoma*. *Schistosoma: Biology, Pathology and Control*, page 440, 2017.

Jarne, P., M. VIANEY-LIAUD, and B. Delay. Selfing and outcrossing in hermaphrodite freshwater gastropods (*basommatophora*): where, when and why. *Biological Journal of the Linnean Society*, 49(2):99–125, 1993.

Jarvis, A., H. I. Reuter, A. Nelson, E. Guevara, et al. Hole-filled SRTM for the globe Version 4. *available from the CGIAR-CSI SRTM 90m Database (http://srtm. csi. cgiar. org)*, 2008.

Jobin, W. R., and E. H. Michelson. Mathematical simulation of an aquatic snail population. *Bulletin of the World Health Organization*, 37(4):657–64, 1967.

Johnson, J. B., and K. S. Omland. Model selection in ecology and evolution. *Trends in Ecology and Evolution*, 19(2): 101–8, 2004. doi: 10.1016/j.tree.2003.10.013.

Kalinda, C., M. Chimbari, and S. Mukaratirwa. Implications of changing temperatures on the growth, fecundity and survival of intermediate host snails of schistosomiasis: a systematic review. *International Journal of Environmental Research and Public Health*, 14(1), 2017a. doi: 10.3390/ijerph14010080.

Kalinda, C., M. J. Chimbari, and S. Mukaratirwa. Effect of temperature on the *Bulinus globosus-Schistosoma haematobium* system. *Infectious Diseases of Poverty*, 6(1):57, 2017b. doi: 10.1186/s40249-017-0260-z.

Kalluri, S., P. Gilruth, D. Rogers, and M. Szczur. Surveillance of arthropod vector-borne infectious diseases using remote sensing techniques: a review. *PLoS Pathogens*, 3(10):e116, 2007. doi: 10.1371/journal.ppat.0030116.

Kariuki, H. C., H. Madsen, J. H. Ouma, A. E. Butterworth, D. W. Dunne, M. Booth, G. Kimani, J. K. Mwatha, E. Muchiri, and B. J. Vennervald. Long term study on the effect of mollusciciding with niclosamide in stream habitats on the transmission of schistosomiasis mansoni after community-based chemotherapy in Makueni District, Kenya. *Parasites & Vectors*, 6(1):107, 2013. doi: 10.1186/1756-3305-6-107.

Kêdowidé, C. M. G., M. P. Sedogo, and G. Cissé. Dynamique spatio temporelle de l'agriculture urbaine à Ouagadougou : Cas du Maraîchage comme une activité montante de stratégie de survie. *VertigO*, 10(2), 2010. doi: 10.4000/vertigo.10312.

Kelly, G. C., C. M. Seng, W. Donald, G. Taleo, J. Nausien, W. Batarii, H. Iata, M. Tanner, L. S. Vestergaard, and A. C. A. Clements. A spatial decision support system for guiding focal indoor residual spraying interventions in a malaria elimination zone. *Geospatial Health*, 6(1):21, 2011. doi: 10.4081/gh.2011.154.

Kennard, M. J., B. J. Pusey, J. D. Olden, S. J. Mackay, J. L. Stein, and N. March. Classification of natural flow regimes in Australia to support environmental flow management. *Freshwater Biology*, 55(1):171–193, 2010. doi: 10.1111/j.1365-2427.2009.02307.x.

Kermack, W. O., and A. G. McKendrick. Contributions to the mathematical theory of epidemics. ii. the problem of endemicity. *Proceedings of the Royal Society of London A: Mathematical, Physical and Engeneering Sciences*, 138 (834):55–83, 1932.

King, A. A. `subplex`*: Unconstrained Optimization using the Subplex Algorithm*, 2015. R package version 1.1-6.

King, C. H. Parasites and poverty: the case of schistosomiasis. *Acta Tropica*, 113(2):95–104, 2010. doi: 10.1016/j.actatropica.2009.11.012.

King, C. H., and M. Dangerfield-Cha. The unacknowledged impact of chronic schistosomiasis. *Chronic illness*, 4(1): 65–79, 2008. doi: 10.1177/1742395307084407.

King, C. H., K. Dickman, and D. J. Tisch. Reassessment of the cost of chronic helmintic infection: a meta-analysis of disability-related outcomes in endemic schistosomiasis. *Lancet*, 365(9470):1561–9, 2005. doi: 10.1016/S0140-6736(05)66457-4.

King, C. H., L. J. Sutherland, and D. Bertsch. Systematic review and meta-analysis of the impact of chemical-based mollusciciding for control of *Schistosoma mansoni* and *S. haematobium* transmission. *PLoS Neglected Tropical Diseases*, 9(12):e0004290, 2015. doi: 10.1371/journal.pntd.0004290.

King, E. G., and K. K. Caylor. Ecohydrology in practice: strengths, conveniences, and opportunities. *Ecohydrology*, 4 (4):608–612, 2011.

Kittur, N., S. Binder, C. H. Campbell Jr, C. H. King, S. Kinung'hi, A. Olsen, P. Magnussen, and D. G. Colley. Defining persistent hotspots: areas that fail to decrease meaningfully in prevalence after multiple years of mass drug administration with praziquantel for control of schistosomiasis. *American Journal of Tropical Medicine and Hygiene*, 2017. doi: 10.4269/ajtmh.17-0368.

Kloos, H. Water resources development and schistosomiasis ecology in the Awash Valley, Ethiopia. *Social Science and Medicine*, 20(6):609–625, 1985. doi: 10.1016/0277-9536(85)90400-9.

Kloos, H. Human behavior, health education and schistosomiasis control: a review. *Social Science and Medicine*, 40 (11):1497–1511, 1995. doi: 10.1016/0277-9536(94)00310-P.

Kloos, H., A. Fulford, A. Butterworth, R. Sturrock, J. Ouma, H. Kariuki, F. Thiongo, P. Dalton, and R. Klumpp. Spatial patterns of human water contact and *Schistosoma mansoni* transmission and infection in four rural areas in Machakos District, Kenya. *Social Science and Medicine*, 44(7):949–968, 1997. doi: 10.1016/S0277-9536(96)00218-3.

Kloos, H., A. Gazzinelli, and P. Van Zuyle. Microgeographical patterns of schistosomiasis and water contact behavior; examples from Africa and Brazil. *Memórias do Instituto Oswaldo Cruz*, 93:37–50, 1998. doi: 10.1590/S0074-02761998000700006.

Kloos, H., L. K. J. Passos, P. LoVerde, R. C. Oliveira, and A. Gazzinelli. Distribution and *Schistosoma mansoni* infection of *Biomphalaria glabrata* in different habitats in a rural area in the Jequitinhonha Valley, Minas Gerais, Brazil: environmental and epidemiological aspects. *Memórias do Instituto Oswaldo Cruz*, 99(7):673–681, 2004. doi: 10.1590/S0074-02762004000700002.

Kloos, H., R. Correa-Oliveira, D. C. dos Reis, E. W. Rodrigues, L. A. S. Monteiro, and A. Gazzinelli. The role of population movement in the epidemiology and control of schistosomiasis in Brazil: a preliminary typology of population movement. *Memórias do Instituto Oswaldo Cruz*, 105(4):578–586, 2010. doi: 10.1590/S0074-02762010000400038.

Klumpp, R. K., and K. Y. Chu. Ecological studies of *Bulinus rohlfsi*, the intermediate host of *Schistosoma haematobium* in the Volta Lake. *Bulletin of the World Health Organization*, 55(6):715–30, 1977.

Klumpp, R. K., and G. Webbe. Focal, seasonal and behavioural patterns of infection and transmission of *Schistosoma haematobium* in a farming village at the Volta Lake, Ghana. *Journal of Tropical Medicine and Hygiene*, 90(5):265–81, 1987.

Knowles, S. C. L., B. L. Webster, A. Garba, M. Sacko, O. T. Diaw, A. Fenwick, D. Rollinson, and J. P. Webster. Epidemiological interactions between urogenital and intestinal human schistosomiasis in the context of praziquantel treatment across three West African countries. *PLoS Neglected Tropical Diseases*, 9(10):e0004019, 2015. doi: 10.1371/journal.pntd.0004019.

Knowles, S. C. L., H. J. W. Sturrock, H. Turner, J. M. Whitton, C. M. Gower, S. Jemu, A. E. Phillips, A. Meite, B. Thomas, K. Kollie, C. Thomas, M. P. Rebollo, B. Styles, M. Clements, A. Fenwick, W. E. Harrison, and F. M. Fleming. Optimising cluster survey design for planning schistosomiasis preventive chemotherapy. *PLoS Neglected Tropical Diseases*, 11 (5):e0005599, 2017. doi: 10.1371/journal.pntd.0005599.

Konar, M., M. J. Todd, R. Muneepeerakul, A. Rinaldo, and I. Rodriguez-Iturbe. Hydrology as a driver of biodiversity: Controls on carrying capacity, niche formation, and dispersal. *Advances in Water Resources*, 51:317–325, 2013.

Konate, D. L., S. Tinga, and M. Seroussi. Enquête Démographique et de Santé Burkina Faso 1993. Technical report, Calverton, Maryland, USA: INSD and ICF International, 1994.

Kosinski, K. C., A. V. Kulinkina, A. F. A. Abrah, M. N. Adjei, K. M. Breen, H. M. Chaudhry, P. E. Nevin, S. H. Warner, and S. A. Tendulkar. A mixed-methods approach to understanding water use and water infrastructure in a schistosomiasis-endemic community: case study of Asamama, Ghana. *BMC public health*, 16(1):322, 2016. doi: 10.1186/s12889-016-2976-2.

Koukounari, A., S. Touré, C. a. Donnelly, A. Ouedraogo, B. Yoda, C. Ky, M. Kaboré, E. Bosqué-Oliva, M.-G. Basáñez, A. Fenwick, and J. P. Webster. Integrated monitoring and evaluation and environmental risk factors for urogenital schistosomiasis and active trachoma in Burkina Faso before preventative chemotherapy using sentinel sites. *BMC Infectious Diseases*, 11(1):191, 2011. doi: 10.1186/1471-2334-11-191.

Kpoda, N. W., H. Sorgho, J.-N. Poda, J. B. Ouédraogo, and G. B. Kabré. Endémie bilharzienne à *Schistosoma mansoni* à la vallée du Kou : caractérisation du système de transmission et impact socioéconomique. *Comptes Rendus Biologies*, 336(5):284–288, 2013.

Kramer-Schadt, S., J. Niedballa, J. D. Pilgrim, B. Schröder, J. Lindenborn, V. Reinfelder, M. Stillfried, I. Heckmann, A. K. Scharf, D. M. Augeri, et al. The importance of correcting for sampling bias in MaxEnt species distribution models. *Diversity and Distributions*, 19(11):1366–1379, 2013.

Krauth, S. J., C. Musard, S. I. Traoré, J. Zinsstag, L. Y. Achi, E. K. N'Goran, and J. Utzinger. Access to, and use of, water by populations living in a schistosomiasis and fascioliasis co-endemic area of northern Côte d'Ivoire. *Acta Tropica*, 149:179–85, 2015. doi: 10.1016/j.actatropica.2015.05.019.

Krauth, S. J., N. Wandel, S. I. Traoré, P. Vounatsou, J. Hattendorf, L. Y. Achi, K. McNeill, E. K. N'Goran, and J. Utzinger. Distribution of intermediate host snails of schistosomiasis and fascioliasis in relation to environmental factors during the dry season in the Tchologo region, Côte d'Ivoire. *Advances in Water Resources*, 108:386–396, 2016. doi: 10.1016/j.advwatres.2016.11.016.

Kulinkina, A., Y. Walz, A. Liss, K. C. Kosinski, N. Biritwum, and E. Naumova. Combining remotely sensed environmental characteristics with social and behavioral conditions that affect surface water use in spatiotemporal modelling of schistosomiasis in Ghana. *International Archives of the Photogrammetry, Remote Sensing and Spatial Information Sciences*, 41, 2016.

Kuznetsov, Y. *Elements of Applied Bifurcation Theory*. Springer-Verlag, New York, NY, USA, 1995.

Lai, Y.-S., P. Biedermann, U. F. Ekpo, A. Garba, E. Mathieu, N. Midzi, P. Mwinzi, E. K. N'Goran, G. Raso, R. K. Assaré, M. Sacko, N. Schur, I. Talla, L.-A. T. Tchuenté, S. Touré, M. S. Winkler, J. Utzinger, and P. Vounatsou. Spatial distribution of schistosomiasis and treatment needs in sub-Saharan Africa: a systematic review and geostatistical analysis. *Lancet Infectious Diseases*, 15(8):927 – 940, 2015. ISSN 1473-3099. doi: https://doi.org/10.1016/S1473-3099(15)00066-3. URL http://www.sciencedirect.com/science/article/pii/S1473309915000663.

Lara, R., M. Islam, S. Yamasaki, S. Neogi, and G. Nair. 10.12 Aquatic ecosystems, human health, and ecohydrology. In *Treatise on Estuarine and Coastal Science*, pages 263–299. Elsevier, 2011. ISBN 9780080878850. doi: 10.1016/B978-0-12-374711-2.01015-9.

Larned, S. T., J. Schmidt, T. Datry, C. P. Konrad, J. K. Dumas, and J. C. Diettrich. Longitudinal river ecohydrology: flow variation down the lengths of alluvial rivers. *Ecohydrology*, 4(4):532–548, 2011. doi: 10.1002/eco.126.

Le Barbé, L., T. Lebel, and D. Tapsoba. Rainfall variability in West Africa during the years 1950-90. *Journal of Climate*, 15(2):187–202, 2002. doi: 10.1175/1520-0442(2002)015<0187:RVIWAD>2.0.CO;2.

Legendre, P., and M. J. Anderson. Distance-based redundancy analysis: Testing multispecies responses in multifactorial ecological experiments. *Ecological Monographs*, 69(1):1–24, 1999. doi: 10.1890/0012-9615(1999)069[0001:DBRATM]2.0.CO;2.

Lehner, B., K. Verdin, and A. Jarvis. New global hydrography derived from spaceborne elevation data. *Eos, Transactions American Geophysical Union*, 89(10):93–94, 2008. doi: 10.1029/2008EO100001.

Levitz, S., C. J. Standley, M. Adriko, N. B. Kabatereine, and J. R. Stothard. Environmental epidemiology of intestinal schistosomiasis and genetic diversity of *Schistosoma mansoni* infections in snails at Bugoigo village, Lake Albert. *Acta Tropica*, 128(2):284–291, 2013. doi: 10.1016/j.actatropica.2012.10.003.

Li, S., L. Xiong, L. Dong, and J. Zhang. Effects of the Three Gorges Reservoir on the hydrological droughts at the downstream Yichang station during 2003-2011. *Hydrological Processes*, 27(26):3981–3993, 2013. doi: 10.1002/hyp.9541.

Li, Z., X. Nie, Y. Zhang, J. Huang, B. Huang, and G. Zeng. Assessing the influence of water level on schistosomiasis in Dongting Lake region before and after the construction of Three Gorges Dam. *Environmental Monitoring and Assessment*, 188(1):28, 2016. doi: 10.1007/s10661-015-5033-1.

Liang, S., D. Maszle, and R. C. Spear. A quantitative framework for a multi-group model of Schistosomiasis japonicum transmission dynamics and control in Sichuan, China. *Acta Tropica*, 82(2):263–277, 2002. doi: 10.1016/S0001-706X(02)00018-9.

Liang, S., E. Y. W. Seto, J. V. Remais, B. Zhong, C. Yang, A. Hubbard, G. M. Davis, X. Gu, D. Qiu, and R. C. Spear. Environmental effects on parasitic disease transmission exemplified by schistosomiasis in western China. *Proceedings of the National Academy of Sciences of the United States of America*, 104(17):7110–5, 2007. doi: 10.1073/pnas.0701878104.

Lima e Costa, M. F. F., R. S. Rocha, M. L. C. Leite, R. G. Carneiro, D. Colley, G. Gazzinelli, and N. Katz. A multivariate analysis of socio-demographic factors, water contact patterns and *Schistosoma mansoni* infection in an endemic area in Brazil. *Revista do Instituto de Medicina Tropical de São Paulo*, 33(1):58–63, 1991. doi: 10.1590/S0036-46651991000100011.

Liu, Z., M. Notaro, J. Kutzbach, and N. Liu. Assessing global vegetation-climate feedbacks from observations. *Journal of Climate*, 19:787–814, 2006. doi: 10.1175/JCLI3658.1.

Livingston, E. H., and S. Lee. Percentage of burned body surface area determination in obese and nonobese patients. *Journal of Surgical Research*, 91(2):106–110, 2000.

Lleo, M. M., M. Lafaye, and A. Guell. Application of space technologies to the surveillance and modelling of waterborne diseases. *Current Opinion in Biotechnology*, 19(3):307–312, 2008. doi: 10.1016/j.copbio.2008.04.001.

Lo, N. C., I. I. Bogoch, B. G. Blackburn, G. Raso, E. K. N'Goran, J. T. Coulibaly, S. L. Becker, H. B. Abrams, J. Utzinger, and J. R. Andrews. Comparison of community-wide, integrated mass drug administration strategies for schistosomiasis and soil-transmitted helminthiasis: a cost-effectiveness modelling study. *Lancet Global health*, 3(10):e629–38, 2015. doi: 10.1016/S2214-109X(15)00047-9.

Lo, N. C., Y.-S. Lai, D.-A. Karagiannis-Voules, I. I. Bogoch, J. T. Coulibaly, E. Bendavid, J. Utzinger, P. Vounatsou, and J. R. Andrews. Assessment of global guidelines for preventive chemotherapy against schistosomiasis and soil-transmitted helminthiasis: a cost-effectiveness modelling study. *Lancet Infectious Diseases*, 16(9):1065 – 1075, 2016. doi: 10.1016/S1473-3099(16)30073-1.

Lo, N. C., D. G. Addiss, P. J. Hotez, C. H. King, J. R. Stothard, D. S. Evans, D. G. Colley, W. Lin, J. T. Coulibaly, A. L. Bustinduy, G. Raso, E. Bendavid, I. I. Bogoch, A. Fenwick, L. Savioli, D. Molyneux, J. Utzinger, and J. R. Andrews. A call to strengthen the global strategy against schistosomiasis and soil-transmitted helminthiasis: the time is now. *Lancet Infectious Diseases*, 17(2):e64 – e69, 2017. ISSN 1473-3099. doi: https://doi.org/10.1016/S1473-3099(16)30535-7. URL http://www.sciencedirect.com/science/article/pii/S1473309916305357.

Lodoun, T., A. Giannini, P. S. Traoré, L. Somé, M. Sanon, M. Vaksmann, and J. M. Rasolodimby. Changes in seasonal descriptors of precipitation in Burkina Faso associated with late 20th century drought and recovery in West Africa. *Environmental Development*, 5(1):96–108, 2013. doi: 10.1016/j.envdev.2012.11.010.

Loker, E. S. A comparative study of the life-histories of mammalian schistosomes. *Parasitology*, 87 (Pt 2)(02):343–369, 1983. doi: 10.1017/S0031182000052689.

Lowe, D., J. Xi, X. Meng, Z. Wu, D. Qiu, and R. Spear. Transport of *Schistosoma japonicum* cercariae and the feasibility of niclosamide for cercariae control. *Parasitology International*, 54(1):83–89, 2005. doi: 10.1016/j.parint.2004.12.003.

Lu, X., E. Wetter, N. Bharti, A. J. Tatem, and L. Bengtsson. Approaching the limit of predictability in human mobility. *Scientific Reports*, 3:2923, 2013. doi: 10.1038/srep02923.

Macdonald, G. The dynamics of helminth infections, with special reference to schistosomes. *Transactions of the Royal Society of Tropical Medicine and Hygiene*, 59(5):489–506, 1965. doi: 10.1016/0035-9203(65)90152-5.

Madsen, H. *Schistosoma* intermediate host snails. *Schistosoma: Biology, Pathology and Control*, page 38, 2017.

Maharaj, J. R., C. C. Appleton, and R. M. Miller. Snail predation by larvae of *Sepedon scapularis* Adams (Diptera: Sciomyzidae), a potential biocontrol agent of snail intermediate hosts of schistosomiasis in South Africa. *Medical and Veterinary Entomology*, 6(3):183–187, 1992. doi: 10.1111/j.1365-2915.1992.tb00604.x.

Mahe, G., G. Lienou, L. Descroix, F. Bamba, J. E. Paturel, A. Laraque, M. Meddi, H. Habaieb, O. Adeaga, C. Dieulin, F. Chahnez Kotti, and K. Khomsi. The rivers of Africa: witness of climate change and human impact on the environment. *Hydrological Processes*, 27(15):2105–2114, 2013. doi: 10.1002/hyp.9813.

Malone, J., R. Bergquist, and L. Rinaldi. Geospatial surveillance and response systems for schistosomiasis. *Schistosoma: Biology, Pathology and Control*, page 479, 2017.

Malone, J. B., N. R. Bergquist, O. K. Huh, M. E. Bavia, M. Bernardi, M. M. El Bahy, M. V. Fuentes, T. K. Kristensen, J. C. McCarroll, J. M. Yilma, and X. N. Zhou. A global network for the control of snail-borne disease using satellite surveillance and geographic information systems. *Acta Tropica*, 79(1):7–12, 2001. doi: 10.1016/S0001-706X(01)00098-5.

Mandahl-Barth, G. Intermediate hosts of *Schistosoma*: African *Biomphalaria* and *Bulinus*: 1. *Bulletin of the World Health Organization*, 16(6):1103, 1957a.

Mandahl-Barth, G. Intermediate hosts of *Schistosoma*: African *Biomphalaria* and *Bulinus*: 2. *Bulletin of the World Health Organization*, 17(1):1, 1957b.

Mande, T., N. C. Ceperley, G. G. Katul, S. W. Tyler, H. Yacouba, and M. B. Parlange. Suppressed convective rainfall by agricultural expansion in southeastern Burkina Faso. *Water Resources Research*, 51(7):5521–5530, 2015. doi: 10.1002/2015WR017144.

Mangal, T. D., S. Paterson, and A. Fenton. Effects of snail density on growth, reproduction and survival of *Biomphalaria alexandrina* exposed to *Schistosoma mansoni*. *Journal of Parasitology Research*, 2010, 2010.

Manyangadze, T., M. J. Chimbari, M. Gebreslasie, and S. Mukaratirwa. Application of geo-spatial technology in schistosomiasis modelling in Africa: a review. *Geospatial Health*, 10(2), 2015.

Manyangadze, T., M. J. Chimbari, M. Gebreslasie, P. Ceccato, and S. Mukaratirwa. Modelling the spatial and seasonal distribution of suitable habitats of schistosomiasis intermediate host snails using Maxent in Ndumo area, KwaZulu-Natal Province, South Africa. *Parasites & Vectors*, 9(1):572, 2016. doi: 10.1186/s13071-016-1834-5.

Mari, L., E. Bertuzzo, L. Righetto, R. Casagrandi, M. Gatto, I. Rodriguez-Iturbe, and A. Rinaldo. Modelling cholera epidemics: the role of waterways, human mobility and sanitation. *Journal of the Royal Society Interface*, 9(67): 376–388, 2012a. doi: 10.1098/rsif.2011.0304.

Mari, L., E. Bertuzzo, L. Righetto, R. Casagrandi, M. Gatto, I. Rodriguez-Iturbe, and A. Rinaldo. On the role of human mobility in the spread of cholera epidemics: towards an epidemiological movement ecology. *Ecohydrology*, 5(5): 531–540, 2012b. doi: 10.1002/eco.262.

Mari, L., R. Casagrandi, E. Bertuzzo, A. Rinaldo, and M. Gatto. Metapopulation persistence and species spread in river networks. *Ecology Letters*, 17(4):426–434, 2014a. doi: 10.1111/ele.12242.

Mari, L., R. Casagrandi, E. Bertuzzo, A. Rinaldo, and M. Gatto. Floquet theory for seasonal environmental forcing of spatially explicit waterborne epidemics. *Theoretical Ecology*, 7:351–365, 2014b. doi: 10.1007/s12080-014-0223-y.

Mari, L., M. Ciddio, R. Casagrandi, J. Perez-Saez, E. Bertuzzo, A. Rinaldo, S. H. Sokolow, G. A. De Leo, and M. Gatto. Heterogeneity in schistosomiasis transmission dynamics. *Journal of Theoretical Biology*, 432:87–99, 2017a. doi: 10.1016/j.jtbi.2017.08.015.

Mari, L., M. Gatto, M. Ciddio, E. D. Dia, S. H. Sokolow, G. A. De Leo, and R. Casagrandi. Big-data-driven modeling unveils country-wide drivers of endemic schistosomiasis. *Scientific Reports*, 7(1):489, 2017b. doi: 10.1038/s41598-017-00493-1.

Marti, H. P., and M. Tanner. Field observations on the influence of low water velocities on drifting of *Bulinus globosus*. *Hydrobiologia*, 157(2):119–123, 1988. doi: 10.1007/BF00006964.

Maszle, D., P. Whitehead, R. Johnson, and R. Spear. Hydrological studies of schistosomiasis transport in Sichuan Province, China. *Science of The Total Environment*, 216(3):193–203, 1998. doi: 10.1016/S0048-9697(98)00152-1.

May, R. M., and R. M. Anderson. Population biology of infectious diseases: Part II. *Nature*, 280(5722):455–461, 1979. doi: 10.1038/280455a0.

Mbabazi, P. S., O. Andan, D. W. Fitzgerald, L. Chitsulo, D. Engels, and J. A. Downs. Examining the relationship between urogenital schistosomiasis and HIV infection. *PLoS Neglected Tropical Diseases*, 5(12):e1396, 2011. doi: 10.1371/journal.pntd.0001396.

McCreesh, N., and M. Booth. Challenges in predicting the effects of climate change on *Schistosoma mansoni* and *Schistosoma haematobium* transmission potential. *Trends in Parasitology*, 29(11):548–555, 2013. doi: 10.1016/j.pt.2013.08.007.

McCreesh, N., and M. Booth. The effect of increasing water temperatures on *Schistosoma mansoni* transmission and *Biomphalaria pfeifferi* population dynamics: an agent-based modelling study. *PLoS ONE*, 9(7):e101462, 2014a. doi: 10.1371/journal.pone.0101462.

McCreesh, N., and M. Booth. The effect of simulating different intermediate host snail species on the link between water temperature and schistosomiasis risk. *PLoS ONE*, 9(7):e87892, 2014b. doi: 10.1371/journal.pone.0087892.

McCreesh, N., M. Arinaitwe, W. Arineitwe, E. M. Tukahebwa, and M. Booth. Effect of water temperature and population density on the population dynamics of *Schistosoma mansoni* intermediate host snails. *Parasites & Vectors*, 7:9, 2014. doi: 10.1186/s13071-014-0503-9.

McCullough, F. S., P. Gayral, J. Duncan, and J. D. Christie. Molluscicides in schistosomiasis control. *Bulletin of the World Health Organization*, 58(5):681–9, 1980.

McDonnell, J. J., and R. Woods. On the need for catchment classification. *Journal of Hydrology*, 299(1-2):2–3, 2004.

McMichael, A. J., R. E. Woodruff, and S. Hales. Climate change and human health: present and future risks. *Lancet*, 367:859–869, 2006.

Meurs, L., M. Mbow, N. Boon, F. Van den Broeck, K. Vereecken, T. N. Dièye, E. Abatih, T. Huyse, S. Mboup, and K. Polman. Micro-geographical heterogeneity in *Schistosoma mansoni* and *S. haematobium* infection and morbidity in a co-endemic community in northern Senegal. *PLoS Neglected Tropical Diseases*, 7(12):e2608, 2013.

Michael, E., and S. Madon. Socio-ecological dynamics and challenges to the governance of neglected tropical disease control. *Infectious Diseases of Poverty*, 6(1):35, 2017. doi: 10.1186/s40249-016-0235-5.

Michelson, E. H. Studies on the biological control of schistosome-bearing snails. Predators and parasites of freshwater mollusca: a review of the literature. *Parasitology*, 47(3-4):413, 2009. doi: 10.1017/S0031182000022101.

Mitchell, K. M., F. Mutapi, N. J. Savill, and M. E. J. Woolhouse. Protective immunity to *Schistosoma haematobium* infection is primarily an anti-fecundity response stimulated by the death of adult worms. *Proceedings of the National Academy of Sciences of the United States of America*, 109(33):13347–52, 2012. doi: 10.1073/pnas.1121051109.

Mitchell, K. M., F. Mutapi, T. Mduluza, N. Midzi, N. J. Savill, and M. E. J. Woolhouse. Predicted impact of mass drug administration on the development of protective immunity against *Schistosoma haematobium*. *PLoS Neglected Tropical Diseases*, 8(7):e3059, 2014. doi: 10.1371/journal.pntd.0003059.

Modiano, D., V. Petrarca, B. Sirima, I. Nebie, D. Diallo, F. Esposito, and M. Coluzzi. Different response to *plasmodium falciparum* malaria in West African sympatric ethnic groups. *Proceedings of the National Academy of Sciences of the United States of America*, 93(23):13206–13211, 1996.

Moliere, D. R., J. B. Lowry, and C. L. Humphrey. Classifying the flow regime of data-limited streams in the wet-dry tropical region of Australia. *Journal of Hydrology*, 367(1):1–13, 2009. doi: 10.1016/j.jhydrol.2008.12.015.

Moore, S. M., A. S. Azman, B. F. Zaitchik, E. D. Mintz, J. Brunkard, D. Legros, A. Hill, H. McKay, F. J. Luquero, D. Olson, et al. El Niño and the shifting geography of cholera in Africa. *Proceedings of the National Academy of Sciences of the United States of America*, 114(17):4436–4441, 2017.

Moradkhani, H., and S. Sorooshian. General review of rainfall-runoff modeling: model calibration, data assimilation, and uncertainty analysis. In *Hydrological Modelling and the Water Cycle*, pages 1–24. Springer, 2009.

Moser, W., H. Greter, C. Schindler, F. Allan, B. N. R. Ngandolo, D. D. Moto, J. Utzinger, and J. Zinsstag. The spatial and seasonal distribution of *Bulinus truncatus*, *Bulinus forskalii* and *Biomphalaria pfeifferi*, the intermediate host snails of schistosomiasis, in N'Djamena, Chad. *Geospatial Health*, 9(1):109–118, 2014.

Mu, Q., M. Zhao, and S. W. Running. MODIS Global Terrestrial Evapotranspiration (ET) Product (NASA MOD16A2/A3). *Algorithm Theoretical Basis Document, Collection*, 5, 2013.

Muneepeerakul, R., E. Bertuzzo, H. J. Lynch, W. F. Fagan, A. Rinaldo, and I. Rodriguez-Iturbe. Neutral metacommunity models predict fish diversity patterns in Mississippi-Missouri basin. *Nature*, 453(7192):220–222, 2008.

Mutapi, F., P. Ndhlovu, P. Hagan, and M. Woolhouse. A comparison of re-infection rates with *Schistosoma haematobium* following chemotherapy in areas with high and low levels of infection. *Parasirte Immunilogy*, 21(5):253–259, 1999.

Mutapi, F., R. Maizels, A. Fenwick, and M. Woolhouse. Human schistosomiasis in the post mass drug administration era. *Lancet Infectious Diseases*, 17(2):e42–e48, 2017.

Mutuku, F. M., C. H. King, A. L. Bustinduy, P. L. Mungai, E. M. Muchiri, and U. Kitron. Impact of drought on the spatial pattern of transmission of *Schistosoma haematobium* in coastal Kenya. *American Journal of Tropical Medicine and Hygiene*, 85(6):1065–1070, 2011.

Myneni, R., Y. Knyazikhin, and T. Park. MOD15A2H MODIS/Terra Leaf Area Index/FPAR 8-Day L4 Global 500 m SIN Grid V006. NASA EOSDIS Land Processes DAAC, 2015.

Ngonghala, C. N., G. A. De Leo, M. M. Pascual, D. C. Keenan, A. P. Dobson, and M. H. Bonds. General ecological models for human subsistence, health and poverty. *Nature Ecology and Evolution*, 1(8):1153, 2017.

N'Goran, E. K., J. Utzinger, A. N. N'Guessan, I. Müller, K. Zamblé, K. L. Lohourignon, M. Traoré, B. A. Sosthéne, C. Lengeler, and M. Tanner. Reinfection with *Schistosoma haematobium* following school-based chemotherapy with praziquantel in four highly endemic villages in Côte d'Ivoire. *Tropical Medicine and International Health*, 6 (10):817–825, 2001. doi: 10.1046/j.1365-3156.2001.00785.x.

Noda, S., N. D. Muhoho, S. Habe, K. Makiya, and Y. Aoki. Interation between *Bulinus globosus* and *Cleopatra ferruginea* at a transmission site of schistosomiasis in Kwale, Kenya. *Japanese Society of Tropical Medicine*, 23(1):15–20, 1995.

Odermatt, P. *Comparative Investigation on the population dynamics of Bulinus globosus (Morelet,1886) and Biomphalaria pfeifferi (Kraus, 1884) (Gastropoda; Planorbidae) with special regard to the assessment of high risk areas for the transmission of intestinal schistomiasis.* PhD thesis, University of Basel, 1994.

Ofoezie, J. E., N. Ø. Christensen, and H. Madsen. Water contact patterns and behavioural knowledge of schistosomiasis in South-West Nigeria. *Journal of Biosocial Science*, 30(2):S0021932098002454, 1998. doi: 10.1017/S0021932098002454.

Ogunkoya, O. Towards a delimitation of southwestern Nigeria into hydrological regions. *Journal of Hydrology*, 99 (1-2):165–177, 1988. doi: 10.1016/0022-1694(88)90085-6.

O'Keeffe, J. H. Population biology of the freshwater snail *Bulinus globosus* on the Kenya Coast. I. Population fluctuations in relation to climate. *Journal of Applied Ecology*, 22(1):73, 1985a. doi: 10.2307/2403328.

O'Keeffe, J. H. Population biology of the freshwater snail *Bulinus globosus* on the Kenya Coast. II. Feeding and density effects on population parameters. *Journal of Applied Ecology*, 22(1):85, 1985b. doi: 10.2307/2403329.

Olden, J. D., M. J. Kennard, and B. J. Pusey. A framework for hydrologic classification with a review of methodologies and applications in ecohydrology. *Ecohydrology*, 5(4):503–518, 2012. doi: 10.1002/eco.251.

Ostfeld, R. S., G. E. Glass, and F. Keesing. Spatial epidemiology: an emerging (or re-emerging) discipline. *Trends in Ecology and Evolution*, 20(6):328–336, 2005. doi: 10.1016/j.tree.2005.03.009.

Ouedraogo, H., F. Drabo, D. Zongo, M. Bagayan, I. Bamba, and T. Pima. Schistosomiasis in school-age children in Burkina Faso after a decade of preventive chemotherapy. *Bulletin of the World Health Organization*, 94(November 2015):37–45, 2016.

Oueslati, O., A. M. De Girolamo, A. Abouabdillah, T. R. Kjeldsen, and A. Lo Porto. Classifying the flow regimes of Mediterranean streams using multivariate analysis. *Hydrological Processes*, 29(22):4666–4682, 2015. doi: 10.1002/hyp.10530.

Ouma, J. H., R. F. Sturrock, R. K. Klumpp, and H. C. Kariuki. A comparative evaluation of snail sampling and cercariometry to detect *Schistosoma mansoni* transmission in a large-scale, longitudinal field-study in Machakos, Kenya. *Parasitology*, 99(03):349, 2009. doi: 10.1017/S0031182000059060.

Palchykov, V., M. Mitrović, H.-H. Jo, J. Saramäki, and R. K. Pan. Inferring human mobility using communication patterns. *Scientific Reports*, 4:6174, 2014. doi: 10.1038/srep06174.

PANA Burkina Faso. Programme d'Action National d'adaptation à la variabilité et aux changements climatiques (PANA du Burkina Faso). Technical report, Ministère de l'Environnement et du Cadre de Vie: Burkina Faso, 2007.

Parkes, M. W. Diversity, emergence, resilience: Guides for a new generation of ecohealth research and practice. *EcoHealth*, 8(2):137–139, 2011. doi: 10.1007/s10393-011-0732-8.

Pascual, M., X. Rodó, S. P. Ellner, R. Colwell, and M. J. Bouma. Cholera dynamics and El Niño-Southern Oscillation. *Science*, 289(5485):1766–1769, 2000. doi: 10.1126/science.289.5485.1766.

Pascual, M., M. Bouma, and A. Dobson. Cholera and climate: revisiting the quantitative evidence. *Microbes and Infection*, 4(2):237–245, 2002.

Pasetto, D., F. Finger, A. Rinaldo, and E. Bertuzzo. Real-time projections of cholera outbreaks through data assimilation and rainfall forecasting. *Advances in Water Resources*, 108:345–356, 2017.

Pedersen, U. B., N. Midzi, T. Mduluza, W. Soko, A. S. Stensgaard, B. J. Vennervald, S. Mukaratirwa, and T. K. Kristensen. Modelling spatial distribution of snails transmitting parasitic worms with importance to human and animal health and analysis of distributional changes in relation to climate. *Geospatial Health*, 8(2):335–343, 2014. doi: 10.4081/gh.2014.23.

Pekel, J.-F., A. Cottam, N. Gorelick, and A. S. Belward. High-resolution mapping of global surface water and its long-term changes. *Nature*, 540(7633):418–422, 2016. doi: 10.1038/nature20584.

Pennance, T., B. Person, M. A. Muhsin, A. N. Khamis, J. Muhsin, I. S. Khamis, K. A. Mohammed, F. Kabole, D. Rollinson, and S. Knopp. Urogenital schistosomiasis transmission on Unguja Island, Zanzibar: characterisation of persistent hot-spots. *Parasites & Vectors*, 9(1):646, 2016.

Perez-Saez, J., L. Mari, E. Bertuzzo, R. Casagrandi, S. H. Sokolow, G. A. De Leo, T. Mande, N. Ceperley, J.-M. Froehlich, M. Sou, H. Karambiri, H. Yacouba, A. Maiga, M. Gatto, and A. Rinaldo. A theoretical analysis of the geography of schistosomiasis in burkina faso highlights the roles of human mobility and water resources development in disease transmission. *PLoS Neglected Tropical Diseases*, 9(10):e0004127, 2015. doi: 10.1371/journal.pntd.0004127.

Perez-Saez, J., T. Mande, N. Ceperley, E. Bertuzzo, L. Mari, M. Gatto, and A. Rinaldo. Hydrology and density feedback control the ecology of intermediate hosts of schistosomiasis across habitats in seasonal climates. *Proceedings of the National Academy of Sciences of the United States of America*, 113(23):6427–6432, 2016. doi: 10.1073/pnas.1602251113.

Perez-Saez, J., T. Mande, J. Larsen, N. Ceperley, and A. Rinaldo. Classification and prediction of river network ephemerality and its relevance for waterborne disease epidemiology. *Advances in Water Resources*, 2017. doi: 10.1016/j.advwatres.2017.10.003.

Phillips, S. J., R. P. Anderson, and R. E. Schapire. Maximum entropy modeling of species geographic distributions. *Ecological Modelling*, 190(3):231–259, 2006. doi: 10.1016/j.ecolmodel.2005.03.026.

Picquet, M., J. Vercruysse, D. J. Shaw, M. Diop, and A. Ly. Efficacy of praziquantel against *Schistosoma mansoni* in northern Senegal. *Transactions of the Royal Society of Tropical Medicine and Hygiene*, 92(1):90–93, 1998.

Pitchford, R., A. Meyling, J. Meyling, and J. Du Toit. Cercarial shedding patterns of various schistosome species under outdoor conditions in the Transvaal. *Annals of Tropical Medicine and Parasitology*, 63(3):359–371, 1969.

Plowright, R. K., S. H. Sokolow, M. E. Gorman, P. Daszak, and J. E. Foley. Causal inference in disease ecology: investigating ecological drivers of disease emergence. *Frontiers in Ecology and the Environment*, 6(8):420–429, 2008.

Poda, J., B. Sellin, and L. Swadago. Dynamique des populations de *Bulinus senegalensis* Müller 1781 dans une mare temporaire située dans une zone climatique nord-soudanienne au Burkina Faso. *Revue d'Elevage et de Médecine Vétérinaire des Pays Tropicaux*, 47(4):375–378, 1994.

Poda, J., L. Sawadogo, B. Sellin, and S. Sanogo. Dynamique des populations de *Bulinus truncatus rohlfsi* Clessin, 1886, dans le barrage de Dyoro en zone nord soudanienne du Burkina Faso. *Agronomie Africaine*, 8(1):61–68, 1996.

Poda, J., A. Traoré, and B. K. Sondo. L'endémie bilharzienne au Burkina Faso. *Société de Pathologie Exotique*, 97(1):47–52, 2004a.

Poda, J.-N. *Distribution spatiale des hotes intermediaires des schistosomes au Burkina Faso: Facteurs infulençant la dynamique des populations de Bulinus truncatus rohlfsi Classin, 1886 et de Bulinus sengalensis Muller, 1781.* PhD thesis, Université de Ouagadougou, 1996.

Poda, J.-N., H. Sorgho, D. Dianou, B. Sawadogo, T. Kambou, G. Parent, and B. Sondo. Profil parasitologique de la schistosomosiase urinaire du complexe hydroagricole du Sourou au Burkina Faso. *Société de Pathologie Exotique*, 94(1):21–24, 2001.

Poda, J.-N., B. Sondo, and G. Parent. Influence des hydro-aménagements sur la distribution des bilharzioses et de leurs hôtes intermédiaires au Burkina Faso. *Cahiers d'études et de recherches francophones / Santé*, 13(1):49–53, 2003.

Poda, J.-N., S. P. Wango, H. Sorgho, and D. Dianou. Évolution récente des schistosomoses dans le complexe hydroagricole du Sourou au Burkina Faso. *Société de Pathologie Exotique*, 1(97):15–18, 2004b.

Pointier, J., A. Théron, D. Imbert-Establet, and G. Borel. Eradication of a sylvatic focus of *Schistosoma mansoni* using biological control by competitor snails. *Biological Control*, 1(3):244–247, 1991. doi: 10.1016/1049-9644(91)90073-9.

Porporato, A., E. Daly, and I. Rodriguez-Iturbe. Soil water balance and ecosystem response to climate change. *American Naturalist*, 164(5):625–32, 2004. doi: 10.1086/424970.

PostGIS Project Steering Committee. PostGIS, Spatial and Geographic objects for PostgreSQL, 2015.

PostgreSQL Global Development Group. Documentation, PostgreSQL, 2006.

Prugnolle, F., T. de Meeûs, J. P. Pointier, P. Durand, A. Rognon, and A. Théron. Geographical variations in infectivity and susceptibility in the host-parasite system *Schistosoma mansoni/Biomphalaria glabrata*: no evidence for local adaptation. *Parasitology*, 133(Pt 3):313–319, 2006. doi: 10.1017/S0031182006000412.

Radke, M. G., L. S. Ritchie, and W. B. Rowan. Effects of water velocities on worm burdens of animals exposed to *Schistosoma mansoni* cercariae released under laboratory and field conditions. *Experimental Parasitology*, 11(4): 323–331, 1961. doi: 10.1016/0014-4894(61)90039-X.

Rambaldi, G., P. A. K. Kyem, M. McCall, and D. Weiner. Participatory spatial information management and communication in developing countries. *Electronic Journal of Information Systems in Developing Countries*, 25, 2006.

Raso, G., P. Vounatsou, B. H. Singer, E. K. N'Goran, M. Tanner, and J. Utzinger. An integrated approach for risk profiling and spatial prediction of *Schistosoma mansoni*-hookworm coinfection. *Proceedings of the National Academy of Sciences of the United States of America*, 103(18):6934–9, 2006. doi: 10.1073/pnas.0601559103.

Remais, J. Modelling environmentally-mediated infectious diseases of humans: transmission dynamics of schistosomiasis in China. In Michael, E., and R. C. Spear, editors, *Modelling Parasite Transmission and Control*, pages 79–98. Springer, 2010.

Remais, J., A. Hubbard, W. Zisong, and R. C. Spear. Weather-driven dynamics of an intermediate host: mechanistic and statistical population modelling of *Oncomelania hupensis*. *Journal of Applied Ecology*, 44(4):781–791, 2007. doi: 10.1111/j.1365-2664.2007.01305.x.

Remais, J., S. Liang, and R. C. Spear. Coupling hydrologic and infectious disease models to explain regional differences in schistosomiasis transmission in southwestern China. *Environmental Science and Technology*, 42(7):2643–2649, 2008. doi: 10.1021/es071052s.

Remais, J., B. Zhong, E. J. Carlton, and R. C. Spear. Model approaches for estimating the influence of time-varying socio-environmental factors on macroparasite transmission in two endemic regions. *Epidemics*, 1(4):213–20, 2009. doi: 10.1016/j.epidem.2009.10.001.

Remais, J., A. Akullian, L. Ding, and E. Seto. Analytical methods for quantifying environmental connectivity for the control and surveillance of infectious disease spread. *Journal of the Royal Society Interface*, 7(49):1181–93, 2010. doi: 10.1098/rsif.2009.0523.

Restif, O., D. T. Hayman, J. R. Pulliam, R. K. Plowright, D. B. George, A. D. Luis, A. A. Cunningham, R. A. Bowen, A. R. Fooks, T. J. O'Shea, J. L. Wood, and C. T. Webb. Model-guided fieldwork: Practical guidelines for multidisciplinary research on wildlife ecological and epidemiological dynamics. *Ecology Letters*, 15(10):1083–1094, 2012. doi: 10.1111/j.1461-0248.2012.01836.x.

Ricker, W. E. Stock and recruitment. *Journal of the Fisheries Board of Canada*, 11(5):559–623, 1954.

Rinaldo, A., E. Bertuzzo, L. Mari, L. Righetto, M. Blokesch, M. Gatto, R. Casagrandi, M. Murray, S. M. Vesenbeckh, and I. Rodriguez-Iturbe. Reassessment of the 2010-2011 Haiti cholera outbreak and rainfall-driven multiseason projections. *Proceedings of the National Academy of Sciences of the United States of America*, 109(17):6602–6607, 2012. doi: 10.1073/pnas.1203333109.

Rinaldo, A., E. Bertuzzo, M. Blokesch, L. Mari, and M. Gatto. Modeling key drivers of cholera transmission dynamics provides new perspectives for parasitology. *Trends in Parasitology*, 33(8):587 – 599, 2017. doi: 10.1016/j.pt.2017.04.002.

Rodell, M., P. Houser, U. Jambor, J. Gottschalck, K. Mitchell, C. Meng, K. Arsenault, B. Cosgrove, J. Radakovich, M. Bosilovich, et al. The global land data assimilation system. *Bulletin of the American Meteorological Society*, 85 (3):381–394, 2004.

Rodríguez-Iturbe, I., and A. Porporato. *Ecohydrology of water-controlled ecosystems: soil moisture and plant dynamics*. Cambridge University Press, 2007.

Rodriguez-Iturbe, I., R. Muneepeerakul, E. Bertuzzo, S. A. Levin, and A. Rinaldo. River networks as ecological corridors: a complex systems perspective for integrating hydrologic, geomorphologic, and ecologic dynamics. *Water Resources Research*, 45(1):1–22, 2009. doi: 10.1029/2008WR007124.

Rohani, P., D. Earn, and B. Grenfell. Opposite patterns of synchrony in sympatric disease metapopulations. *Science*, 286:968–971, 1999.

Rollinson, D. *Biomphalaria*: Natural history, ecology and schistosome transmission. In *Biomphalaria Snails and Larval Trematodes*, pages 57–79. Springer New York, New York, NY, 2011. doi: 10.1007/978-1-4419-7028-2_3.

Rollinson, D., J. R. Stothard, and V. R. Southgate. Interactions between intermediate snail hosts of the genus *Bulinus* and schistosomes of the *Schistosoma haematobium* group. *Parasitology*, 123(07):245–260, 2003. doi: 10.1017/S0031182001008046.

Rollinson, D., J. P. Webster, B. L. Webster, S. Nyakaana, A. Jorgensen, and J. R. Stothard. Genetic diversity of schistosomes and snails: implications for control. *Parasitology*, 136(13):1801, 2009. doi: 10.1017/S0031182009990412.

Rollinson, D., S. Knopp, S. Levitz, J. R. Stothard, L.-A. Tchuem Tchuenté, A. Garba, K. A. Mohammed, N. Schur, B. Person, D. G. Colley, and J. Utzinger. Time to set the agenda for schistosomiasis elimination. *Acta Tropica*, 128 (2):423–40, 2013. doi: 10.1016/j.actatropica.2012.04.013.

Ross, G. J. Parametric and nonparametric sequential change detection in R: the `cpm` package. *Journal of Statistical Software*, 66(3):1–20, 2015. doi: 10.18637/jss.v066.i03.

Rubaba, O., M. Chimbari, and S. Mukaratirwa. The role of snail aestivation in transmission of schistosomiasis in changing climatic conditions. *African Journal of Aquatic Science*, 41(2):143–150, 2016. doi: 10.2989/16085914.2016.1145103.

Rudge, J. W., J. R. Stothard, M.-G. Basáñez, A. F. Mgeni, I. S. Khamis, A. N. Khamis, and D. Rollinson. Micro-epidemiology of urinary schistosomiasis in Zanzibar: local risk factors associated with distribution of infections among schoolchildren and relevance for control. *Acta Tropica*, 105(1):45–54, 2008. doi: 10.1016/j.actatropica.2007.09.006.

Rudge, J. W., J. P. Webster, D.-B. Lu, T.-P. Wang, G.-R. Fang, and M.-G. Basáñez. Identifying host species driving transmission of schistosomiasis japonica, a multihost parasite system, in China. *Proceedings of the National Academy of Sciences of the United States of America*, 110(28):11457–62, 2013. doi: 10.1073/pnas.1221509110.

Rumisha, S. F., T. Smith, S. Abdulla, H. Masanja, and P. Vounatsou. Modelling heterogeneity in malaria transmission using large sparse spatio-temporal entomological data. *Global Health Action*, 7(1):22682, 2014.

Sandbach, F. The history of schistosomiasis research and policy for its control. *Medical history*, 20(3):259, 1976.

Sarr, B. Present and future climate change in the semi-arid region of west africa: a crucial input for practical adaptation in agriculture. *Atmospheric Science Letters*, 13(2):108–112, 2012.

Savadogo, B., A. G. Adjami, D. Zongo, J. Hattendorf, J.-N. Poda, and A. Traoré. Schistosomiasis assessment among school children and malacological factors in Burkina Faso: case of Daguilma, Koubri and Yamtenga. *Current Research in Microbiology and Biotechnology*, 3(4):701–706, 2015.

Schneider, D. C. *Quantitative ecology: measurement, models and scaling*. Academic Press, 2009.

Schur, N., P. Vounatsou, J. Utzinger, J. Stothard, and L. Tchuem-Tchuenté. Determining treatment needs at different spatial scales using geostatistical model-based risk estimates of schistosomiasis. *PLoS Neglected Tropical Diseases*, 6(9):e1773, 2012. doi: 10.1371/journal.pntd.0001773.

Scott, J. T., M. Diakhate, K. Vereecken, A. Fall, M. Diop, A. Ly, D. de Clercq, S. J. de Vlas, D. Berkvens, L. Kestens, and B. Gryseels. Human water contacts patterns in *Schistosoma mansoni* epidemic foci in northern Senegal change according to age, sex and place of residence, but are not related to intensity of infection. *Tropical Medicine and International Health*, 8(2):100–108, 2003. doi: 10.1046/j.1365-3156.2003.00993.x.

Sebastian, K. Agro-ecological Zones of Africa. Harvard Dataverse, 2009. URL http://hdl.handle.net/1902.1/22616. V2.

Secor, W. E. The effects of schistosomiasis on HIV/AIDS infection, progression and transmission. *Current Opinion in HIV and AIDS*, 7(3):254–259, 2012.

Senghor, B., O. T. Diaw, S. Doucoure, S. N. Sylla, M. Seye, I. Talla, C. T. Bâ, A. Diallo, and C. Sokhna. Efficacy of praziquantel against urinary schistosomiasis and reinfection in Senegalese school children where there is a single well-defined transmission period. *Parasites & Vectors*, 8(1):362, 2015. doi: 10.1186/s13071-015-0980-5.

Servat, E., J.-M. Lapetite, J.-C. Bader, and J.-F. Boyer. Satellite data transmission and hydrological forecasting in the fight against onchocerciasis in West Africa. *Journal of Hydrology*, 117(1-4):187–198, 1990.

Seto, E. Y. W., W. Wu, H.-Y. Liu, H.-G. Chen, A. Hubbard, A. Holt, and G. M. Davis. Impact of changing water levels and weather on *oncomelania hupensis hupensis* populations, the snail host of *schistosoma japonicum*, downstream of the Three Gorges Dam. *EcoHealth*, 5(2):149–158, 2008. doi: 10.1007/s10393-008-0169-x.

Seto, E. Y. W., J. C. Sousa-Figueiredo, M. Betson, C. Byalero, N. B. Kabatereine, and J. Russell Stothard. Patterns of intestinal schistosomiasis among mothers and young children from Lake Albert, Uganda: water contact and social networks inferred from wearable global positioning system dataloggers. *Geospatial Health*, 7(1):1–13, 2013. doi: 10.4081/gh.2012.99.

Shankman, D., B. D. Keim, and J. Song. Flood frequency in china's poyang lake region: trends and teleconnections. *International Journal of Climatology*, 26(9):1255–1266, 2006.

Shiff, C. J. Studies of *Bulinus (physopsis) globosus* in Rhodesia. I. The influence of temperature on the intrinsic rate of natural increase. *Annals of Tropical Medicine and Parasitology*, 58:94–105, 1964a.

Shiff, C. J. Studies of *Bulinus (physopsis) globosus* in Rhodesia. II. Factors influencing the relationship between age and growth. *Annals of Tropical Medicine and Parasitology*, 58:106–115, 1964b.

Shiff, C. J. Studies of *Bulinus (physopsis) globosus* in Rhodesia. III. Bionomics of a natural population existing in a temporary habitat. *Annals of Tropical Medicine and Parasitology*, 58:240–255, 1964c.

Shiff, C. J. Why reinvent the wheel? Lessons in schistosomiasis control from the past. *PLoS Neglected Tropical Diseases*, pages 1–6, 2017.

Shiff, C. J., W. Coutts, C. Yiannakis, and R. Holmes. Seasonal patterns in the transmission of *Schistosoma haematobium* in Rhodesia, and its control by winter application of molluscicide. *Transactions of the Royal Society of Tropical Medicine and Hygiene*, 73(4):375–380, 1979.

Silvester, J. Determinants of block matrices. *Mathematical Gazette*, 84:460–467, 2000.

Simini, F., M. C. Gonzalez, A. Maritan, and A.-L. Barabasi. A universal model for mobility and migration patterns. *Nature*, 484(7392):96–100, 2012. doi: 10.1038/nature10856.

Simoonga, C., J. Utzinger, S. Brooker, P. Vounatsou, C. C. Appleton, A. S. Stensgaard, A. Olsen, and T. K. Kristensen. Remote sensing, geographical information system and spatial analysis for schistosomiasis epidemiology and ecology in Africa. *Parasitology*, 136(13):1683–93, 2009. doi: 10.1017/S0031182009006222.

Sire, C., J. Langand, V. Barral, and A. Théron. Parasite (*Schistosoma mansoni*) and host (*Biomphalaria glabrata*) genetic diversity: population structure in a fragmented landscape. *Parasitology*, 122(5):545–554, 2001. doi: 10.1017/S0031182001007727.

Sivakumar, B., V. P. Singh, R. Berndtsson, and S. K. Khan. Catchment classification framework in hydrology: challenges and directions. *Journal of Hydrologic Engineering*, 20(1):A4014002, 2015. doi: 10.1061/(ASCE)HE.1943-5584.0000837.

Sivakumar, M., and G. Faustin. *Agroclimatology of West Africa: Burkina Faso.* International Crops Research Institute for the Semi-Arid Tropics, Patancheru, A.P. 502 324, India, 1987. Information Bulletin no.23.

Snelder, T. H., N. Lamouroux, J. R. Leathwick, H. Pella, E. Sauquet, and U. Shankar. Predictive mapping of the natural flow regimes of France. *Journal of Hydrology*, 373(1-2):57–67, 2009. doi: 10.1016/j.jhydrol.2009.04.011.

Snelder, T. H., T. Datry, N. Lamouroux, S. T. Larned, E. Sauquet, H. Pella, and C. Catalogne. Regionalization of patterns of flow intermittence from gauging station records. *Hydrology and Earth System Sciences*, 17(7):2685–2699, 2013. doi: 10.5194/hess-17-2685-2013.

Soares Magalhães, R. J., A. G. Barnett, and A. C. a. Clements. Geographical analysis of the role of water supply and sanitation in the risk of helminth infections of children in West Africa. *Proceedings of the National Academy of Sciences of the United States of America*, 108(50):20084–9, 2011. doi: 10.1073/pnas.1106784108.

Sokolow, S. H., K. D. Lafferty, and A. M. Kuris. Regulation of laboratory populations of snails (*Biomphalaria and Bulinus spp.*) by river prawns, *macrobrachium* spp. (Decapoda, Palaemonidae): implications for control of schistosomiasis. *Acta Tropica*, 132:64–74, 2014.

Sokolow, S. H., E. Huttinger, N. Jouanard, M. H. Hsieh, K. D. Lafferty, A. M. Kuris, G. Riveau, S. Senghor, C. Thiam, A. N'Diaye, et al. Reduced transmission of human schistosomiasis after restoration of a native river prawn that preys on the snail intermediate host. *Proceedings of the National Academy of Sciences of the United States of America*, pages 9650–9655, 2015.

Sokolow, S. H., C. L. Wood, I. J. Jones, S. J. Swartz, M. Lopez, M. H. Hsieh, K. D. Lafferty, A. M. Kuris, C. Rickards, and G. A. De Leo. Global assessment of schistosomiasis control over the past century shows targeting the snail intermediate host works best. *PLoS Neglected Tropical Diseases*, 10(7):e0004794, 2016. doi: 10.1371/journal.pntd.0004794.

Sokolow, S. H., C. L. Wood, I. J. Jones, K. D. Lafferty, A. M. Kuris, M. H. Hsieh, and G. A. De Leo. To reduce the global burden of human schistosomiasis, use ’old fashioned’ snail control. *Trends in Parasitology*, 2017.

Sonwa, D. J., A. Dieye, E.-H. El Mzouri, A. Majule, F. T. Mugabe, N. Omolo, H. Wouapi, J. Obando, and N. Brooks. Drivers of climate risk in African agriculture. *Climate and Development*, 9(5):383–398, 2017.

Sood, A., L. Muthuwatta, and M. McCartney. A SWAT evaluation of the effect of climate change on the hydrology of the Volta River basin. *Water International*, 38(3):297–311, 2013.

Soti, V., C. Puech, D. L. Seen, A. Bertran, C. Vignolles, B. Mondet, N. Dessay, and A. Tran. The potential for remote sensing and hydrologic modelling to assess the spatio-temporal dynamics of ponds in the Ferlo Region (Senegal). *Hydrology and Earth System Sciences*, 14:1449–1464, 2010.

Soti, V., A. Tran, P. Degenne, V. Chevalier, D. L. Seen, Y. Thiongane, M. Diallo, J.-F. Guégan, and D. Fontenille. Combining hydrology and mosquito population models to identify the drivers of Rift Valley fever emergence in semi-arid regions of West Africa. *PLoS neglected tropical diseases*, 6(8):e1795, 2012.

Southgate, V. R. Schistosomiasis in the Senegal River Basin: before and after the construction of the dams at Diama, Senegal and Manantali, Mali and future prospects. *Journal of Helminthology*, 71(2):125–132, 1997. doi: 10.1017/S0022149X00015790.

Southgate, V. R., D. de Clercq, M. Sène, D. Rollinson, a. Ly, and J. Vercruysse. Observations on the compatibility between *Bulinus spp.* and *Schistosoma haematobium* in the Senegal River basin. *Annals of Tropical Medicine and Parasitology*, 94(2):157–64, 2000. doi: 10.1080/00034980057491.

Souza, R., X. Feng, A. Antonino, S. Montenegro, E. Souza, and A. Porporato. Vegetation response to rainfall seasonality and interannual variability in tropical dry forests. *Hydrological Processes*, 30(20):3583–3595, 2016. doi: 10.1002/hyp.10953.

Sow, S., K. Polman, K. Vereecken, J. Vercruysse, B. Gryseels, and S. J. de Vlas. The role of hygienic bathing after defecation in the transmission of *Schistosoma mansoni*. *Transactions of the Royal Society of Tropical Medicine and Hygiene*, 102(6):542–547, 2008. doi: 10.1016/j.trstmh.2008.02.016.

Sow, S., S. J. de Vlas, F. Stelma, K. Vereecken, B. Gryseels, and K. Polman. The contribution of water contact behavior to the high *Schistosoma mansoni* infection rates observed in the Senegal river basin. *BMC infectious diseases*, 11 (1):198, 2011. doi: 10.1186/1471-2334-11-198.

Standley, C. J., N. B. Kabatereine, C. N. Lange, N. J. S. Lwambo, and J. R. Stothard. Molecular epidemiology and phylogeography of *Schistosoma mansoni* around Lake Victoria. *Parasitology*, 137(13):1937–49, 2010. doi: 10.1017/S0031182010000788.

Steinmann, P., J. Keiser, R. Bos, M. Tanner, and J. Utzinger. Schistosomiasis and water resources development: systematic review, meta-analysis, and estimates of people at risk. *Lancet Infectious Diseases*, 6(7):411–25, 2006. doi: 10.1016/S1473-3099(06)70521-7.

Stensgaard, A. S., A. Jørgensen, N. B. Kabatereine, C. Rahbek, and T. K. Kristensen. Geospatial Health - Modeling freshwater snail habitat suitability and areas of potential snail-borne disease transmission in Uganda. *Geospatial Health*, pages 93–104, 2006.

Stensgaard, A.-S., J. Utzinger, P. Vounatsou, E. Hürlimann, N. Schur, C. F. L. Saarnak, C. Simoonga, P. Mubita, N. B. Kabatereine, L.-A. Tchuem Tchuenté, C. Rahbek, and T. K. Kristensen. Large-scale determinants of intestinal schistosomiasis and intermediate host snail distribution across Africa: does climate matter? *Acta Tropica*, 128(2): 378–390, 2013. doi: 10.1016/j.actatropica.2011.11.010.

Stensgaard, A.-S., M. Booth, G. Nikulin, and N. McCreesh. Combining process-based and correlative models improves predictions of climate change effects on *Schistosoma mansoni* transmission in eastern Africa. *Geospatial Health*, 11(1s), 2016. doi: 10.4081/gh.2016.406.

Stokols, D. Translating social ecological theory into guidelines for community health promotion. *American Journal of Health Promotion*, 10(4):282–298, 1996. doi: 10.4278/0890-1171-10.4.282.

Stothard, J. R. Improving control of African schistosomiasis: towards effective use of rapid diagnostic tests within an appropriate disease surveillance model. *Transactions of the Royal Society of Tropical Medicine and Hygiene*, 103(4): 325–32, 2009. doi: 10.1016/j.trstmh.2008.12.012.

Stothard, J. R., and A.-F. Gabrielli. Schistosomiasis in african infants and preschool children: to treat or not to treat? *Trends in Parasitology*, 23(3):83–86, 2007.

Stothard, J. R., J. C. Sousa-Figueiredo, M. Betson, E. Y. W. Seto, and N. B. Kabatereine. Investigating the spatial micro-epidemiology of diseases within a point-prevalence sample: a field applicable method for rapid mapping of households using low-cost GPS-dataloggers. *Transactions of the Royal Society of Tropical Medicine and Hygiene*, 105(9):500–6, 2011. doi: 10.1016/j.trstmh.2011.05.007.

Stothard, J. R., J. C. Sousa-Figueiredo, M. Betson, A. Bustinduy, and J. Reinhard-Rupp. Schistosomiasis in african infants and preschool children: let them now be treated! *Trends in Parasitology*, 29(4):197–205, 2013.

Stothard, J. R., M. C. Stanton, A. L. Bustinduy, J. C. Sousa-Figueiredo, G. J. Van Dam, M. Betson, D. Waterhouse, S. Ward, F. Allan, A. A. Hassan, M. A. Al-Helal, Z. A. Memish, and D. Rollinson. Diagnostics for schistosomiasis in Africa and Arabia: a review of present options in control and future needs for elimination. *Parasitology*, 141(14): 1947–61, 2014. doi: 10.1017/S0031182014001152.

Stothard, J. R., S. J. Campbell, M. Y. Osei-Atweneboana, T. Durant, M. C. Stanton, N.-K. Biritwum, D. Rollinson, D. R. E. Ombede, and L.-A. Tchuem-Tchuenté. Towards interruption of schistosomiasis transmission in sub-Saharan Africa: developing an appropriate environmental surveillance framework to guide and to support "end game" interventions. *Infectious Diseases of Poverty*, 6(1):10, 2017.

Strong, D. R. Density-vague population change. *Trends in Ecology and Evolution*, 1(2):39 – 42, 1986. doi: 10.1016/0169-5347(86)90071-6.

Sturrock, H. J. W., P. W. Gething, A. C. A. Clements, and S. Brooker. Optimal survey designs for targeting chemotherapy against soil-transmitted helminths: effect of spatial heterogeneity and cost-efficiency of sampling. *American Journal of Tropical Medicine and Hygiene*, 82(6):1079–87, 2010. doi: 10.4269/ajtmh.2010.09-0702.

Sturrock, R. F. Current concepts of snail control. *Memórias do Instituto Oswaldo Cruz*, 90(2):241–248, 1995. doi: 10.1590/S0074-02761995000200020.

Südmeier-Rieux, K., H. Masundire, A. Rizvi, and R. Rietbergen. *Ecosystems, livelihoods and disasters: An integrated approach to disaster risk managment*, volume 4. IUCN, Gland, Switzerland and Cambridge, UK, 2006. ISBN 9782831709284.

Suter, R., M. Tanner, C. Borel, K. Hostettmann, and T. A. Freyvogel. Laboratory and field trials at Ifakara (Kilombero District, Tanzania) on the plant molluscicide Swartzia madagascariensis. *Acta Tropica*, 43(1):69–83, 1986.

Suzuki, R., and H. Shimodaira. `pvclust`*: Hierarchical clustering with p-values via multiscale bootstrap resampling*, 2015. R package version 2.0-0.

Swartz, S. J., G. A. De Leo, C. L. Wood, and S. H. Sokolow. Infection with schistosome parasites in snails leads to increased predation by prawns: implications for human schistosomiasis control. *Journal of Experimental Biology*, 218(24):3962–3967, 2015.

Talla, I., A. Kongs, P. Verle, J. Belot, S. Sarr, A. Coll, et al. Outbreak of intestinal schistosomiasis in the Senegal river basin. *Annales de la Societe Belge de Medecine Tropicale*, 70(3):173–180, 1990.

Tambo, E., L. Ai, X. Zhou, J.-H. Chen, W. Hu, R. Bergquist, J.-G. Guo, J. Utzinger, M. Tanner, and X.-N. Zhou. Surveillance-response systems: the key to elimination of tropical diseases. *Infectious Diseases of Poverty*, 3 (1):1–11, 2014. doi: 10.1186/2049-9957-3-17.

Tambo, E., J. Tei-Wu, X. Ning, W. Hu, and Z. Xiao-Nong. Impact evaluation of schistosomiasis control into elimination interventions models in P. R. of China. *Journal of Microbiology and Infectious Diseases*, 7(2):104–118, 2017.

Tchuem Tchuenté, L. A., V. R. Southgate, J. Jourdane, B. L. Webster, and J. Vercruysse. *Schistosoma intercalatum*: An endangered species in Cameroon? *Trends in Parasitology*, 19(9):389–393, 2003. doi: 10.1016/S1471-4922(03)00193-4.

Tchuem Tchuenté, L.-A., S. C. Momo, J. R. Stothard, and D. Rollinson. Efficacy of praziquantel and reinfection patterns in single and mixed infection foci for intestinal and urogenital schistosomiasis in Cameroon. *Acta Tropica*, 128(2):275 – 283, 2013. doi: 10.1016/j.actatropica.2013.06.007.

Tchuem Tchuenté, L.-A., D. Rollinson, J. R. Stothard, and D. Molyneux. Moving from control to elimination of schistosomiasis in sub-Saharan Africa: time to change and adapt strategies. *Infectious Diseases of Poverty*, 6(1):42, 2017. doi: 10.1186/s40249-017-0256-8.

Theron, A., A. Rognon, B. Gourbal, and G. Mitta. Multi-parasite host susceptibility and multi-host parasite infectivity: a new approach of the *Biomphalaria glabrata/Schistosoma mansoni* compatibility polymorphism. *Infection, Genetics and Evolution*, 26:80–88, 2014. doi: 10.1016/j.meegid.2014.04.025.

Thomas, J. D., and M. Benjamin. The effects of population density on growth and reproduction of *Biomphalaria glabrata* (Say)(Gasteropoda: Pulmonata). *Journal of Animal Ecology*, pages 31–50, 1974.

Tilman, D., R. M. May, C. L. Lehman, and M. A. Nowak. Habitat destruction and the extinction debt. *Nature*, 371(1): 65–66, 1994. doi: 10.1038/371065a0.

Tompkins, A. M., and V. Ermert. A regional-scale, high resolution dynamical malaria model that accounts for population density, climate and surface hydrology. *Malaria Journal*, 12(1):65, 2013.

Toms, J. D., and M. L. Lesperance. Piecewise regression: a tool for identifying ecological thresholds. *Ecology*, 84(8): 2034–2041, 2003.

Touré, S., Y. Zhang, E. Bosqué-Oliva, C. Ky, A. Ouedraogo, A. Koukounari, A. F. Gabrielli, S. Bertrand, J. P. Webster, and A. Fenwick. Two-year impact of single praziquantel treatment on infection in the national control programme on schistosomiasis in Burkina Faso. *Bulletin of the World Health Organization*, 86(10):780–787A, 2008. doi: 10.1590/S0042-96862008001000014.

Trancoso, R., J. R. Larsen, C. McAlpine, T. R. McVicar, and S. Phinn. Linking the Budyko framework and the Dunne diagram. *Journal of Hydrology*, 535:581–597, 2016. doi: 10.1016/j.jhydrol.2016.02.017.

Trancoso, R., S. Phinn, T. R. McVicar, J. R. Larsen, and C. A. McAlpine. Regional variation in streamflow drivers across a continental climatic gradient. *Ecohydrology*, page e1816, 2017. doi: 10.1002/eco.1816.

Traoré, I. *Geographic determinants of human schistosomiasis transmission in the Sourou Valley, Burkina Faso*. PhD thesis, University of Goettingen, 2013.

Traoré, I., A. Sié, B. Coulibaly, M. Yé, D. Karthe, and M. Kappas. Rapid screening and mapping of urinary schistosomiasis prevalence at the village scale in the Sourou Valley, Burkina Faso: Adapting the school-base questionnaire method. Technical report, Gottingen Internation Health Network (GIHN), 2012.

Traoré, I., D. Karthe, A. Sié, V. Coulibaly, and M. Kappas. Influence of air temperature on children water contacts with respect to schistosomiasis transmission risk in the Sourou Valley, Burkina Faso. *Stochastic Environmental Research and Risk Assessment*, 2016. doi: 10.1007/s00477-016-1214-x.

Troch, P. A., T. Lahmers, A. Meira, R. Mukherjee, J. W. Pedersen, T. Roy, and R. Valdés-Pineda. Catchment coevolution: a useful framework for improving predictions of hydrological change? *Water Resources Research*, 51(7):4903–4922, 2015. doi: 10.1002/2015WR017032.

Truscott, J., D. Gurarie, R. Alsallaq, J. Toor, N. Yoon, S. Farrell, H. Turner, A. Phillips, H. Aurelio, J. Ferro, C. King, and R. Anderson. A comparison of two mathematical models of the impact of mass drug administration on the transmission and control of schistosomiasis. *Epidemics*, 18:29–37, 2017. doi: 10.1016/j.epidem.2017.02.003.

Tuite, A. R., J. Tien, M. Eisenberg, D. J. D. Earn, J. Ma, and D. N. Fisman. Cholera Epidemic in Haiti, 2010: Using a transmission model to explain spatial spread of disease and identify optimal control interventions. *Annals of Internal Medicine*, 154(9):593–U59, 2011. doi: 10.1059/0003-4819-154-9-201105030-00334.

Turchin, P. Rarity of density dependence or population regulation with lags? *Nature*, 344(6267):660–663, 1990.

Turchin, P. *Complex Population Dynamics: a Theoretical/Empirical Synthesis*, volume 35. Princeton University Press, 2003.

Uchoa, E., S. M. Barreto, J. O. Firmo, H. L. Guerra, F. G. Pimenta, and M. F. F. L. e Costa. The control of schistosomiasis in Brazil: an ethno-epidemiological study of the effectiveness of a community mobilization program for health education. *Social Science and Medicine*, 51(10):1529 – 1541, 2000. doi: 10.1016/S0277-9536(00)00052-6.

Utzinger, J., and D. de Savigny. Control of neglected tropical diseases: integrated chemotherapy and beyond. *PLoS Medicine*, 3(5):e112, 2006. doi: 10.1371/journal.pmed.0030112.

Utzinger, J., E. K. N'Goran, M. Tanner, and C. Lengeler. Simple anamnestic questions and recalled water-contact patterns for self-diagnosis of *Schistosoma mansoni* infection among schoolchildren in western Côte d'Ivoire. *American Journal of Tropical Medicine and Hygiene*, 62(5):649–655, 2000.

Utzinger, J., E. K. N'Goran, C. R. Caffrey, and J. Keiser. From innovation to application: social-ecological context, diagnostics, drugs and integrated control of schistosomiasis. *Acta Tropica*, 120:S121–S137, 2011.

Van Bocxlaer, B., C. Albrecht, and J. R. Stauffer. Growing population and ecosystem change increase human schistosomiasis around Lake Malawi. *Trends in Parasitology*, 30(5):217–220, 2014. doi: 10.1016/j.pt.2014.02.006.

van den Broeck, F., G. E. Maes, M. H. Larmuseau, D. Rollinson, I. Sy, D. Faye, F. A. Volckaert, K. Polman, and T. Huyse. Reconstructing colonization dynamics of the human parasite *Schistosoma mansoni* following anthropogenic environmental changes in Northwest Senegal. *PLoS Neglected Tropical Diseases*, 9(8):1–21, 2015. doi: 10.1371/journal.pntd.0003998.

van der Werf, M. J., S. J. de Vlas, S. Brooker, C. W. Looman, N. J. Nagelkerke, J. F. Habbema, and D. Engels. Quantification of clinical morbidity associated with schistosome infection in sub-Saharan Africa. *Acta Tropica*, 86(2):125–139, 2003.

Vazquez-Prokopec, G. M., T. A. Perkins, L. A. Waller, A. L. Lloyd, R. C. Reiner, T. W. Scott, and U. Kitron. Coupled heterogeneities and their impact on parasite transmission and control. *Trends in Parasitology*, 32(5):356–367, 2016. doi: 10.1016/j.pt.2016.01.001.

Vercruysse, J., D. J. Shaw, and J. De Bont. Index of potential contamination for schistosomiasis. *Trends in Parasitology*, 17(6):256–261, 2001.

Vico, G., S. E. Thompson, S. Manzoni, A. Molini, J. D. Albertson, J. S. Almeida-Cortez, P. A. Fay, X. Feng, A. J. Guswa, H. Liu, T. G. Wilson, and A. Porporato. Climatic, ecophysiological, and phenological controls on plant ecohydrological strategies in seasonally dry ecosystems. *Ecohydrology*, 8(4):660–681, 2015. doi: 10.1002/eco.1533.

Wagener, T., M. Sivapalan, P. Troch, and R. Woods. Catchment Classification and Hydrologic Similarity. *Geography Compass*, 1:1–31, 2007. doi: 10.1111/j.1749-8198.2007.00039.x.

Walz, Y., M. Wegmann, S. Dech, G. Raso, and J. Utzinger. Risk profiling of schistosomiasis using remote sensing: approaches, challenges and outlook. *Parasites & Vectors*, 8(1):163, 2015a. doi: 10.1186/s13071-015-0732-6.

Walz, Y., M. Wegmann, S. Dech, P. Vounatsou, J. N. Poda, E. K. N'Goran, J. Utzinger, and G. Raso. Modeling and validation of environmental suitability for schistosomiasis transmission using remote sensing. *PLoS Neglected Tropical Diseases*, 9(11):e0004217–e0004217, 2015b.

Wan, Z. MYD11A2 MODIS/Aqua Land Surface Temperature/Emissivity 8-Day L3 Global 1km SIN Grid V006. NASA EOSDIS Land Processes DAAC, 2015.

Wang, D., and L. Wu. Similarity between runoff coefficient and perennial stream density in the Budyko framework. *Hydrology and Earth System Sciences*, 9(6):7571–7589, 2012. doi: 10.5194/hess-17-315-2013.

Wang, L., J. Utzinger, and X. N. Zhou. Schistosomiasis control: experiences and lessons from China. *Lancet*, 372 (9652):1793–1795, 2008. doi: 10.1016/S0140-6736(08)61358-6.

Wang, R., T. Wang, L. Wang, J. Guo, Q. Yu, J. Xu, F. Gao, Z. Yin, and X. Zhou. Study on the re-emerging situation of schistosomiasis epidemics in areas already under control and interruption. *Zhonghua liu xing bing xue za zhi= Zhonghua liuxingbingxue zazhi*, 25(7):564–567, 2004.

WASHwatch. Burkina faso - country statistics. WASHwatch, 2017.

Webbe, G. Observations on the seasonal fluctuation of snail-population densities in the northern province of Tanganyika. *Annals of Tropical Medicine and Parasitology*, 54(1):54–9, 1960.

Webster, B. L., V. R. Southgate, and L. A. T. Tchuente. Mating interactions between *Schistosoma haematobium* and *S. mansoni*. *Journal of Helminthology*, 73(4):351–356, 1999.

Webster, J. P., and C. M. Davies. Coevolution and compatibility in the snail schistosome system. *Parasitology*, 123 (2001):S41–S56, 2001.

Webster, J. P., C. M. Gower, and A. J. Norton. Evolutionary concepts in predicting and evaluating the impact of mass chemotherapy schistosomiasis control programmes on parasites and their hosts. *Evolutionary Applications*, 1: 66–83, 2008. doi: DOI10.1111/j.1752-4571.2007.00012.x.

Weijs, S. V., R. Mutzner, and M. B. Parlange. Could electrical conductivity replace water level in rating curves for alpine streams? *Water Resources Research*, 49(1):343–351, 2013.

Weiss, D. J., S. Bhatt, B. Mappin, T. P. Van Boeckel, D. L. Smith, S. I. Hay, and P. W. Gething. Air temperature suitability for *Plasmodium falciparum* malaria transmission in Africa 2000-2012: a high-resolution spatiotemporal prediction. *Malaria Journal*, 13(1):171, 2014.

Weiss, D. J., B. Mappin, U. Dalrymple, S. Bhatt, E. Cameron, S. I. Hay, and P. W. Gething. Re-examining environmental correlates of plasmodium falciparum malaria endemicity: a data-intensive variable selection approach. *Malaria Journal*, 14(1):68, 2015.

Wesolowski, A., N. Eagle, A. M. Noor, R. W. Snow, and C. O. Buckee. The impact of biases in mobile phone ownership on estimates of human mobility. *Journal of the Royal Society Interface*, 10(81):20120986, 2013. doi: 10.1098/rsif.2012.0986.

White, F. The vegetation of Africa, a descriptive memoir to accompany the UNESCO/AETFAT/UNSO vegetation map of Africa (3 Plates, Northwestern Africa, Northeastern Africa, and Southern Africa, 1: 5,000,000), 1983.

Wiegand, R. E., P. N. M. Mwinzi, S. P. Montgomery, Y. L. Chan, K. Andiego, M. Omedo, G. Muchiri, M. O. Ogutu, F. Rawago, M. R. Odiere, D. M. S. Karanja, and W. E. Secor. A persistent hotspot of *Schistosoma mansoni* infection in a five-year randomized trial of praziquantel preventative chemotherapy strategies. *Journal of Infectious Diseases*, page jix496, 2017. doi: 10.1093/infdis/jix496.

Williams, G. M., A. C. Sleigh, Y. Li, Z. Feng, G. M. Davis, H. Chen, A. G. P. Ross, R. Bergquist, and D. P. McManus. Mathematical modelling of schistosomiasis japonica: comparison of control strategies in the People's Republic of China. *Acta Tropica*, 82(2):253–262, 2002. doi: 10.1016/S0001-706X(02)00017-7.

Woolhouse, M. On the application of mathematical models of schistosome transmission dynamics. I. Natural transmission. *Acta Tropica*, 49(4):241–270, 1991. doi: 10.1016/0001-706X(91)90077-W.

Woolhouse, M., and S. Chandiwana. Population dynamics model for *Bulinus globosus*, intermediate host for *Schistosoma haematobium*, in river habitats. *Acta Tropica*, 47(3):151–160, 1990a. doi: 10.1016/0001-706X(90)90021-Q.

Woolhouse, M. E. A mark-recapture method for ecological studies of schistosomiasis vector snail populations. *Annals of tropical medicine and parasitology*, 82(5):485–97, 1988a.

Woolhouse, M. E., and S. K. Chandiwana. Temporal patterns in the epidemiology of schistosome infections of snails: a model for field data. *Parasitology*, 100 Pt 2:247–253, 1990b.

Woolhouse, M. E., C. Dye, J.-F. Etard, T. Smith, J. Charlwood, G. Garnett, P. Hagan, J. Hii, P. Ndhlovu, R. Quinnell, et al. Heterogeneities in the transmission of infectious agents: implications for the design of control programs. *Proceedings of the National Academy of Sciences of the United States of America*, 94(1):338–342, 1997.

Woolhouse, M. E. J. Passive dispersal of *Bulinus globosus*. *Annals of Tropical Medicine and Parasitology*, 82(3):315–317, 1988b. doi: 10.1080/00034983.1988.11812250.

Woolhouse, M. E. J. On the application of mathematical models of schistosome transmission dynamics. II. Control. *Acta Tropica*, 50(3):189–204, 1992a. doi: 10.1016/0001-706X(92)90076-A.

Woolhouse, M. E. J. Population biology of the freshwater snail *Biomphalaria pfeifferi* in the Zimbabwe highveld. *Journal of Applied Ecology*, 29(3):687–694, 1992b.

Woolhouse, M. E. J., and S. K. Chandiwana. Spatial and temporal heterogeneity in the population dynamics of *Bulinus globosus* and *Biomphalaria pfeifferi* and in the epidemiology of their infection with schistosomes. *Parasitology*, 98 (01):21–34, 1989.

Woolhouse, M. E. J., and S. K. Chandiwana. Population biology of the freshwater snail *bulinus globosus* in the zimbabwe highveld. *Journal of Applied Ecology*, 27(1):41–59, 1990c. doi: 10.2307/2403567.

Woolhouse, M. E. J., and P. Taylor. Survival rates of *Bulinus globosus* during aestivation. *Annals of Tropical Medicine and Parasitology*, 84(3):293–294, 1990.

Woolhouse, M. E. J., C. H. Watts, and S. K. Chandiwana. Heterogeneities in transmission rates and the epidemiology of schistosome infection. *Proceedings of the Royal Society of London B: Biological Sciences*, 245(1313):109–114, 1991.

Woolhouse, M. E. J., J.-F. Etard, K. Dietz, P. D. Ndhlovu, and S. K. Chandiwana. Heterogeneities in schistosome transmission dynamics and control. *Parasitology*, 117(05):475–482, 1998.

World Health Organization. World Health Assembly Resolution WHA 54.19 Elimination of schistosomiasis. *Geneva: World Health Organization*, 2001.

World Health Organization. *Helminth control in school-age children: a guide for managers of control programmes*. Geneva: World Health Organization, 2011.

World Health Organization. World Health Assembly Resolution WHA 65.21 Elimination of schistosomiasis. *Geneva: World Health Organization*, 2012a.

World Health Organization. WHO | Public health surveillance. World Health Organization, 2012b.

World Health Organization. The London Declaration on Neglected Tropical Diseases. *Geneva: World Health Organization*, 2012c.

World Health Organization. *Schistosomiasis: progress report 2001-2011, strategic plan 2012-2020*. World Health Organization, WHO Press, World Health Organization, 20 Avenue Appia, 1211 Geneva 27, Switzerland, 2013a. ISBN 9789241503174.

World Health Organization. World Health Assembly Resolution WHA 66.12 Neglected tropical diseases. *Geneva: World Health Organization*, 2013b.

World Health Organization. *Water, sanitation and hygiene for accelerating and sustaining progress on neglected tropical diseases: a new Global Strategy 2015-2020*, volume 8. Oxford University Press, 2016.

World Health Organization. *Field use of molluscicides in schistosomiasis control programmes: an operational manual for programme managers*. World Health Organization, 2017a. ISBN 978-92-4-151199-5.

World Health Organization. Schistosomiasis: number of people treated worldwide in 2016. *Weekly Epidemiological Record*, 92(49):749–760, 2017b.

World Health Organization and UNICEF. Progress on drinking water, sanitation and hygiene: 2017 update and sdg baselines. Technical report, World Health Organization, 2017.

Wu, J.-Y., Y.-B. Zhou, Y. Chen, S. Liang, L.-H. Li, S.-B. Zheng, S.-p. Zhu, G.-H. Ren, X.-X. Song, and Q.-W. Jiang. Three Gorges Dam: impact of water level changes on the density of schistosome-transmitting snail *oncomelania hupensis* in dongting lake area, china. *PLoS Neglected Tropical Diseases*, 9(6):e0003882, 2015. doi: 10.1371/journal.pntd.0003882.

Xiang, J., H. Chen, and H. Ishikawa. A mathematical model for the transmission of *Schistosoma japonicum* in consideration of seasonal water level fluctuations of Poyang Lake in Jiangxi, China. *Parasitology International*, 62 (2):118–126, 2013. doi: 10.1016/j.parint.2012.10.004.

Xie, P., and P. A. Arkin. Global precipitation: a 17-year monthly analysis based on gauge observations, satellite estimates, and numerical model outputs. *Bulletin of the American Meteorological Society*, 78(11):2539–2558, 1997.

Xu, B., P. Gong, E. Seto, S. Liang, C. Yang, S. Wen, D. Qiu, X. Gu, and R. Spear. A spatial-temporal model for assessing the effects of intervillage connectivity in schistosomiasis transmission. *Annals of the Association of American Geographers*, 96(1):31–46, 2006. doi: 10.1111/j.1467-8306.2006.00497.x.

Xu, J., J.-F. Xu, S.-Z. Li, L.-J. Zhang, Q. Wang, H.-H. Zhu, and X.-N. Zhou. Integrated control programmes for schistosomiasis and other helminth infections in P.R. China. *Acta Tropica*, 141(Part B):332 – 341, 2015a. doi: 10.1016/j.actatropica.2013.11.028.

Xu, J., Q. Yu, L.-A. T. Tchuenté, R. Bergquist, M. Sacko, J. Utzinger, D.-D. Lin, K. Yang, L.-J. Zhang, Q. Wang, S.-Z. Li, J.-G. Guo, and X.-N. Zhou. Enhancing collaboration between china and african countries for schistosomiasis control. *Lancet Infectious Diseases*, 16(3):376 – 383, 2016. doi: 10.1016/S1473-3099(15)00360-6.

Xu, R., and D. Wunsch. Survey of clustering algorithms. *IEEE Transactions on Neural Networks*, 16(3):645–678, 2005.

Xu, X., W. Liu, B. R. Scanlon, L. Zhang, and M. Pan. Local and global factors controlling water-energy balances within the Budyko framework. *Geophysical Research Letters*, 40(23):6123–6129, 2013. doi: 10.1002/2013GL058324.

Xu, X., D. Medvigy, and I. Rodriguez-Iturbe. Relation between rainfall intensity and savanna tree abundance explained by water use strategies. *Proceedings of the National Academy of Sciences of the United States of America*, 112(42): 12992–12996, 2015b. doi: 10.1073/pnas.1517382112.

Yakob, L., R. J. S. Magalhães, D. J. Gray, G. Milinovich, N. Wardrop, R. Dunning, J. Barendregt, F. Bieri, G. M. Williams, and A. C. Clements. Modelling parasite aggregation: disentangling statistical and ecological approaches. *International Journal for Parasitology*, 44(6):339–342, 2014.

Yang, G.-J., M. Tanner, J. Utzinger, J. B. Malone, R. Bergquist, E. Y. Chan, Q. Gao, X.-N. Zhou, and others. Malaria surveillance-response strategies in different transmission zones of the People's Republic of China: preparing for climate change. *Malaria Journal*, 11(1):426, 2012a.

Yang, K., L.-P. Sun, Y.-X. Huang, G.-J. Yang, F. Wu, D.-R. Hang, W. Li, J.-F. Zhang, Y.-S. Liang, and X.-N. Zhou. A real-time platform for monitoring schistosomiasis transmission supported by Google Earth and a web-based geographical information system. *Geospatial Health*, 6(2):195–203, 2012b.

Yang, K., X. N. Zhou, T. W. Jia, G. J. Yang, X. H. Wu, X. W. Shi, H. J. Li, P. Steinmann, J. Utzinger, and R. Bergquist. Eco-social determinants of *Schistosoma japonicum* infection supported by multi-level modelling in Eryuan county, People's Republic of China. *Acta Tropica*, 141(Part B):391–398, 2015. doi: 10.1016/j.actatropica.2014.04.013.

Yu, K., and J. Zhang. A three-parameter asymmetric Laplace distribution and its extension. *Communications in Statistics - Theory and Methods*, 34(9-10):1867–1879, 2005. doi: 10.1080/03610920500199018.

Zhang, L., N. Potter, K. Hickel, Y. Zhang, and Q. Shao. Water balance modeling over variable time scales based on the Budyko framework - model development and testing. *Journal of Hydrology*, 360(1-4):117–131, 2008. doi: 10.1016/j.jhydrol.2008.07.021.

Zhang, Y., and F. Chiew. Estimation of mean annual runoff across southeast Australia by incorporating vegetation types into Budyko-framework. *Australian Journal of Water Resources*, 15(2):109–121, 2012. doi: 10.7158/W10-840.2012.15.2.

Zhou, X., L. Dandan, Y. Huiming, C. Honggen, S. Leping, Y. Guojing, H. Qingbiao, L. Brown, and J. Malone. Use of landsat TM satellite surveillance data to measure the impact of the 1998 flood on snail intermediate host dispersal in the lower Yangtze River Basin. *Acta Tropica*, 82(2):199–205, 2002. doi: 10.1016/S0001-706X(02)00011-6.

Zhou, X.-N., G.-J. Yang, K. Yang, X.-H. Wang, Q.-B. Hong, L.-P. Sun, J. B. Malone, T. K. Kristensen, N. R. Bergquist, and J. Utzinger. Potential impact of climate change on schistosomiasis transmission in china. *American Journal of Tropical Medicine and Hygiene*, 78(2):188–194, 2008.

Zhou, X.-N., R. Bergquist, and M. Tanner. Elimination of tropical disease through surveillance and response. *Infectious Diseases of Poverty*, 2(1):1, 2013. doi: 10.1186/2049-9957-2-1.

Zhou, Y.-B., S. Liang, Y. Chen, and Q.-W. Jiang. The Three Gorges Dam: does it accelerate or delay the progress towards eliminating transmission of schistosomiasis in China? *Infectious Diseases of Poverty*, 5(1):63, 2016.

Zida, A., J. Briegel, I. Kabré, M. P. Sawadogo, I. Sangaré, S. Bamba, A. Yacouba, A. Ouédraogo, D. Yonli, F. Drabo, L. K. Traoré, R. Ouédraogo-Traoré, R. T. Guiguemdé, and J. Wacker. Epidemiological and clinical aspects of urogenital schistosomiasis in women, in Burkina Faso, West Africa. *Infectious Diseases of Poverty*, 5(1):81, 2016. doi: 10.1186/s40249-016-0174-1.

Zongo, D., B. Kabre, D. Dianou, B. Savadogo, and J. Poda. Importance of malacological factors in the transmission of *schistosoma haematobium* in two dams in the Province of Oubritenga (Burkina Faso). *Research Journal of Environmental Sciences*, 3(1):127–133, 2009. doi: 10.3923/rjes.2009.127.133.

Zongo, D., B. G. Kabre, D. Dayeri, B. Savadogo, and J. N. Poda. [Comparative study of schistosomiasis transmission (urinary and intestinal forms) at 10 sites in Burkina Faso (in sub-Saharan Africa)]. *Médecine et Santé Tropicales*, 22 (3):323–9, 2012. doi: 10.1684/mst.2012.0089.

Zongo, D., B. G. Kabre, D. Dayeri, B. Savadogo, and J.-N. Poda. Parasitological profile of two forms of schistosomiasis (urinary and intestinal forms) at ten sites in Burkina Faso (Sub-Saharan African country). *Comptes Rendus Biologies*, 336(5-6):317–9, 2013. doi: 10.1016/j.crvi.2013.04.014.

Zorom, M., B. Barbier, O. Mertz, and E. Servat. Diversification and adaptation strategies to climate variability: A farm typology for the sahel. *Agricultural Systems*, 116(0):7 – 15, 2013. doi: 10.1016/j.agsy.2012.11.004.

Francisco Javier Perez-Saez

Av. Mon-Loisir 4; 1006 Lausanne; Suisse;
Tel: +41 78 824 5990; Email: javier.perezsaez@gmail.com
Born 01/07/1990;
Venezuelian- Italian.

EDUCATION

Since 2014	PhD student in the Ecohydrology Laboratory supervised by prof. Andrea Rinaldo at the Ecole Polytechnique Fédérale de Lausanne (EPFL) Switzerland on field and modeling studies of schistosomiasis transmission in Burkina Faso.
2013	Msc in Environmental Science and Engineering. Specialization in Water, Soil and Ecosystem Engineering from the EPFL (grade of 5,84/6).
Spring 2013	Master Thesis supervised by prof. Andrea Rinaldo on endemic cholera modelling in Dhaka, Bangladesh, co-supervised by prof. Mercedes Pascual and prof. Aaron King at the Ecology and Evolutionary Biology Department of the University of Michigan.
2008-2013	Environmental Science and Engineering studies (BA/MA) at the EPFL. 1-year exchange at the Royal Institute of Technology (KTH), Stockholm, Sweden.
1998-2008	School and High School at the Lycée Français de Rome – Lycée Chateaubriand, Italy. Science Baccalauréat, Earth and Life Sciences option (grade of 19/20).

PUBLICATIONS

Perez-Saez, Javier, Theophile Mande, Joshua Larsen, Natalie Ceperley, and Andrea Rinaldo. "Classification and prediction of river network ephemerality and its relevance for waterborne disease epidemiology." *Advances in Water Resources* 110C (2017): 263-278.

Mari, Lorenzo, Manuela Ciddio, Renato Casagrandi, **Javier Perez-Saez**, Enrico Bertuzzo, Andrea Rinaldo, Susanne H. Sokolow, Giulio A. De Leo, and Marino Gatto. "Heterogeneity in schistosomiasis transmission dynamics." *Journal of Theoretical Biology* 432 (2017): 87-99.

Perez-Saez, Javier, Theophile Mande, Natalie Ceperley, Enrico Bertuzzo, Lorenzo Mari, Marino Gatto, and Andrea Rinaldo. "Hydrology and density feedbacks control the ecology of intermediate hosts of schistosomiasis across habitats in seasonal climates." *Proceedings of the National Academy of Sciences of the United States of America*113, no. 23 (2016): 6427-6432.

Perez-Saez, Javier, Aaron A. King, Andrea Rinaldo, Mohammad Yunus, Abu SG Faruque, and Mercedes Pascual. "Climate-driven endemic cholera is modulated by human mobility in a megacity." *Advances in Water Resources* 108 (2016) : 367-376.

Perez-Saez, Javier, Lorenzo Mari, Enrico Bertuzzo, Renato Casagrandi, Susanne H. Sokolow, Giulio A. De Leo, Theophile Mande, Natalie Ceperley, Jean-Marc Froehlich, Mariam Sou, Harouna Karambiri, Hamma Yacouba, Amadou Maiga, Marino Gatto, and Andrea Rinaldo "A theoretical analysis of the geography of schistosomiasis in Burkina Faso highlights the roles of human mobility and water resources development in disease transmission." *PLoS Neglected Tropical Diseases* 9, 10 (2015): e0004127.

AWARDS

2015	Mobility award for an exchange at Stanford University by the Doctoral school in Civil and Environmental Engineering (EDCE-EPFL).
2014	Prix Pralong of the University of Lausanne for Swiss students to work on development issues.
2013	Prix « Société Suisse de géomatique et de gestion du territoire » for the best Master average grade in the Environmental Sciences and Engineering section.

TEACHING EXPERIENCE

Undergraduate

2011-2012	Introduction to Environmental Engineering (B.A.1) Engineering Informatics (B.A. 2) Quantitative Methods II (B.A. 3)
2016-2017	Hydrology for engineers (B.A. 3)

Graduate

2014-2017	Water Resources Management (M.A.)
2011-2012	Soil Water Regime Management (M.A.)

RESEARCH EXPERIENCE

My doctoral project involved field and theoretical work on a waterborne disease in West Africa. The research project required planning and managing field campaigns, including ecological sampling and environmental monitoring using wireless stations in collaboration with academic, governmental and non-governmental partners in Burkina Faso. Theoretical work focuses on spatially explicit models of schistosomiasis transmission, inclusive of climatic, ecological and socio-economic drivers.

PROFESSIONAL EXPERIENCE

2011-2012	**Environmental Engineering Student Association** (associative experience) Founder and head of the inter-class work group in charge of putting together the dossier for the creation of the student association. The dossier was accepted by the EPFL and the association founded in October 2012 – called TREE - with wide student participation.
2011	**Instituto Argentino de Investigacion de Zonas Aridas** (2-month internship) Evaluation of the Environmental Impact Assessment (EIA) procedure in the province of Mendoza and investigation of the potential of GIS-based best practices implementation in arid and marginalized areas.
2009	**American Overseas School of Rome** (2-month summer job) Summer camp counselor. Responsible for Lacrosse and co-responsible of the 12-14 year old group (animation and English classes). Mainly Italian and American children.

LANGUAGES

Spanish	Native Language
French	Native level
Italian	Native level - 10 years in Rome
English	Fluent C2 – Born in England and 1 year in Sweden